New Aspects of the Theory of Electron Transfer Reaction Dynamics

Thesis by

José Nelson Onuchic

In Partial Fulfillment of the Requirements

for the Degree of

Doctor of Philosophy

California Institute of Technology

1987

(submitted March 9, 1987)

To My Father,

Who Taught Me To Love Science

Acknowledgments

It is a pleasure to acknowledge John Hopfield, a brillant advisor and a very good friend during this period. To do science in collaboration with him was always a pleasant activity, never an obligation. The scientific and life experience he provided me is something very precious, and I will always be in debt to him for that.

Life in the Hopfield group was very nice and interesting. Science and social activities always played a very important role. It was fun to interact with David Beratan, Noam Agmon, Alvin Joran, Burt Leland, John Reinitz, Bo Cartling, Eric Baum, and Jimmy Hanson. Interaction with David Beratan played a important role in the development of this work. He is a talented scientific collaborator and a very good friend.

Also at Caltech, collaboration outside the Hopfield group was very important. In particular, I have enjoyed discussions with and learned from Rudi Marcus, Harry Gray, Walther Ellis, and Arnóbio da Gama. Part of this work was developed in collaboration outside of Caltech with Anupam Garg, Vinay Ambegaokar, and William Bialek. I also want to thank Peter Wolynes for inspirational scientific discussions. Thanks also go to Debbie Chester for her secretarial work during this period.

I want to thank all my Brazilian friends here at Caltech during this period. Also, I want to thank all my friends and colleagues at the Instituto de Física e Química de São Carlos, in particular, those in the Biophysics group.

I am also indebted to Sérgio Mascarenhas. As my advisor in Brazil, he inspired me to work on biophysics and gave me full support in the beginning

of my scientific life. He is also a very good friend, and he was supportive and understanding when I decided to come to Caltech.

I want to conclude by thanking my family. Mayra was just wonderful during this period. Thanks to her, life outside Caltech was very pleasant. In her company, I had five wonderful years in the United States. Her support and understanding, even during a few difficult periods, was essential during the development of this thesis. Lucas arrived less than one year ago. He came to fill an important space in our family. Special thanks go to my mother who took very good care of us from Brazil. Thanks to everyone in our families who were very supportive during this period and understanding of our need to live far away from them.

Financial support for this work was provided by the Brazilian Agency Conselho Nacional de Desenvolvimento Científico e Tecnológico (CNPq). They provided me with a fellowship, and they paid all of my university fees. Support was also provided by the Universidade de São Paulo and by the National Science Foundation (NSF).

Abstract

This thesis deals basically with some new aspects of the electron transfer theory. It is divided into four parts: (1) Chapter I gives an introduction to the electron transfer problem; (2) Chapter II addresses the subject of how nuclear dynamics influences the electron transfer rate; (3) Chapter III explains how to calculate electron transfer matrix elements for non–adiabatic electron transfer systems, in particular protein systems; and (4) Chapter IV discusses some preliminary ideas about new problems I intend to work on the future.

In Chapter II the following dynamical problems are addressed. For the case of one overdamped reaction coordinate, the problem of adiabaticity and non–adiabaticity is considered in details. For an underdamped reaction coordinate, a preliminary discussion is given. All this formalism is developed using a density matrix formalism and path integral techniques. One of the advantages of using this formalism is that, by analyzing the spectral density, we can connect our microscopic Hamiltonian with macroscopic quantities. It also gives us a natural way of including friction in the problem. We also determine when the Hopfield semiclassical or the Jortner "quantum" models are good approximations to the "complete" Hamiltonian. In the limit that the reaction coordinates are "classical," we discuss how we can obtain the Fokker–Planck equation associated with the Hamiltonian.

By adding more than one reaction coordinate to the problem (normally two), several other problems are studied. The separation of "fast" quantum modes from "slow" semiclassical modes, where the fast modes basically renormalize the electronic matrix element and the driving force of the electron trans-

fer reaction, is discussed. Problems such as exponential and non–exponential decay in time of the donor survival probability, and the validity of the Born–Oppenheimer and Condon approximations are also carefully addressed. This chapter is concluded with a calculation of the reaction rate in the inverted region for the extreme adiabatic limit.

In Chapter III we discuss calculations of electronic matrix elements, which are essential for the calculation of non–adiabatic rates. It starts with a discussion of why, through bond rather than through space, electron transfer is the important mechanism in model compounds. Also, it explains why tight–binding Hückel calculations are reasonable for evaluating these matrix elements, and why, through space and through bond, matrix element decays with distance have a different functional dependence on energy. Bridge effects due to different hydrocarbon linkers are also calculated.

This chapter concludes with a model for the calculation of matrix elements in proteins. The model assumes that the important electron transfer "pathways" are composed of both, through bond and through space parts. Finally, we describe how medium (bridge) fluctuations may introduce a new form of temperature dependence by modulating the matrix element.

In Chapter IV we discuss some experimental results obtained for electron transfer in the porphyrin–phenyl –(bicyclo[2.2.2]octane)$_n$–quinone molecule, and we propose some new experiments that should help to clarify our interpretation. It concludes with some preliminary discussions of how we can include entropy in the finite mode formalism described in Chapter II, and how we intend to use the formalism described in Chapter III in order to understand electron transfer in real protein systems.

Table of Contents

List of Figures

CHAPTER I – Introduction to the Electron Transfer Problem

I.1 Overview

Electron transfer is an important reaction in several chemical and biological processes.[1] Of the reactions that occur in condensed matter, it is the simplest one to be studied, and therefore a natural target when trying to develop microscopic models for chemical reactions.

Chemical electron transfer can be divided basically into two types. The first one is electron transfer between ions and molecules in solution. In this case, it is necessary that the two molecules involved in the transfer form a precursor complex before the electron is able to transfer.[1] In the second type the transfer occurs between two fixed sites. In the latter case, the donor and acceptor are in the same molecule or bound to some rigid matrix.[3] This second class of reactions is very important in several biological processes, and it is the kind of reaction we mainly address in this work.

Some important examples of electron transfer reactions in biology are the oxidative phosphorylation and photosynthetic reactions, which take electrons through a potential gradient. In both respiratory and photosynthetic systems the primary action of the energy source (combustion of the substrate by oxygen in respiration and absorption of light by chlorophyll or bacteriochlorophyll in photosynthesis) is to move electrons along an electron transport chain. The biological system then extracts energy from the resulting electrical potential in order to phosphorylate ADP (adenosine diphosphate) to ATP (adenosine triphosphate) or to transport ions across membranes. Details about the biological process are given in Refs. 1a and 1b.

One of the most studied electron transfer systems is the reaction center iso-

lated from the antenna pigments of the purple bacterium *Rhodopseudomonas sphaeroids.*[1a,1b] This reaction center contains four molecules of bacteriochlorophyll a (BChl), two molecules of bacteriopheophytin (BPh), one ubiquinone-10 (Q), and one non–heme iron. All these components, together with external cytochromes, are packed in a lipid membrane. A summary of the electron transfer events in such a system is shown in Figure I.1. Of all the reactions shown in this figure, the one that received early attention was the electron transfer from the cyt. *c* to $BChl^+$ in *Chromatium*, a different type of photosynthetic bacterium, which was studied by DeVault and Chance (Figure I.2).[4] This reaction is particularly interesting because it shows a normal Arrhenius behavior at high temperatures (above 200° K), but is temperature–independent at low temperatures. The semiclassical and "quantum" electron transfer theories were used to explain this behavior. These theories are described in the next section.

In an attempt to understand the main features of the above biological problems, several rigid electron transfer model compounds have been built, and an enormous amount of new experimental data is available.[2] One such system is the porphyrin–quinone system linked by a bridge of (0, 1, or 2) bicyclo[2.2.2]octane units.[2a] Also, electron transfer in native and modified proteins has been studied.[5] Gray's group Ru-modified proteins,[5a] Hoffman's group modified hemoglobin,[5b] and McLendon's modified cytochrome *c*[5c] are examples of such systems. To develp new theoretical methods that will be applied to interpret some of the experimental data from these systems is one of the goals of this thesis.

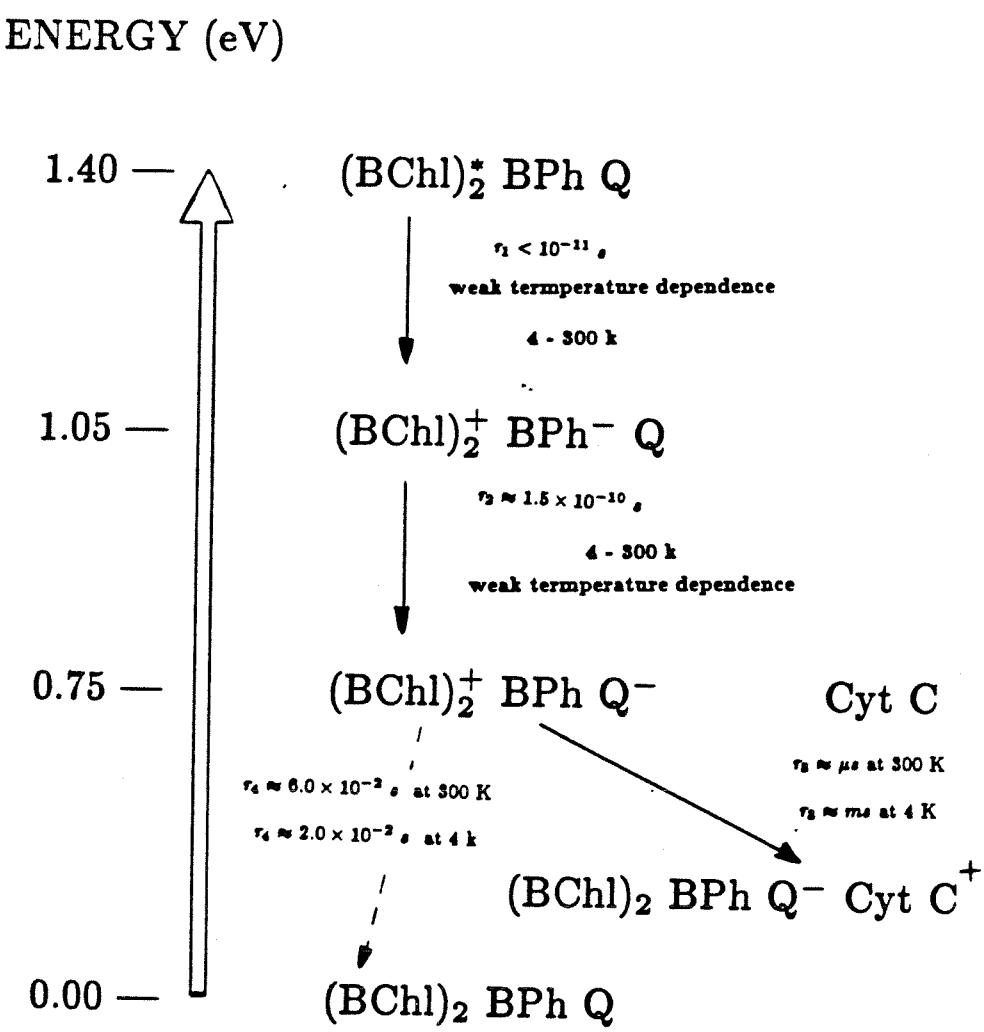

Figure I.1 – Schematic representation of the primary electron transfer processes in the reaction center of the photosynthetic bacteria *Rhodopseudomonas sphaeroids.*

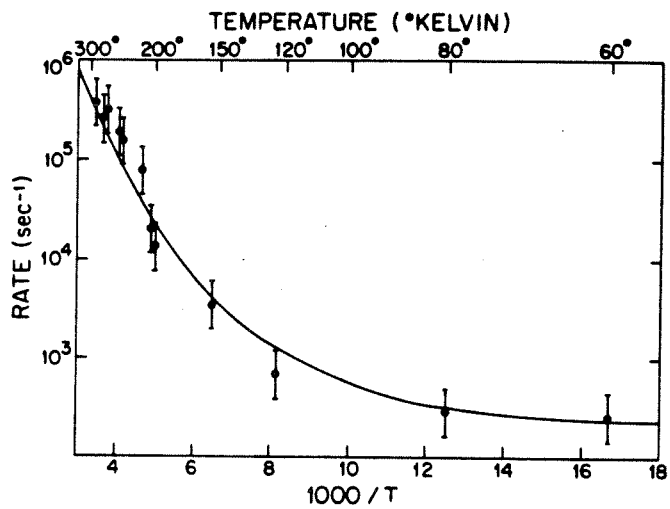

Figure I.2 – Cytochrome *c* oxidation rate in *Chromatium vinosum* as a function of temperature. The solid line shows a fit of the data by Hopfield's model (Eq. I.10) with the parameters given in Ref. 9d.

I.2 Summary of Theoretical Models

Several theoretical models have been developed to understand long-distance electron transfer (donor–acceptor separation larger than $\sim$ 5 Å). These reactions are the focus of this thesis. We summarize these models in this section, and briefly describe the new models that are developed in this thesis and the reason why they are needed. Also, the theory described in this thesis is designed mainly to calculate unimolecular rates, i.e., electron transfer rates between donor and acceptor in the same molecule, or between two molecules after a precursor complex is formed.[1c,1d] The summary presented here gives enough information to introduce the reader to the problem, but is in no way a complete review of all the theoretical work developed to date.

Initially, we describe the classical theory of Marcus[1c,6] for bimolecular electron transfer. Assume that electron transfer occurs between two molecules, and that it occurs only after they form the precursor complex. The rate of formation of such a complex can be described as

$$A + B \underset{k_{-D}}{\overset{k_D}{\rightleftharpoons}} A\cdot\cdot B \ . \qquad (I.1)$$

If, during the encounter, the electron transfers with a unimolecular rate k_1, the observed bimolecular transfer rate is

$$\frac{1}{k_{obs}} = \frac{1}{k_D} + \frac{1}{K_A k_1} \ , \qquad (I.2)$$

where $K_A = k_D/k_{-D}$ is the equilibrium constant for formation of the $A\cdot\cdot B$ complex. When the electronic and "nuclear" motions can be separated using the Born–Oppenheimer approximation (adiabatic limit, and this point

is more carefully addressed later in this section), the first–order rate constant, k_1, is taken to be an effective frequency, ν_N, for motion along the "reaction coordinate (vibrational and "solvational" contributions) multiplied by $\exp(-\Delta G^*/k_BT)$, where ΔG^* is the activation "free energy."

To better illustrate how k_1 is calculated we now consider the electron transfer problem coupled to two "nuclear modes," one vibrational (mode 1) and one solvational (mode 2). The reorganization energy is defined as

$$\lambda = \lambda_1 + \lambda_2 = \frac{m_1\omega_1^2 a_1^2}{2} + \frac{m_2\omega_2^2 a_2^2}{2} \quad , \qquad (I.3)$$

where a_1 and a_2 are the displacement of the modes from their pretransfer equilibrium positions after the electron transfer. If the the electron transfer rate is calculated using transition state theory,[1,7] the rate is

$$k_1 = \nu_N \exp\left\{-\frac{(\lambda + \Delta U_0)^2}{4k_BT\lambda}\right\} \quad , \qquad (I.4a)$$

where ΔU_0 is the driving force (or energy gap) of the electron transfer reaction. Here[7]

$$\nu_N = \frac{1}{2\pi}\left(\frac{\sum_{i=1}^{2}\lambda_i\omega_i^2}{\sum_{i=1}^{2}\lambda_i}\right)^{1/2} \quad , \qquad (I.4b)$$

and

$$\Delta U^* = \frac{(\lambda + \Delta U_0)^2}{4\lambda} \quad . \qquad (I.4c)$$

Eq. I.4 can be easily generalized for as many nuclear coordinates as must be included. If we compare the rate described in the paragraph before Eq. I.3 with Eq. I.4, we notice that in one of them we have free energy, and in the other one we have real potential energy U. On the one hand, the problem is well defined only if we actually have potential energies. How to think about dynamics along a free energy coordinate has been a controversy in this field for

some time. On the other hand, large entropic changes have been observed in several electron transfer reactions,[8] and Eq. I.4 is unable to properly account for this large ΔS. In the final chapter of this thesis we present some comments about the meaning of dynamics on a free energy surface, but this point is not carefully addressed in this thesis. Some work by Marcus[6a,6g] also addressed this point. In most of this thesis we consider motion only on potential energy surfaces.

For simplicity we now consider only one nuclear mode coupled to the electron. The Hamiltonian for the entire electron transfer system (neglecting coupling to the environment) can be written as[1]

$$H_{ET} = T_{DA}\sigma_x + \frac{p_y^2}{2M} + \frac{1}{2}M\Omega^2(y + y_0\sigma_z)^2 + \frac{\Delta U_0}{2}\sigma_z \quad . \qquad (I.5)$$

Here y is the reaction coordinate, $\lambda = 2M\Omega^2 y_0$, and T_{DA} is the electronic matrix element coupling the donor and acceptor states.[9a] This Hamiltonian assumes a Born–Oppenheimer approximation for the donor and acceptor states, and a Condon approximation for the electronic matrix element. The validity of these approximations is discussed in Chapter II. Non–adiabatic and adiabatic potential wells are shown in Figure I.3. If the rate is adiabatic, the "reaction coordinate" potential surface is shown in Figure I.3c, and, if $T_{DA} \ll k_B T$, the rate calculated using transition state theory (exactly as in Eq. I.4) is

$$k_1 = \frac{\Omega}{2\pi} \exp\left\{-\frac{(\lambda + \Delta U_0)^2}{4k_B T\lambda}\right\} \quad . \qquad (I.6)$$

But the reaction is not always adiabatic, principally when the electron is transferred a long distance. In this case (still a transition state theory approach), the rate k_1 must be multiplied by an adiabaticity factor κ_{EL}, which is calculated in the Landau–Zener framework,[10] and in the high–temperature limited

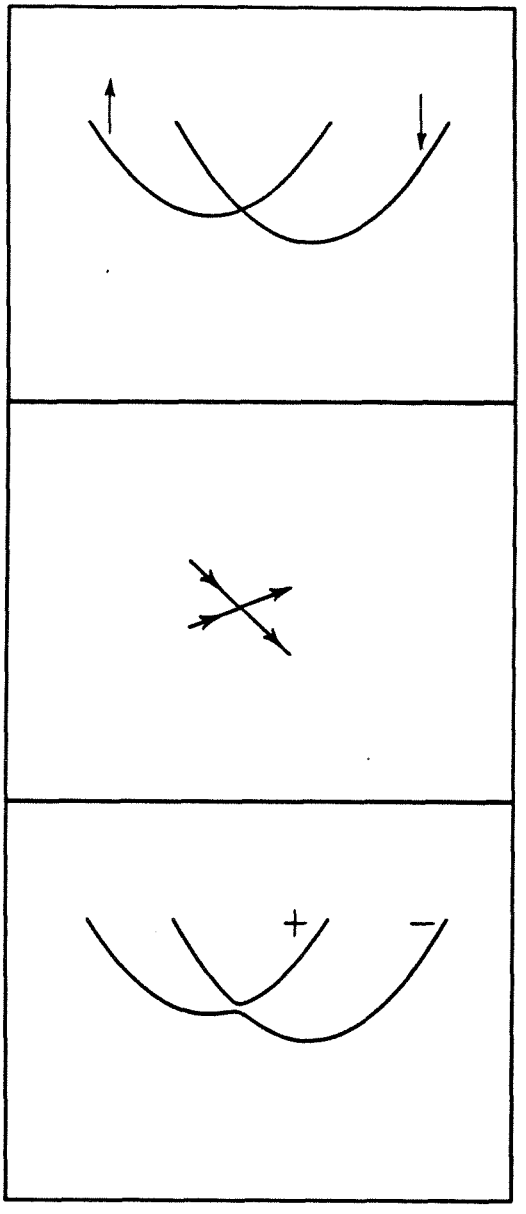

Figure I.3 – (a) Upper panel. Energy of the electronic (spin) states $|\uparrow\rangle$ and $|\downarrow\rangle$ as a function of the reaction coordinate y (see Eq. I.5). (b) Middle panel. The region where the potential surfaces in (a) cross, with arrows denoting the reactive trajectory. (c) Lower panel. Adiabatic surfaces corresponding to the zero–order (non–adiabatic) surfaces in (a).

can be written as[11]

$$\kappa_{EL} = \frac{2\left[1-\exp(-\nu_{EL}/2\nu_N)\right]}{2-\exp(-\nu_{EL}/2\nu_N)} \quad , \tag{I.7a}$$

where

$$\nu_{EL} = \frac{2\pi T_{DA}^2}{\hbar}\,\frac{1}{\sqrt{4\pi k_B T\lambda}} \quad . \tag{I.7b}$$

When $\kappa_{EL} \ll 1$ the rate becomes non–adiabatic, and thus

$$k_1 = \frac{2\pi T_{DA}^2}{\hbar}\,\frac{1}{\sqrt{4\pi k_B T\lambda}}\,\exp\left\{-\frac{(\lambda+\Delta U_0)^2}{4k_B T\lambda}\right\} \quad . \tag{I.8}$$

To this point the nuclear coordinates are treated classically, and rates have been calculated using transition state theory.

The importance of the non–adiabatic theory for biological electron transfer was observed by Hopfield in 1974.[9] He developed a semiclassical non–adiabatic theory for electron transfer with one nuclear mode coupled to the acceptor and one to the donor. The rate obtained is

$$k_1 = \frac{2\pi}{\hbar}T_{DA}^2\int_{-\infty}^{\infty} D_d(E)D'_a(E)\,dE \quad , \tag{I.9}$$

where $D_d(E)$ describes the electron removal spectral density, and $D'_a(E)$ the insertion energy of an electron into the acceptor state. Thus, if $\Delta U_0 = E_d - E_a$, then

$$D_d(E) = \frac{1}{\sqrt{2\pi\sigma_d^2}}\,\exp\left\{-\frac{(E-E_d+\lambda_d)^2}{2\sigma_d^2}\right\} \quad , \tag{I.10a}$$

$$D'_a(E) = \frac{1}{\sqrt{2\pi\sigma_a^2}}\,\exp\left\{-\frac{(E-E_a-\lambda_a)^2}{2\sigma_a^2}\right\} \quad , \tag{I.10b}$$

where

$$\sigma_i^2 = \hbar\Omega_i\lambda_i\coth\left(\frac{\hbar\Omega_i}{2k_B T}\right) \quad \text{with} \quad i = d \text{ or } a \quad . \tag{I.10c}$$

If instead of two modes we consider only one (donor or acceptor), the rate becomes

$$k_1 = \frac{2\pi}{\hbar} T_{DA}^2 \frac{1}{\sqrt{2\pi\sigma^2}} \exp\left\{-\frac{(\Delta U_0 - \lambda)^2}{2\sigma^2}\right\} \quad . \qquad (I.11)$$

From Eq. I.10c we can explain the cyt. *c* oxidation rate in *Chromatium* (Figure I.2). σ_i^2 is temperature–independent at low T and varies linearly in T at high temperatures. There is a need to treat the reaction coordinate quantum mechanically in order to get this temperature–independent rate at low temperatures. If $k_B T \gg \hbar\Omega$, the classical limit is valid, and Eq. I.11 becomes exactly Eq. I.8.

As a final theoretical model we discuss the "quantum" model developed by Jortner and collaborators.[12] The rate is calculated using a Fermi golden rule approach. The one mode rate in such a model is formally written as

$$k_1 = \frac{2\pi}{\hbar} T_{DA}^2 \times F \quad , \qquad (I.12a)$$

where F is the thermally averaged nuclear vibrational Franck–Condon overlap factor

$$F = \sum_{n_D, m_A} \rho_{n_D} \mid < \chi_{n_D} | \chi_{m_A} > |^2 \, \delta(E_{d,n_D} - E_{a,m_A}) \quad . \qquad (I.12b)$$

Here χ_{n_D} (χ_{m_A}) are the nuclear wave functions for the donor(acceptor) states of the Hamiltonian I.5 or of a more complicated Hamiltonian. n_D and m_A are the quantum numbers for each of these states. ρ_{n_D} is the thermal probability of the donor being in the state n_D. The delta functions in Eq. I.12b are purely formal. We do not give further details about this formalism but, as expected, at high temperatures all three formalisms agree.

All the theories described here lack a careful description for the dynamics of the nuclear coordinates. Without a good description of the nuclear dynamics, it is impossible to determine when the non–adiabatic limit is valid, and

when it starts to break down. Only the classical model tries to take dynamics into account, but it does not explain how the system relaxes after the particle goes through the crossing point of the surfaces (Landau–Zener region). The weakness of the models can be noticed from Hamiltonian I.5, which does not take into account how the "reaction coordinate" interacts with the environment and is damped. A detailed study of the dynamics of the problem is given in Chapter II. Also, as mentioned earlier, all of these theories make two basic approximations, the Born–Oppenheimer and Condon approximations, without adequate justification. When these approximations are valid and what happens when they break down are discussed in Chapter II.

For completeness, it is useful to mention that theoretical work has been done for a diffusive reaction coordinate. Such an approach is used to describe electron transfer reactions in polar solvents. If the solvent polarization is the only reaction coordinate considered, the diffusive dynamics may be valid, and in the adiabatic limit the rate has a Kramer's behavior instead of a transition state one.[13] A careful discussion about this macroscopic model for solvent polarization and all relevant references can be found in Ref. 1c. Recall that Kramer's limit is the opposite of the transition state theory limit.

Assume we understand the nuclear dynamics. When the rate is non–adiabatic, the problem of predicting the electronic matrix element, T_{DA}, is an important problem. If we write the electronic Hamiltonian in a basis of donor and acceptor localized states, the interaction between these two states is given by the the non–diagonal matrix element T_{DA}. One of the first attempts to calculate electron transfer matrix elements in biological systems was made by Hopfield using a square well model,[9] and therefore treating the medium in an

average sense. This model was used to calculate the electron transfer matrix element of light–initiated transfer of an electron from cytochrome to $BChl^+$ in *Chromatium*.[4] Also treating the medium in an average sense is the model developed by Siders, Cave and Marcus.[14] In that case an angular dependence between donor and the acceptor is included. But, no "detailed" description of the medium is included.

It is generally accepted that the electron transfer rate is dependent on the details of the medium the electron tunnels through. Experiments performed on model compounds,[2] which have the donor and acceptor covalently linked (through–bond electron transfer), have shown that different bridges connecting donor and acceptor lead to different transfer rates. On the theoretical side, Halpern and Orgel[15] in 1960 first identified the importance of orbital symmetry, overlap, and energetics on the bridge–mediated electronic interaction. McConnell[16] in 1961 used a one–electron one–orbital–per–bridge–site model to describe electron exchange through a saturated bridge. A literature is emerging that allows estimates of the importance of electron (conduction band) or hole (valence band) tunneling, and dependence of the electronic donor–acceptor interaction on redox potentials and bridge geometry.[17] In some theoretical work, using tight binding Hückel calculations, our group tried to quantify these effects.[17c,17h] A discussion of the validity of the average medium description or the tight binding one is one of the topics presented in Chapter III.

From model compounds, we learned that covalent pathways really assist electron transfer. Therefore, they must be important for electron transfer in proteins. However, if we look at protein structures, we come to the conclusion that the covalent pathways are, in most proteins, prohibitively long, and

some through–space electron "jumps" (tunneling) are probably important. In Chapter III we develop a model that includes both possibilities; i.e., the electron transfer pathway is composed of many covalent pathways joined by a few through–space jumps. Initially we present the model, assuming that the electron tunnels through a rigid medium and then we discuss how these medium fluctuations affect the transfer rate.

The plan of this thesis is as follows:

(a) Chapter II describes new theoretical approaches to describe the dynamics of electron transfer reactions. The topics discussed are the following: (1) The effect of friction on electron transfer reactions is studied. A discussion of the validity, depending on friction, of Hopfield's semiclassical[9] or the Jortner's "quantum"[12] models is presented. Criteria for adiabaticity and non–adiabaticity are discussed. (2) A model is presented for separating the fast local modes (such as CO vibrations) from the slow reaction coordinates and the bath in the electron transfer problem. In this case the fast mode overlap "renormalizes" the electronic matrix element. How this affects the adiabatic and non–adiabatic limits is discussed. (3) We also discuss how, starting from the Hamiltonian, we can write the Fokker–Planck equation associated with the electron transfer problem if the reaction coordinate(s) is(are) "classical." (4) In the case of multiple "slow" reaction coordinates (i.e., those that can not be treated as "renormalizing" the matrix element), a discussion is given about the point at which the donor survival probability decays exponentially in time or not. (5) A discussion is given about the validity of the Born–Oppenheimer and Condon approximations, and about what happens to the rate when these approximations

fail. (6) A calculation is presented of the electron transfer rate in the inverted region and extreme adiabatic limit.

(b) Chapter III describes the effect of the transfer medium between donor and acceptor on the electron transfer rate. A discussion is presented of through–bond versus through–space electron transfer matrix elements. Here we also discuss how different hydrocarbon bridges affect the through–bond electron transfer matrix element in several model compounds. We also use these two mechanisms to propose a model for matrix elements through protein environments. This chapter is concluded with a discussion of how the protein environment motions may modulate the electron transfer rate and therefore give rise to a new form of temperature dependence.

(c) Chapter IV describes some preliminary ideas that will be further developed in the future. A discussion is presented of the experimental results available for electron transfer in the model compound porphyrin–linker–quinone molecule, where the linker is composed of 0, 1, or 2 bicyclo[2.2.2]octane units. Some new experiments are proposed to clarify our understanding of this system. To conclude this chapter, we discuss one way that large entropic changes may be included in simple electron transfer models, and how we intend to apply the protein model described in Chapter III to real systems.

I.3 References – Chapter I

(1) (a) D.DeVault, *Quantum Mechanical Tunneling in Biological Systems*, 2nd edition; Cambridge Univ. Press: New York, 1984; (b) B. Chance, D.C. DeVault, H. Frauenfelder, R.A. Marcus, J.R. Schrieffer, and N. Sutin, eds., *Tunneling in Biological Systems*; Academic Press: New York, 1979; (c) R.A. Marcus and N. Sutin, *Biochim. Biophys. Acta* **811**, 265 (1985); (d) M.D. Newton and N. Sutin, *Ann. Rev. Phys. Chem.* **35**, 437 (1984).

(2) (a) B.A. Leland, A.D. Joran, P.M. Felker, J.J. Hopfield, A.H. Zewail, and P.B. Dervan, *J. Phys. Chem.* **89**, 5571 (1985); (b) S.S. Isied *Prog. Inorg. Chem.* **32**, 443 (1984); (c) H. Heitele and M.E. Michel–Beyerle, *J. Am. Chem. Soc.* **107**, 8286 (1985); (d) M.R. Wasielewski and M.P. Niemczyk, *J. Am. Chem. Soc.* **106**, 5043 (1984); (e) D.E. Richardson and H. Taube, *J. Am. Chem. Soc.* **105**, 40 (1985); (f) G.L. Closs, L.T. Calcaterra, N.J. Green, K.W. Penfield, and J.R. Miller, *J. Phys. Chem.* **90**, 3673 (1986); (g) J. Verhoeven *J. Pure and Appl. Chem* **58**, 1285 (1986); (h) C.A. Stein, N.A. Lewis, and G.J. Seitz, *J. Am. Chem. Soc.* **104**, 2596 (1982).

(3) (a) J.R. Miller, J.V. Beitz, and R.K. Huddleston, *J. Am. Chem. Soc.* **106**, 5057 (1984).

(4) D. Devault and B. Chance, *Biophys. J.* **6**, 825 (1966).

(5) (a) S.L. Mayo, W.R. Ellis, R.J. Crutchley, and H.B. Gray, *Science* **233**, 948 (1986); (b) S.E. Peterson–Kennedy, J.L. McGourty, J.A. Kalweit, and B.M. Hoffman, *J. Am. Chem. Soc.* **108**, 1739 (1986); (c) G. McLendon and J.R. Miller, *J. Am. Chem. Soc.* **107**, 7811 (1985); (d) S.G. Boxer,

Biochim. Biophys. Acta **726**, 265 (1983).

(6) R.A. Marcus, (a) *J. Chem. Phys.* **24**, 966 (1956); (b) *Discuss. Faraday Soc.* **29**, 21 (1960); (c) *J. Phys. Chem.* **67**, 853, 2889 (1963); (d) *Ann. Rev. Phys. Chem.* **15**, 155 (1964); (e) *J. Chem. Phys.* **43**, 679 (1963); (f) in *Oxidases and Related Redox Systems*, T.E. King, H.S. Mason, and M. Morrison, eds.; Pergamon Press: New York, 1982, p. 3; (g) *J. Chem. Phys.* **81**, 4494 (1984).

(7) (a) V.G. Levich and R.R. Dogonadze, *Dokl. Acad. Nauk SSSR* **124**, 123 (1959); (b) V.G. Levich, *Adv. Electroch. Electroch. Eng.* **4**, 249 (1965).

(8) W.R. Ellis, *Ph.D. Thesis*, California Institute of Technology, 1986.

(9) (a) J.J. Hopfield, *Proc. Nat. Acad. Sci. (USA)* **7**, 3640 (1974); (b) J.J. Hopfield, *Biophys. J.* **18**, 311 (1977); (c) M. Redi and J.J. Hopfield, *J. Chem. Phys.* **72**, 6651 (1980); (d) J.J. Hopfield, in *Electrical Phenomena at the Biological Membrane Level*; Elsevier Scientific Publishing Co.: Amsterdam, 1977.

(10) L.D. Landau and E.M. Lifshitz, *Quantum Mechanics*; Pergamon Press: New York, 1977, 3rd edition, §90.

(11) N. Sutin, *Acc. Chem. Res.* **9**, 275 (1982).

(12) (a) N.R. Kestner, J. Logan, and J. Jortner, *J. Phys. Chem.* **78**, 2148 (1974); (b) J. Jortner, *J. Chem. Phys.* **64**, 4860 (1976); (c) J. Jortner, *Biochim. Biophys. Acta* **594**, 193 (1980); (d) M. Bixon and J. Jortner, *Faraday Discuss. Chem. Soc.* **74**, 17 (1982).

(13) D.F. Calef and P.G. Wolynes, *J. Phys. Chem.* **87**, 3387 (1983).

(14) P. Siders, R.J. Cave, and R.A. Marcus, *J. Chem. Phys.* **81**, 5613 (1984).

(15) J. Halpern and L. Orgel, *Discuss. Faraday Soc.* **29**, 32 (1960).

(16) H.M. McConnell, *J. Chem. Phys.* **35**, 508 (1961).

(17) (a) S. Larsson, *J. Chem. Soc., Faraday Trans. 2* **79**, 1375 (1983); (b) S. Larsson, *J. Am. Chem. Soc.* **103**, 4034 (1981); (c) D.N. Beratan and J.J. Hopfield, *J. Am. Chem. Soc.* **106**, 1584 (1984); (d) P.D. Hale and M.A. Ratner, *Int. J. Quantum Chem.: Quantum Chem. Symp.* **18**, 195 (1984); (e) A.A.S. da Gama, *Theor. Chim. Acta* **68**, 159 (1985); (f) D.E. Richardson and H. Taube, *J. Am. Chem. Soc.* **105**, 40 (1983); (g) D.E. Richardson and H. Taube, *Coord. Chem. Revs.* **60**, 107 (1984); (h)(c) D.N. Beratan *J. Am. Chem. Soc.* **108**, 4321 (1986).

CHAPTER II – Theoretical Models for the Dynamics of the Nuclear Coordinates

II.1 Summary

This section gives a summary of the work presented in the following four sections of this chapter. The most important results are emphasized in order to help the reader to proceed through the chapter. Also, some supplemental discussion of these results is given. Besides the results presented below, it is important to remark that to perform these calculations we had to introduce new methods to this field. In our work (details in Secs. II.2, II.3 and II.4), we describe how to use a density matrix approach combined with Path Integral techniques[1] to calculate rates for chemical and biological reactions.

Adiabaticity vs. Non–Adiabaticity

Effect of Friction on Electron Transfer Rates

Consider Hamiltonian I.5, but with the nuclear mode y coupled to the remaining nuclear degrees of freedom of the problem (the bath). The Hamiltonian is

$$H_{ET} = T_{DA}\,\sigma_x + \frac{p_y^2}{2M} + \frac{1}{2}M\Omega^2(y + y_0\sigma_z)^2 + \frac{\varepsilon}{2}\sigma_z + \sum_{b(bath)} \frac{P_b^2}{2M_b} + \frac{1}{2}M_b\omega_b^2\left[x_b + \frac{c_b}{M_b\omega_b^2}y\right]^2 \qquad (II.1)$$

where x_b's are the bath coordinates. A schematic representation of the parameters used in the equation above is given in Figure II.1. To model the bath as a set of independent harmonic oscillators linearly coupled to the reaction coordinate is correct as long as the bath modes are all weakly coupled to the reaction coordinate. This prescription will start to provide quantitatively inaccurate answers if, in reality, some of the bath degrees of freedom are strongly

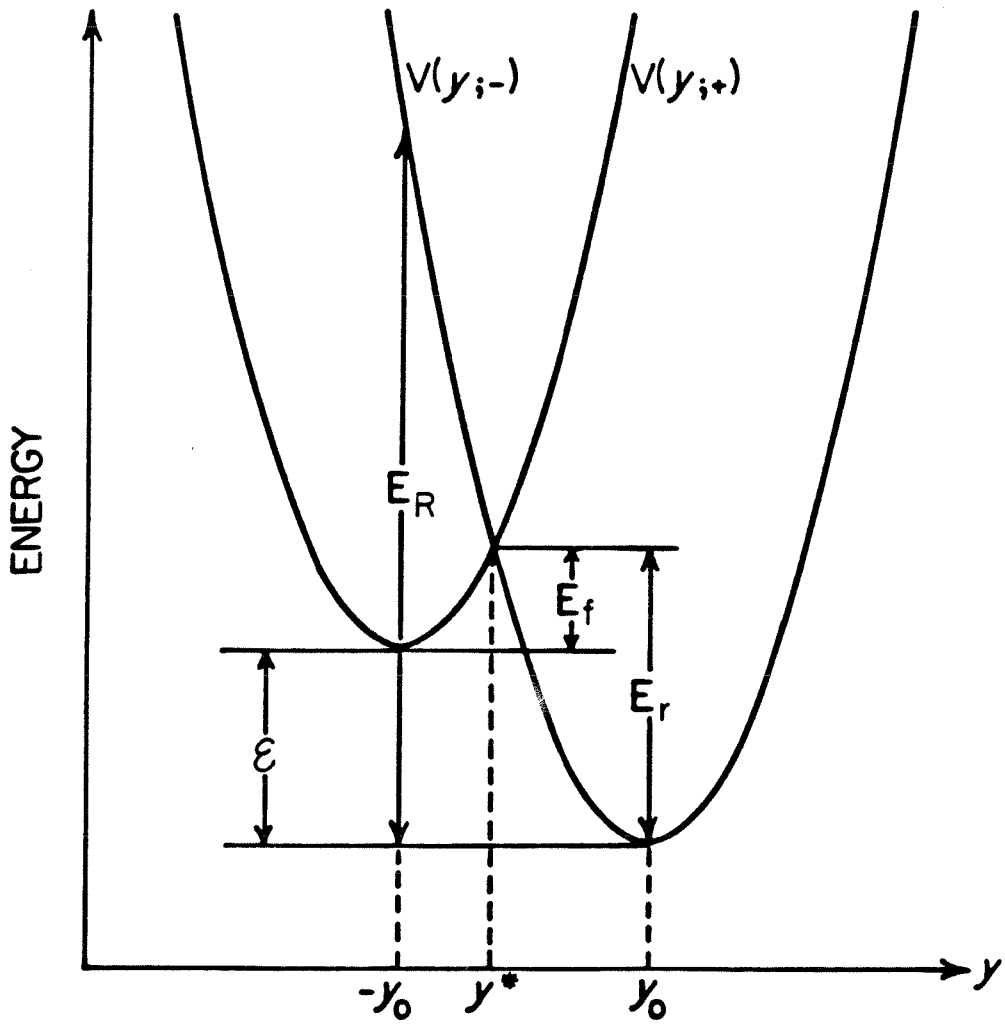

Figure II.1 – Potential energy surfaces for the reaction coordinate. The labels + and − refer to the donor and acceptor sites. The energies E_f, E_r, and E_R are the forward and reverse activation energies, and the reorganization energy, respectively.

excited. If that is the case, the mode should be treated separately, not with the continuum of modes. More details about this assumption are given in Secs. II.2 and II.3.

As discussed by Caldeira and Leggett,[2] details of the bath are unnecessary; only how the "reduced dynamics" of the electron and reaction coordinate are affected by the bath is important. Therefore, the bath oscillators' influence on the reaction coordinate is determined by the following relation, which is known as the spectral density,

$$J_0(\omega) \;=\; \frac{\pi}{2} \sum_{b(bath)} \frac{c_b^2}{M_b \omega_b} \, \delta(\omega - \omega_b) \quad . \qquad (II.2)$$

In this section we work mainly with the ohmic form of the spectral density

$$J_0(\omega) \;=\; \eta\omega \;\exp(-\omega/\Lambda) \;\text{ and }\; \gamma = \eta/2M \quad , \qquad (II.3)$$

where Λ is a high frequency cutoff that is required on both physical and mathematical grounds. It must be much faster than any time scale associated with the problem. As discussed in Sec. II.2, if other forms for the spectral density were considered, a frequency–dependent damping constant η would be necessary. Because at the level we want to address the problem here there is no reason to further complicate it, we use (in this section) the ohmic form for the spectral density. (See Secs. II.3 for details.)

Because the bath and the reaction coordinate are assumed harmonic, and the coupling between them is linear, we can diagonalize the quadratic part of Eq. II.1 and get

$$H_{ET} = T_{DA}\,\sigma_x + \frac{\varepsilon}{2}\sigma_z + \sigma_z \sum_\alpha \tilde{c}_\alpha \tilde{x}_\alpha$$

$$+ \sum_\alpha \left\{ \frac{\tilde{p}_\alpha^2}{2\tilde{m}_\alpha} + \frac{1}{2}\tilde{m}_\alpha \tilde{\omega}_\alpha^2 \tilde{x}_\alpha^2 + \frac{\tilde{c}_\alpha^2}{2\tilde{m}_\alpha \tilde{\omega}_\alpha^2} \right\} \quad , \qquad (II.4)$$

where $\tilde{x}_\alpha$ are the normal coordinates, and $\tilde{p}_\alpha$, $\tilde{m}_\alpha$, and $\tilde{\omega}_\alpha$ are the corresponding canonical momenta, masses, and frequencies. In analogy to Eqs. II.2 and II.3, the effective spectral density becomes

$$J_{eff}(\omega) = \frac{\pi}{2} \sum_\alpha \frac{\tilde{c}_\alpha^2}{\tilde{m}_\alpha \tilde{\omega}_\alpha} \delta(\omega - \tilde{\omega}_\alpha) = \frac{\eta \Omega^4 y_0^2 \omega}{(\Omega^2 - \omega^2)^2 + 4\omega^2\gamma^2} \quad . \qquad (II.5)$$

This technique can be applied to more complex Hamiltonians where several reaction coordinates exist. These Hamiltonians can also be transformed to the form given in Eq. II.4 but with a different spectral density. Details about this case are given in Sec. II.3.

We now calculate electron transfer rates in the non–adiabatic limit. Here we discuss two interesting limits of the coupling between the reaction coordinate and the bath. (See Secs. II.3 and II.4 for details.) Initially we consider the weak coupling limit. By weak coupling we mean that the widths of the reaction coordinate energy levels, which are important for the electron transfer, are much smaller than $\hbar\Omega$, but large enough so that the non–adiabatic limit still holds (this point is discussed more carefully in the end of this subsection and Secs. II.3 and II.4). When this condition is satisfied, the rate is

$$\Gamma_{na}^{f;r} = \frac{2\pi}{\hbar} T_{DA}^2 \, (F.C.)^{f;r} \quad , \qquad (II.6)$$

where $(F.C.)$ is the thermally averaged Franck-Condon factor

$$(F.C.)^{f;r} = \sum_{i_D} \sum_{i_A} \rho(E_{i_D;i_A}^{D;A}, T) \; |< \phi_{i_D}^D \mid \phi_{i_A}^A >|^2 \; h^{D;A}(E_{i_D}^D - E_{i_A}^A) \; . \; (II.7)$$

$\rho(E^{D;A}_{i_D;i_A})$ is the donor (acceptor) thermal density of states, and ϕ's are the reaction coordinate eigenfunctions, neglecting the coupling to the bath. Here $f(r)$ is the forward (reverse) electron transfer rate. The function $h(E^D - E^A)$ has $\int h(E)dE = 1$ and is highly peaked when $E^D = E^A$ (see Secs. II.3 and II.4 for details). Because the width of $h(E)$ is much smaller than $\hbar\Omega$, $\delta(E)$ is normally substituted for it to simplify the algebra, although here the delta function has only formal meaning.

In this limit, the electron transfer rate has the functional form of the Jortner "quantum" model. Eq. II.6 gives a rate that is peaked for values of ε, which are multiples of $\hbar\Omega$. This peaked behavior can be eliminated only if there is enough inhomogeneous broadening.

The second limit considered is the case of strong coupling between the reaction coordinate and the bath. In this case the density of states varies smoothly with energy. Initially, consider the case where y is underdamped. When both of these conditions are met we call it the moderate–friction limit. A quantitative estimate of this condition is given in Sec. II.4. Here the probability of having the electron on the acceptor at time t (assuming that $P^A(0) = 0$) is

$$P^A(t) \;=\; P^A_\infty - P^A_\infty \exp(-\Gamma_{na} t) \quad , \qquad (II.8)$$

where

$$\Gamma_{na} \;=\; \Gamma^f_{na} + \Gamma^r_{na} \quad , \qquad (II.9a)$$

with

$$\Gamma^{f,r}_{na} \;=\; \frac{2\pi}{\hbar}\frac{T^2_{DA}}{\sqrt{4\pi E_R k T_{eff}}} \exp\left\{-(\varepsilon \mp E_R)^2/4kT_{eff}E_R\right\}$$

$$= \frac{2\pi}{\hbar F_\Delta} T^2_{DA} \rho^{f;r}_{DA}(y^*) \quad , \qquad (II.9b)$$

and

$$P_{\infty}^{A} = \frac{1+\tanh(\varepsilon/2kT_{eff})}{2} \quad . \qquad (II.9c)$$

$E_R = 2M\Omega^2 y_0^2$ is the reorganization energy and $\rho_{D,A}(y^*)$ is the probability of finding the nuclear mode ("particle") in the intersection point between donor and acceptor wells when the electron is on the donor (acceptor). F_Δ is the difference of slopes of the donor and acceptor potential wells at the crossing point. The effective temperature, T_{eff}, is

$$kT_{eff} = M\Omega^2\mu^2(\eta,T) \quad , \qquad (II.10)$$

where $\mu^2(\eta,T)$ is the mean–square displacement of the reaction coordinate about its equilibrium value. (See Sec. II.2 for details.) At high temperatures $T_{eff} \approx T$. This functional form for the electron transfer rate (Eq. II.9) is similar to the one proposed by Hopfield in his semiclassical model. This rate is valid when we are in the strong coupling limit and when *each transit of the "particle" through the Landau–Zener region* is too rapid for the electron to make many transitions from donor to acceptor. This last statement is the point of discussion for the remainder of this subsection.

A particular case of the strong coupling limit is one in which the nuclear coordinate is overdamped ($\gamma \gg \Omega$). In this case the characteristic time of the reaction coordinate is given by $\tau_c = \omega_c^{-1}$, where $\omega_c = \Omega^2/2\gamma$. In this situation (assuming $kT \gg \hbar\Omega^2/2\gamma$, which is true for real diffusive modes such as solvent polarization), the electron transfer rate is

$$\Gamma^{f;r} = \frac{2\pi}{\hbar} T_{DA}^2 \left(\frac{1}{4\pi E_R kT}\right)^{1/2} \left[\frac{1}{1+(2\pi T_{DA}^2/\hbar\omega_c E_R)}\right] \exp\left\{-\frac{(\varepsilon \mp E_R)^2}{4kTE_R}\right\} \quad . \qquad (II.11)$$

If an "adiabaticity" parameter g is defined

$$g = \frac{2\pi T_{DA}^2}{\hbar\omega_c E_R} \quad , \qquad (II.12)$$

the reaction is adiabatic or non–adiabatic, depending on whether g is large or small.

The condition given by Eq. II.12 is especially interesting because it provides a quantitative estimate for the validity of the non–adiabatic limit. In order to simplify the discussion, we now define two characteristic times:

$$t_{drift}^{LZ} \approx \frac{2T_{DA}}{E_R\omega_c} = \frac{\ell_{LZ}}{y_0\omega_c} \quad , \qquad (II.13)$$

which is the average time the "particle" stays in the Landau–Zener region each times it reaches it, and

$$t_{diff}^{LZ} \approx \frac{(2T_{DA})^2}{E_R kT\ \omega_c} \quad , \qquad (II.14)$$

which is the time taken by the particle for each transit through the Landau–Zener region. Also, it is important to point out that because $2\ T_{DA} \ll kT$, for the problems we are interested in, $t_{drift}^{LZ} \gg t_{diff}^{LZ}$.

Considering the two characteristic times above, we note that the adiabaticity condition, $g \gg 1$, is satisfied when $t_{drift}^{LZ} \gg (T_{DA}/\hbar)^{-1}$, and we need not meet the condition $t_{diff}^{LZ} \gg (T_{DA}/\hbar)^{-1}$. The latter condition, $t_{diff}^{LZ} \gg (T_{DA}/\hbar)^{-1}$, is the conventional adiabatic limit, and when it is true, the conventional picture of split nuclear wells is valid. But, as we showed in the case of $t_{drift}^{LZ} \gg (T_{DA}/\hbar)^{-1}$, "adiabaticity" holds under a much weaker condition than the conventional one.

As can be seen from Sec. II.2, Eq. II.11 was developed, assuming that the motion of the particle is diffusive even when it is in the Landau–Zener

region. Thus, if $t_{diff}^{LZ} \ll (T_{DA}/\hbar)^{-1} \ll t_{drift}^{LZ}$, when the particle crosses the Landau–Zener region, each of its transits is associated with a very small transfer probability proportional to T_{DA}^2, but adiabaticity results because the particle crosses this region many times before it drifts away. Otherwise, i.e., if $t_{diff}^{LZ} \gg (T_{DA}/\hbar)^{-1}$, we should look at the problem in the conventional way, where we have the "adiabatic" splitting of the nuclear wells. This latter limit in the inverted region is discussed at the end of this section.

If the motion of the nuclear coordinate is classical, an extension of the above discussion is possible for the underdamped case. We are interested in the low–friction limit, i.e., when every crossing through the Landau–Zener region is ballistic. Even so, the discussion we present here does not give quantitative estimates as in the overdamped case; it permits some preliminary understanding of the problem. As in the overdamped situation, it is not necessarily only the time involved for each Landau–Zener crossing that is important to decide whether or not the rate is non–adiabatic. Also, similarly to the case we solved for the overdamped problem, we assume that the activation energies are much larger than kT. In the Landau–Zener picture, if a particle goes accross the crossing region with velocity v, the time it stays in this region is of the order

$$t_{LZ} \sim \frac{l_{LZ}}{v} \sim \frac{T_{DA} y_0}{E_R v} \quad . \qquad (II.15)$$

But every time this particle is excited so that it is able to cross the Landau–Zener region, the average value of $1/v$ with which it goes through the crossing region is about

$$\left\langle \frac{1}{v} \right\rangle \sim \sqrt{\frac{M}{kT}} \quad , \qquad (II.16a)$$

and therefore

$$t_{LZ} \sim l_{LZ} \sqrt{\frac{M}{kT}} \quad . \qquad (II.16b)$$

In the underdamped limit, before the particle relaxes, i.e., it does not have energy to traverse the crossing region any more, it may go through the Landau–Zener region several times. This point is discussed next.

Recall that the size of the transition state region (l_{TS}) is $\sim kTy_0/E_R$, and the average free path (l_{free}) is $\sim (kT/M)^{1/2}/\gamma$. As discussed by Frauenfelder and Wolynes,[3] if $l_{LZ} \gg l_{TS}$, the curves split and the standard adiabatic theory is valid. This is not the situation we are interested in. If $l_{LZ} \ll l_{TS}$, the number of times it goes across the Landau–Zener region may depend on two factors:

(1) $l_{LZ} \ll l_{TS} \ll l_{free}$ every transit through the transition region is ballistic. But if $l_{LZ} \ll l_{free} \ll l_{TS}$, then on each passage through the transition region multiple crossings of the Landau–Zener region occur, and

$$N_{crosses} \sim l_{TS}/l_{free} \quad . \qquad (II.17a)$$

This last case is not important in the low–friction limit because the crossings through the Landau–Zener region are not ballistic.

(2) If the friction is very low, the system does not lose enough energy after leaving the transition state to avoid recrossing it. The number of forward crossings in this case was estimated by Kramer

$$N_{crosses} - 1 \sim \frac{\text{time to lose } kT}{\text{time traverse the well}} \sim \frac{2\Omega}{\gamma}\sqrt{\frac{kT}{E_f}} \quad , \qquad (II.17b)$$

where E_f is the activation barrier.

Therefore, similar to the overdamped case, the condition for non–adiabaticity is expected to be about $\hbar/T_{DA} \gg N_{crosses}\, t_{LZ}$. In the limit that we can consider the crosses to be uncorrelated, i.e., $N_{crosses}$ of order unity, and the crossing is ballistic, the condition above is very similar to the one given by Eq. 3.11 of Sec. II.2.

All of the discussion presented here for the underdamped case is based on some qualitative arguments. As can be seen in Secs. II.2, II.3 and II.4, when the nuclear coordinate is classical, we can write the Fokker–Planck equation associated with the problem. How to solve this equation in the overdamped regime is presented in Sec. II.2. In order to quantify and obtain a clear understanding of the conditions described above for the underdamped case, we intend, in the future, to solve the Fokker–Planck equation in this limit. Because the differential equation in this limit is much more complicated, we are still not sure whether an analytical solution will be possible.

For completeness, we conclude this subsection, pointing out that the conditions for the validity of the non–adiabatic rate in the limit of weak coupling to the bath (Eqs. II.6 and II.7) are presented in Appendix B of Sec. II.3. Recall that by weak coupling we mean that mixing between the energy levels of the reaction coordinate is "small." In this case quantum effects are important, and to calculate the transition from the non–adiabatic to the adiabatic problem is a very complex problem, which we do not intend to address in this thesis, although it deserves more careful attention in the future.

Separation of Fast and Slow Modes

All of the previous discussion assumes that the cutoff frequency, Λ (see Eq. II.3), is the fastest frequency of the problem. We now consider the possibility of a a fast mode (here associated with the coordinate y) whose motion is much faster than Λ. We also consider a "slow" mode, z, coupled to the problem, which satisfies the conditions described in Eq. II.3, i.e., much slower

than Λ. For simplicity, the z mode is considered strongly coupled to the bath. Although this is not a necessary assumption for the formalism, it is a good one for the slow modes of interest discussed at the end of this subsection. In this subsection, we describe how the dynamics of these two modes can be separated. This point is carefully addressed in Secs. II.3 and II.4.

Assuming that $\hbar\Omega_y \gg kT$, the energy fluctuations of the z mode are much smaller than the spacing of the y energy levels. Therefore, because the fast mode y is the fastest frequency associated with the problem, its effect can be separated by "renormalizing" the electronic matrix element. The forward rate for the electron transfer can be written as a sum of several two–level system problems coupled to one nuclear mode z. The renormalized matrix elements and driving forces are

$$T_{DA}^{eff} \;=\; T_{DA} < n_D^y = 0 | m_A^y > \;\;, \qquad (II.18a)$$

where n_D^y (m_A^y) are the vibrational states of the y mode when the electron is on the donor (acceptor), and

$$\varepsilon^y(m_A^y) \;=\; \varepsilon \;-\; m_A^y \hbar\Omega_y \;\;. \qquad (II.18b)$$

In Sec. II.4 we calculate the non–adiabatic rate in general, and the adiabatic rate when z is overdamped. We do not write the rates in this section but they are basically a sum of rates given by Eq. II.9 summed over all values of m_A^y.

This description, in which we separate the influence of fast modes from that of the slow modes, is useful for describing electron transfer coupled to both fast modes (such as CO vibrations) and to "slow," sometimes diffusive, modes (such as solvent polarization or gross protein motions). After separating the fast "quantum" modes, the slow modes left in the problem can normally

be treated in the strong coupling limit, and therefore the entire formalism developed for strong coupling can be applied. Applications of this model to calculate electron transfer between quinones and oxidized bacteriochlorophyll dimer, and between rigidly linked porphyrin and quinone systems are discussed in Sec. II.4. The second case is discussed in more detail in Chapter IV.

In the case that the z mode is diffusive, the condition for adiabaticity is different for each term of the sum because *each has a different* T_{DA}^{eff}. The forward rate can be written as

$$\Gamma^f = \sum_{m_A} \frac{2\pi}{\hbar} \left(T_{DA}^{eff}(m_A)\right)^2 \left(\frac{1}{4\pi E_R^z kT}\right)^{1/2}$$

$$\times \left[\frac{1}{1+\left(2\pi \left(T_{DA}^{eff}(m_A)\right)^2 / \hbar\omega_c^z E_R^z\right)}\right] \exp - \left\{\frac{(\varepsilon^y(m_A) - E_R^z)^2}{4kTE_R^z}\right\} \quad . \quad (II.19)$$

Notice that in the adiabatic limit the rate becomes independent of T_{DA}^{eff}, and is basically ε independent for large driving forces. This is discussed in Sec. II.4, and this model was applied to understand intramolecular electron transfers in 6–(4–methylphenyl)amino–2–naphthalenesulfon–N,N–dimethylamide(TNS-DMA) and 1–cyano–4–dimethyl–aminobenzene (DMAB).[4]

The Fokker–Planck equation

Here we discuss how, beginning with Hamiltonian II.1, we obtain a differential equation of motion – a Fokker–Planck equation – for the reduced density matrix of the electron plus the reaction coordinate. This conversion can not always be performed. It can be done if $kT/\hbar$ is much larger than the charac-

teristic frequency of the reaction coordinate ($\sqrt{\Omega^2 - \gamma^2}$ in the underdamped case and ω_c in the overdamped one).

Suppose that at some time, t_0, the total density matrix of the system can be factored into one part for the bath alone (which we shall take to be at a temperature T), and a part for the electron plus the reaction coordinate. The reduced density matrix $\rho_{\sigma\lambda}(x,y;t_0)$ for the electron and reaction coordinate at a later time t is (see Sec. II.2)

$$\rho_{\sigma\lambda}(x,y;t) \;=\; \sum_{\sigma',\lambda'} \int_{-\infty}^{\infty}\int_{-\infty}^{\infty} dx'\; dy'\; \hat{J}_{\sigma\lambda,\sigma'\lambda'}(x,y;t:x',y';t_0)\; \rho_{\sigma'\lambda'}(x',y';t_0)\;, \tag{II.20a}$$

where

$$\hat{J} \;=\; \int_{\sigma'}^{\sigma} \mathcal{D}\sigma \int_{\lambda'}^{\lambda} \mathcal{D}\lambda \int_{x'}^{x} \mathcal{D}x \int_{y'}^{y} \mathcal{D}y \Big[\; A[\sigma]A^*[\lambda]$$

$$\times exp\frac{i}{\hbar}\Big\{S_{r+e}[x,\sigma] - S_{r+e}[y,\lambda]\Big\}\;\Big]\;.\;\mathcal{F}[x,y]\;. \tag{II.20b}$$

The limits on the functional integration signs indicate the boundary conditions that the trajectories must satisfy; e.g., $\sigma(t_0) = \sigma'$, $\sigma(t) = \sigma$. The quantity $A[\sigma]$ is the bare amplitude associated with a spin trajectory $\sigma(\tau)$, as defined in Sec. II.2, and $S_{r+e}[y,\lambda]$ is the classical action for the reaction coordinate to follow a trajectory $y(\tau)$, given that the electron trajectory is $\lambda(\tau)$, ignoring the coupling to the bath. Performing the calculation as described in Sec. II.2 we get

$$\frac{\partial\rho}{\partial t} \;=\; \frac{i\hbar}{2M}\Big(\frac{\partial^2\rho}{\partial x^2} - \frac{\partial^2\rho}{\partial y^2}\Big) - \frac{i}{\hbar}(U(x) - U(y))\rho - \frac{i}{\hbar}[H_\sigma,\rho]$$

$$-\frac{i}{\hbar}\Big(\sigma_z f(x)\rho - \rho\sigma_z f(y)\Big) - \gamma(x-y)\Big(\frac{\partial\rho}{\partial x} - \frac{\partial\rho}{\partial y}\Big) - \frac{\eta kT}{\hbar^2}(x-y)^2\rho\;. \tag{II.21}$$

After performing a Wigner transform on this equation, it can be written in the

well–known momentum–position representation

$$\frac{\partial W}{\partial t} = -\frac{1}{M}\frac{\partial}{\partial y}(pW) + \frac{\partial}{\partial p}(U'(y)W) + 2\gamma\frac{\partial}{\partial p}(pW) + \eta kT\frac{\partial^2}{\partial p^2}W$$

$$+ \frac{1}{2}\frac{df}{dy}\frac{\partial}{\partial p}\{\sigma_z, W\} - \frac{i}{\hbar}[H_\sigma + \sigma_z f(y), W] \ , \qquad (II.22)$$

where the commutators and anticommutators now involve only the spin degrees of freedom, and

$$W_{\alpha,\beta}(y,p) = \frac{1}{2\pi\hbar}\int_{-\infty}^{\infty} \exp(ipu/\hbar)\ \rho_{\alpha\beta}\left(y - \frac{u}{2}, y + \frac{u}{2}\right)\ du \ . \qquad (II.23)$$

The solution of this equation for the overdamped case is shown in Sec. II.2, and it gives a rate very similar to the one given by Eq. II.11. As previously discussed in this section, the solution of the underdamped limit is especially relevant to the question of adiabaticity, but we have not yet been able to solve it analytically. Also, Eqs. II.21 and II.22 assume only one reaction coordinate. In Sec. II.4, we solved the case for two reaction coordinates and showed when the models of Agmon and Hopfield[5] or of Sumi and Marcus[6] are valid. The case of two reaction coordinates is discussed in more detail in the following subsection.

To conclude, we notice that much will have been gained if it is possible to reduce these problems to Fokker–Planck equations, since the latter can be solved numerically. More important, this is a clear way to understand how the microscopic quantum mechanical model can be related to "macroscopic" models for electron transfer.

Exponential or Non-Exponential Time Decay

for Donor Survival Probability

So far we have calculated electron transfer rates, which means that the donor survival probability decays exponentially with time as can be seen from Eqs. II.8 and II.9. Assume now that we have an electron transfer problem, which after we renormalize the effect of all fast vibrations, is still coupled to several "slow" modes. For the point we want to make, two coordinates are sufficient. Here we discuss two possibilities. The first possibility is that the slow mode is coupled to σ_z (as the reaction coordinate described until now), and therefore modulates the activation barrier. The second possibility is that the slow mode is coupled to σ_x, and it modulates the electronic matrix element. These two possibilities are carefully discussed in Sec. II.4.

In the first case we assume the following Hamiltonian

$$H_{ET} = T_{DA}\,\sigma_x + \frac{P_y^2}{2M_y} + \frac{1}{2}M_y\Omega_y^2(y + y_0\sigma_z)^2 + \frac{\varepsilon}{2}\sigma_z$$

$$+\frac{P_z^2}{2M_z} + \frac{1}{2}M_z\Omega_z^2(z + z_0\sigma_z)^2 + \frac{1}{2}\sum_\alpha\left[\frac{p_\alpha^2}{m_\alpha} + m_\alpha\omega_\alpha^2\left(x_\alpha + \frac{c_\alpha y}{m_\alpha\omega_\alpha^2}\right)^2\right]$$

$$+\frac{1}{2}\sum_\beta\left[\frac{p_\beta^2}{m_\beta} + m_\beta\omega_\beta^2\left(x_\beta + \frac{c_\beta z}{m_\beta\omega_\beta^2}\right)^2\right] \quad , \qquad (II.24)$$

where y and z can be treated in the strong coupling limit. We also assume ohmic forms of the spectral density for both coordinates

$$J_0^{y,z} = \eta_{y,z}\omega\ \exp(-\omega/\Lambda), \quad \text{and} \quad \gamma_{y,z} = \eta_{y,z}/2M_{y,z}\ . \qquad (II.25)$$

Λ is the cutoff frequency, which was discussed earlier.

In Sec. II.4 we solve this problem in two limits. In the first one both coordinates relax much faster than the electron transfer rate, and the donor survival probability decays exponentially in time. In the second limit the z coordinate moves much slower than the electron transfer, so the donor suvival probability is non-exponential in time. As an example, in this subsection we summarize the results only for the overdamped case, because it is the only one for which we can analytically connect the non–adiabatic and the adiabatic limits.

In the first limit, the donor survival probability is exponential in time, and the electron transfer rates rates are

$$\Gamma^{f;r} = \frac{2\pi}{\hbar} T_{DA}^2 \left[\frac{1}{4\pi(E_R^y + E_R^z)kT} \right]^{1/2} \times \left\{ \frac{1}{1 + \left[2\pi T_{DA}^2 / \hbar(\omega_c^y E_R^y + \omega_c^z E_R^z) \right]} \right\} \exp\left\{ -\frac{E_{f;r}}{kT} \right\} \quad , \qquad (II.26a)$$

where

$$E_{f;r} = \frac{\left[\varepsilon \mp (E_R^y + E_R^z) \right]^2}{4kT(E_R^y + E_R^z)} \quad . \qquad (II.26b)$$

As before, we define the adiabaticity parameter $\bar{g}$,

$$\bar{g} = \frac{2\pi T_{DA}^2}{\hbar\omega_c^y E_R^y + \hbar\omega_c^z E_R^z} \quad , \qquad (II.27)$$

which can be written as

$$\frac{1}{\bar{g}} = \frac{1}{g_y} + \frac{1}{g_z} \quad , \qquad (II.28)$$

where g_y and g_z are the adiabaticity parameters for the y and z modes, respectively.

If $\bar{g} \ll 1$, the non–adiabatic limit is valid, and the above rates can be written as the following integral

$$\Gamma_{na}^{f;r} = \int_{-\infty}^{\infty} k_{y,na}^{f;r}(z) P_{eq}^{+,-}(z)\, dz \quad , \qquad (II.29)$$

where $k^{f;r}_{y,na}(z)$ are the forward and reverse rates when the system is frozen at a particular value of z, and $P^{+,-}_{eq}(z)$ are the equilibrium distributions of z when the electron is on the donor (+) or the acceptor (−), respectively. $k^{f;r}_{y,na}(z)$ is calculated exactly as in the one mode case, but using a z dependent driving force, $\varepsilon^y(z) = \varepsilon + 2M_z\Omega_z^2 z_0 z$. This expression is basically the result obtained by Agmon and Hopfield[5] or Sumi and Marcus[6] when the transfer is exponential in time. The final rate is the rate in the y direction averaged over the z coordinate. If the non–adiabatic limit is not valid, we can use Eq. II.29 to calculate the rate only if $g_y \ll g_z$. This means that every crossing through the Landau–Zener region is basically in the y direction or that Eq. II.29 is not valid. The reason why the non–adiabatic limit can be calculated, using Eq. II.29, independent of the y and z modes chosen, is that the dynamics of the nuclear coordinates are not important when this limit is valid ($\bar{g} \ll 1$ anyway).

In the second limit we can calculate the electron transfer expectation value $P(t)$ ($< \sigma_z(t) >$), and we get (assuming that we have an equilibrium distribution for z when the electron is on the donor)

$$P(t) = \int_{-\infty}^{\infty} dz \left[P^y_\infty(z) + \Big(1 - P^y_\infty(z)\Big) \exp\big(-k_y(z)t\big) \right] \times P^+_{eq}(z) \quad , \quad (II.30a)$$

where

$$k_y(z) = k^f_y(z) + k^r_y(z) \quad . \qquad (II.30b)$$

Here $P^y_\infty(z)$ and k_y are, respectively, the equilibrium value for $< \sigma_z >$ and the electron transfer rate when we freeze the system at a particular z value. Current work in Hoffman's group involves looking for this non–exponential behavior in electron transfer between heme groups in Zn modified hemoglobin at low temperatures.[7]

In this second limit, the formalism presented by Agmon and Hopfield or Sumi and Marcus works without any difficulties because the z coordinate is much slower than y, and therefore every crossing through the Landau–Zener region is basically in the y direction. It is also important to point out that because $\varepsilon^y(z)$ appears only on the exponent of the rate expression, the non–exponential behavior is the same for the adiabatic and non–adiabatic limits.

Also in Sec. II.4, we develop the Fokker–Planck equation associated with this two–mode problem, and with this formalism we show which approximations have to be made to obtain the diffusion equation used by Agmon and Hopfield. This is a particular limit of a more general equation developed there.

To conclude this subsection, we discuss the case in which the slow mode is coupled to σ_x, and this coupling is not necessarily linear in this slow coordinate (anharmonic coupling is allowed). As an example, we apply this formalism to electron transfer in the porphyrin–bridge–quinone molecule.[8] This problem is more carefully described in Sec. II.4. Figure II.2 shows the structure of this molecule. Because we are interested in the problem of exponential versus non–exponential decay in time, we wrote the simplest Hamiltonian to describe this effect, and therefore the matrix element is assumed to be renormalized by the fast mode(s), and we consider only one mode coupled to σ_z. The slow mode here is the rotation of the dihedral angle between the porphyrin and the quinone, θ, because the electronic matrix element depends on relative orientation of the two molecules. Thus, the simplest Hamiltonian that can be written is

$$H_{ET} = \frac{\hbar\Delta_0(\theta)}{2}\sigma_x + \frac{\varepsilon}{2}\sigma_z + \frac{P_x^2}{2M_x} + V_x(x) + \sigma_z f(x) + Bath_x + \frac{P_\theta^2}{2M_\theta} + U_\theta(\theta) + Bath_\theta \quad . \qquad (II.31)$$

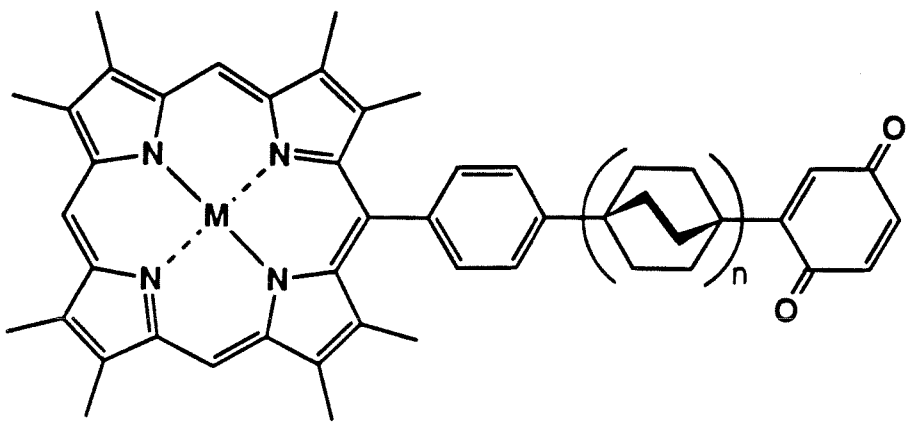

Figure II.2 – Structure of the molecule Porphyrin–Phenyl–(Bicyclo[2.2.2]octane)$_n$–Quinone. $n = 0, 1, 2$. M is a metal, normally Zn.

Here V_x and U_θ are the potentials associated with x and θ. $f(x)$ is the coupling of coordinate x to the z component of the spin.

In the limit that x is diffusive and θ is very slow, and considering $V_x(x) = M_x\Omega_x^2(x^2 + x_0^2)/2$ and $f(x) = M_x\Omega_x^2 x_0 x$, we obtain

$$\frac{\partial}{\partial t}\bar{n}_{11}(\theta,t) = D_\theta\frac{\partial^2}{\partial\theta^2}\bar{n}_{11}+\frac{\partial}{\partial\theta}\left(\frac{U'_\theta(\theta)}{\eta_z}\bar{n}_{11}\right)-k_x^f(\theta)\bar{n}_{11}+k_x^r(\theta)\bar{n}_{22} \ , \quad (II.32a)$$

$$\frac{\partial}{\partial t}\bar{n}_{22}(\theta,t) = D_\theta\frac{\partial^2}{\partial\theta^2}\bar{n}_{22}+\frac{\partial}{\partial\theta}\left(\frac{U'_\theta(\theta)}{\eta_z}\bar{n}_{22}\right)+k_x^f(\theta)\bar{n}_{11}-k_x^r(\theta)\bar{n}_{22} \ , \quad (II.32b)$$

where

$$k_x^{f;r} = \frac{\Delta_0^2(\theta)}{4}\left(\frac{\pi\hbar^2}{E_R^x kT}\right)^{1/2}\left[\frac{1}{1+g'}\right]\exp\left\{-\frac{(\varepsilon\mp E_R^x)^2}{4kTE_R^x}\right\} \ , \quad (II.33a)$$

and

$$g' = \frac{\Delta_0^2(\theta)\pi\hbar}{2E_R^x\omega_c^x}\left(\frac{x_0}{|x^*+x_0|}+\frac{x_0}{|x^*-x_0|}\right) \ . \quad (II.33b)$$

Here x^* is the crossing point for the donor and acceptor curves. (See Sec. II.4 for details.)

Solutions to Eqs. II.32 are straightforward when the transfer rate is much slower or much faster than the θ coordinate. In the first case,

$$P(t) = P_\infty + (1-P_\infty)\exp\left[-(\Gamma^f+\Gamma^r)t\right] \ , \quad (II.34a)$$

where

$$\Gamma^{f;r} = \int_0^{2\pi} k_x^{f;r}(\theta)\ P_{eq}(\theta)\ d\theta \ . \quad (II.34b)$$

In the second case,

$$P(t) = \int_0^{2\pi} d\theta\left[P_\infty+\left(1-P_\infty\right)\exp\left\{-\left(k_x^f(\theta)+k_x^r(\theta)\right)t\right\}\right]\times P_{eq}(\theta) \ . \quad (II.35)$$

When the transfer is adiabatic, the rates $k_x^{f,r}$ become independent of Δ_0, and therefore of θ. In this limit Eqs. II.34 and II.35 are exactly the same, and the decay is exponential in time.

We now discuss a result that, although very simple, is useful to illustrate the difference between a slow mode coupled to σ_z and a slow mode coupled to σ_x. If the slow mode is coupled to σ_x, it modulates only the matrix element. Therefore, in the adiabatic limit, the rate is not modulated by the slow coordinate. Then, in this limit, the donor survival probability always decays exponentially in time. This is not true when the slow mode is coupled to σ_z. Thus, the non–exponential behavior at low temperatures for the electron transfer in the porphyrin–bridge–quinone with one linker group[8] (see Figure II.2 with n=1) shows us that the rate is probably not adiabatic, because it appears to depend on the slow coordinate, θ. An interesting problem to pursue now is to try to obtain the potential U_θ. Whether this potential has only one or many minima may lead to different dynamics at low temperature. For example, if this potential has two minima, non–exponentiality appears when the barrier between the two minima becomes larger than kT. Non–exponentiality exists independent of the dynamics of the slow mode. If there is only one minimum, non–exponentiality is due to a dynamical effect; i.e., it appears only when the electron transfer rate is much faster than the slow coordinate.

The Spectral Density

Looking at the spectral density function, $J_{eff}(\omega)$, given by Eq. II.5, we see that it is directly proportional to the imaginary part of the dynamic sus-

ceptibility of a damped harmonic oscillator with undamped frequency Ω and friction coefficient η; i.e.,

$$J_{eff}(\omega) = M^2\Omega^4 y_0^2 \chi''(\omega) \quad . \qquad (II.36)$$

This spectral density was generalized for several reaction coordinates in Secs. II.3 and II.4. Thus, these spectral densities describe particular ways that the environment affects the transferring electron. Therefore, when treating real systems, we need the response function (susceptibility) of the medium modes because of the electron transfer. The most interesting part of that is that the spectral density permits an understanding of how the microscopic Hamiltonian is related to macroscopic parameters.

As a warning (discussed in Secs. II.2 and II.3), if there are medium degrees of freedom that are strongly excited, this linear treatment of the environmental modes breaks down and anharmonic corrections are necessary. However, in several problems, after the fast local modes are separated in the way described in this section, all we need is the response function of the "slow" medium modes.

The Born–Oppenheimer and Condon Approximations

In the standard treatment of non–adiabatic electron transfer, the Born–Oppenheimer approximation is used to calculate the donor and acceptor wave functions, and on top of that the Condon approximation is applied to calculate the matrix element, T_{DA}. After performing these approximations, the electron transfer Hamiltonian is of the form of Eq. II.1 (when we have only one nuclear mode, but generalization is straightforward). Here we discuss the validity of

such approximations for the case of a model Hamiltonian where the electron tunnels through a chain of identical orbitals. In this subsection we describe two examples; in the first one we have only one mode coupled to the donor or acceptor, and in the second there is one mode coupled to the donor and one to the acceptor. Details of this subsection are presented in Sec. II.3.

We work in the non-adiabatic weak coupling to the bath limit. For the fast quantum modes, for which we expect that the Born–Oppenheimer and Condon approximations breakdown may occur, this weak coupling limit is applicable (see Sec. IV of Sec. II.3). Without including the bath, the Hamiltonian is

$$H_{ET} = H^e + H^{n-e} + H^n, \qquad (II.37)$$

where e is electron and n, nuclei. Here we present models for each part of Eq. II.37 and solve the following equations for the localized states:

$$H_{D,\,M}\Psi_D(\vec{x}, R_1, \ldots, R_{N_{RC}}) = \{T_{\vec{r}} + V_D + V_M + H^n\}\,\Psi_D = E\Psi_D \quad (II.38a)$$

$$H_{A,\,M}\Psi_A(\vec{x}, R_1, \ldots, R_{N_{RC}}) = \{T_{\vec{r}} + V_A + V_M + H^n\}\,\Psi_A = E\Psi_A\,, \quad (II.38b)$$

where D, M, and A are the donor, medium, and acceptor respectively, and R_i is the i^{th} reaction coordinate.

Recall that, in the weak coupling limit, the energy broadening due to the bath guarantees non-adiabaticity but is not strong enough so that the vibronic levels are mixed. In this case, the forward transfer rate from a single donor state is (see Eqs. II.6 and II.7)

$$\Gamma^f_{na} = \frac{2\pi}{\hbar}\sum_F |< \Psi_D \mid V_A \mid \Psi^F_A >|^2\, h(E_D - E^F_A) \qquad (II.39a)$$

$$\Gamma^f_{na} \stackrel{\text{def}}{=} \frac{2\pi}{\hbar}\,|\sum_F H^F_{DA}|^2 h(E_D - E^F_A)\ . \qquad (II.39b)$$

Applying the Born-Oppenheimer and Condon approximations to the sum of matrix elements gives

$$\sum_F | < \Psi_D(\vec{x}, R_1 \ldots R_{N_{RC}}) \mid V_A \mid \Psi_A^F(\vec{x}, R_1 \ldots R_{N_{RC}}) > |^2 h(E_D - E_A^F)$$

$$\simeq T_{DA}^2 \quad \sum_F | < \phi_D(R_1 \ldots R_{N_{RC}}) \mid \phi_A^F(R_1 \ldots R_{N_{RC}}) > |^2 h(E_D - E_A^F). \tag{II.40}$$

First, we consider one nuclear mode linearly coupled to a single bound electron (donor state, for example). The electronic Hamiltonian we use in this subsection is described in Figure II.3. For this electronic Hamiltonian we have

$$H^e_{D,\,M} = \Delta_D a_D^\dagger a_D + \beta_D(a_0^\dagger a_D + a_D^\dagger a_0) + \sum_n \beta(a_n^\dagger a_{n+1} + a_n^\dagger a_{n-1}) \quad (II.41a)$$

$$H^e_{A,\,M} = \Delta_A a_A^\dagger a_A + \beta_A(a_N^\dagger a_A + a_A^\dagger a_N) + \sum_n \beta(a_n^\dagger a_{n+1} + a_n^\dagger a_{n-1}). \quad (II.41b)$$

Δ_D and Δ_A are negative and are the binding energies of the isolated donor and acceptor relative to the energy of an isolated bridge orbital. The fermion operators create ($\dagger$) or annihilate an electron on a donor($\theta_D(\vec{r})$), acceptor ($\theta_A(\vec{r})$), or bridge site orbital ($\theta_n(\vec{r}-n\vec{a})$, $n = 0, \pm 1, \pm 2, \ldots$). $\beta_{D(A)}$ is the donor (acceptor) interaction ($< \theta_{D(A)}(\vec{r})|H|\theta_{0(N)}(\vec{r}) >$) with the nearest bridge orbital. This electronic Hamiltonian is the simplest possible one we can consider for through–bond electron transfer. The importance of through–bond pathways for electron transfer is discussed in the next chapter.

The Hamiltonian for the one vibrational mode coupled to the donor is

$$H^n + H^{n-e} = (b^\dagger b + \frac{1}{2})\hbar\Omega - \lambda(b^\dagger + b)a_D^\dagger a_D \quad . \tag{II.42}$$

The boson operators create ($b^\dagger$) or annihilate (b) a vibration on the oscillator and $(b^\dagger + b) = \sqrt{2M\Omega/\hbar}\; y$.

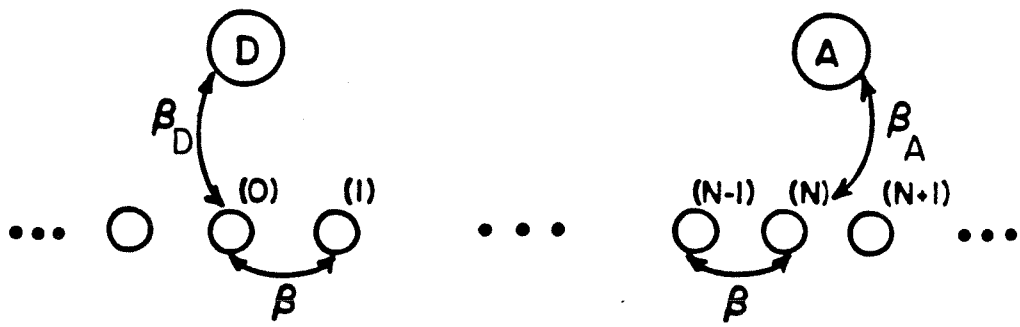

Figure II.3 – Arrangement of the donor, acceptor, and bridging orbitals for Hamiltonian II.41.

As described in Sec. II.3, the donor wave function is

$$\Psi^D(\vec{r},y)=\sum_j\left\{g_j\phi_j(y)\left[\theta_D(\vec{r})+\frac{\beta_D}{\sqrt{E_j^2-4\beta^2}}\sum_n\epsilon_j^{|n|}\theta_n(\vec{r}-n\vec{a})\right]\right\}, \quad (II.43)$$

where

$$\epsilon_j+\frac{1}{\epsilon_j}=\frac{E_j}{\beta}, \quad (II.44a)$$

$$E_j=E^{total}-(j+1/2)\hbar\Omega, \quad (II.44b)$$

and

$$g_j\left[\Delta_D-\frac{\beta_D^2}{\sqrt{E_j^2-4\beta^2}}-E_j\right]-\lambda(g_{j+1}\sqrt{j+1}+g_{j-1}\sqrt{j})=0\ . \quad (II.45)$$

$\phi_j(y)$ solves the nuclear Schrödinger equation (Eq. II.42) in the absence of the electron (harmonic oscillator with origin $y=0$). In the Born–Oppenheimer approximation

$$\Psi^D_{B.O.}(\vec{r},y)=\sum_j\left\{g_j\phi_j(y)\right.$$

$$\left.\times\left[\theta_D(\vec{r})+\frac{\beta_D}{\sqrt{(\Delta_D-\lambda' y)^2-4\beta^2}}\sum_n\epsilon(y)^{|n|}\theta_n(\vec{r}-n\vec{a})\right]\right\}\ , \quad (II.46)$$

where

$$\epsilon(y)+\frac{1}{\epsilon(y)}=\frac{E^e(y)}{\beta}\ , \quad (II.47)$$

and $\lambda'=\lambda(2M\Omega/\hbar)^{1/2}$. The Born-Oppenheimer wave function is qualitatively wrong because it assumes an electronic decay for each possible value of the nuclear coordinate.

For simplicity we consider the $T=0$ case. Because the bridge orbitals are orthogonal, and the driving force of the reaction must be left on the single donor

oscillator (for energy conservation), just one matrix element H_{DA} contributes to the rate:

$$H_{DA} = \beta_A \frac{\beta_D}{\sqrt{E_j^2 - 4\beta^2}} \epsilon_j^N g_j. \qquad (II.48a)$$

Now, if $4\beta^2 \ll E_j^2$ and g_j can be expanded as described in Appendix C of Sec. II.3, the equation above becomes

$$H_{DA} \simeq \frac{\beta_D \beta_A}{\beta} \left[\frac{e^{-\gamma}\gamma^j}{j!}\right]^{1/2} \left[\frac{\beta}{\Delta_D - \lambda^2/\hbar\Omega - j\hbar\Omega}\right]^{N+1}, \qquad (II.49a)$$

where

$$\gamma = (E_R/\hbar\Omega) = (\lambda/\hbar\Omega)^2, \qquad (4.28)$$

$$\epsilon_j \simeq \beta/E_j \ . \qquad (II.49b)$$

In the Born–Oppenheimer/Condon limit

$$H_{DA}^{Condon} \simeq \frac{\beta_D \beta_A}{\beta} \left(\frac{\beta}{\Delta_D - \lambda' \bar{y}(j)}\right)^{N+1} \left(\frac{e^{-\gamma}\gamma^j}{j!}\right)^{1/2}. \qquad (II.50)$$

$\bar{y}$ is the chosen value of y in the tunneling matrix element. There is an ε (reorganization energy) dependence in the so–called "electronic" matrix element as was found in the exact solution because the choice of $\bar{y}$ is ε dependent. Condon breakdown arises when *more than one* matrix element enters the rate expression at *fixed* ε (as we discuss next in this subsection) *or* when $\beta/E(y)$ varies rapidly in the range of y, which maximizes the product of nuclear functions for different ε. For a fixed value of ε, the Born–Oppenheimer Condon result becomes the exact result for the choice $\bar{y} = (\Delta_D - \Delta_A)/\lambda'$. This $\bar{y}$ is the value at the crossing point of the surfaces.

The interpretation of this result is simple but important. With coupling on the donor, the exact donor wave fuction includes admixtures of many ϵ_j's.

However, the acceptor can only access the portion of the wave function that propagates, leaving $\epsilon/\hbar\Omega$ vibrations on the donor. This particular part of the wave function decays as $(\beta/\Delta_A)^N$. The Born-Oppeheimer/Condon approximations match the exact result in this limit because energy conservation forces the decay to the correct value. More profound problems with these approximations arise when there is coupling on both the donor *and* acceptor sites.

In the case of one nuclear mode on both donor and acceptor, the situation is different. Here we assume the simplest situation, same frequency and same coupling. The exact result becomes

$$\sum_F | < \Psi_D | H' | \Psi_A^F > |^2 =$$

$$\left(\frac{\beta_A \beta_D}{\beta}\right)^2 \sum_{j=0}^{M} \left[\epsilon_j^{N+1} \left(\frac{e^{-\gamma}\gamma^j}{j!}\right)^{1/2} \left(\frac{e^{-\gamma}\gamma^{M-j}}{(M-j)!}\right)^{1/2}\right]^2, \qquad (II.51a)$$

where $M = \epsilon/\hbar\Omega$ and

$$\epsilon_j = \frac{\beta}{\Delta_D - \lambda^2/\hbar\Omega - j\hbar\Omega} \quad . \qquad (II.51b)$$

In the Born-Oppenheimer/Condon approach, it becomes

$$\sum_F | < \Psi_D | H' | \Psi_A^F > |^2 \; = \; \left| \frac{\beta_A \beta_D}{\beta} \left(\frac{\beta}{\Delta - \lambda' \bar{y}^D}\right)^{N+1} \right|^2$$

$$\times \sum_j | < \phi_0(y^D) | \phi_j(y^D - 2y_0^D) > < \phi_0(y^A) | \phi_{M-j}(y^A - 2y_0^A) > |^2 \quad . \quad (II.52)$$

The minimum crossing of the two nuclear potential surfaces occurs at

$$y^D = \frac{\lambda'}{2k} + \frac{\Delta_A - \Delta_D}{2\lambda'} \quad . \qquad (II.53a)$$

The decay constant at this point is

$$\epsilon(\bar{y}) \simeq \frac{\beta}{(\Delta_D + \Delta_A)/2 - \lambda^2/\hbar\Omega} \quad . \qquad (II.53b)$$

The nuclear factor in the Condon expression is maximized when half of the vibrational excitation is left on the donor and half on the acceptor (because couplings were chosen equal), or $j\hbar\Omega = (\Delta_D - \Delta_A)/2$. ϵ_j^{exact} for this value of j, and this value only, is equal to the approximate value. Because many ϵ_j's enter the sum, as transfer distance increases, the large ϵ's (with smaller j's) may dominate, and the driving force dependence of the rate may vary with transfer distances. No choice of $\bar{y}$ gives the Born-Oppenheimer/Condon rate the proper distance dependence.

In summary, there are two kinds of errors in the Born-Oppenheimer/ Condon approach to the problem: (1) The incorrect functional form of the Born-Oppenheimer decay length. The true electronic decay is not modulated by the reaction coordinate position when the electron is on the bridge orbitals. It is sensitive only to the vibrational energy left behind. (2) The assumption that ϵ is ε independent (Condon approximation).

Analyzing Eqs. II.51 and II.53, we understand why the Born–Oppenheimer and Condon approximations "work" in most cases. The reason is that the energetic distance to the center of the band (Δ_D or Δ_A which are energies in order of 5 eV) is much larger than the nuclear energy fluctuations involved (reorganization energies are fractions of eV). In order to observe the breakdown of these approximations we need long distances, so that N is large in Eqs. II.51a and II.52. As discussed in Sec. II.3, that is exactly the case of the radiolysis–initiated electron transfer study in glassy MTHF by Miller, Beitz and Huddleston.[9] In their measurements they observed a shift in the peak of the rate vs. ΔG plot to larger exothermicity for longer distance transfer. In Sec. II.3 we discuss this result, and we show that such a behavior may be due

to Born–Oppenheimer/Condon breakdown.

The "Adiabatic" Rate in the Inverted Region

In the adiabatic limit, as can be seen from Eq. I.5 and Figure I.3, the nuclear motion occurs only on the lowest energy surface, and the electron transfer rate limiting step is the way in which the nuclear coordinate flips between the two minima. This approach works when we are in the "normal" region, but in the "inverted" region it would lead to no transfer. This is the point of discussion of this subsection and Sec. II.5.

In Sec. II.5, we solve Eq. II.1 in the extreme adiabatic limit (very large T_{DA}), and we get, using a semiclassical approximation

$$\Gamma^f = \frac{\hbar\tilde{\omega}^2}{T_{DA}} \sqrt{\frac{2\pi k T_{eff}}{E_f}} \exp\left\{-\frac{E_f}{kT_eff}\right\} \quad , \qquad (II.54)$$

where E_f is the forward activation energy, and $\tilde{\omega}$ is the effective frequency of the coordinate y. This expression is equal to Eq. II.9b at $T_{DA} \sim \alpha\hbar\tilde{\omega}$, with α of order unity for reasonable parameters values. This is exactly what we expect; the crossover from small T_{DA} to large T_{DA} occurs when the matrix element is comparable to the spacing $\hbar\tilde{\omega}$ between vibrational energy levels.

References – Section II.1

(1) R.P. Feynman and A.R. Hibbs, *Quantum Mechanics and Path Integrals*; McGraw–Hill: New York, 1965.

(2) A.O. Caldeira and A.J. Leggett (a) *Ann. Phys (N.Y.)* **149**, 374 (1983); (b) *Physica A* **121**, 587 (1983).

(3) H. Frauenfelder and P.G. Wolynes, *Science* **229**, 337 (1985).

(4) E.M. Kosower and D. Huppert, *Chem. Phys. Lett.* **96**, 433 (1983).

(5) N. Agmon and J.J. Hopfield, *J. Chem. Phys.* **78**, 6947 (1983).

(6) H. Sumi and R.A. Marcus, *J. Chem. Phys.* **84**, 4272 (1986).

(7) B.M Hoffman, personal communication.

(8) (a) A.D. Joran, B.A. Leland, G.G. Geller, J.J. Hopfield, and P.B. Dervan, *J. Am. Chem. Soc.* **106**, 6090 (1984); (b) B.A. Leland, A.D. Joran, Felker, P. , J.J. Hopfield, A.H. Zewail, and P.B. Dervan, *J. Phys. Chem.* **89**, 5571 (1985).

(9) J.R. Miller, J.V. Beitz, and R.K. Huddleston, *J. Am. Chem. Soc.* **106**, 5057 (1984).

II.2 Effect of Friction on Electron Transfer in Biomoleculecules

J. Chem. Phys. **83**, 4491 (1985)

Effect of friction on electron transfer in biomolecules

Anupam Garg[a)]
Department of Physics, University of Illinois at Urbana-Champaign, Urbana, Illinois 61801

José Nelson Onuchic[b)]
Division of Chemistry and Chemical Engineering,[c)] California Institute of Technology, Pasadena, California 91125

Vinay Ambegaokar[a)]
Laboratory of Atomic and Solid State Physics, Cornell University, Ithaca, New York 14853

(Received 16 April 1985; accepted 23 July 1985)

In biological and chemical electron transfer, a nuclear reaction coordinate is coupled to other nuclear and/or "solvent" coordinates. This coupling, or friction, if strong enough, may substantially slow down motion along the reaction coordinate, and thus vitiate the assumption of electron transfer being nonadiabatic with respect to the nuclei. Here, a simple, fully quantum mechanical model for electron transfer using a one mode treatment which incorporates this coupling is studied. Path integral methods are used to study the dependence of the reaction rate on friction, and the limits of the moderate and the high friction are analyzed in detail. The first limit will prevail if the reaction coordinate is, e.g., an underdamped nuclear vibration, whereas the second limit will prevail if it corresponds to a slow or diffusive degree of freedom. In the high-friction limit, the reaction rate is explicitly shown to vary between the nonadiabatic and adiabatic expressions as the tunneling matrix element and/or the friction are varied. Starting from a path integral expression for the time evolution of the reduced density matrix for the electron and reaction coordinate, a Fokker–Planck equation is obtained which reduces in the high-friction limit to a Smoluchowski equation similar to one solved by Zusman.

I. INTRODUCTION: THE ROLE OF FRICTION

The migration of an electron from one molecule to another, or between two localized sites in the same molecule is a very common phenomenon and plays a central role in important biological and chemical processes such as oxidative phosphorylation, photosynthesis, and oxy-reduction reactions.[1] Naturally, in all these processes, it is not merely one electron that changes its state; the nuclei in the molecule(s) along with the electrons that are tightly bound to them must also readjust. This important fact, has, of course, been realized by earlier workers.[2–7] References 2 to 7 vary in their treatment of the nuclear degrees of freedom, but they all share the view that whether or not the electron adiabatically follows the nuclei in the transfer process is a question of the size of the electronic tunneling matrix element. In many chemical processes the electronic state does readjust rapidly as the nuclei move, and the reaction is said to be *adiabatic*. In biological processes, however, the distance between the sites of electron localization can be as much as 15 Å, which leads to small tunneling matrix elements with experimental values in the range 10^{-3}–10^{-5} eV. The vibronic energies, in contrast, are typically of the order of 10^{-2} eV. This has led to the belief that since the change of state of the electron can take place on the time scales associated with nuclear motion, most biological electron transfer is *nonadiabatic*, i.e., the electronic matrix element determines the efficacy of the transfer.[8]

What has been omitted in this simple picture are the many other degrees of freedom corresponding to the other atoms of the molecule(s) and the solvent which is present in many cases (particularly those involving biomolecules). The frequencies associated with gross motions of proteins, relaxation of solvent polarization, and the motion of counterions, etc., can often be very small, even in comparison with the electronic tunneling frequency. (Reference 9 provides experimental evidence for slow modes in the context of adiabatic chemical electron transfer.) More importantly, even if it is possible to identify a single "reaction coordinate" (representing, e.g., the direction in the multidimensional coordinate space along which the potential energy barrier is lowest), this coordinate will, in general, be coupled to all the others. This coupling will, among other things, result in a transfer of energy from the reaction coordinate to the other coordinates, and give rise to what would classically be interpreted as dissipation or friction.

It is of course clear that some such energy removal mechanism must be present if an exothermic reaction is ever to take place. More interestingly, however, it can also affect the dynamics of the electron transfer itself. To see this let us assume for the moment that the temperature is high enough to permit us to think of the motion of the reaction coordinate classically. Let us associate with this coordinate, y, an *adiabatic* potential $V(y;+)$ or $V(y;-)$ depending on whether the electron is in the donor or acceptor site, respectively. (See Fig. 1.) (These potentials should be thought of in the same spirit as the potentials used to solve the vibronic eigenvalue problem in the Born–Oppenheimer approximation.) If we denote the tunneling matrix element by $(\hbar\Delta_0/2)$, it follows

[a)] Also Institute for Theoretical Physics, University of California, Santa Barbara, California 93106. This is also the present address of the first author.
[b)] On leave of absence from Instituto de Física e Química de São Carlos, Universidade de São Paulo, 13560, São Carlos, SP, Brazil.
[c)] Contribution No. 7233.

 0021-9606/85/214491-13$02.10

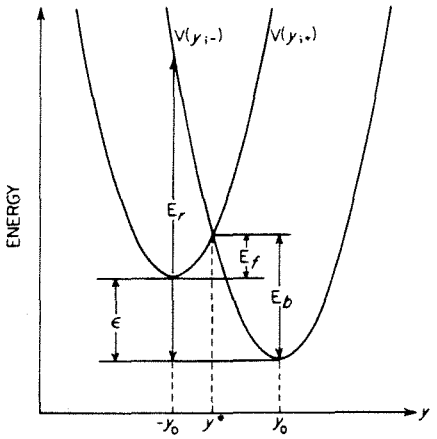

FIG. 1. Potential energy surfaces for the reaction coordinate when the electronic transition is forbidden (adiabatic potential wells). The labels + and − refer to the donor and acceptor sites, respectively. The energies E_f, E_b, and E_r are the forward and backward activation energies, and the reorganization energy, respectively.

that most of the tunneling can occur only within a length of order l_{LZ} of the crossing point y^*, where l_{LZ} is the so called *Landau–Zener length* [10]:

$$l_{LZ} = \hbar\Delta_0/|F_+ - F_-|, \tag{1.1}$$

where

$$F_\pm = -[\partial V(y;\pm)/\partial y]_{y=y^*}. \tag{1.2}$$

If the friction is low enough (but not too low–see Sec. III), and the temperature is high enough, then each transit of the reaction coordinate through the Landau–Zener region will appear ballistic, and the probability of tunneling will be small and calculable perturbatively in $\hbar\Delta_0$, leading to the standard picture of a nonadiabatic reaction. If, on the other hand, the friction is high enough (see Sec. IV), the motion of the reaction coordinate through the Landau–Zener region may appear diffusive rather than ballistic, and it may slow down to the point where the electronic change of state is once again rapid by comparison. The electron will then be able to make many transitions between the two states, and it is clear that in order to ascribe a definite state to it, we must study how the phase coherence between these states is lost. This can only come about because of the motion of the nuclei, and this suggests that the reaction rate in this limit will be similar to what one would get by assuming that the electron followed the nuclei adiabatically all the time, even though the vaule of $\hbar\Delta_0$ itself would have suggested that the reaction was nonadiabatic.[11]

Although there is as yet no evidence for biological electron transfer processes being coupled mainly to a diffusive nuclear coordinate, it is still worthwhile to study the effects on electron transfer of the coupling between the reaction coordinate and the remaining degrees of freedom for several reasons. The first is conceptual: The simplest pictures of adiabatic and nonadiabatic reactions are very different from each other, and it is interesting to see how they emerge from a unified treatment in which the relative time scales of the electron and the reaction coordinate can be continuously varied from the limit in which the electron is "slow" and the reaction coordinate "fast" to the opposite limit where the roles are reversed. Such a variation is most naturally brought about by the coupling studied in this paper since on *a priori* grounds alone it would seem to be present in reactions involving complex molecules. Secondly, even though the effects of this coupling would be most clearly evident in an adiabatic electron transfer, they are by no means absent in the nonadiabatic limit. (See Sec. III.) Finally, these considerations are not limited to electron transfer, and many of them apply to some other situations such as ligand binding to heme proteins.[11]

In this paper we present a simple but fully quantum mechanical model for electron transfer which incorporates friction in the sense of coupling together the nonelectronic degrees of freedom. For simplicity, we take the Hilbert space of the electron to consist of just those two states that are involved in the transfer. It is convenient to use the Pauli matrices for the operators in this space, and we shall often refer to the electron as a "spin." We shall employ a basis such that the reactant (electron in the donor site) and product (electron in the acceptor site) states are eigenstates of σ_z with eigenvalues + 1 and − 1, respectively. We further assume that the electronic degree of freedom is directly coupled to only one reaction coordinate y, which we shall sometimes call the "particle," and which in turn is coupled to the remaining nuclear and solvent degrees of freedom, hereafter referred to as the "bath" or "environment." As shown by Caldeira and Leggett,[12] provided the physical situation is such that none of the bath degrees of freedom are strongly excited, then *for the purposes of understanding the behavior of the nonenvironmental degrees of freedom*, it is possible to represent the bath by a collection of harmonic oscillators, and take the coupling to be linear in the oscillator coordinates. Thus, the Hamiltonian that we shall consider is[13,14]

$$H_{ET} = \frac{\hbar\Delta_0}{2}\sigma_x + \frac{1}{2M}P_y^2 + V(y;\sigma_z) + \sum_\alpha\left[\frac{p_\alpha^2}{2m_\alpha} + \tfrac{1}{2}m_\alpha\omega_\alpha^2\left\{x_\alpha + \frac{c_\alpha}{m_\alpha\omega_\alpha^2}y\right\}^2\right]. \tag{1.3}$$

Here, y and P_y are the reaction coordinate and the corresponding momentum, and $\{x_\alpha, p_\alpha\}$ are the coordinates and momenta of the bath oscillators. The quantities $V(y;\sigma_z = +1)$ and $V(y;\sigma_z = -1)$ are the adiabatic potential surfaces introduced earlier. Many of our results are true for fairly general choices of $V(y;\sigma_z)$, but we shall perform explicit calculations only for the special case

$$V(y;\sigma_z) = \tfrac{1}{2}M\Omega^2(y + y_0\sigma_z)^2 + \tfrac{1}{2}\epsilon\sigma_z. \tag{1.4}$$

We expect our results to be valid for more general potentials since experience with the problem of a particle diffusing over a one-dimensional barrier indicates that the reaction rate is sensitive only to gross features of the potential such as the barrier height, etc.[15,16] We shall, accordingly, cast our results, as far as possible, in terms of such quantities.

It might appear at first sight that we need to specify the masses m_α, frequencies ω_α, and coupling constants c_α, for

all the oscillators in order to completely specify the problem. This is however unnecessary because we are not interested in the detailed dynamical behavior of the bath oscillators. As shown in Ref. 12, the *reduced dynamics* of just the electron and the reaction coordinate are influenced by the bath only through the following combination of parameters known as the spectral density:

$$J_0(\omega) = \frac{\pi}{2}\sum_\alpha \frac{c_\alpha^2}{m_\alpha \omega_\alpha}\delta(\omega - \omega_\alpha). \tag{1.5}$$

The spectral density, in turn, can be determined provided one knows the semiclassical equation of motion satisfied by the particle. In particular, if, for fixed σ_z, the particle experiences a frictional force linearly proportional to its velocity with a coefficient η, that is if the equation of motion is

$$M\frac{d^2y}{dt^2} + \eta\frac{dy}{dt} + \frac{d}{dy}V(y;\sigma_z) = F_{\rm ext}, \tag{1.6}$$

where $F_{\rm ext}$ is any external force, then one can show that $J_0(\omega)$ is given by

$$J_0(\omega) = \eta\omega \exp(-\omega/\Lambda). \tag{1.7}$$

Here, Λ is a high frequency cutoff that is required on both physical and mathematical grounds, and that is much larger than the domain of frequencies over which Eq. (1.6) is a reasonable approximation to the exact equation of motion. We shall, in fact, take $J_0(\omega)$ to be given by Eq. (1.7). The main reason for doing this is that it leads to a well-characterized form of dissipation, and allows us to make contact with the conventional problem of diffusion over a one-dimensional barrier.[15,16]

It should be noted that if $J_0(\omega)$ is not given by Eq. (1.7), the classical equation of motion is no longer Eq. (1.6), and has to be generalized to have a frequency dependent friction coefficient.[17] In particular, it is no longer possible to define a simple friction coefficient or a diffusion constant. The question of what the correct spectral density for a given biomolecular reaction should be is open at this time, but we believe that many of the techniques of our paper should prove useful in any case.

We emphasize that the use of harmonic oscillators is *not* equivalent to expanding the full particle-plus-bath potential to second order in the displacements of the bath coordinates about their equilibrium values. Further, there is no limit to the overall strength of the dissipation that can be treated via such a prescription. The prescription will start to provide quantitatively inaccurate answers if in reality some of the bath degrees of freedom are strongly excited, but it represents, nevertheless, a first step in arriving at a comprehensive understanding of how friction affects electron transfer.

To summarize, our model consists of an electron (with a two-dimensional Hilbert space) that is directly coupled to a single nuclear coordinate. The latter is assumed to move on an adiabatic potential surface of the form (1.4) and is in turn coupled to an environment which we represent by a set of harmonic oscillators following Caldeira and Leggett.[12] The oscillators have a spectral density $J_0(\omega)$ of form (1.7), where η is a parameter that quantifies the strength of the coupling between the reaction coordinates and the environment, and which we shall regard as given. Our aim in this paper is to analyze as completely as possible the rate of electron transfer as a function of the tunneling matrix element Δ_0, the exothermicity ϵ, the parameters of the reaction coordinate potential, i.e., M, y_0, and Ω, and the friction coefficient η. We would like to obtain the conditions under which the reaction is adiabatic or nonadiabatic, and also to construct simple physical arguments for understanding these conditions, in particular the dependence on the friction coefficient η. As far as we know there is at present no information on what the spectral density for any particular reaction should be. Therefore, our emphasis in this paper shall be on understanding the conceptual issues associated with the introduction of friction into the problem, and on developing techniques which we think will be useful for dealing with generalizations that may be necessitated by future experimental and theoretical work on its nature and source.

The plan of our paper is as follows:

(1) In Sec. II we shall present a formally exact path integral expression for an inclusive probability that we interpret to be the probability that electron transfer has occured at a time t after some specified initial state for the system as a whole. Except for a trick that eliminates a large amount of tedious algebra, this section consists mainly of a recapitulation of formal results already in the literature, and the reader who is not interested in the details should note the definition of the inclusive probability [up to Eq. (2.3)], and proceed to the answer for it [Eqs. (2.14), (2.15), and (2.23) onward].

(2) In Sec. III, we shall show that it is possible to simplify this formal expression very considerably for moderate values of friction. We shall obtain an answer for the reaction rate [Eqs. (3.7) and (3.8)] that is quite similar in functional form to the one obtained by Hopfield[6] in its overall temperature dependence but differs in some details ($T_{\rm eff}$ is different). We shall see that the calculation itself provides an upper limit on the friction for this result to be valid, and we shall give some plausible arguments for what the lower limit should be. We shall then provide a very simple interpretation of our results.

(3) In Sec. IV we shall analyze the formal path integral expression in the limit of very high friction, and show that with some very plausible approximations it is possible to obtain a relatively simple expression for the reaction rate for all values of the tunneling amplitude $\hbar\Delta_0$. [See Eq. (4.18)]. As expected, we find that if the tunneling matrix element and/or the friction is large enough, the rate is independent of $\hbar\Delta_0$, and is very similar to the rate at which a particle diffuses over a one-dimensional barrier obtained by considering only the lower of the curves $V(y;+)$ and $V(y;-)$ for each value of y, whereas in the opposite limit it reduces to the nonadiabatic result of Sec. III. The important ratio turns out to be that of the time spent in the Landau–Zener region to the "tunneling time" Δ_0^{-1}.

(4) In order to understand the result of Sec. IV better, we show in Sec. V how to obtain a Fokker–Planck equation for the reduced system consisting of the electron and the reaction coordinate. This equation is valid over a wide range of values of temperature and friction, and should be useful for a detailed study of the crossover from the nonadiabatic to adiabatic regime. Rather than do this, we shall limit ourselves to the very high friction regime and convert the

Fokker–Planck equation into a Smoluchowski equation, which is identical (except for minor corrections) to a set of equations arrived at by Zusman through the use of a stochastic Liouville equation.[18]

(5) In Sec. VI we shall summarize Zusman's solution of this equation. The reaction rate thus obtained is almost but not quite the same as that of Sec. IV.

(6) We conclude this paper in Sec. VII with some remarks about the possible future extensions of our work.

II. PATH INTEGRAL CALCULATIONS OF INCLUSIVE PROBABILITY

In this section, we shall derive a formally exact expression for the conditional expectation value $P(t)$ defined as follows. Suppose that for $t<0$, the electron is held fixed in the donor site, or equivalently, that the spin is in the "up" state, and the reaction coordinate and the bath are in equilibrium with it. In other words, the entire system is described by the density matrix

$$\rho(t) = |+\rangle\langle +|\exp(-\beta H_0^+), \quad t<0, \tag{2.1}$$

where $\sigma_z|\pm\rangle = \pm|\pm\rangle$, $\beta \equiv (kT)^{-1}$, with T being the temperature, and

$$H_0^{\pm} = \frac{1}{2M}P_y^2 + V(y;\sigma_z = \pm 1) + H_{\text{bath}}, \tag{2.2}$$

where H_{bath} consists of all the terms in the sum in Eq. (1.3). The electron is let go at $t=0$, and the entire system is allowed to evolve according to the full Hamiltonian H_{ET}. We define $W(t)$ to be the probability that the spin will be found in the up state at a later time t, irrespective of the state of the reaction coordinate or the bath. The conditional expectation value $\langle\sigma_z(t)\rangle$, denoted $P(t)$, is then given by

$$P(t) = 2W(t) - 1. \tag{2.3}$$

We shall calculate $P(t)$ for the special choice (1.4) of the potential $V(y;\sigma_z)$, following the method of Chakravarty and Leggett,[19] and Leggett *et al.*,[20] which in turn is based on the Feynman–Vernon influence functional method.[21,22] Since the spin is coupled only to harmonic oscillators (bath as well as the reaction coordinate) it is clear that one can integrate out the oscillators. The only complication is that the spin is not directly coupled to all the oscillators, and although one can first eliminate the bath and then the reaction coordinate, it is simpler to proceed as follows.

Let us consider the purely quadratic part of the Hamiltonian (1.3) that is not coupled to the spin, and imagine diagonalizing it via a transformation to normal modes. Since y can be written as a linear combination of these normal modes, we can write the Hamiltonian H_{ET} as follows:

$$H_{ET} = \frac{\hbar\Delta_0}{2}\sigma_x + \tfrac{1}{2}\epsilon\sigma_z + y_0\sigma_z\sum_\alpha \tilde{c}_\alpha\tilde{x}_\alpha + \sum_\alpha\left[\frac{\tilde{p}_\alpha^2}{2\tilde{m}_\alpha} + \tfrac{1}{2}\tilde{m}_\alpha\tilde{\omega}_\alpha^2\tilde{x}_\alpha^2 + \frac{\tilde{c}_\alpha^2}{2\tilde{m}_\alpha\tilde{\omega}_\alpha^2}y_0^2\right], \tag{2.4}$$

where $\tilde{x}_\alpha$ are the normal coordinates, and $\tilde{p}_\alpha$, $\tilde{m}_\alpha$, and $\tilde{\omega}_\alpha$ are the corresponding canonical momenta, masses, and frequencies. The quantities $\tilde{c}_\alpha$ are proportional to the coefficients in the expansion of y in terms of $\tilde{x}_\alpha$'s.

Since H_{ET} now consists of a spin coupled to a set of mutually *noninteracting oscillators*, it follows from Refs. 21 and 22 that $P(t)$ is influenced by the oscillators only through a spectral density $J_{\text{eff}}(\omega)$ defined in exact analogy with Eq. (1.5):

$$J_{\text{eff}}(\omega) = \frac{\pi}{2}\sum_\alpha \frac{\tilde{c}_\alpha^2}{\tilde{m}_\alpha\tilde{\omega}_\alpha}\delta(\omega - \tilde{\omega}_\alpha). \tag{2.5}$$

The problem is therefore reduced to finding $J_{\text{eff}}(\omega)$ since once it is known we can write[19,20] a formal expression for $P(t)$. [See the discussion following Eq. (2.16). The reader who is not interested in the details of the derivation of $J_{\text{eff}}(\omega)$ should skip to this point after noting its form—Eq. (2.14)].

It is not even necessary to find $\tilde{c}_\alpha$, etc., explicitly in order to determine $J_{\text{eff}}(\omega)$. Since the transformation from Eqs. (1.3) and (1.4) to Eq. (2.4) does not involve the spin, the same $J_{\text{eff}}(\omega)$ will control the dynamics of a continuous variable q moving in some potential $U(q)$ and coupled to coordinates y and $\{x_\alpha\}$ in the same way as the spin. In fact, as shown by Leggett,[17] it suffices to know the equation of motion for q in the classical limit in order to deduce $J_{\text{eff}}(\omega)$, and this allows us to circumvent the calculation of the normal modes.

To this end, let us consider the Hamiltonian

$$H_q = \frac{p_q^2}{2\mu} + U(q) + \frac{1}{2M}P_y^2 + \tfrac{1}{2}M\Omega^2(y+q)^2 + \sum_\alpha\left[\frac{p_\alpha^2}{2m_\alpha} + \tfrac{1}{2}m_\alpha\omega_\alpha^2\left\{x_\alpha + \frac{c_\alpha}{m_\alpha\omega_\alpha^2}y\right\}^2\right], \tag{2.6}$$

where p_q is the momentum conjugate to q. The classical equations of motion (with $U'(q) = dU/dq$, $\dot{q} = dq/dt$, etc.) are

$$\begin{aligned}\mu\ddot{q} &= -U'(q) - M\Omega^2(y+q),\\ M\ddot{y} &= -M\Omega^2(y+q) - \sum_\alpha c_\alpha x_\alpha - y\sum_\alpha\frac{c_\alpha^2}{m_\alpha\omega_\alpha^2},\\ m_\alpha\ddot{x}_\alpha &= -m_\alpha\omega_\alpha^2 x_\alpha - c_\alpha y.\end{aligned} \tag{2.7}$$

The Leggett prescription for obtaining $J_{\text{eff}}(\omega)$ is as follows. We define the Fourier transform

$$\hat{q}(z) = \int_{-\infty}^{\infty} q(t)\exp(-izt)dt, \quad \text{Im}(z) < 0, \tag{2.8}$$

and write the equation satisfied by q as

$$\hat{K}(z)\hat{q}(z) = -U_z'(q), \tag{2.9}$$

where $\hat{K}(z)$ is a function of z alone, and $U_z'(q)$ is the Fourier transform of $U'(q)$. Then, $J_{\text{eff}}(\omega)$ is given by

$$J_{\text{eff}} = \lim_{\epsilon\to 0+}\text{Im}[\hat{K}(\omega - i\epsilon)]; \quad \omega \text{ real}. \tag{2.10}$$

Carrying out these steps, and using the definitions (1.5) and (1.7), one obtains

$$\hat{K}(z) = -\mu z^2 + M\Omega^2\hat{L}(z)/[M\Omega^2 + \hat{L}(z)] \tag{2.11}$$

with

$$\hat{L}(z) = -z^2\left[M + \frac{2\eta}{\pi}\int_0^\infty \frac{\exp(-\omega'/\Lambda)}{(\omega')^2 - z^2}d\omega'\right]. \tag{2.12}$$

The cutoff Λ can now be taken to infinity, which then leads to the expression

$$\hat{L}(z) = -Mz^2 + i\eta z. \tag{2.13}$$

Substituting this in Eq. (2.11), and using Eq. (2.10), we get

$$J_{\text{eff}}(\omega) = \frac{\eta\omega\Omega^4}{(\Omega^2-\omega^2)^2 + 4\omega^2\gamma^2}, \tag{2.14}$$

where we have defined

$$\gamma = \eta/2M. \tag{2.15}$$

Note that $J_{\text{eff}}(\omega)$ is directly proportional to the imaginary part of the dynamic susceptibility of a damped harmonic oscillator with undamped frequency Ω and a friction coefficient η:

$$J_{\text{eff}}(\omega) = M^2\Omega^4\chi''(\omega). \tag{2.16}$$

We can now use the results obtained in Refs. 19 and 20 directly, and write[23]

$$W(t) = \int\mathscr{D}\sigma\int\mathscr{D}\lambda\, A[\sigma]A^*[\lambda] \times\exp\left\{\frac{-4y_0^2}{\pi\hbar}\int_{-\infty}^{t}d\tau\int_{-\infty}^{\tau}ds\,\xi(\tau) \times[\xi(s)K_2(\tau-s) - i\chi(s)K_1(\tau-s)]\right\}. \tag{2.17}$$

Here, $\int\mathscr{D}\sigma$ denotes an integral over all spin trajectories $\sigma(\tau)$ (see below), and $A[\sigma]$ is the amplitude that any given trajectory $\sigma(\tau)$ would have in the absence of coupling to the reaction coordinate. The exponential factor is the influence functional of Feynman and Vernon for a bath of harmonic oscillators, which we have written out explicitly with the following notations:

$$\xi(\tau) = [\sigma(\tau) - \lambda(\tau)]/2, \quad \chi(\tau) = [\sigma(\tau) + \lambda(\tau)]/2, \tag{2.18}$$

$$K_1(\tau) = \int_0^\infty d\omega\, J_{\text{eff}}(\omega)\sin(\omega\tau), \tag{2.19a}$$

$$K_2(\tau) = \int_0^\infty d\omega\, J_{\text{eff}}(\omega)\cos(\omega\tau)\coth\left(\frac{\beta\hbar\omega}{2}\right). \tag{2.19b}$$

The spin trajectory $\sigma(\tau)$ [and similarly $\lambda(\tau)$] consists of any function that takes values on the set $+1$ and -1 with discontinuities at an arbitrary, countable number of points $t_1, t_2, \ldots, t_m < t$, subject to the conditions[24]

$$\sigma(\tau) = \lambda(\tau) = 1, \quad -\infty < \tau < 0; \quad \tau = t. \tag{2.20}$$

The values ± 1 correspond to eigenvalues of σ_z, so that for any pair of trajectories $\sigma(\tau)$ and $\lambda(\tau)$, the segments in which $\xi(\tau) = 0$ can be thought of, roughly, as states in which the spin density matrix is in a diagonal state; following Ref. 19, we shall call such segments *sojourns*. Similarly, segments in which $\chi(\tau) = 0$ represent off-diagonal states of the density matrix and we shall call them *blips*.

The identification of the amplitude $A[\sigma]$ and the measure to be associated with the spin paths is most easily done by examining the amplitudes K_{++} to go from the state $|+\rangle$ at time zero to the state $|+\rangle$ at time t under the influence of the Hamiltonian

$$H_\sigma = \frac{\hbar\Delta_0}{2}\sigma_x + \tfrac{1}{2}\epsilon\sigma_z. \tag{2.21}$$

If we consider the first term as a perturbation and work in the interaction picture, then it is simple to construct the Dyson series for the time evolution operator, and we get

$$K_{++} = \sum_{m=0,2,4\ldots}^{\infty}\left(\frac{-i\Delta_0}{2}\right)^m\int_0^t dt_m\int_0^{t_m}dt_{m-1}\cdots\int_0^{t_2}dt_1 \times\exp\left\{\frac{-i\epsilon}{2\hbar}\int_0^t\sigma(\tau)d\tau\right\}, \tag{2.22}$$

where $\sigma(\tau)$ equals $+1$ for $\tau < t_1$, flips to -1, and stays at that value until $\tau = t_2$, when it flips to $+1$, and so on. Equation (2.22) is the precise meaning of the formal expression $K_{++} = \int\mathscr{D}\sigma\, A[\sigma]$.

The last step is to rewrite the expression (2.17) in terms of a *single* sum over all possible *pairs* of paths $\{\sigma(\tau),\lambda(\tau)\}$. We do this by considering each double path as a succession of alternating blips and sojourns. Note that there are two kinds of blips [$\xi(\tau) = +1$ or -1], and similarly, two kinds of sojourns [$\chi(\tau) = +1$ or -1]. Since $\xi(\tau)$ and $\chi(\tau)$ can both be written as a sum of piecewise continuous functions taking on values $+1$, 0, or -1, the double integrals of the kernels K_1 and K_2 in the influence functional are easily performed. Finally, summing over all possible numbers of blips, and integrating over their locations, we get

$$P(t) = \sum_{n=0}^{\infty}(-\Delta_0^2)^n\int_0^t dt_{2n}\int_0^{t_{2n}}dt_{2n-1}\cdots \times\int_0^{t_2}dt_1\,\tilde{F}_n(t_1,t_2,\ldots,t_{2n}), \tag{2.23}$$

where

$$\tilde{F}_n(\{t_i\}) = 2^{-n}\exp\left(-\sum_{j=1}^{n}A_j\right)\sum_{\{\zeta_i\}}\left[\exp\left(-\sum_{k>j=1}^{n}\zeta_j\zeta_k B_{jk}\right) \times\prod_{k=1}^{n-1}\cos\left(\sum_{j=k+1}^{n}\zeta_j\Phi_{kj}\right) \times\prod_{j=1}^{n}\exp\left\{-i\zeta_j\left(\frac{\epsilon}{\hbar}t_{2j,2j-1} + \Phi_{0j}\right)\right\}\right]. \tag{2.24}$$

Here, $t_{n,m} \equiv t_n - t_m$, and the ζ_i's are variables indicating the signs of the blips; each of them can equal $+1$ or -1. Further,

$$A_j = G_2(t_{2j,2j-1}), \tag{2.25a}$$

$$B_{jk} = G_2(t_{2k,2j-1}) + G_2(t_{2k-1,2j}) - G_2(t_{2k,2j}) - G_2(t_{2k-1,2j-1}), \tag{2.25b}$$

$$\Phi_{kj} = G_1(t_{2j,2k}) + G_1(t_{2j-1,2k+1}) - G_1(t_{2j-1,2k}) - G_1(t_{2j,2k+1}), \tag{2.25c}$$

where G_1 and G_2 are second integrals of the kernels K_1 and K_2:

$$G_1(t) = \frac{4y_0^2}{\pi\hbar}\int_0^\infty d\omega\,\frac{J_{\text{eff}}(\omega)}{\omega^2}\sin(\omega t), \tag{2.26a}$$

$$G_2(t) = \frac{4y_0^2}{\pi\hbar}\int_0^\infty d\omega\,\frac{J_{\text{eff}}(\omega)}{\omega^2}[1-\cos(\omega t)]\coth\left(\frac{\beta\hbar\omega}{2}\right), \tag{2.26b}$$

and it is to be understood that the limit $t_0 \to -\infty$ is to be taken in evaluating Φ_{0j}. Formulas for G_1 and G_2 are given in the Appendix.

The expression (2.23) for $P(t)$ can be thought of as a generalized, grand partition function for a one-dimensional system of charged rods, or blips. The term A_j can be interpreted

as the energy of a blip. It is always positive, and grows both with increasing temperature and with increasing blip width for wide enough blips. Consequently, very wide blips are always suppressed. The term B_{jk} represents the interaction energy of two blips, and because it is multiplied by the factor $\zeta_j\zeta_k$, blips can both attract and repel one another. Finally, Φ_{kj} is the phase factor arising from the interference between trajectories with sojourns of opposite sign.

Despite its formidable appearance, Eq. (2.23) can be made to yield useful results in the limits of moderate and high friction. This is the subject of Secs. III and IV.

III. MODERATE FRICTION AND NONADIABATIC LIMIT

In this section we shall show that if the friction is moderate (we shall make this more precise) then the expression (2.23) for $P(t)$ can be approximated by a very simple form characteristic of exponential decay with clearly identifiable forward and backward reaction rates (i.e., electron going from donor site to acceptor site and vice versa). Our strategy is motivated by the simple picture given in Sec. I. We expect there to be a range of values of friction in which it is small enough that each transit of the Landau–Zener region is too rapid for the electron to make many transitions, and at the same time large enough that there is no precise relation between the times at which these transits occur. Since a blip can be thought of, loosely speaking, as an interval in which the electron is "making up its mind" about which state to end up in, or as a single tunneling event, we should expect that different blips are uncorrelated, and that interblip interactions are unimportant. This is indeed the case, as we shall see.

Let us suppose that the decay rate has a value Γ_{na} (which must, of course, be calculated) so that we can associate with $P(t)$, for not too short values of t, a variation of the form $\exp(-\Gamma_{na}t)$. If such a form is to rise from the series (2.23), it follows that $\Delta_0^2\tilde{F}_n$ must act as a probability distribution such that the mean length of a blip *plus* its neighboring sojourn equals Γ_{na}^{-1}. Quite generally, however, we expect Γ_{na} to contain an activation factor, which in the high temperature limit equals $\exp(-E_f/kT)$ etc., which merely reflects the frequency with which a particle has enough energy to reach the Landau–Zener region. Within each transit of the Landau–Zener region, however, we can have several tunneling events, corresponding to a mean blip-plus-sojourn length t_{b+s}, which can be obtained by dividing Γ_{na} by the activation factor. If we can self-consistently impose the condition that the self-energy of a blip forces the mean length of a blip, which we denote $t_{\rm blip}$, to be much smaller than t_{b+s}, it follows from Eqs. (2.25) and (2.26) that it is reasonable to neglect the interblip interactions B_{jk}, and all the phase factors Φ_{kj} except those with $j=k+1$. Since we are assuming that $t_{\rm blip} \ll t_{b+s}$, we can approximate $\Phi_{k,k+1}$ as follows:

$$\Phi_{k,k+1} = G_1(t_{2k+2,2k}) - G_1(t_{2k+1,2k}) - G_1(t_{2k+2,2k+1}) \approx -G_1(t_{2k+2}-t_{2k+1}). \tag{3.1}$$

The partially averaged influence functional $\tilde{F}_n(\{t_i\})$ [see Eq. (2.24)] now decomposes into a product of functions depending on the blip lengths alone.

$$\tilde{F}_n(\{t_i\}) = \left[\prod_{j=1}^{n}\exp\{-G_2(b_j)\}\right] \times\left[\prod_{j=2}^{n}\cos\{G_1(b_j)\}\cos\{\epsilon b_j/\hbar\}\right] \times\cos\{G_1(b_1)-\epsilon b_1/\hbar\}, \tag{3.2}$$

where b_j, the length of the jth blip, is defined by

$$b_j = t_{2j} - t_{2j-1}. \tag{3.3}$$

We now substitute Eq. (3.2) in Eq. (2.23), and rewrite the multiple integral as an integral over the lengths of all the blips and sojourns (with the constraint that they add up to t). Since G_2 is a rapidly increasing function of its argument, we can extend the upper limits of the blip integrals to $+\infty$. The sojourn integrals then give a factor of $t^n/n!$ in the nth term of the series, which is easily summed to give

$$P(t) = P_\infty + (1-P_\infty)\exp(-\Gamma_{na}t), \tag{3.4}$$

where

$$\Gamma_{na} = \Delta_0^2\int_0^\infty \exp[-G_2(t)]\cos[G_1(t)]\cos(\epsilon t/\hbar)dt, \tag{3.5}$$

$$P_\infty = 1 - \frac{\Delta_0^2}{\Gamma_{na}}\int_0^\infty \exp[-G_2(t)]\cos[G_1(t)-\epsilon t/\hbar]dt. \tag{3.6}$$

As stated earlier, the time scale Γ_{na}^{-1} is determined by the argument, and we must ensure that the self-consistency condition is satisfied, i.e., $t_{\rm blip} \ll t_{b+s}$. We can evaluate Γ_{na} explicitly if the time scale τ_0 defined in the Appendix is much less than the lesser of $\beta\hbar$ and γ^{-1}. (Recall that $\gamma = \eta/2M$.) This will be the case if the barrier heights E_f, E_b are large in comparison with both the thermal energy kT and the vibrational enegy $\hbar\Omega$. Equation (A8) of the Appendix is then a good approximation to $G_2(t)$ over the region where the exponential in Eq. (3.5) is appreciable, and $t_{\rm blip}$ is equal to τ_0. In the same region $G_1(t)$ can be approximated by Eq. (A5). It follows that

$$\Gamma_{na} = \Gamma_{na,f} + \Gamma_{na,b}, \tag{3.7}$$

where

$$\Gamma_{na,f} = \frac{\Delta_0^2}{4}\left(\frac{\pi\hbar^2}{E_r kT_{\rm eff}}\right)^{1/2}\exp(-E_f/kT_{\rm eff}) \tag{3.8}$$

is the forward rate. The backward rate $\Gamma_{na,b}$ is given by the same equation with E_f replaced by E_b. (See Fig. 1 for the definition of E_f, E_b, and E_r.) We have introduced an effective temperature $T_{\rm eff}$, through

$$kT_{\rm eff} = M\Omega^2\mu^2(\eta, T), \tag{3.9}$$

where $\mu^2(\eta, T)$ is the mean square displacement of the reaction coordinate about its equilibrium value in either potential well $V(y;\pm)$. From the discussion of the T and η dependence of μ^2 in the Appendix it follows that $T_{\rm eff} \approx T$ at high temperatures, so that the forward and backward rates satisfy detailed balance, and P_∞, which is the equilibrium expectation value $\langle\sigma_z\rangle$, and is generally given by

$$P_\infty = -\tanh(\epsilon/2kT_{\rm eff}), \tag{3.10}$$

reduces to the answer we would get from the Boltzmann distribution.

The expression (3.8) is quite similar to the one found by Hopfield[6(a)] in that the effective temperature $T_{\rm eff}$ changes from T to a temperature-independent value as the actual temperature decreases, although the detailed manner in which it does so is different. As states in the Appendix, the crossover temperature depends on the strength of the friction, and measuring it should provide an indication of how important friction is in any given reaction.

The self-consistency condition now reads, approximately,

$$\left(\frac{\hbar^2\Delta_0^2}{4E_r kT_{\rm eff}}\right) \ll 1. \tag{3.11}$$

Since $\hbar\Delta_0$ is usually much smaller than E_r, this condition will always be satisfied unless the friction is very large.

The determination of how large the friction must be in order for Eq. (3.8) to hold is a more delicate question. Indeed, if the friction is very low, we should expect $P(t)$ to depend sensitively on the choice of the potentials $V(y;\pm)$, and answers obtained by studying the parabolic form (1.4) may have rather limited validity. We shall therefore make only rough, qualitative statements about the behavior of $P(t)$ in this case.[25]

Let us imagine, to begin with, that there is no friction. In this case we will have in each well a whole ladder of energy levels with a nonuniform spacing. Further, any level in the left well will, in general, be separated from the one closest to it in the right well by a *detuning*, $\hbar\delta$, which we expect to be of order $\hbar\Omega/2$. This detuning will be much larger than the tunneling matrix element $\hbar\tilde{\Delta}$ between these levels, where $\tilde{\Delta}$ is given by Δ_0 times the overlap integral of the levels in question. If we now start our system in one of the levels on the left, and assume that we can neglect the mixing of this level with all but its closest partner in the right well, the system will oscillate back and forth between these two levels. The probability of finding the system on the right, however, will be very small, or order $(\tilde{\Delta}/\delta)^2$. This oscillation will continue *ad infinitum* unless there is a mechanism for the system to equilibrate, and so we must reintroduce the coupling to the bath. Then, given that the system is in the right well in a level with an energy E as measured from its bottom, it will lose energy by making transitions to other levels at a rate $2\gamma E/\hbar\Omega$. The net rate at which the reaction will proceed is then approximately given by the product of these two factors, suitably weighted over the levels of the left well so as to reflect the initial density matrix. Although this sum is difficult to evaluate, we can argue that the rate should be proportional to (i) an activation factor $\exp-(E_f/kT)$ arising from the initial Boltzmann distribution, (ii) a factor of order $(\Delta_0/\Omega)^2$ arising from the mixing of individual levels in each well, and (iii) the frequency γ associated with the rate of energy loss. Recall that this last factor is also present in the rate at which a particle diffuses over a simple one-dimensional barrier when the friction is low.

One can now get a rough understanding of the effects of increasing the friction by thinking of the levels in each well as acquiring a width. This tends to increase the reaction rate by decreasing the detuning between the levels. It also tends to reduce the time over which phase coherence between two neighboring levels can be maintained, i.e., it tends to dampen the oscillations. It follows that by the time $\gamma \approx \Omega/2$, there are neither sharp levels, nor any coherence between them, so the results stated in this section should hold.

We conclude this section with a simple semiclassical interpretation of the result [Eq. (3.8)]. Let us consider a particle in the left well, traversing the Landau–Zener region with a velocity v. Then, the probability $p(v)$ that the electron will tunnel to the state $|-\rangle$ during one forward and return transit is given by[10]

$$p(v) = \pi\hbar\Delta_0^2/F_\Delta v, \tag{3.12}$$

where F_Δ is the difference in the slopes of the potentials at the crossing point:

$$F_\Delta = F_- - F_+ = \frac{d}{dy}\{V(y;+) - V(y;-)\}_{y=y^*}. \tag{3.13}$$

The probability $W_{++}(y^*,v)$ of finding a particle in the state $|+\rangle$ at $y = y^*$ and with velocity v can be taken to be the Wigner transform of the reduced density matrix $\rho_{++}(y, y')$ for the reaction coordinate, evaluated at the position y^*, and at a momentum Mv:

$$W_{++}(y^*,v) = \frac{M}{2\pi\hbar}\int_{-\infty}^{\infty} dx \times \exp(iMvx/\hbar)\rho_{++}(y^* - x/2, y^* + x/2). \tag{3.14}$$

Since the flux of particles with velocity v at the point y^* is given by $vW_{++}(y^*,v)$, the forward rate $\Gamma_{na,f}$ is given by

$$\Gamma_{na,f} = \int_0^\infty dv\, p(v) v W_{++}(y^*,v) = \frac{\pi\hbar\Delta_0^2}{2F_\Delta}\rho_{++}(y^*, y^*). \tag{3.15}$$

Using the fact that $\rho_{++}(y, y)$ is a Gaussian probability distribution centered at $y = -y_0$ with mean square deviation μ^2, it is simple to show that Eq. (3.15) is identical to Eq. (3.8).

IV. HIGH FRICTION AND THE ADIABATIC LIMIT

In this section we analyze the formal path integral expression [Eq. (2.23)] for $P(t)$ in the high friction limit and show that the reaction rate may become independent of the matrix element $\hbar\Delta_0$. The arguments of this section are not quite as robust as those of the previous one, and we believe that a better answer for the rate in this limit can be obtained by solving the Smoluchowski equation derived in the next section. We nevertheless include this section because (a) it is the only instance known to us where one can sum many orders of perturbation theory in a real-time path integral, albeit approximately, and (b) the fact that the results so obtained do not differ substantially from those of Sec. VI indicates that the mental picture of the process in this limit on which our approximations are predicted is valid and useful.

Since we shall work entirely in the overdamped limit in this section, the relevant approximations to $G_1(t)$ and $G_2(t)$ are given by Eqs. (A3) and (A7) of the Appendix. The characteristic time over which these functions vary (and over which the reaction coordinate, or "particle," moves) is given by $\tau_c = \omega_c^{-1}$, where

$$\omega_c = \Omega^2/2\gamma. \tag{4.1}$$

Let us imagine restricting the electron to the $|+\rangle$ state. Then the time taken by the particle to traverse the Landau–Zener region in a single visit is of order $\tau_c l_{LZ}/(y^* + y_0)$. For large enough γ and/or Δ_0, this time can become much larger than the mean blip time which is of order $(E_r kT/\hbar^2)^{-1/2}$. In contrast, different passages of the Landau–Zener region will be separated by a mean time of order $\tau_c \exp(E_f/kT)$, which is much longer than τ_c if E_f is more than a few times kT. This suggests that for times $t \gg \tau_c$, the electron trajectories which contribute appreciably to $P(t)$ consist of well separated *blocks*, with each block consisting of closely spaced blips. We indicate this pictorially in Fig. 2, where the lower and upper horizontal segments represent sojourns and blips, respectively. We shall call the long intervals between blocks *super-sojourns*, and label them as indicated in the figure.

In analyzing Eq. (2.25), we shall, therefore, use the asymptotic form for $G_2(t)$ (linear function of t) if the argument spans a super-sojourn, and the short time form (A8) otherwise. Similarly, we shall take $G_1(t)$ to be a constant [given by the first term of Eq. (A3)] in the first case, and to be given by the first two terms in the $t \to 0$ expansion of Eq. (A3) in the second. With the definitions

$$b_j = t_{2j} - t_{2j-1}, \tag{4.2a}$$

$$s_j = t_{2j+1} - t_{2j}, \tag{4.2b}$$

it is straightforward to show that

$$A_j = b_j^2/2\tau_0^2, \tag{4.3}$$

$$B_{jk} = \begin{cases} b_j b_k/\tau_0^2, & b_j \text{ and } b_k \text{ in the same block,} \\ 0, & \text{otherwise.} \end{cases} \tag{4.4}$$

The phase factors Φ_{kj} are a little more complicated. If the blip b_j and sojourn s_k are in the same block, then

$$\Phi_{kj} = -(\omega_c E_r/\hbar) b_j s_k, \tag{4.5}$$

whereas if they are in different blocks, Φ_{kj} vanishes unless the sojourn s_k is a super-sojourn, and b_j lies in the block immediately following it. (This is true even for $k = 0$.) In that case,

$$\Phi_{kj} = -E_r b_j/\hbar. \tag{4.6}$$

It now follows that as in the previous section, the influence functional decomposes into a product of functions, depending this time only on the lengths of the blocks. If we denote the length of the J th block by B_J (this should not be confused with the interblip interaction B_{jk} which always has two subscripts), and that of the following supersojourn by S_J, then we can write

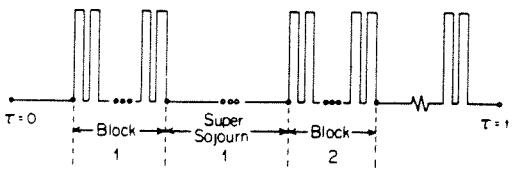

FIG. 2. Schematic representation of the important electronic trajectories in the limit of high friction. The short horizontal segments are the blips which bunch together into *blocks*. Different blocks are separated by long intervals called *super-sojourns*. The labeling in such that the jth super-sojourn follows the jth block.

$$P(t) = \sum_{N=0}^{\infty} \int dS_0 \left(\prod_{J=1}^{N} \int\int dS_J\, dB_J \right) R'(B_1) \prod_{J=2}^{N} R(B_J), \tag{4.7}$$

where it is understood that the block and super-sojourn lengths are constrained to add up to t. The functions R and R' are given by

$$\begin{Bmatrix} R(B) \\ R'(B) \end{Bmatrix} = \sum_{n=1}^{\infty} (-\Delta_0^2)^n \int ds_0 \left(\prod_{j=1}^{n} \int\int ds_j\, db_j \right) \begin{Bmatrix} \hat{F}_n(\{s_i, b_i\}) \\ \hat{F}'_n(\{s_i, b_i\}) \end{Bmatrix}, \tag{4.8}$$

where it is similarly understood that the blip and sojourn lengths must add up to B, and where

$$\begin{Bmatrix} \hat{F}_n \\ \hat{F}'_n \end{Bmatrix} = \frac{1}{2^n} \sum_{\{\zeta_i\}} \exp\left(-\frac{\Lambda_1^2}{2\tau_0^2} \right) \begin{Bmatrix} \cos(\epsilon \Lambda_1/\hbar) \cos(E_r \Lambda_1/\hbar) \\ \cos[(\epsilon - E_r)\Lambda_1/\hbar] \end{Bmatrix} \times \prod_{k=1}^{n-1} \cos\left(\frac{\omega_c E_r}{\hbar} \Lambda_{k+1} s_k \right), \tag{4.9}$$

with the definition

$$\Lambda_j = \sum_{i=j}^{n} \zeta_i b_i. \tag{4.10}$$

The evaluation of $P(t)$ is most easily organized by taking Laplace transforms. Defining

$$\tilde{P}(\lambda) = \int_0^{\infty} \exp(-\lambda t) P(t)\, dt, \tag{4.11}$$

and similarly $\tilde{R}(\lambda)$ and $\tilde{R}'(\lambda)$, we get

$$\tilde{P}(\lambda) = \frac{1}{\lambda} \left[1 + \frac{\tilde{R}'(\lambda)}{\lambda - \tilde{R}(\lambda)} \right]. \tag{4.12}$$

We explicitly show the evaluation only of $\tilde{R}'(\lambda)$, since that of $\tilde{R}(\lambda)$ is very similar:

$$\tilde{R}'(\lambda) = \sum_{n=1}^{\infty} (-\Delta_0^2)^n \int_0^{\infty} \cdots \int_0^{\infty} \exp[-\lambda (b_1 + b_2 + \cdots + b_n + s_1 + \cdots + s_{n-1})] \times \hat{F}'_n(\{s_i, b_i\})\, ds_{n-1} \ldots db_1. \tag{4.13}$$

The evaluation of the sojourn integrals is easy; the k th integral gives a factor

$$\frac{\lambda}{\lambda^2 + (\omega_c E_r \Lambda_{k+1}/\hbar)^2}. \tag{4.14}$$

We now note that we are interested in $P(t)$ for times much longer than ω_c^{-1}, and so any singularities of $\hat{P}(\lambda)$ with $\mathrm{Re}(\lambda) \ll -\omega_c$ are not of interest. We can accordingly consider Eq. (4.14) in the limit $\lambda \to 0$, where it reduces to

$$\frac{\pi\hbar}{\omega_c E_r} \delta(\Lambda_{k+1}). \tag{4.15}$$

The delta functions render all but one of the blip integrals trivial, which is easily done. The final result is

$$\tilde{R}'(\lambda) \approx -\frac{\Delta_0^2 (\pi\hbar^2/E_r kT)^{1/2}}{2[1 + \Delta_0^2 (\pi\hbar/2\omega_c E_r)]} \exp(-E_f/kT). \tag{4.16}$$

$\tilde{R}(\lambda)$ is similarly evaluated, and $\tilde{P}(\lambda)$ is inverted to give

$$P(t) = P_{\infty} + (1 - P_{\infty}) \exp(-\Gamma t), \tag{4.17}$$

where

$$\Gamma = \frac{\Delta_0^2(\pi\hbar^2/E_r kT)^{1/2}}{4[1+\Delta_0^2(\pi\hbar/2\omega_c E_r)]} \times [\exp(-E_f/kT)+\exp(-E_b/kT)], \quad (4.18)$$

and

$$P_\infty = -\tanh(\epsilon/2kT). \quad (4.19)$$

If we now define an "adiabaticity parameter" g,

$$g = \Delta_0^2(\pi\hbar/2\omega_c E_r), \quad (4.20)$$

then the reaction is adiabatic or nonadiabatic depending on whether g is large or small. If $g \ll 1$, Eq. (4.18) reduces to the nonadiabatic rate of Sec. III, while if $g \gg 1$, we get a Δ_0 independent, or adiabatic rate

$$\Gamma_{ad} \simeq \frac{\omega_c}{2}\left(\frac{E_r}{\pi kT}\right)^{1/2}[\exp(-E_f/kT)+\exp(-E_b/kT)]. \quad (4.21)$$

The interpretation of the condition for adiabaticity or nonadiabaticity is simple: g is the ratio between the time spent by the particle in the Landau–Zener region when the friction is high and the time taken for one spin precession (which is the inverse of the tunneling frequency Δ_0^{-1}).

It is worth noting that Eq. (4.21) is almost exactly the rate we would write down on the basis of a Kramers-like calculation for a particle diffusing in a potential obtained by keeping the smaller of $V(y;+)$ and $V(y;-)$ for each y.[15] (There are small corrections to the preexponential factor.)

In Sec. VI, we shall see how almost exactly the same results are obtained by solving the Smoluchowski equation which we derive in the next section.

V. DERIVATION OF THE FOKKER–PLANCK AND SMOLUCHOWSKI EQUATIONS

In this section we shall show how, starting from a Hamiltonian of the form (1.3), one can integrate out the bath and obtain an equation of motion—a Fokker–Planck equation, in other words—for the reduced density matrix of the electron *plus* the reaction coordinate. It is very useful to have such a description since it is much less cumbersome than a path integral, and is, even in the worst case, amenable to numerical solution. Of course, it is not always possible to achieve such a description, and the criterion for being able to do so is, as we shall argue, that $kT/\hbar$ be much larger than the characteristic frequency of the reaction coordinate $[(\Omega^2-\gamma^2)^{1/2}$ in the underdamped case, and $\Omega^2/2\gamma$ in the overdamped one]. This covers a wide range of parameters, and so our Fokker–Planck equation should be useful even for studying the underdamped, nonadiabatic case, and should allow a more detailed analysis of the crossover from nonadiabatic to adiabatic behavior. We shall not, however, do that here. Instead, we shall show how the Fokker–Planck equation reduces to a Smoluchowski equation in the limit of very high friction, whose solution we shall then outline in Sec. VI following Zusman.[18] We also note that the Fokker–Planck equation is not limited to the special quadratic potential [Eq. (1.4)] for the reaction coordinate.

Our argument follows that of Caldeira and Leggett for ordinary Brownian motion very closely.[26] Suppose that at some time t_0, the total density matrix of the system can be factorized into a part for the bath alone (which we shall take to be at a temperature T), and a part for the electron *plus* the reaction coordinate.[27] (Note that this part does *not* have to factorize any further.) Then the reduced density matrix $\rho_{\sigma\lambda}(x,y;t_0)$ for the electron and reaction coordinate at a later time t is given by[28]

$$\rho_{\sigma\lambda}(x,y;t) = \sum_{\sigma'\lambda'}\int_{-\infty}^{\infty}\int_{-\infty}^{\infty} dx'\,dy' \times \hat{J}_{\sigma\lambda,\sigma'\lambda'}(x,y;t;x',y';t_0)\rho_{\sigma'\lambda'}(x',y';t_0), \quad (5.1)$$

where

$$\hat{J} = \int_{\sigma'}^{\sigma}\mathcal{D}\sigma\int_{\lambda'}^{\lambda}\mathcal{D}\lambda\int_{x'}^{x}\mathcal{D}x\int_{y'}^{y}\mathcal{D}y \times\left[A[\sigma]A^*[\lambda]\exp\frac{i}{\hbar}\{S_{r+e}[x,\sigma]-S_{r+e}[y,\lambda]\}\right] \times\mathcal{F}[x,y]. \quad (5.2)$$

The limits on the functional integration signs indicate the boundary conditions that the trajectories must satisfy, e.g., $\sigma(t_0)=\sigma'$, $\sigma(t)=\sigma$. The quantity $A[\sigma]$ is the bare amplitude associated with a spin trajectory $\sigma(\tau)$, as defined in Sec. II, and $S_{r+e}[y,\lambda]$ is the classical action for the reaction coordinate to follow a trajectory $y(\tau)$, given that the electron trajectory is $\lambda(\tau)$, and ignoring the coupling to the bath. That is,

$$S_{r+e}[y,\lambda] = \int_{t_0}^{t}\left\{\tfrac{1}{2}M\left(\frac{dy(\tau)}{dt}\right)^2 - V[y(\tau),\lambda(\tau)]\right\}d\tau. \quad (5.3)$$

Note that $V(y,\lambda)$ does not need to be given by Eq. (1.4). Finally, $\mathcal{F}[x,y]$ is the influence functional for a system coupled to a set of harmonic oscillators. It has a structure identical to that for the spin coupled to a bath that we discussed in Sec. II. We rewrite it here for ease of reference:

$$\mathcal{F}[x,y] = \exp\left[-\frac{1}{\pi\hbar}\int_{t_0}^{t}\int_{t_0}^{\tau}u(\tau)\{u(s)\tilde{K}_2(\tau-s) - iv(s)\tilde{K}_1(\tau-s)\}ds\,d\tau\right], \quad (5.4)$$

$$\begin{pmatrix}u(\tau)\\ v(\tau)\end{pmatrix} = [x(\tau)\mp y(\tau)], \quad (5.5)$$

$$\tilde{K}_1(\tau) = \int_0^\infty d\omega\, J_0(\omega)\sin(\omega\tau), \quad (5.6a)$$

$$\tilde{K}_2(\tau) = \int_0^\infty d\omega\, J_0(\omega)\cos(\omega\tau)\coth(\beta\hbar\omega/2). \quad (5.6b)$$

Note that it is $J_0(\omega)$ and not $J_{\rm eff}(\omega)$ that appears in Eqs. (5.6).

As discussed in Ref. 26, the kernel $\tilde{K}_1$ can be replaced by $-\pi\eta$ times the derivative of a delta function since most particle trajectories will vary on a frequency scale much smaller than Λ. The kernel $\tilde{K}_2$ has a somewhat longer range, namely $\hbar/kT$. From a semiclassical argument we would expect that the most important particle trajectories vary on a time scale characteristic of damped motion in the potentials $V(y;\pm)$. Thus, if this time scale is much longer than $\hbar/kT$, we can replace $\tilde{K}_2(\tau)$ by a delta function times a constant. Specifically, we write

$$\tilde{K}_1(\tau) = -\pi\eta\delta'(\tau), \quad (5.7a)$$

$$\tilde{K}_2(\tau) = 2\eta kT\delta(\tau), \tag{5.7b}$$

so that

$$\mathscr{F}[x,y] = \exp\left\{\frac{-i\eta}{2\hbar}\int_{t_0}^{t}(x-y)\frac{d}{d\tau}(x+y)d\tau - \frac{\eta kT}{\hbar^2}\int_{t_0}^{t}(x-y)^2 d\tau\right\}. \tag{5.8}$$

The propagator $\hat{J}$ now has no nonlocal terms in it, and so the reduced density matrix of interest at any given time t can be related to itself at *any* earlier time t_0, which means that we can find a differential equation of motion for it. If we symbolically write, for infintesimal δ,

$$\hat{J}(t+\delta; t) = \hat{1} + \delta\hat{\mathscr{L}} + \mathscr{O}(\delta^2), \tag{5.9}$$

where $\hat{1}$ is the unit operator and $\hat{\mathscr{L}}$ is some other linear operator (which we shall find), then

$$\partial\rho/\partial t = \hat{\mathscr{L}}\rho. \tag{5.10}$$

We now find $\hat{\mathscr{L}}$ by doing a stationary phase analysis as in Ref. 26 or Sec. 4-1 of Ref. 22. Let us take the Hamiltonian describing the electron and the reaction coordinate to be of the general form

$$\tilde{H} = \frac{p^2}{2M} + U(y) + \sigma_z f(y) + H_\sigma, \tag{5.11}$$

where H_σ is a part that depends on the electronic degree of freedom only and which we shall take to be

$$H_\sigma = (\hbar\Delta_0/2)\sigma_x + (\epsilon/2)\sigma_z. \tag{5.12}$$

[The choice (1.4) corresponds to $U(y) = M\Omega^2(y^2 + y_0^2)/2$, $f(y) = M\Omega^2 y_0 y$.] Combining Eqs. (5.2), (5.3), (5.7), (5.8), and (5.11), we can write (with $\dot{y}\equiv dy/d\tau$, etc.),

$$\hat{J} = N^{-2}\int_\sigma^\sigma \mathscr{D}\sigma\int_\lambda^\lambda \mathscr{D}\lambda\, A[\sigma]A^*[\lambda]\exp\frac{i}{\hbar}\times\left\{\int_t^{t+\delta}[\tfrac{1}{2}M(\dot{x}^2-\dot{y}^2) - U(x) + U(y) - \sigma(\tau)f(x) + \lambda(\tau)f(y)] - \frac{\eta}{2}\times\int_t^{t+\delta}(x-y)(\dot{x}+\dot{y}) + \frac{i}{\hbar}\eta kT\int_t^{t+\delta}(x-y)^2\right\}. \tag{5.13}$$

Here, N is a normalization constant. Let us take the paths $x(\tau)$ and $y(\tau)$ to be straight line segments connecting x, y to x', y'. Replacing $f(x)$ and $f(y)$ by $f(\bar{x})$ and $f(\bar{y})$, where

$$\bar{x} = (x+x')/2, \quad \bar{y} = (y+y')/2, \tag{5.14}$$

we can do the σ and λ path integrals as explained in Sec. II. Thus, we find

$$K_{\sigma\sigma'}(\bar{x}) \equiv \int_\sigma^\sigma \mathscr{D}\sigma\, A_\sigma \exp\left\{-\frac{i}{\hbar}\int_t^{t+\delta}\sigma(\tau)f(\bar{x})\right\} = \delta_{\sigma\sigma'} - \frac{i\delta}{\hbar}\langle\sigma|H_\sigma + \sigma_z f(\bar{x})|\sigma'\rangle + \mathscr{O}(\delta^2). \tag{5.15}$$

If we now define

$$\xi_1 = (x-x') - \gamma\delta.(\bar{x}-\bar{y}), \tag{5.16a}$$

$$\xi_2 = (y-y') + \gamma\delta.(\bar{x}-\bar{y}), \tag{5.16a}$$

it is easy to show that $\hat{J}$ becomes the exponential of a diagonal quadratic form times the electronic propagators:

$$\hat{J} \simeq N^{-2}\exp\frac{i}{\hbar}\left[\frac{M}{2\delta}(\xi_1^2 - \xi_2^2) - \delta.U(\bar{x}) + \delta.U(\bar{y}) + \frac{\eta}{4}(\xi_1^2 - \xi_2^2) + \frac{i\eta kT}{\hbar}\delta.(\bar{x}-\bar{y})^2 + o(\delta)\right]K_{\sigma\sigma'}(\bar{x})K^*_{\lambda\lambda'}(\bar{y}). \tag{5.17}$$

There is an ambiguity at this point about whether or not the term $\eta(\xi_1^2 - \xi_2^2)/4$ should be included in N. If it is not, one can show that the resulting Fokker–Planck equation does not conserve probability. On the other hand, if it is included (which is what we shall do), the normalization constant is not what one would obtain from other considerations, such as those in Sec. 4-1 of Ref. 22. This is somewhat disturbing since unitarity has been built into expressions (5.1) and (5.2) and should not have to be reimposed. A solution of this conundrum would be most welcome.

It follows from Eq. (5.17) that

$$\frac{\partial\rho}{\partial t} = \frac{i\hbar}{2M}\left(\frac{\partial^2\rho}{\partial x^2} - \frac{\partial^2\rho}{\partial y^2}\right) - \frac{i}{\hbar}[U(x) - U(y)]\rho - \frac{i}{\hbar}[H_\sigma, \rho] - \frac{i}{\hbar}[\sigma_z f(x)\rho - \rho\sigma_z f(y)] - \gamma(x-y)\left(\frac{\partial\rho}{\partial x} - \frac{\partial\rho}{\partial y}\right) - \frac{\eta kT}{\hbar^2}(x-y)^2\rho. \tag{5.18}$$

This can be written more concisely in operator notation as

$$\frac{\partial\rho}{\partial t} = -\frac{i}{\hbar}[\tilde{H}, \rho] - \frac{\eta kT}{\hbar^2}[y, [y, \rho]] - \frac{i\gamma}{\hbar}[y, \{p, \rho\}]. \tag{5.19}$$

To convert this to a more familiar form we take the Wigner transform, i.e., we define

$$W_{\alpha,\beta}(y,p) = \frac{1}{2\pi\hbar}\int_{-\infty}^{\infty}\exp(ipu/\hbar)\rho_{\alpha\beta}\left(y - \frac{u}{2}, y + \frac{u}{2}\right)du. \tag{5.20}$$

Dropping terms of order $\hbar$, Eq. (5.18) becomes

$$\frac{\partial W}{\partial t} = -\frac{1}{M}\frac{\partial}{\partial y}(pW) + \frac{\partial}{\partial p}[U'(y)W] + 2\gamma\frac{\partial}{\partial p}(pW) + \eta kT\frac{\partial^2}{\partial p^2}W + \frac{1}{2}\frac{df}{dy}\frac{\partial}{\partial p}\{\sigma_z, W\} - \frac{i}{\hbar}[H_\sigma + \sigma_z f(y), W], \tag{5.21}$$

where the commutators and anticommutators now involve only the spin degrees of freedom.

The structure of Eq. (5.21) is illuminated by thinking of a classical object with some internal degrees of freedom—for example, angles associated with moments of inertia—moving in a medium that exerts viscous forces only on the center of mass of the object, and not on the internal degrees of freedom. (The latter may or may not experience external fields

depending on the position of the center of mass.) In this case the dynamics of the internal variables will be purely convective—and governed by Liouville's equation, i.e., by the classical analog of the first term on the right-hand side of Eq. (5.19)—whereas the diffusive terms will only involve the center of mass. This is precisely the form of Eq. (5.21), reflecting our assumption that friction enters the problem via the reaction coordinate. Note, however, that for the problem at hand, the dynamics of the internal coordinate, i.e., the electron or "spin," are intrinsically quantum mechanical as evidenced by the persistence of Planck's constant in Eq. (5.21).

If the friction is very high, we can assume that the momentum equilibrates to a Maxwellian distribution at each point y independently, so that W takes the form

$$W_{\alpha\beta}(y,p;t)=(2\pi MkT)^{-1/2}\exp(-p^2/2MkT)n_{\alpha\beta}(y,t). \tag{5.22}$$

This distribution has a momentum space width $\sqrt{MkT}$, which in one collision time $(2\gamma)^{-1}$ translates into a position space width $\sqrt{MkT}/\eta$. Equation (5.22) will be a reasonable *ansatz* provided $U(y)$, $f(y)$, and *all* the components $n_{\alpha\beta}$ vary slowly on this length scale. It is clear that this condition will be met for $U(y)$, $f(y)$, and the diagonal components n_{11} and n_{22} provided the friction is large enough. (We use the subscripts 1 and 2 rather than + and − in this and the next section to prevent confusion with the operations of addition and subtraction.) We shall see in the next section that the condition is also met for n_{12}, but that it is more stringent than that for $U(y)$, $f(y)$, and n_{11} and n_{22}.

The momentum can now be integrated out in the standard way,[15,16] leading to Smoluchowski-like equations, which we write down here for the special choice (1.4) only for simplicity:

$$\frac{\partial n_{11}}{\partial t}=\frac{1}{\eta}\frac{\partial}{\partial y}\left[M\Omega^2(y+y_0)+kT\frac{\partial}{\partial y}\right]n_{11}+\frac{i\Delta_0}{2}(n_{12}-n_{21}), \tag{5.23a}$$

$$\frac{\partial n_{22}}{\partial t}=\frac{1}{\eta}\frac{\partial}{\partial y}\left[M\Omega^2(y-y_0)+kT\frac{\partial}{\partial y}\right]n_{22}-\frac{i\Delta_0}{2}(n_{12}-n_{21}), \tag{5.23b}$$

$$\frac{\partial n_{12}}{\partial t}=\frac{1}{\eta}\frac{\partial}{\partial y}\left[M\Omega^2 y+kT\frac{\partial}{\partial y}\right]n_{12}+\frac{i\Delta_0}{2}(n_{11}-n_{22})-\frac{i}{\hbar}(\epsilon+F_\Delta y)n_{12}. \tag{5.23c}$$

The equation for n_{21} can be obtained from Eq. (5.23c) by complex conjugation.

These are essentially the same equations as those of Zusman.[18] Our derivation of them, starting from a Hamiltonian, unambiguously resolves the difficulty faced by him in deciding what systematic force to associate with the off-diagonal components of n. In the next section we shall summarize his solution to these equations and obtain an answer for the reaction rate that is almost identical to that found in Sec. IV. We do this for the sake of completeness and also because it is useful to have a feeling for the approximations involved in real space as opposed to energy space which is what Zusman works in.

VI. SOLUTION OF THE SMOLUCHOWSKI EQUATION À LA ZUSMAN

The first step in solving Eqs. (5.23) is to Laplace transform them with respect to time. This is especially advantageous if one is looking for a solution in terms of an eigenfunction expansion as one often does for the ordinary Smoluchowski equation.[29,30] That is, suppose we assume a solution of the form

$$n_{\alpha\beta}(y,t)=\sum_i a_i n^{(i)}_{\alpha\beta}(y)\exp(-\Gamma_i t), \tag{6.1}$$

where $\mathrm{Re}(\Gamma_i)>0$, then its Laplace transform $\tilde{n}_{\alpha\beta}(y,\lambda)$ is given by

$$\tilde{n}_{\alpha\beta}(y,\lambda)=\sum_i a_i n^{(i)}_{\alpha\beta}(y)/(\lambda+\Gamma_i), \tag{6.2}$$

so that if we have an approximate solution for $\tilde{n}_{\alpha\beta}(y,\lambda)$, an examination of the poles and residues gives the eigenvalues and eigenfunctions. We shall be concerned mainly with the pole closest to the origin (which is then interpreted to be the decay rate), although some of the higher eigenvalues and eigenfunctions can also be found by simple extensions of what follows.

The crucial step is to argue that $\tilde{n}_{12}$ varies on a length scale, α, that is much shorter than μ, the length scale for $\tilde{n}_{11}$ and $\tilde{n}_{22}$. An estimate of α can be found by using the uncertainty principle, since a large value of $\tilde{n}_{12}$ implies a large uncertainty in the electronic state of the system. Thus, if n_{12} is appreciable over a region of width α near the crossing point y^*, the energy uncertainty is $F_\Delta\alpha$, while the time spent by the particle in this region is given by $\alpha^2\eta/kT$. Thus, since

$$(\Delta E)(\Delta t)\simeq(F_\Delta\alpha)(\alpha^2\eta/kT)\simeq\hbar, \tag{6.3}$$

$$\alpha=(\hbar kT/F_\Delta\eta)^{1/3}. \tag{6.4}$$

Note that as stated in the previous section, $\alpha\gg\sqrt{MkT}/\eta$ for large enough η, so the passage from the Fokker–Planck equation to the Smoluchowski equation is justified.

Under the assumptions that $\alpha y^*\ll\mu^2$, $\alpha^2\ll\mu^2$, and as long as we are interested in λ values less than $F_\Delta\alpha/\hbar$, the equation for $\tilde{n}_{12}(y,\lambda)$ can be simplified to an inhomogeneous Airy equation. The inhomogeneity is proportional to $(\tilde{n}_{11}-\tilde{n}_{22})$, which can be treated as a constant equal to its value at $y=y^*$ since it varies little over a length α. We now argue that for purposes of solving the $\tilde{n}_{11}$ and $\tilde{n}_{22}$ equations, the imaginary part of $\tilde{n}_{12}$ can be replaced by a delta function at $y=y^*$. Specifically, we write

$$\mathrm{Im}[\tilde{n}_{12}(y,\lambda)]=\frac{\pi}{2}l_{LZ}[\tilde{n}_{11}(y^*,\lambda)-\tilde{n}_{22}(y^*,\lambda)]\delta(y-y^*). \tag{6.5}$$

The resulting equations for $\tilde{n}_{11}$ and $\tilde{n}_{22}$ are nothing but the Laplace transforms of the decoupled equations for the time evolution of the probability distribution in either well with an initial delta function source at $y=y^*$. It is straightforward to solve them and obtain the eigenvalues and eigenfunctions. The procedure fails if $|\lambda_i|>F_\Delta\alpha/\hbar$, but this still allows us to get quite a few λ_i and $n^{(i)}$. For example, the eigenvalue second nearest to the origin is at $\lambda_2\simeq-\omega_c$, which is well separated from $\lambda_1=-\Gamma$, and indicates that a reaction rate can be sensibly defined. The result for Γ is

$$\Gamma = \frac{\Delta_0^2(\pi\hbar^2/E_r kT)^{1/2}}{4(1+g')} \times [\exp(-E_f/kT) + \exp(-E_b/kT)], \quad (6.6)$$

where g' is an adiabaticity parameter given by

$$g' = \frac{\pi}{2}(\Delta_0\tau_c)I_{LZ}(|y^* + y_0|^{-1} + |y^* - y_0|^{-1}). \quad (6.7)$$

Note that this is very similar to the adiabaticity parameter g defined in Eq. (4.20).

VII. CONCLUSIONS

We have shown in this paper how path integral techniques can be used to study a simple model for the coupling of a reaction coordinate to the many degrees of freedom present in a biomolecule. Our methods should be applicable to more complicated situations where it is necessary, e.g., to treat the direct coupling of the electronic degree of freedom to more than one coordinate. In particular, much will have been gained if it is possible to reduce these problems to Fokker–Planck equations since the latter can then be numerically solved. One of the possible interesting extensions is to consider two nuclear coordinates coupled to the electron transfer problem, one fast mode (e.g., an underdamped nuclear coordinate), and one slow mode (e.g., solvent polarization). The analysis of the different limits of this problem may lead us to understand several important biological electron transfers.

It is somewhat surprising that even when Δ_0 is large the rate obtained in the adiabatic limit is the one appropriate to diffusion over a one-dimensional potential with a cusp barrier and not the potential we would get by diagonalizing the electronic part of the Hamiltonian for each value of the reaction coordinate. While the distinction may not be important in practical terms, the conceptual point involved is important and interesting in itself. In hindsight, it is possible to understand it by invoking the "watched pot effect" which says that a quantum system in a state that is continually monitored by an external agency cannot evolve out of that state.[31] In our system, the bath, via the reaction coordinate, can be thought of as "observing" the z component of the spin. The higher the friction, the more frequent the observation. The electron is thus prevented from evolving out of the $|\pm\rangle$ states, and the one-dimensional potential in which the reaction coordinate diffuses is the one in which the electron has definite σ_z quantum numbers.

Perhaps the most important question that arises from this work is how the phenomenological friction coefficient η, or more generally, the spectral density, would be experimentally determined in any given situation. We feel it is important to address this issue, since the concept of a spectral density is a powerful tool in reducing the complex details of the bath-system interactions to a manageable degree, and retaining only those features that bear on the properties of the interesting degrees of freedom.

ACKNOWLEDGMENTS

We are indebted to J. J. Hopfield for introducing us to this problem, and to him, A. J. Leggett, and P. G. Wolynes for many fruitful discussions. In addition, A. G. would like to thank H. Frauenfelder and E. Shyamsunder for many informative and thought-provoking conversations, and J. N. O. would like to thank D. Beratan and A. da Gama in the same regard. The authors are supported, respectively, by the MacArthur professorship endowed by the John D. and Catherine T. MacArthur foundation; by the Brazilian Agency CNPq, the Universidade de São Paulo and the NSF (Grant No. PCM-8406049); and by the NSF (Grant No. DMR-8314625). This work was begun while A. G. and V. A. were at the Institute for Theoretical Physics at Santa Barbara; they were partially supported by the NSF (Grant No. PHY-7727084) supplemented by funds from the National Aeronautics and Space Administration, and they are grateful to the members of the Institute for their hospitality.

APPENDIX: FORMULAS FOR $G_1(t)$, $G_2(t)$, AND THE DAMPED HARMONIC OSCILLATOR

This Appendix contains formulas for the kernels G_1 and G_2 defined in Sec. II [see Eq. (2.26)] as well as some relevant information on the quantum mechanical damped harmonic oscillator.

It is straightforward to show that with $J_{eff}(\omega)$ given by Eq. (2.12), $G_1(t)$ is given by

$$G_1(t) = \frac{2My_0^2}{\hbar}[\omega_0 \sin(\omega_0 t)\exp(-\gamma t) + 2\gamma\{1 - \cos(\omega_0 t)\exp(-\gamma t)\}], \quad (A1)$$

where

$$\omega_0 = (\Omega^2 - \gamma^2)^{1/2}. \quad (A2)$$

Note that Eq. (A1) remains valid even if $\gamma > \Omega$. In particular, in the extreme overdamped limit, $\gamma \gg \Omega$, $G_1(t)$ can be approximated for all times large in comparison to γ^{-1} by

$$G_1(t) \simeq \frac{4My_0^2\gamma}{\hbar}[1 - \exp(-\omega_c t)], \quad (A3)$$

$$\omega_c = \Omega^2/2\gamma. \quad (A4)$$

For short times [$t \ll \omega_c^{-1}(\Omega^{-1})$ in the overdamped (underdamped) case], on the other hand,

$$G_1(t) \simeq 2My_0^2\Omega^2 t/\hbar = E_r t/\hbar. \quad (A5)$$

The evaluation of $G_2(t)$ is not quite so simple, and we shall limit ourselves to statements valid only if $\gamma \gtrsim \Omega/2$. If $kT/\hbar$ is large compared to the characteristic frequency ω_J associated with the maximum of $J_{eff}(\omega)$ (which varies from ω_0 for small γ/Ω to ω_c for large γ/Ω), we can use the small argument expansion of $\coth(\hbar\omega/2kT)$ in Eq. (2.26b). This gives

$$G_2(t) \simeq \frac{4My_0^2 kT}{\hbar^2}\left[2\gamma t - \left(\frac{4\gamma^2}{\Omega^2} - 1\right) + \exp(-\gamma t) \times \left\{\left(\frac{4\gamma^2}{\Omega^2} - 1\right)\cos(\omega_0 t) + \frac{\gamma}{\omega_0}\left(\frac{4\gamma^2}{\Omega^2} - 3\right)\sin(\omega_0 t)\right\}\right] + \cdots . \quad (A6)$$

In the highly overdamped limit this becomes (for $t \gg \gamma^{-1}$),

$$G_2(t) \simeq \frac{4My_0^2kT}{\hbar^2}\left(\frac{4\gamma^2}{\Omega^2}\right)[\omega_c t - 1 + \exp(-\omega_c t)] + \cdots . \tag{A7}$$

It should be noted that Eqs. (A6) and (A7) do *not* give the correct asymptotic behavior of $G_2(t)$ as $t \to \infty$. The leading term is linear in t with the indicated coefficient, but the next term, which is a constant, is not given correctly. What is more important is the time scale on which $G_2(t)$ is accurately given by the two leading terms in the asymptotic expansion. We expect this time scale to be the larger of $\hbar/kT$ and γ^{-1} in the underdamped case, and the larger of $\hbar/kT$ and ω_c^{-1} in the overdamped case. For times less than the smaller of these two times in either case, we can approximate $G_2(t)$ by expanding in powers of t. This gives (with $\beta \equiv 1/kT$),

$$G_2(t) \simeq t^2/2\tau_0^2 + \cdots , \tag{A8}$$

$$\tau_0^{-2} = \frac{4y_0^2}{\pi\hbar}\int_0^\infty d\omega\, J_{\rm eff}(\omega)\coth(\beta\hbar\omega/2). \tag{A9}$$

By using results contained in Appendix B of Ref. 12, this integral can be expressed entirely in terms of the mean square displacement of the reaction coordinate about its equilibrium position in either of the potentials wells $V(y;\pm)$, *provided* $V(y;\sigma_z)$ is given by the special form (1.4). In other words, suppose we constrain the electron to be in the $|+\rangle$ state, and couple the bath to the reaction coordinate as in Sec. I. The system is then effectively described by the Hamiltonian

$$H_{\rm osc} = \frac{1}{2M}P_y^2 + \tfrac{1}{2}M\Omega^2(y+y_0)^2 + \sum_\alpha\left[\frac{p_\alpha^2}{2m_\alpha} + \tfrac{1}{2}m_\alpha\omega_\alpha^2\left\{x_\alpha + \frac{c_\alpha}{m_\alpha\omega_\alpha^2}y\right\}^2\right] \tag{A10}$$

and the bath parameters satisfy Eq. (1.5). If we now construct the reduced density matrix $\rho_{++}(y,y')$ of the reaction coordinate by taking the trace of the full thermal equilibrium density matrix $\exp(-\beta H_{\rm osc})$ (suitably normalized) over the bath degrees of freedom, the mean square displacement μ^2 is given by

$$\mu^2 = \int_{-\infty}^{\infty} dy(y+y_0)^2\rho_{++}(y,y). \tag{A11}$$

Caldeira and Leggett[12] show that

$$\mu^2 = \frac{\hbar}{\pi M^2\Omega^4}\int_0^\infty d\omega\, J_{\rm eff}(\omega)\coth(\beta\hbar\omega/2). \tag{A12}$$

Therefore,

$$\tau_0^{-2} = (2M\Omega^2y_0\mu/\hbar)^2. \tag{A13}$$

Note that μ^2 is a function of both the temperature and the friction. For any given temperature it is always less than its zero-friction value:

$$\mu^2(\eta=0) = \frac{\hbar}{2M\Omega}\coth(\beta\hbar\Omega/2). \tag{A14}$$

Further, at high temperatures, irrespective of the damping, μ^2 acquires its "equipartition theorem" value $kT/M\Omega^2$. As the temperature decreases, so does μ^2, and it eventually crosses over to a low temperature value depending on the friction. The crossover temperature is also determined by the friction. Thus, in the underdamped regime

$$\mu^2 \simeq \frac{\hbar}{2M\omega_0}\left(\frac{2}{\pi}\tan^{-1}(\omega_0/\gamma)\right) \quad \text{for } kT \lesssim \hbar\Omega, \tag{A15}$$

while in the heavily overdamped regime

$$\mu^2 \simeq \frac{\hbar}{\pi M\gamma}\ln(2\gamma/\omega_0) \quad \text{for } kT \lesssim \hbar\omega_c\ln(\gamma/\Omega). \tag{A16}$$

[1](a) D. De Vault, Q. Rev. Biophys. **13**, 387 (1980); (b) *Tunneling in Biological Systems*, edited by B. Chance *et al.* (Academic, New York, 1977).
[2](a) R. A. Marcus, J. Chem. Phys. **24**, 966 (1956); (b) Discuss. Faraday Soc. **29**, 21 (1960); (c) J. Phys. Chem. **67**, 853, 2889 (1983); (d) Annu. Rev. Phys. Chem. **15**, 155 (1964); (e) J. Chem. Phys. **43**, 679 (1963).
[3](a) N. S. Hush, Trans. Faraday Soc. **57**, 557 (1961); (b) Electrochim. Acta **13**, 1005 (1968).
[4](a) V. G. Levich and R. R. Dogonadze, Dokl. Acad. Nauk SSSR **124**, 123 (1959); (b) V. G. Levich, Adv. Electrochem. Electrochem. Eng. **4**, 249 (1965).
[5]L. N. Grigorov and D. S. Chernavskii, Biofizica **17**, 195 (1972).
[6](a) J. J. Hopfield, Proc. Natl. Acad. Sci. U.S.A. **71**, 3640 (1974); (b) M. Redi and J. J. Hopfield, J. Chem. Phys. **72**, 6651 (1980).
[7](a) J. Jortner, J. Chem. Phys. **64**, 4860 (1976); (b) Biochim. Biophys. Acta **594**, 193 (1980).
[8]See, for example, J. J. Hopfield in Ref. 1(b).
[9](a) E. M. Kosower and D. Huppert, Chem. Phys. Lett. **96**, 433 (1983); (b) E. M. Kosower, Acc. Chem. Res. **15**, 259 (1982).
[10]L. D. Landau and E. M. Lifshitz, *Quantum Mechanics*, 3rd ed. (Pergamon, New York, 1977), Sec. 90.
[11]H. Frauenfelder and P. G. Wolynes [Science, **229**, 337 (1985)] have given a qualitative discussion of this point in the context of ligand binding to heme proteins. Their arguments, however, are more generally applicable.
[12]A. O. Caldeira and A. J. Leggett, Ann. Phys. (N.Y.) **149**, 374 (1983). This reference contains an exhaustive discussion of the justification for this procedure.
[13]P. G. Wolynes has been studying the same Hamiltonian and obtains results similar to ours (private communication to be published).
[14]To assist the reader, we note that the ensuing discussion [up to the end of the paragraph containing Eq. (1.7)] is devoted to a specification of the parameters in Eq. (1.3).
[15]H. A. Kramers, Physica (Utrecht) **7**, 284 (1940).
[16]S. Chandrasekhar, Rev. Mod. Phys. **15**, 3 (1943).
[17]A. J. Leggett, Phys. Rev. B **30**, 1208 (1984).
[18]L. D. Zusman, Chem. Phys. **49**, 295 (1980).
[19]S. Chakravarty and A. J. Leggett, Phys. Rev. Lett. **53**, 5 (1984).
[20]A. J. Leggett, S. Chakravarty, A. Dorsey, M. P. A. Fisher, A. Garg, and W. Zwerger (to be published).
[21]R. P. Feynman and F. L. Vernon, Ann. Phys. (N.Y.) **24**, 118 (1963).
[22]R. P. Feynman and A. R. Hibbs, *Quantum Mechanics and Path Integrals* (McGraw-Hill, New York, 1965).
[23]We reemphasize that the above maneuver for finding $J_{\rm eff}(\omega)$ is merely a labor saving device, and that the result [Eq. (2.17)] can be obtained by starting with the Hamiltonian [Eqs. (1.3) and (1.4)] and integrating out the bath oscillators $\{x_\alpha\}$ and then the reaction coordinate y by brute force.
[24]The reason for considering trajectories $\sigma(\tau)$ and $\lambda(\tau)$ extending all the way to $\tau \to -\infty$ has to do with subtle differences between the quantities $P^{(1)}(t)$ and $P^{(2)}(t)$ defined in Sec. 3 and Appendix B of Ref. 20.
[25]A more detailed discussion of this case has been given by (a) W. S. Bialek, Ph.D. thesis, University of California at Berkeley, 1983 (unpublished); (b) R. F. Goldstein and W. S. Bialek, Phys. Rev. B **27**, 7431 (1983).
[26]A. O. Caldeira and A. J. Leggett, Physica A **121**, 587 (1983).
[27]A further discussion of initial conditions is contained in V. Hakim and V. Ambegaokar, Phys. Rev. A **32**, 423 (1985).
[28]Since the equations that follow are somewhat complicated in appearance, it is worthwhile to summarize our notation here. Both x and y denote values of the reaction coordinate with $x(\tau)$ and $y(\tau)$ being the "forward" and the "backward" trajectories, respectively. Since we do not need to refer to the bath coordinates explicitly in this section, this should not cause any confusion. Similarly, σ and λ denote values of σ_z and $\sigma(\tau)$ and $\lambda(\tau)$ are the forward and backward spin trajectories. Finally, all initial values at time t_0 are denoted with primes, and all final values are unprimed.
[29]N. G. van Kampen, J. Stat. Phys. **17**, 71 (1977).
[30]H. Riskin, *The Fokker–Planck Equation* (Springer, Berlin, 1984), Sec. 5.4.
[31]M. Simonius, Phys. Rev. Lett. **40**, 980 (1978).

II.3 Some Aspects of Electron Transfer Dynamics

J. Phys. Chem. **90**, 3707 (1986)

Reprinted from The Journal of Physical Chemistry, 1986, 90, 3707

Some Aspects of Electron-Transfer Reaction Dynamics

José Nelson Onuchic,*†

Division of Chemistry and Chemical Engineering,‡ California Institute of Technology, Pasadena, California 91125

David N. Beratan,

Jet Propulsion Laboratory, California Institute of Technology, Pasadena, California 91109

and J. J. Hopfield§

Division of Chemistry and Chemical Engineering, California Institute of Technology, Pasadena, California 91125 *(Received: January 14, 1986)*

We present a simple, but complete, quantum mechanical model for electron transfer. It contains the elements necessary to calculate a rate: electron, reaction coordinate(s), and bath. The completeness of the model allows analysis of the dynamical aspects of the transfer (validity of the nonadiabatic, Born–Oppenheimer, and Condon approximations, for example). Interaction between the reaction coordinate(s) and the bath is discussed for "weak" and "strong" coupling, and the rate expression is derived in these limits. A model for donor and acceptor vibronic wave functions is solved exactly by using a molecular orbital approach. The rates are calculated from these states and a comparison with the standard Born–Oppenheimer/Condon result is made. The nature of the "inverted" effect is found to depend on transfer distance and details of the vibronic coupling.

I. Introduction

Simple electron-transfer reactions, reactions which do not involve bond formation or rupture, are of theoretical and experimental interest in physics, chemistry, and biology.[1] The success of the theoretical foundations provided by the Marcus, Hush, and Levich schools has been remarkable. Current theories provide a firm foundation for understanding the source of reaction rate differences as large as 10 orders of magnitude for similar reactions.[2-7] The electron-transfer problem nominally contains three elements: (1) an electron which is localized in distinct regions of space before and after transfer; (2) a "reaction coordinate(s)" which represents a combination of degrees of freedom of the environment directly coupled to the oxidation/reduction; (3) all other degrees of freedom of the environment which are not directly coupled to the electronic coordinate but create a bath which facilitates energy flow into and out of the reaction coordinate.

Standard approaches for calculating electron-transfer rates are generally useful in the adiabatic or nonadiabatic limit. The first one assumes that the relaxation of the reaction coordinate is much slower than electron exchange between trapping sites. This is the condition for adiabatic electron transfer and it has been extensively used for chemical electron-transfer rate calculations.[1d] In some long distance biological and other electron-transfer reactions[8] the opposite limit is assumed and a nonadiabatic analysis of the experiments is performed. In the latter case there are a few fundamental theoretical problems. Because the bath is not generally included in the Hamiltonian, a quantitative constraint on the condition that relaxation must be much faster than electron exchange cannot be obtained. Interest is growing in understanding the validity of this assumption.[9,10] Also, the dynamics of the motion along the reaction coordinate depends on the environment. In the quantum regime, the standard nonadiabatic calculations are unable to take this into account. Recent work in this group[9] and by Bialek and Goldstein[11] has considered this problem. We intend to address this point in some detail. There are also circumstances in which details of the coupling between electronic and reaction coordinate motion cannot be treated with the standard (Born–Oppenheimer, Condon) approximations. These difficulties with the conventional theories arise when time-scale separations are not valid.

The goal of this paper is to consider more general formulations of the electron-transfer problem. These models consider the dynamics of the electron transfer and relevant time scales needed to define a transfer event as being adiabatic or nonadiabatic. The Born–Oppenheimer and Condon approximations are considered in detail. Finally, connections are drawn with existing and proposed experiments.

This paper is structured as follows. Section II presents an electron-transfer Hamiltonian which includes the electron, reaction coordinate, and environment. Section III discusses the calculation of a transfer rate from the Hamiltonian of section II. The two-level nature of the problem and the Born–Oppenheimer approximations for the wave functions are discussed. The influence on the rate of the relationship between environmental and reaction coordinate

† On leave of absence from Instituto de Física e Química de São Carlos, Universidade de São Paulo, 13560, São Carlos, SP, Brazil.
‡ Contribution No. 7355.
§ Also Caltech Division of Biology and AT&T Bell Laboratories, Murray Hill, NJ 07974.

(1) (a) DeVault, D. *Quantum Mechanical Tunneling in Biological Systems*, 2nd ed.; Cambridge University Press: New York, 1984. (b) Chance, B.; DeVault, D. C.; Frauenfelder, H.; Marcus, R. A.; Schrieffer, J. R.; Sutin, N. Eds. *Tunneling in Biological Systems*; Academic Press: New York, 1979. (c) Marcus, R. A.; Sutin, N. *Biochim. Biophys. Acta* **1985**, *811*, 265. (d) Newton, M. D.; Sutin, N. *Annu. Rev. Phys. Chem.* **1984**, *35*, 437.
(2) (a) Marcus, R. A. *J. Chem. Phys.* **1956**, *24*, 966. (b) *Discuss. Faraday Soc.* **1960**, *29*, 21. (c) *J. Phys. Chem.* **1963**, *67*, 853, 2889. (d) *Annu. Rev. Phys. Chem.* **1964**, *15*, 155. (e) *J. Chem. Phys.* **1963**, *43*, 679. (f) In *Oxidases and Related Redox Systems*; King, T. E., Mason, H. S., Morrison, M., Eds.; Pergamon Press: New York, 1982; p 3.
(3) (a) Hush, N. S. *Trans. Faraday Soc.* **1961**, *57*, 557. (b) *Electrochim. Acta* **1965**, *13*, 1005.
(4) (a) Levich, V. G.; Dogonadze, R. R. *Dokl. Acad. Nauk SSSR* **1959**, *124*, 123. (b) Levich, V. G. *Adv. Electrochem. Electrochem. Eng.* **1965**, *4*, 249.
(5) Grigorov, L. N.; Chernavskii, D. S. *Biofizica* **1972**, *17*, 195.
(6) (a) Hopfield, J. J. *Proc. Natl. Acad. Sci. U.S.A.* **1974**, *7*, 3640. (b) Hopfield, J. J. *Biophys. J.* **1977**, *18*, 311. (c) Redi, M.; Hopfield, J. J. *J. Chem. Phys.* **1980**, *72*, 6651.
(7) (a) Kestner, N. R.; Logan, J.; Jortner, J. *J. Phys. Chem.* **1974**, *78*, 2148. (b) Jortner, J. *J. Chem. Phys.* **1976**, *64*, 4860. (c) Jortner, J. *Biochim. Biophys. Acta* **1980**, *594*, 193. (d) Bixon, M.; Jortner, J. *Faraday Discuss. Chem. Soc.* **1982**, *74*, 17.
(8) Mayo, S. L.; Ellis, W. R.; Crutchley, R. J.; Gray, H. B. *Science*, in press.
(9) Garg, A.; Onuchic, J. N.; Ambegaokar, V. *J. Chem. Phys.* **1985**, *83*, 4491.
(10) Frauenfelder, H.; Wolynes, P. G. *Science* **1985**, *229*, 337. (b) Wolynes, P. G. preprint, 1985.
(11) Goldstein, R. F.; Bialek, W. *Phys. Rev. B* **1983**, *27*, 7431.

0022-3654/86/2090-3707$01.50/0

frequencies is also considered. Section IV presents matrix element calculations for the nonadiabatic rate expression. The Born–Oppenheimer and Condon approximations are considered independently for electron-transfer mediated by a molecular bridge. Section V discusses the relevance of these theories to some experimental systems.

II. The Electron-Transfer Hamiltonian: Electron plus Reaction Coordinate plus Environment

The electron-transfer problem consists of an electron which moves between two trapping sites (donor and acceptor). This is not a purely electronic motion, because it is influenced by motions of some nuclei, which are called nuclear modes. In this section we write the "simplest" possible Hamiltonian necessary to represent this problem. By simplest, we mean that we use many crude approximations such as the one-electron model and a quadratic expansion of environmental degress of freedom. The validity of these approximations is discussed.

We consider, therefore, the following Hamiltonian

$$H_{ET} = \sum_{i=1}^{n} T_{\vec{r}_i} + \sum_{j=1}^{N} T_{R_j} + V_e(\vec{r}_1,...,\vec{r}_n) + V_N(R_1,...,R_N) + f(\vec{r}_1,...,\vec{r}_n,R_1,...,R_N) \quad (2.1)$$

where $\vec{r}_i$ represent the electronic coordinates (n electrons) and R_j the "nuclear" (environmental) coordinates (N modes). The corresponding many-dimensional nuclear potentials must have two well-separated minima which correspond to the states D^+A^- and DA^-. In eq 2.1 T is the kinetic energy, V is the electronic or "nuclear" potential energy, and f is the coupling between the electronic and the nuclear coordinates.

As an initial approximation, we choose a one-electron model for $V_e(\vec{r}_1,...,\vec{r}_n)$. This approach can be justified if only one electron moves between trapping sites and the others are closed core shells. Therefore, the interactions of the core electrons with each other and with the transfer electron are treated by establishing an effective potential $V_e(\vec{r})$ for the transfer electron. This is a reasonable approximation because the important part of the wave function, when there is weak coupling between orbitals, is its tail far from the atomic cores of the trapping sites. Far from the sites, the wave function can be factored as Ψ(transfer electron) × Ψ(core electrons). To normalize this state we need to know the entire wave function. This is done artifically by choosing the appropriate "depth" of the one-electron potential.[6c,12,13] The depth is chosen to give the wave function the proper asymptotic behavior far from the nuclei. This approximation is not expected to give realistic details of the states near the nuclei. When the transfer distance is small the one-electron model may no longer be valid. The adiabatic rate, however, is shown to be nearly independent of details of electronic structure.

The one-electron approximation has been used extensively in the electron-transfer literature. Textbook examples of wave function propagation in one-dimensional barriers provide the simplest description of long distance wave-function decay in a one-electron model.[14] Early considerations of the bridge mediated electron transfer problem employed one-electron models. Halpern and Orgel[15a] in 1960 first identified the importance of orbital symmetry, overlap, and energetics on the bridge mediated electronic interaction. McConnell[15b] in 1961 used a one-electron one orbital per bridge site model to describe electron exchange through a saturated bridge. A literature which allows estimates of the importance of electron or hole tunneling, and dependence of the electronic donor–acceptor interaction on redox potentials and bridge geometry is emerging.[16] Orientation effects on the tunneling matrix element for spheroidal constant potential models of porphyrins are under study as well.[12a] Information learned about these numerous effects is expected to carry through in some fashion to the many-electron problem. Quantitative experimental tests of one-electron models lie in the future.

The long distance electron-transfer problem is rather unique from a quantum chemical point of view. Variational methods which calculate long distance donor wave function propagation must be calculated with wave functions containing asymptotically accurate "tails" for a given tunneling energy. Variational calculations performed on wave functions expanded in incomplete or asymptotically incorrect basis sets can yield accurate energies because the calculation is insensitive to the low-amplitude details of the state. Accurate (or convergent) energies do not validate the asymptotic details of the calculated wave function. A discussion of the functional forms for the one-electron wave-function decay in a bridging medium has recently been given and a connection has been drawn between square well potential and molecular orbital models.[13a] Electronic potential models suppress the nuclear motion and vibronic coupling, considering only the electronic potential in a single nuclear configuration "corresponding" to the transition state. The current model includes both nuclear and electronic coordinates as well as coupling between them.

We now discuss the "nuclear" potential, $V_N(R_1,...,R_N)$. As previously described, $V_N(R_1,...,R_N)$ is the potential energy for all the degrees of freedom of the medium that surround the electron. We assume that $V_N(R_1,...,R_N)$ is quadratic in the coordinate space. This is a common assumption and is used mainly because it simplifies the mathematics and qualitatively, at least, models a binding energy surface. The harmonic approximation would provide inaccurate predictions if, in reality, some of the environmental degrees of freedom were strongly excited. The final part of the Hamiltonian (2.1), namely the coupling between electron and environment, $f(\vec{r},R_j)$, is a subject of section IV. It represents, for example, the observed changes in bond length and frequency accompanying reduction/oxidation.

The interesting electron-transfer problems are rather complicated. Because the environment or protein matrix has a very large number of degrees of freedom, it is helpful to write the electron–medium coupling in the Hamiltonian as depending only on a few nuclear coordinates, representing the notion that "most" of the medium modes are insensitive to the transfer event. A simple theoretical view of a single reaction coordinate is as follows. After performing a Born–Oppenheimer separation of the electronic and nuclear coordinates, the problem is left with a many-dimensional "nuclear" potential surface. One may then be able to identify a single "reaction coordinate" representing, for example, the direction in the multidimensional space along which the potential energy barrier is lowest. This is never done in practice. When it is known experimentally that the transferring electron is strongly coupled to medium modes with radically different dynamics, it is essential to use several nuclear coordinates. Some examples of reaction coordinates are localized vibrations of the donor or the acceptor molecules, solvent polarization, and gross protein motion.

We approximate $f(\vec{r},R_j)$ as being linear in R_j. This is consistent with the fact that $V_N(R_1,...,R_N)$ is assumed quadratic in the coordinate space; i.e., if higher order terms were necessary the harmonic approximation for the reaction coordinates would not be valid. If f had a term quadratic in R_j it would shift the frequency of the oscillators. However, even linear coupling of a nuclear mode to the electron causes small changes in the curvature of the potential surfaces. In most cases this shift is small and is neglected (see section IV). After making the approximations

(12) (a) Siders, P.; Cave, J.; Marcus, R. A. *J. Chem. Phys.* **1984**, *81*, 5613. (b) Cave, R. J. Ph.D. Thesis, California Institute of Technology, 1986. (c) Siders, P. Ph.D. Thesis, California Institute of Technology, 1983.

(13) (a) Beratan, D. N.; Onuchic, J. N.; Hopfield, J. J. *J. Chem. Phys.* **1985**, *83*, 5325. (b) Beratan, D. N. Ph.D. Thesis, California Institute of Technology, 1986.

(14) Bell, R. P. *The Tunnel Effect in Chemistry*; Chapman and Hall: New York, 1980.

(15) (a) Halpern, J.; Orgel, L. *Discuss. Faraday Soc.* **1960**, *29*, 32. (b) McConnell, H. M. *J. Chem. Phys.* **1961**, *35*, 508.

(16) (a) Larsson, S. *J. Chem. Soc., Faraday Trans. 2* **1983**, *79*, 1375. (b) Larsson, S. *J. Am. Chem. Soc.* **1981**, *103*, 4034. (c) Beratan, D. N.; Hopfield, J. J. *J. Am. Chem. Soc.* **1984**, *106*, 1584. (d) Hale, P. D.; Ratner, M. A. *Int. J. Quantum Chem. Quantum Chem. Symp.* **1984**, *18*, 195. (e) da Gama, A. A. S. *Theor. Chim. Acta* **1985**, *68*, 159. (f) Richardson, D. E.; Taube, H. *J. Am. Chem. Soc.* **1983**, *105*, 40. (g) Richardson, D. E.; Taube, H. *Coord. Chem. Rev.* **1984**, *60*, 107.

described above (one electron, quadratic wells, choice of reaction coordinate, linear coupling), we can rewrite the Hamiltonian (2.1) in the form

$$H_{ET} = T_{\vec{r}} + V_e(\vec{r}) + \sum_a \left[f_a(\vec{r})R_a + \frac{P_a^2}{2M_a} + \frac{1}{2}M_a\Omega_a^2 R_a^2 \right] + \sum_{b(bath)} \left\{ \frac{P_b^2}{2M_b} + \frac{1}{2}M_b\omega_b^2 \left[x_b + \sum_a \frac{c_{a,b}}{M_b\omega_b^2}R_a \right]^2 \right\} \quad (2.2)$$

$\vec{r}$ is the electronic coordinate, R_a's are the reactions coordinates, and x_b's are the remaining degrees of freedom of the environment coupled to the reaction coordinates. These coordinates (x_b's) are called "bath" in the remainder of this paper. The bath consists of all nuclear coordinates of the system which are coupled to the reaction coordinates.

For convenience the Hamiltonian (2.2) is written

$$H_{ET} = H^e + H^{m-e} + H^m + H^{m-b} \quad (2.3)$$

where

$$H^e = T_{\vec{r}} + V_e(\vec{r}) \quad (2.4a)$$

is the one-electron Hamiltonian

$$H^{m-e} = \sum_a f_a(\vec{r})R_a \quad (2.4b)$$

is the Hamiltonian including the coupling between the reaction (nuclear) coordinates and the electron

$$H^m = \sum_a \left\{ \frac{P_a^2}{2M_a} + \frac{1}{2}M_a\Omega_a^2 R_a^2 \right\} \quad (2.4c)$$

is the reaction coordinate(s) Hamiltonian, and

$$H^{m-b} = \sum_{b(bath)} \left\{ \frac{P_b^2}{2M_b} + \frac{1}{2}M_b\omega_b^2 \left[x_b + \sum_a \frac{c_{a,b}}{M_b\omega_b^2}R_a \right]^2 \right\} \quad (2.4d)$$

is the bath plus bath–reaction coordinate(s) coupling Hamiltonian.

Because this model utilizes a quadratic "nuclear" potential, we can diagonalize the bath Hamiltonian H^{m-b} via a transformation of normal modes, and write it in the form of eq 2.4d without loss of generality. This transformation of the bath to uncoupled harmonic oscillators, coupled only via the reaction coordinates, simplifies the algebra significantly. Including anharmonic interactions makes it impossible to uncouple the coordinates.[17]

With the electron-transfer Hamiltonian now defined, we calculate the associated electron-transfer rate. We define this rate as the negative time derivative of the natural logarithm of the absolute value of the probability of finding the electron on the acceptor minus its equilibrium probability. If this rate is much slower than the relaxation times of all reaction coordinates, it is constant in time and the probability of finding the electron on the donor varies exponentially in time. When this condition is not met, i.e., this derivative is not constant in time, the concept of a rate is meaningless. Comparisons of rates obtained with "standard" methods and those calculated with more complete models are made. "Standard" in this context means treatments which omit parts of the Hamiltonian in eq 2.2, make separations of coordinates, or make other simplifying assumptions when developing a rate expression.

III. The Two-Level Representation of the Electron-Transfer Problem: Approximation for the Donor/Acceptor Wave Function

The first two terms of Hamiltonian (eq 2.2), i.e., eq 2.4a and 2.4b, can be rewritten in the form

$$H^e + H^{m-e} = T_{\vec{r}} + V_D^e(\vec{r}) + V_A^e(\vec{r}) + V_M^e(\vec{r}) + \sum_{a=1}^{N_{RC}} [f_a^D(\vec{r}) + f_a^M(\vec{r}) + f_a^A(\vec{r})]R_a \quad (3.1)$$

or

$$H^e + H^{m-e} = T_{\vec{r}} + V_D(\vec{r},R_1,...,R_{N_{RC}}) + V_M(\vec{r},R_1,...,R_{N_{RC}}) + V_A(\vec{r},R_1,...,R_{N_{RC}}) \quad (3.2)$$

where

$$V_i = V_i^e(\vec{r}) + \sum_{a=1}^{N_{RC}} f_a^i(\vec{r})R_a, \quad \text{with i = D, M, or A} \quad (3.3)$$

Here D, M, and A are the donor, medium, and acceptor respectively. N_{RC} is the number of reaction coordinates. Models for this reaction coordinate–electronic coupling are shown in the next section and in the literature.[18,19] Usually f_a^M is neglected because most reaction coordinates are known to be locally coupled to the donor or acceptor.

Substituting 3.1 in 2.2, we get a Hamiltonian that can be characterized by two distinct zero-order electronic states, donor and acceptor, with some residual electronic coupling between them. To calculate the rate of the electron transfer, we assume that the electron is initially on the donor, neglecting the donor–acceptor exchange interaction, and that all the environmental coordinates of the system are in equilibrium. Then the coupling is turned on starting the time evolution of the entire system. The coupling between the two zero-order states is calculated by using first-order perturbation theory.

Now, we introduce two critical approximations to the problem. First we use the Born–Oppenheimer approximation. Then, for fixed nuclear coordinates (reaction and bath), we find[7a,12]

$$|T_{\vec{r}} + V_D + V_M|\Psi_D(\vec{r};R_1,...,R_{N_{RC}}) = |E_D^0 + \sum_a \lambda_a^D R_a|\Psi_D(\vec{r};R_1,...,R_{N_{RC}}) \quad (3.4a)$$

$$|T_{\vec{r}} + V_A + V_M|\Psi_A(\vec{r};R_1,...,R_{N_{RC}}) = |E_A^0 + \sum_a \lambda_a^A R_a|\Psi_D(\vec{r};R_1,...,R_{N_{RC}}) \quad (3.4b)$$

The coupling between the states is

$$T_{DA}(R_1,...,R_{N_{RC}}) = \langle\Psi_A|V_A|\Psi_D\rangle \quad \text{if } \langle\Psi_A|\Psi_D\rangle \ll 1 \quad (3.4c)$$

The Schrödinger equation (eq 3.4) is written for the electron and all nuclear coordinates directly coupled to the electron. The values of λ_a depend on the details of H^{m-e} and H^e. The condition in eq 3.4c is satisfied for large distance electron transfer. The assumption that the electronic energies in 3.4a and 3.4b are linear in R_a is consistent with the harmonic approximation. The second approximation used to calculate the rate is the Condon approximation, which fixes R_a's in all T_{DA}'s contributing to the rate at a *single* value. It is reasonable only when T_{DA} is weakly dependent on the λR_a terms. The validity of these approximations is discussed in section IV.

Using eq 3.4, the two localized electronic states can be represented as spins with $\sigma_z = \pm 1$. When Pauli matrices are used for the operators in this space, the Hamiltonian becomes

$$H_{ET} = T_{DA}\sigma_x + \frac{(E_D^0 + E_A^0)}{2} + \frac{(E_D^0 - E_A^0)}{2}\sigma_z + \sum_a \left[\frac{(\lambda_a^D + \lambda_a^A)}{2} + \frac{(\lambda_a^D - \lambda_a^A)}{2}\sigma_z \right] R_a + \frac{P_a^2}{2M_a} + \frac{1}{2}M_a\Omega_a^2 R_a^2 + \sum_{b(bath)} \left\{ \frac{P_b^2}{2M_b} + \frac{1}{2}M_b\omega_b^2 \left[x_b + \sum_a \frac{c_{a,b}}{M_b\omega_b^2}R_a \right]^2 \right\} \quad (3.5)$$

where we have employed a basis such that the localized electronic states are eigenstates of σ_z with eigenvalues +1 and −1. All details of the electronic structure of D, A, and M are contained in T_{DA}. Use of a single value for T_{DA} shows that a Condon separation was used. This representation yields the same Hamiltonian matrix equation as does eq 3.4. Replacing σ_x by $(a_D^\dagger a_A + a_A^\dagger a_D)$ and

(17) Bialek, W.; Goldstein, R. F. *Biophys. J.* **1985**, *48*, 1027.

(18) (a) Beratan, D. N.; Hopfield, J. J. *J. Chem. Phys.* **1984**, *81*, 5753. (b) Ivanov, G. K.; Kozhushner, M. A. *Sov. J. Chem. Phys.* **1984**, *1*, 1813.

(19) Ratner, M. A.; Madhukar, A. *Chem. Phys.* **1978**, *30*, 201.

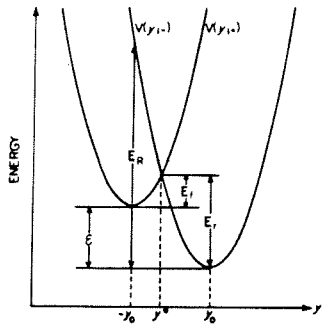

Figure 1. Potential energy surfaces for the reaction coordinate. The labels + and − refer to the donor and acceptor sites. The energies E_f, E_r, and E_R are the forward and reverse activation energies, and the reorganization energy, respectively.

σ_z by $(a_D^\dagger a_D - a_A^\dagger a_A)$ converts the Hamiltonian to the operator notation where $a^\dagger$ (a) creates (destroys) an electron on the donor (D) or acceptor (A).

Shifting the origins of all nuclear (reaction and bath) coordinates and the energy scale, and defining the driving force

$$\epsilon = E_D^0 - E_A^0 - \sum_\alpha \frac{(\lambda_\alpha^D)^2 - (\lambda_\alpha^A)^2}{2M_\alpha\Omega_\alpha^2} \tag{3.6a}$$

and the displacement

$$y_0^\alpha = \frac{\lambda_\alpha^D - \lambda_\alpha^A}{2M_\alpha\Omega_\alpha^2} \tag{3.6b}$$

Hamiltonian 3.5 can be rewritten as

$$H_{ET} = T_{DA}\sigma_x + \sum_\alpha \left\{ \frac{P_\alpha^2}{2M_\alpha} + \frac{1}{2}M_\alpha\Omega_\alpha^2(R_\alpha + y_0^\alpha\sigma_z)^2 \right\} + \frac{\epsilon}{2}\sigma_z + \sum_{b(bath)} \left\{ \frac{P_b^2}{2M_b} + \frac{1}{2}M_b\omega_b^2\left[x_b + \sum_\alpha \frac{c_{\alpha,b}}{M_b\omega_b^2}R_\alpha \right]^2 \right\} \tag{3.7}$$

If only one reaction coordinate is considered, this is the Hamiltonian used by Garg, Onuchic, and Ambegaokar.[9] In this section we generalize their results for the case of weak coupling to the bath, and consider some cases with two reaction coordinates. Two reaction coordinates, one representing the fast local vibrational modes and another the slow (perhaps "diffusive") modes such as solvent polarization, are needed to address many of the interesting dynamical questions concerning electron-transfer reactions. After solving the electron-transfer problem for one and two reaction coordinates, extensions to systems with larger numbers of coordinates is direct and simple.

Initially we analyze the one reaction coordinate problem with

$$H_{ET} = T_{DA}\sigma_x + \frac{P_y^2}{2M_y} + \frac{1}{2}M_y\Omega^2(y + y_0\sigma_z)^2 + \frac{\epsilon}{2}\sigma_z + \sum_{b(bath)} \left\{ \frac{P_b^2}{2M_b} + \frac{1}{2}M_b\omega_b^2\left[x_b + \frac{c_b}{M_b\omega_b^2}y \right]^2 \right\} \tag{3.8}$$

where y is the reaction coordinate. A schematic representation of the donor potential well $V(y;+)$ $(\sigma_z = 1)$ and acceptor potential well $V(y;-)$ $(\sigma_z = -1)$ is shown in Figure 1. It is not necessary to specify all the masses M_b, frequencies ω_b, and coupling constants c_b for bath oscillators, because we are not interested in the detailed dynamical behavior of the oscillators, but only how they influence motion along the reaction coordinates.[9,20] The *reduced* dynamics of the electron and reaction coordinate are influenced by the bath only through the spectral density[20]

$$J_0(\omega) = \frac{\pi}{2}\sum_{b(bath)} \frac{c_b^2}{M_b\omega_b}\delta(\omega - \omega_b) \tag{3.9}$$

How to experimentally measure the spectral density is still an open question (see also section V). Theoretically, it can be determined from the semiclassical equation of motion satisfied by the "particle".[20] In our case for fixed σ_z, if the motion on the reaction coordinate experiences a frictional force linearly proportional to its velocity with coefficient η; i.e., if

$$M_y\frac{d^2y}{dt^2} + \eta\frac{dy}{dt} + M_y\Omega^2(y + y_0) = F_{ext} \tag{3.10}$$

where F_{ext} is any external force, then

$$J_0(\omega) = \eta\omega\exp(-\omega/\Lambda), \quad \text{with } \Lambda \gg \Omega \tag{3.11}$$

If $J_0(\omega)$ is not given by the equation above, the classical equation of motion is no longer eq 3.10 and must be written with a frequency-dependent friction coefficient. In the quantum limit for a fixed σ_z, as shown in Appendix B, the spectral density is related to the broadening of the reaction coordinate energy levels. We show in this section that detailed knowledge about the bath is needed only when the nonadiabatic limit is invalid. In the nonadiabatic limit, it is only required that the reaction coordinate relaxation time be fast enough so that transitions from donor to acceptor are uncorrelated (see also Appendix B and in ref 9 and 10).

Because the reaction and bath coordinates are assumed harmonic, and the coupling between them is linear, we can diagonalize the quadratic part of Hamiltonian 3.8 (more generally 3.7), via a transformation to normal modes, and obtain the Hamiltonian

$$H_{ET} = T_{DA}\sigma_x + \frac{\epsilon}{2}\sigma_z + \sigma_z\sum_\beta \tilde{c}_\beta\tilde{x}_\beta + \sum_\beta \left[\frac{\tilde{p}_\beta^2}{2\tilde{m}_\beta} + \frac{1}{2}\tilde{m}_\beta\tilde{\omega}_\beta^2\tilde{x}_\beta^2 + \frac{\tilde{c}_\beta^2}{2\tilde{m}_\beta\tilde{\omega}_\beta^2} \right] \tag{3.12}$$

where $\tilde{x}_\beta$ are the normal (reaction plus bath) coordinates, and $\tilde{p}_\beta$, $\tilde{m}_\beta$, and $\tilde{\omega}_\beta$ are the corresponding canonical momenta, masses, and frequencies. H_{ET} now consists of a spin coupled to a set of mutually *noninteracting oscillators*. The spin is influenced by the oscillators (as in eq 3.9) only through the spectral density

$$J_{eff}(\omega) = \frac{\pi}{2}\sum_\beta \frac{\tilde{c}_\beta^2}{\tilde{m}_\beta\tilde{\omega}_\beta}\delta(\omega - \tilde{\omega}_\beta) \tag{3.13}$$

Calculations of $J_{eff}(\omega)$ for the situations considered in this paper are given in Appendix A.

Now we can calculate transfer rates. Let us consider two types of $J_0(\omega)$. The first distribution couples the reaction coordinate to modes with frequencies which vary from very slow to ones much faster than itself. The second distribution couples to bath modes much slower than the reaction coordinate. Let us consider the first case. Garg, Onuchic, and Ambegaokar[9] considered the spectral density $J_0(\omega)$ given by eq 3.11. As is shown in Appendix A, in the first case

$$J_{eff}(\omega) = \frac{\eta\omega\Omega^4 y_0^2}{(\Omega^2 - \omega^2)^2 + 4\omega^2\gamma^2} \tag{3.14}$$

where $\gamma = \eta/2M_y$ is the relaxation frequency of the reaction coordinate.

The results summarized here are valid only when friction is large enough so that there is no phase coherence between neighboring energy levels of the reaction coordinate, i.e., there are no sharp levels. (This is always true for $\gamma > \Omega/2$.)[9] Then, in the nonadiabatic limit, the probability of having the electron on the acceptor at time t is

$$P^A(t) = P_-^A - P_-^A\exp(-\Gamma_{na}t) \tag{3.15}$$

where

$$\Gamma_{na} = \Gamma_{na}^f + \Gamma_{na}^r \tag{3.16}$$

(20) (a) Caldeira, A. O.; Legget, A. J. *Ann. Phys. (N.Y.)* **1983**, *149*, 374. (b) *Physica A* **1983**, *121*, 587.

with

$$\Gamma_{na}^{f,r} = \frac{2\pi}{\hbar}\frac{|T_{DA}|^2}{(4\pi E_R kT_{eff})^{1/2}}\exp(-E_{f,r}/kT_{eff}) = \frac{2\pi}{\hbar F_\Delta}|T_{DA}|^2\rho_{D,A}(y^*) \quad (3.17)$$

$$P_\infty^A = \frac{1+\tanh(\epsilon/2kT_{eff})}{2} \quad (3.18)$$

Γ_{na}^{f} and Γ_{na}^{r} are the forward and reverse rates, and $\rho_{D,A}(y^*)$ is the probability of finding the nuclear mode ("particle") in the *intersection point between donor and acceptor wells when the* electron is on the donor (acceptor). F_Δ is the difference of slopes of the donor and acceptor potential wells at the crossing point. Figure 1 defines E_R (reorganization energy), E_f (forward activation energy), and E_r (reverse activation energy). The effective temperature, T_{eff}, is

$$kT_{eff} = M_y\Omega^2\mu^2(\eta,T) \quad (3.19)$$

where $\mu(\eta,T)$ is the mean square displacement of the reaction coordinate about its equilibrium value.[9] At high temperatures $T_{eff} = T$. Equation 3.15 is exactly the solution of the system of equations

$$\frac{dP^A(t)}{dt} = \Gamma_{na}^{f}P^D(t) - \Gamma_{na}^{r}P^A(t)$$

$$\frac{dP^D(t)}{dt} = -\Gamma_{na}^{f}P^D(t) + \Gamma_{na}^{r}P^A(t) \quad (3.20a)$$

with

$$P^A(t) + P^D(t) = 1 \qquad P^A(0) = 0 \quad (3.20b)$$

From 3.15 we note that P_∞^A is the equilibrium probability of finding the electron on the acceptor, exactly as expected from detailed balance.

The quantum rates given in eq 3.17 are valid only when there is no phase coherence between the energy levels of the reaction coordinate. They are identical with the semiclassical rates[9] obtained from a Landau–Zener[21] approach. The homogeneous broadening is large enough to generate a smoothly varying density of states for the reaction coordinate. The density of states is *not* a sequence of peaks separated by $\hbar\Omega$ and with width of order $\hbar\gamma$ ($\hbar\gamma$ is a lower bound for the width, see Appendix B for details). This form for the density of states is identical with that considered by Hopfield,[6] in his semiclassical model for electron transfer, although friction was never clearly included in the model. Generalization of eq 3.17 for more than one reaction coordinate can be done as proposed by Hopfield.[6a] When γ is not large enough to satisfy this condition, eq 3.17 is no longer valid (see eq 3.23 *and Appendix B*).

The nonadiabatic rate given by eq 3.17 is valid only when *each transit of the "particle" through the Landau–Zener region* is too rapid for the electron to make many transitions from donor to acceptor. A quantitative estimate for this condition is known.[9,10] The form of $J_0(\omega)$ does not have to be exactly the one considered in ref 9 (eq 3.11) but can have any form which broadens the energy levels enough to make the density of states smooth. For low temperatures, increasing friction reduces μ^2, but how friction acts is not important. When temperature is increased quantum effects are unimportant, $T \approx T_{eff}$, and no information about the bath can be obtained from the rate. Different $J_0(\omega)$'s give slightly different μ^2's, but the nonadiabatic rate is basically the same. Therefore, *if the nonadiabatic limit holds, details about* $J_0(\omega)$ *cannot be* extracted from electron-transfer rates.

When $\gamma \gg \Omega$, the motion of the reaction coordinate is overdamped. In this case the characteristic time of the reaction coordinate is given by $\tau_c = \omega_c^{-1}$, where $\omega_c = \Omega^2/2\gamma$. In this situation (assuming $kT \gg \hbar\Omega^2/2\gamma$, which is true for real diffusive modes such as solvent polarization), the electron-transfer rate is

$$\Gamma^{f,r} = \frac{2\pi}{\hbar}\frac{|T_{DA}|^2}{(4\pi E_R kT)^{1/2}}\left[\frac{1}{1+(2\pi|T_{DA}|^2/\hbar\omega_c E_R)}\right]\exp(-E_{f,r}/kT) \quad (3.21)$$

If an "adiabaticity" parameter g is defined

$$g = \frac{2\pi|T_{DA}|^2}{\hbar\omega_c E_R} \quad (3.22)$$

the reaction is adiabatic or nonadiabatic depending on whether g is large or small. g is the ratio between the time spent by the "particle" (reaction coordinate) in the Landau–Zener region (exactly the time it takes the particle to drift out of this region) and the time taken by one transition from donor to acceptor ($\hbar/|T_{DA}|$).

The rates in eq 3.21 are valid only when $J_0(\omega)$ is given by eq *3.11 and* $\gamma \gg \Omega$. *Under these circumstances the reaction coordinate* is diffusive[9] with diffusion constant $D = kT/\eta$. In this situation, principally in the adiabatic limit, details about the spectral density are important. If $J_0(\omega)$ is not given by eq 3.11 then η is frequency-dependent. Equation 3.21 shows that the adiabatic correction to the nonadiabatic limit is a function of ω_c, the relaxation time of the reaction coordinate. When the adiabatic limit is reached, the rate becomes proportional to ω_c and independent of T_{DA}. In this limit the condition for validity of eq 3.21, $\Gamma^{f,r} \ll \omega_c$, depends on the size of $E_{f,r}$. If this condition is violated, the transfer is nonexponential in time.

Therefore, we conclude that when "adiabatic" corrections are important, knowledge about how relaxation of the reaction coordinate occurs is necessary. Equation 3.21 is a particular example for $J_0(\omega)$ given by eq 3.11 and $\gamma \gg \Omega$. For a different spectral density, the "adiabatic" result depends on it, and the rates given by eq 3.21 are no longer valid; i.e., the rates depend strongly on the reaction coordinate relaxation time, which is not true in the nonadiabatic limit.

Although assuming η *frequency-independent is an oversim*plification, this kind of approach (in the overdamped limit) has proven to be useful in cases such as solvent polarization.[33] The results of ref 33, and experimental measurements of dielectric constants for polar solvents which obey the Debye form,[22] are experimental examples which justify this model in these particular cases.

We now consider the situation where the width of the reaction coordinate energy levels is much smaller than $\hbar\Omega$, but large enough so that the nonadiabatic limit still holds. We call this situation the extreme nonadiabatic limit, and the detailed evaluation of the electron-transfer rate is given in Appendix B. When this condition is satisfied, the rate is

$$\Gamma_{na}^{f} = \frac{2\pi}{\hbar}|T_{DA}|^2(FC) \quad (3.23)$$

where (FC) is the thermally averaged Franck–Condon factor

$$(FC) = \sum_{i_d}\sum_{i_a}\rho(E_{i_d}^D,T)|\langle\phi_{i_d}^D|\phi_{i_a}^A\rangle|^2\hbar(E_{i_d}^D - E_{i_a}^A) \quad (3.24)$$

$\rho(E_{i_d}^D)$ is the donor thermal density of states and ϕ's are the reaction coordinate eigenfunctions, neglecting the coupling to the bath. The function $\hbar(E^D - E^A)$ has $\int\hbar(E)\,dE = 1$ and is highly peaked when $E^D = E^A$ (see Appendix B). Because the width of $\hbar(E)$ is much smaller than $\hbar\Omega$, $\delta(E)$ is normally substituted for it to simplify the algebra, although the delta function is conceptually wrong. Generalization of this Franck–Condon factor for larger numbers of reaction coordinates is straightforward.[7b,23]

To eliminate the peaks of the Franck–Condon factor, it is necessary to include inhomogeneous broadening to generate a smooth density of states on the acceptor. Under this assumption

(21) Landau, L. D.; Lifshitz, E. M. *Quantum Mechanics*, 3rd ed.; Pergamon Press: New York, 1977; Section 90.

(22) McConnell, J. *Rotational Brownian Motion and Dielectric Theory*; Academic Press: New York, 1980.

(23) Siders, P.; Marcus, R. A. *J. Am. Chem. Soc.* **1981**, *103*, 741, 747.

we can change $\sum_{i_q}$ to $\int dE^A/\hbar\Omega$, and the Franck–Condon factor (FC) becomes

$$(FC) = \sum_{i_q} \frac{\rho(E_{i_q}{}^D, T)}{\hbar\Omega} |\langle \phi_{i_q}{}^D | \phi_{i_q}{}^A{}_{+n} \rangle|^2 \qquad (3.25)$$

where $\epsilon = n\hbar\Omega$ and n is an integer.

The rate given by eq 3.23 is exactly the one calculated by Jortner,[7c,d] and is usually referred to as the quantum model in the electron-transfer literature. In this case, details of $J_0(\omega)$ are unnecessary, as long as there is very little broadening of the reaction coordinate energy levels, but sufficient brodening to guarantee the nonadiabatic limit.

In summary, the nonadiabatic rate is given by eq 3.17 *or* eq 3.23, depending on the strength of the coupling to the bath. Eq 3.23 is correct in the weak damping limit. When friction becomes large enough so that the reaction coordinate density of states is smooth, the rates in eq 3.17 are the correct ones. These rates have the same functional form as the ones obtained in Hopfield's semiclassical model.[6]

In the remainder of this section, we consider the situation where *one reaction coordinate is much faster than the remaining nuclear* coordinates, bath, or other reaction coordinates. Calling the frequency of this fast mode Ω_f, we only work in the limit of $\hbar\Omega_f \gg kT, \epsilon$. These conditions are necessary so that thermal excitations of this fast coordinate are unimportant. In this case, we can simplify the problem to a new two-level problem including the electron plus the fast reaction coordinate.

We now consider the second type of $J_0(\omega)$ for the one reaction coordinate case; i.e., all the bath modes are much slower than Ω in eq 3.8. For this case, we transform eq 3.8 to eq 3.12, and get (see Appendix A)

$$J_{eff}(\omega) \approx J_0(\omega) y_0^2 + \frac{\pi}{2} M_y \Omega^3 y_0^2 \delta(\omega - \Omega) \qquad (3.26)$$

In this case the reaction coordinate is weakly influenced by the bath modes because it is much faster than them.

Because $J_{eff}(\omega)$ has two well-defined frequency regions, the problem is solved by using the method of Leggett et al.[24a] The calculation proceeds in two stages. First, we replace $J_{eff}(\omega)$ with its high-frequency component

$$J'_{eff}(\omega) \approx \frac{\pi}{2} M_y \Omega^3 y_0^2 \delta(\omega - \Omega) \qquad (3.27)$$

so the Hamiltonian to be solved is

$$H'_{ET} = T_{DA}\sigma_x + \frac{P_y^2}{2M_y} + \frac{1}{2} M_y \Omega^2 (y + y_0\sigma_z)^2 + \frac{\epsilon}{2}\sigma_z \qquad (3.28)$$

Assuming that the reaction coordinate is much faster than the spin, a kind of Born–Oppenheimer approximation can be performed. The Born–Oppenheimer solution for this ground state is

$$H'_{ET}\phi(y;\sigma_z) = \left\{ T_{DA}\sigma_x + E_0(\sigma_z) + \frac{\epsilon}{2}\sigma_z \right\} \phi(y;\sigma_z) \qquad (3.29)$$

Using the fact that for eq 3.28 $E_0(\sigma_z{=}1) = E_0(\sigma_z{=}-1)$, and making the appropriate shift in the origin of the energy scale, the Hamiltonian we have to solve is then

$$H'_{ET} = T_{DA}{}^{eff}\sigma_x + \frac{\epsilon}{2}\sigma_z \qquad (3.30a)$$

where

$$T_{DA}{}^{eff} = T_{DA}\langle \phi_0(y;\sigma_z{=}1) | \phi_0(y;\sigma_z{=}-1) \rangle = T_{DA}\langle \phi_0{}^D | \phi_0{}^A \rangle \qquad (3.30b)$$

We can now proceed to stage two. Taking into account the low-frequency modes, the Hamiltonian is

$$H_{ET} = T_{DA}{}^{eff}\sigma_x + \frac{\epsilon}{2}\sigma_z + \sigma_z \sum_\beta \tilde{c}_\beta \tilde{x}_\beta + \sum_\beta \left[\frac{\tilde{p}_\beta^2}{2\tilde{m}_\beta} + \frac{1}{2}\tilde{m}_\beta \tilde{\omega}_\beta^2 \tilde{x}_\beta^2 + \frac{\tilde{c}_\beta^2}{2\tilde{m}_\beta \tilde{\omega}_\beta^2} \right] \qquad (3.31a)$$

where

$$J''_{eff}(\omega) = \frac{\pi}{2} \sum_\beta \frac{\tilde{c}_\beta^2}{\tilde{m}_\beta \tilde{\omega}_\beta} \delta(\omega - \tilde{\omega}_\beta) = J_0(\omega) y_0^2 \qquad (3.31b)$$

Calculation of rates for this problem, principally when $J_0(\omega)$ satisfies 3.11, has been performed extensively by Leggett et al.[24] They have shown that the condition for validity of the nonadiabatic limit is that spin flips (transfer from donor to acceptor) to incoherent. When this condition holds, the rate is proportional to $|T_{DA}{}^{eff}|^2$ with

$$\Gamma_{na} = \frac{2\pi}{\hbar} |T_{DA}{}^{eff}|^2 \tilde{\rho}(\epsilon, T, J'') \qquad (3.32)$$

where $\tilde{\rho}$ has dimension of reciprocal energy, and depends on the coupling to the bath, ϵ, and temperature.

We finally consider electron transfer coupled to two reaction coordinates. The Hamiltonian is

$$H_{ET} = T_{DA}\sigma_x + \frac{P_y^2}{2M_y} + \frac{1}{2} M_y \Omega_y^2 (y + y_0\sigma_z)^2 + \frac{\epsilon}{2}\sigma_z + \frac{P_z^2}{2M_z} + \frac{1}{2} M_z \Omega_z^2 (z + z_0\sigma_z)^2 + \sum_{b(bath)} \left\{ \frac{P_b^2}{2M_b} + \frac{1}{2} M_b \omega_b^2 \left[x_b + \frac{c_b{}^y}{M_b \omega_b{}^2} y + \frac{c_b{}^z}{M_b \omega_b{}^2} z \right]^2 \right\} \qquad (3.33)$$

and $J_0{}^y(\omega)$ and $J_0{}^z(\omega)$ are the spectral densities for the y and z coordinates, respectively.

A particular case of eq 3.33, which may be very useful for real systems, has y, a fast local vibrational mode, and z, a slow reaction coordinate. Solvent polarization might be modeled with the z coordinate. It is reasonable to assume that Ω_y is much faster than all bath modes. We consider the case in which the bath has frequencies which vary from very slow to much faster than Ω_z. Under these circumstances eq 3.33 can be transformed to eq 3.12 (see Appendix A) with the spectral density

$$J_{eff}(\omega) \approx J_{eff}{}^z(\omega) + J_{eff}{}^y(\omega) \qquad (3.34a)$$

Because the $J_{eff}{}^z(\omega)$ satisfies eq A.11, it is strongly peaked around Ω_z. The slow part of $J_{eff}{}^y(\omega)$ can be neglected, and the equation above can be rewritten as

$$J_{eff}(\omega) \approx J_{eff}{}^z(\omega) + \frac{\pi}{2} M_y \Omega_y{}^3 y_0{}^2 \delta(\omega - \Omega_y) \qquad (3.34b)$$

In a way similar to eq 3.30, the fast mode y renormalizes T_{DA}, i.e.

$$T_{DA}{}^{eff} = T_{DA}\langle \phi_{0,y}{}^D | \phi_{0,y}{}^A \rangle \qquad (3.35)$$

and the problem we are left with is exactly the first case of the single reaction coordinate. By analogy to the beginning of the section, when the nonadiabatic limit holds the rates are exactly as in eqs 3.17 and 3.23

$$\Gamma_{na}{}^f = \frac{2\pi}{\hbar} \frac{|T_{DA}{}^{eff}|^2}{(4\pi E_R{}^z kT_{eff})^{1/2}} \exp(-E_f{}^z / kT_{eff}) \qquad (3.36a)$$

if damping is strong enough, or

$$\Gamma_{na}{}^f = \frac{2\pi}{\hbar} |T_{DA}{}^{eff}|^2 \sum_{i_q} \frac{\rho(E_{i_q}{}^D, T)}{\hbar\Omega_z} |\langle \phi_{i_q,z}{}^D | \phi_{i_q+n,z}{}^A \rangle|^2 \qquad (3.36b)$$

in the weak damping limit, and $\epsilon = n\hbar\Omega_z$.

The conditions for the validity of the nonadiabatic limit are exactly the same for the single-mode problem. The fast-mode

(24) (a) Leggett, A. J.; Chakravarty, S.; Dorsey, A.; Fisher, M. P. A.; Garg, A.; Zwerger, W., preprint, 1985. (b) Chakravarty, S.; Leggett, A. J. *Phys. Rev. Lett.* **1984**, *53*, 5.

y only renormalizes T_{DA}. If, for example, z is overdamped, we can calculate the rate in analogy to eq 3.21, and get

$$\Gamma^{f,r} = \frac{2\pi}{\hbar}\frac{|T_{DA}^{eff}|^2}{(4\pi E_R{}^z kT)^{1/2}}\left[\frac{1}{1+(2\pi|T_{DA}^{eff}|^2/\hbar\omega_c E_R{}^z)}\right]\times \exp(-E_{f,r}{}^z/kT) \quad (3.37)$$

The adiabaticity parameter g is the same as eq 3.22 replacing T_{DA} by T_{DA}^{eff}.

Another interesting case of eq 3.31 occurs when the relaxation of the fast mode is faster than the motion of the slow mode. In this case we can define a "rate" for the fast part of the problem which is a function of the slow-mode coordinate. Some work in this limit has been performed.[25]

IV. Matrix Element Calculation: Exact and Born–Oppenheimer/Condon Results

In the previous section some nonadiabatic rates were found to be proportional to the sum of squared Hamiltonian matrix elements. The matrix elements were approximated as the product of electronic and nuclear factors. The nuclear wave functions in such a calculation neglect the damping effects. These rates (eq 3.24, 3.32, and 3.36b) are appropriate when coupling to the bath is weak and/or when there is a fast reaction coordinate which renormalizes the electronic matrix element. The goal of this section is to calculate these nonadiabatic matrix elements exactly for a simple model, and to investigate the validity of the Born–Oppenheimer and Condon approximations.

When the nonadiabatic weak damping limit is applicable the bath broadens the vibronic levels of the donor and acceptor. We work in the limit that the broadening guarantees nonadiabaticity but is not so large that the vibronic levels are mixed. The transfer rate from a single donor state is (see Appendix B and eq 3.24)

$$\Gamma_{na}{}^f = \frac{2\pi}{\hbar}\sum_F |(\Psi_D|V_A|\Psi_A{}^F)|^2\hbar(E_D - E_A{}^F) \quad (4.1)$$

Applying the Born–Oppenheimer and Condon approximations to the sum of matrix elements gives

$$\sum_F |(\Psi_D(\vec{x},R_1...R_{N_{RC}})|V_A|\Psi_A{}^F(\vec{x},R_1...R_{N_{RC}}))|^2\hbar(E_D - E_A{}^F) \quad (4.2a)$$

$$\simeq |T_{DA}|^2\sum_F |(\phi_D(R_1...R_{N_{RC}})|\phi_A{}^F(R_1...R_{N_{RC}}))|^2\hbar(E_D - E_A{}^F) \quad (4.2b)$$

If the model includes vibrations on both sites, the nuclear coordinates appear in both donor and acceptor wave functions. We must first formulate a vibronic Hamiltonian relevant to the initial and final states and find the wave functions for these states, in order to evaluate the perturbation matrix element. Qualitative estimates of the errors which arise from approximations in all stages of the calculation are beginning to emerge.[1d,2f,13a,18] The goal of this section is to complete a nonadiabatic rate calculation from beginning to end evaluating the validity of the common approximations (Born–Oppenheimer and Condon) which are made along the way.

We connect with the previous section by considering the electron-transfer Hamiltonian

$$H_{ET} = H^e + H^{n-e} + H^n \quad (4.3)$$

We present models for each part of eq 4.3 and solve eqs 4.4 for the localized states:

$$H_{D,M}\Psi_D(\vec{x},R_1,...,R_{N_{RC}}) = [T_r + V_D + V_M + H^n]\Psi_D = E\Psi_D \quad (4.4a)$$

$$H_{A,M}\Psi_A(\vec{x},R_1,...,R_{N_{RC}}) = [T_r + V_A + V_M + H^n]\Psi_A = E\Psi_A \quad (4.4b)$$

(25) (a) Agmon, N.; Hopfield, J. J. *J. Chem. Phys.* **1983**, *78*, 6947. (b) Sumi, H.; Marcus, R. A. *J. Chem. Phys.* **1986**, *84*, 4272.

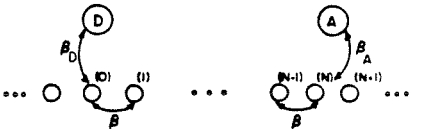

Figure 2. Arrangement of the donor, acceptor, and bridging orbitals.

The first model includes one-nuclear mode linearly coupled to a single bound electron. The electronic potential is assumed to be of a form[13a] so that a tight-binding or molecular orbital model is appropriate. For systems with polymeric bridges of variable length, a periodic approximation for V_M is expected to be a good starting point. If the amplitude near the boundary is small it is an adequate approximation to continue the "bridging" medium indefinitely to the left and right of the donor and acceptor sites. The transfer rate is calculated for the exact and Born–Oppenheimer states. The conventional Condon approximation is discussed for the Born–Oppenheimer states. Next, we consider models with one oscillator on the donor and one on the acceptor. Finally, we present a prescription for calculating exact wave functions when more than one oscillator is on the donor or acceptor site. The relevance of the approximate and exact expressions to experimentally measured transfer rates is discussed in section V.

Vibronic Model for One-Nuclear Mode. Wave functions decay in regions of space where the potential energy exceeds the energy of the state. This decay may be calculated with surprisingly few free parameters if the potential in the nonclassical regions is periodic and the amplitude of the donor or acceptor state at the boundary of the periodic potential is very small (i.e., minimal reflection at the boundary).[13] In the periodic molecular orbital limit such a model allows us to write the donor (acceptor) plus medium electronic Hamiltonian

$$H^e{}_{D,M} = \Delta_D a_D{}^\dagger a_D + \beta_D(a_0{}^\dagger a_D + a_D{}^\dagger a_0) + \sum_n \beta(a_n{}^\dagger a_{n+1} + a_n{}^\dagger a_{n-1}) \quad (4.5a)$$

$$H^e{}_{A,M} = \Delta_A a_A{}^\dagger a_A + \beta_A(a_N{}^\dagger a_A + a_A{}^\dagger a_N) + \sum_n \beta(a_n{}^\dagger a_{n+1} + a_n{}^\dagger a_{n-1}) \quad (4.5b)$$

Δ_D and Δ_A are negative and are the binding energies of the isolated donor and acceptor relative to the energy of an isolated bridge orbital. The fermion operators create (†) or annihilate an electron on a donor ($\theta_D(\vec{r})$), acceptor ($\theta_A(\vec{r})$), or bridge site orbital ($\theta_n(\vec{r}-n\vec{a})$, $n = 0, \pm1, \pm2, ...$). $\beta_{D(A)}$ is the donor (acceptor) interaction ($(\theta_{D(A)}(\vec{r})|H|\theta_{0(N)}(\vec{r}))$) with the nearest bridge orbital. Eigenfunctions of these electronic Hamiltonians have been discussed at length.[15b,26]

The Hamiltonian for the one vibrational mode coupled to the electron is

$$H^n + H^{n-e} = (b^\dagger b + \tfrac{1}{2})\hbar\Omega - \lambda(b^\dagger + b)a_D{}^\dagger a_D \quad (4.6)$$

The boson operators create ($b^\dagger$) or annihilate (b) a vibration on the oscillator and $(b^\dagger + b) = (2M_y\Omega/\hbar)^{1/2}y$. The mode is localized on the donor in this example. Coupling between the electron and the nuclear mode is linear in the nuclear coordinate so a term proportional to y is added to the Hamiltonian "when" the electron is on the donor. Exact eigenfunctions of H^e and H^n are well-known.[15b,26] However, the electron-vibrational coupling adds considerable complexity to the problem.

Because the bridging potential is periodic, wave function decay far from the donor is determined by the exchange interaction between bridging sites and the energy of the bound state.[16c] For simplicity only one basis function is placed on each bridging group, leading to one band of bridge localized states to assist the tunneling. Since the bridges of interest are saturated, the energies of the donor and acceptor localized states are outside of this band.

(26) Davydov, A. S. *Phys. Status Solidi B* **1978**, *90*, 457.

Exact Eigenfunctions. Since the Hamiltonian is a function of two variables, the eigenfunctions of

$$H_{D,M} = H^{e}_{D,M} + H^{n} + H^{n-e} \tag{4.7}$$

are

$$\Psi^{D} = \sum_j g_j \chi_j(\vec{r})\phi_j(y) \tag{4.8}$$

where $\phi_j(y)$ solves the nuclear Schrödinger equation in the absence of the electron (harmonic oscillator with origin $y = 0$) and the $\chi_j(\vec{r})$'s are not orthogonal states. In analogy with the solution of the electronic Schrödinger equation described by Davydov,[26] integration of the complete donor Schrödinger equation yields

$$\Psi^{D}(\vec{r},y) = \sum_j \left\{ g_j\phi_j(y)\left[\theta_D(\vec{r}) + \frac{\beta_D}{(E_j^2 - 4\beta^2)^{1/2}} \sum_n \tilde{\epsilon}_j^{|n|}\theta_n(\vec{r} - n\vec{a}) \right] \right\} \tag{4.9}$$

$$\tilde{\epsilon}_j + \frac{1}{\tilde{\epsilon}_j} = \frac{E_j}{\beta} \tag{4.10a}$$

$$E_j = E^{\text{total}} - (j + 1/2)\hbar\Omega \tag{4.10b}$$

where

$$g_j\left[\Delta_D - \frac{\beta_D^2}{(E_j^2 - 4\beta^2)^{1/2}} - E_j \right] - \lambda[g_{j+1}(j+1)^{1/2} + g_{j-1}j^{1/2}] = 0 \tag{4.11}$$

$\tilde{\epsilon}$ is used here to distinguish the wave function decay constant[16c] from the driving force of the reaction, ϵ. The donor localized state has $|\tilde{\epsilon}_j| < 1$. This result is valid when the energy shift of the donor localized state caused by the bridge is small relative to the binding energy of the donor. g_j is a mixing constant defined by the energy of the state. A similar calculation was performed with δ function binding and coupling potentials.[18a] The main difference between the molecular orbital and the δ function coupled wave functions is that the decay length of $\chi_j(\vec{r})$ in the orbital model has a logarithmic dependence on the binding energy (if $\tilde{\epsilon} \ll 1$, $\tilde{\epsilon}_j \simeq E_j/\beta$) rather than a square root dependence.[13a]

Two methods can be used to find the energy eigenvalues. One calculates the g_j's for a particular energy guess (from the Born–Oppenheimer energy) and examines the behavior of g_j for large j. These coefficients converge to zero for large j when the eigenvalue is found and diverge rapidly otherwise. An alternate method is to cast the recursion relation in matrix form:

$$\begin{pmatrix} \Delta_D - E_0 & -\lambda & 0 & 0 & \cdots \\ -\lambda & \Delta_D - E_1 & -\lambda\sqrt{2} & 0 & \cdots \\ 0 & -\lambda\sqrt{2} & \Delta_D - E_2 & -\lambda\sqrt{3} & \cdots \\ 0 & 0 & -\lambda\sqrt{3} & \Delta_D - E_3 & \cdots \\ \vdots & \vdots & \vdots & \vdots & \ddots \end{pmatrix} \begin{pmatrix} g_0 \\ g_1 \\ g_2 \\ g_3 \\ g_4 \\ \vdots \end{pmatrix} = 0 \tag{4.12}$$

β_D and β are small compared to the binding energy of the localized state in the case of interest, so terms of order $\beta_D^2/(E_j^2 - 4\beta^2)^{1/2}$ have been neglected in 4.12. The first condition is true if the presence of a bridge is known *not* to affect the energy of the transferring localized electron. The second condition is necessary for the tight-binding model to be applicable. $\Delta_D - E_j$ is of the order $\lambda^2/\hbar\Omega + n\hbar\Omega$ for the ground state. The validity of these assumptions in real systems has been discussed elsewhere.[13a]

The g_j's decay very rapidly with j (as $[\exp(-\gamma)\gamma^j/j!]^{1/2}$ in the ground state, $\gamma = (\lambda/\hbar\Omega)^2$, see Appendix C) and excellent approximations can be made by truncating the matrix and finding the roots numerically. More generally, Appendix C proves that for any coupled state $n, g_j^{(n)} \simeq \langle j|n\rangle$ where j and n are harmonic oscillator eigenstates with equilibrium positions differing by $2y_0$.

The amplitude of the wave function on the Nth orbital of the bridge is proportional to $\tilde{\epsilon}_j^N$ where j is the number of vibrations in the donor oscillator. For $|\tilde{\epsilon}| \ll 1$, $\tilde{\epsilon}_j \simeq \beta/[E - (j + 1/2)\hbar\omega]$. A coupled donor state presents a *linear combination* of exponentially decaying parts to the acceptor and the observed rate can include contributions from one or more of these tails depending on the vibronic details of the acceptor. The oscillator states in which the wave function was expanded have the equilibrium displacement of the ionized donor. Hence, when $|\vec{r}|$ is very small g_i must correspond to the projection of the oscillator states for the system with the electron on the states of the shifted oscillator. Coupling problems of this form, when solved exactly, are rather complex because the coupling introduces small shifts in the oscillator frequency and anharmonicity. In nearly all conventional electron-transfer models these effects are neglected.

Equation 4.9 solves the initial-state Schrödinger equation *without* Born–Oppenheimer separations *in order to give asymptotically correct wave function propagation at long distance.* The Born–Oppenheimer energies are expected to be quite reliable because they are sensitive to the bulk properties of the wave functions rather than the asymptotic tails.

Born–Oppenheimer Eigenstates. The Born–Oppenheimer electronic donor Hamiltonian is

$$H^{e}_{BO} = H^{e}_{D,M} - \lambda y\left(\frac{2M_y\Omega}{\hbar} \right)^{1/2} \tag{4.13}$$

and the electronic energy for the one-mode problem is

$$E^{e}_{BO}(y) \simeq (\Delta_D - \lambda' y) - \frac{\beta_D^2}{[(\Delta_D - \lambda' y)^2 - 4\beta^2]^{1/2}} \tag{4.14}$$

if the binding energy of the isolated donor $(\Delta_D - \lambda' y)$ relative to the energy of an isolated bridge orbital $(E = 0)$ is much larger than the energy shift of the level due to the presence of the bridge $(|\Delta_D - \lambda' y| \gg \beta_D^2/[(\Delta_D - \lambda' y)^2 - 4\beta^2]^{1/2})$. We define $\lambda' = \lambda(2M_y\Omega/\hbar)^{1/2}$.

The electronic donor wave function is

$$\Psi^{e}_{BO} = \theta_D(\vec{r}) + \frac{\beta_D}{[(\Delta_D - \lambda' y)^2 - 4\beta^2]^{1/2}} \sum_n \tilde{\epsilon}^{|n|}\theta_n(\vec{r} - n\vec{a}) \tag{4.15}$$

Since the bridge is infinite and periodic

$$\tilde{\epsilon} + \frac{1}{\tilde{\epsilon}} = \frac{E^{e}(y)}{\beta} \tag{4.16a}$$

and

$$\tilde{\epsilon} \simeq \frac{\beta}{E^{e}(y)} \quad \text{if } \tilde{\epsilon}^2 \ll 1 \tag{4.16b}$$

The Born–Oppenheimer nuclear Hamiltonian is

$$H^{n}_{BO} = T_y + \frac{1}{2}M_y\Omega^2\left(y - \frac{\lambda}{\hbar\Omega}\left[\frac{2\hbar}{M_y\Omega} \right]^{1/2} \right)^2 - \frac{\lambda^2}{\hbar\Omega} + \Delta_D - \frac{\beta_D^2}{[(\Delta_D - \lambda' y)^2 - 4\beta^2]^{1/2}} \tag{4.17}$$

The nuclear eigenfunction is

$$\Psi^{n}_{BO}(y) = \phi_j(y - 2y_0), \quad 2y_0 = \frac{\lambda}{\hbar\Omega}\left[\frac{2\hbar}{M_y\Omega} \right]^{1/2} \tag{4.18}$$

provided that the β_D^2 term can be ignored. ϕ_j is a harmonic oscillator eigenstate with origin at $2y_0$. The nuclear wave functions are harmonic oscillator states with frequency Ω and shifted origin compared to the uncoupled state. (If the β_D^2 term is not neglected, anharmonicity is introduced and the two parabolic well model is not adequate.) To the extent that energy corrections due to the bridge are small compared to the energy of the state

$$E_j^{BO} \simeq \Delta_D + (j + 1/2)\hbar\Omega - \lambda^2/\hbar\Omega \tag{4.19}$$

The Born–Oppenheimer wave function has a pathological behavior in the region where $\lambda' y$ is of the order of Δ_D.[27] Such

(27) Freed, K. F. *J. Chem. Phys.*, **1986**, *84*, 2108.

behavior is not present in the exact wave function. Because this region of configuration space is not important for the electron-transfer states, this problem may be eliminated by including a cutoff value for y, so that this region is avoided. Such a cutoff can be introduced to the Hamiltonian with no noticeable effect on the exact or Born–Oppenheimer states in the region of interest to the electron-transfer problem. The exact solution is basically the same whether this cutoff is included or not.

Comparison of Wave Functions. Expanding $\phi(y - 2y_0)$ in terms of $\phi(y)$, the Born–Oppenheimer donor states are

$$\Psi_{BO}(\vec{r},y) = \sum_j \left\{ g_j \phi_j(y) \times \left[\theta_D(\vec{r}) + \frac{\beta_D}{[(\Delta_D - \lambda' y)^2 - 4\beta^2]^{1/2}} \sum_n \xi(y)^{|n|} \theta_n(\vec{r} - n\vec{a}) \right] \right\} \quad (4.20)$$

using the result of Appendix C for g_j. $\xi(y)$ is defined in eq 4.16a. Comparing this equation with the exact wave function, eq 4.9, we see that when the electron is on the donor the wave functions are identical. When the electron is on the bridging orbitals, the wave functions are different. In the exact wave function, when the electron is on the bridge it has no interaction with the donor oscillator. However, when on the bridge it tunnels with an energy equal to the total energy of the initial state minus the energy left on the oscillator. The Born–Oppenheimer wave function is qualitatively wrong because it assumes an electronic decay for each possible value of the nuclear coordinate. The Born–Oppenheimer form would be correct if the time taken by the electron to sample its "relevant" space *including the bridge* were short compared to the characteristic time of reaction coordinate (y) motion. In the weak donor–bridge coupling limit this condition for Born–Oppenheimer validity does not hold. Because the exact and Born–Oppenheimer states have identical properties in the high-amplitude region, their eigenvalues are nearly identical.

The differences between the decay of the exact and Born–Oppenheimer donor states is unimportant on the Nth bridge orbital if

$$|\Delta_D| \gg [(N+1)(\lambda^2/\hbar\Omega) + |\epsilon|] \quad (4.21)$$

Recall that ϵ is the driving force of the reaction. In this case fluctuations in the tunneling energy due to the reaction coordinate are much smaller than the binding energy.

Exact Wave Functions, Exact Matrix Elements. When the nuclear mode is on the donor the exchange matrix element is

$$\langle \Psi^D(\vec{r},y^D) | \beta_A (a_N^\dagger a_A + a_A^\dagger a_N) | \Psi^A(\vec{r},y^D) \rangle \quad (4.22)$$

where

$$\Psi^D(\vec{r},y^D) = \sum_i g_i \phi_i(y^D) \chi_i^D(\vec{r}) \quad (4.23)$$

$$\Psi_k^A(\vec{r},y^D) = \chi^A(\vec{r} - R_{DA}) \phi_k(y^D) \quad (4.24)$$

and y is replaced by y^D. $\phi_i(y^D)$ is the ith vibrational state of the ionized donor. The acceptor state can be written in the factored form (eq 4.24) because the two sites are vibrationally distinct and uncoupled.

We only consider the donor ground state (zero temperature) for purposes of illustration. In the one-mode case the driving force in units of $\hbar\Omega$ is $j = \epsilon/\hbar\Omega$. Since the donor state has no amplitude on the acceptor, only the second operator in 4.22 contributes to the matrix element and

$$a_N^\dagger a_A | \Psi^A(x - R_{DA}) \rangle \simeq |\theta_N(\vec{r} - N\vec{a}) \phi_k(y^D)\rangle \quad (4.25)$$

Because the bridge orbitals are orthogonal and the driving force of the reaction must be left on the single-donor oscillator for energy conservation just one matrix element H_{DA} contributes to the rate:

$$H_{DA} = \beta_A \frac{\beta_D}{(E_j^2 - 4\beta^2)^{1/2}} \xi_j^N g_j \quad (4.26)$$

Now, if $4\beta^2 \ll E_j^2$ and g_j can be expanded as described in Appendix C (valid when $\beta_D^2/(E_j^2 - 4\beta^2)^{1/2} \ll |\Delta - E_j|$), the matrix element can be written ($\xi^2 \ll 1$)

$$H_{DA} \simeq \frac{\beta_D \beta_A}{\beta} \left[\frac{e^{-\gamma} \gamma^j}{j!} \right]^{1/2} \left[\frac{\beta}{\Delta_D - \lambda^2/\hbar\Omega - j\hbar\Omega} \right]^{N+1} \quad (4.27)$$

where

$$\gamma = (E_R/\hbar\Omega) = (\lambda/\hbar\Omega)^2 \quad (4.28)$$

$$\xi_j \simeq \beta/E_j \quad (4.29)$$

and the total energy is

$$E_{gs}^{\text{total}} \simeq \Delta_D - \lambda^2/\hbar\Omega + \hbar\Omega/2 \quad (4.30)$$

Because terms in the denominator of the distance (N)-dependent term in eq 4.27 are negative, increasing the exothermicity by increasing $-\Delta_A$ *decreases* the distance-dependent part of the transfer matrix element. The term involving γ and j is peaked at $j = \gamma$. Clearly, the distance decay of the matrix element is driving-force-dependent. This dependence is especially strong when the donor and acceptor energies lie near a band of bridge states ($\xi \propto 1/E$ in the one-band model). Notice also that *different* dependences of rate on ϵ result depending on whether Δ_D or Δ_A is varied.[13a,16c]

Born–Oppenheimer/Condon Approach. The Born–Oppenheimer states are asymptotically incorrect in the limits described above. When the exact and Born–Oppenheimer states are the same (i.e., ξ a very slowly varying function) the Condon approximation for the matrix element of Born–Oppenheimer states is excellent. However, when the Born–Oppenheimer approximation is poor, we cannot directly judge the quality of the Condon approximation by comparing Born–Oppenheimer/Condon rates with the exact rates.

The Born–Oppenheimer matrix element is

$$\langle \Psi_D^e(\vec{r},y) \phi_0 | \beta_A a_N^\dagger a_A | \Psi_A^e(\vec{r},y) \phi_j \rangle \quad (4.31)$$

and is strongly peaked around the maximum of $\phi_0(y - 2y_0)\phi_j(y)$. The Condon approximation fixes y in the electronic wave function at a position where the product of nuclear factors is maximized. Since the Born–Oppenheimer states are qualitatively invalid, we can take this position as the one which gives the matrix element a value as close as possible to the exact value.

The matrix element for the Born–Oppenheimer states in the one-mode example may be approximated by

$$H_{DA} \simeq \left\langle \frac{\beta_D}{[(\Delta_D + \lambda' y)^2 - 4\beta^2]^{1/2}} (\xi(y))^{N+1} \phi_0(y^D - 2y_0^D) \middle| \beta_A \phi_j(y^D) \right\rangle \quad (4.32)$$

Because the product of nuclear wave functions is strongly peaked and $\xi(y)$ is slowly varying in this region, for $\xi^2 \ll 1$

$$H_{DA}^{\text{Condon}} \simeq \frac{\beta_D \beta_A}{\beta} \left(\frac{\beta}{\Delta_D - \lambda' \bar{y}(j)} \right)^{N+1} \left(\frac{e^{-\gamma} \gamma^j}{j!} \right)^{1/2} \quad (4.33)$$

$\bar{y}$ is the chosen value of y in the tunneling matrix element. There is an ϵ (reorganization energy) dependence in the so called "electronic" matrix element as was found in the exact solution because the choice of $\bar{y}$ is ϵ dependent. Condon breakdown arises when *more than one* matrix element enters the rate expression at *fixed* ϵ *or* when $\beta/E(y)$ varies rapidly in the range of y which maximizes the product of nuclear functions.

Comparison of Exact and Born–Oppenheimer/Condon Calculations for One Mode. The differences between the exact and Born–Oppenheimer/Condon rates arise from the coupling between electronic and nuclear motion when the electron is on the bridge. This coupling is manifest in the ξ terms. The nuclear overlap terms in the approximate rate expression are identical, in the limits of interest, with the corresponding g's. The decay constants for the ground-state donor in the one-mode case is

$$\tilde{\epsilon}_j^{\text{exact}} = \frac{\beta}{\Delta_D - \lambda^2/\hbar\Omega - j\hbar\Omega}, \quad j\hbar\Omega = \epsilon \tag{4.34}$$

for the exact solution, and

$$\tilde{\epsilon}(\bar{y}) = \frac{\beta}{\Delta_D - \lambda'\bar{y}(j)} \tag{4.35}$$

for the Born–Oppenheimer/Condon solution. Because *only one* mode is coupled to the transfer event just one $\tilde{\epsilon}_j$ enters the rate expression in the exact case. The Born–Oppenheimer surfaces are

$$U_D^{\text{nuc}} = \Delta_D + \frac{1}{2}k(y - 2y_0)^2 - \frac{\lambda^2}{\hbar\Omega}$$

$$U_A^{\text{nuc}} = \Delta_A + \frac{1}{2}ky^2; \quad 2y_0 = \lambda'/k \tag{4.36}$$

Because the driving force of the reaction is

$$\epsilon \simeq \left(\Delta_D - \frac{\lambda^2}{\hbar\Omega}\right) - \Delta_A \tag{4.37a}$$

$$\tilde{\epsilon}^{\text{exact}} \simeq \frac{\beta}{\Delta_A} \tag{4.37b}$$

$\tilde{\epsilon}(\bar{y})$ is identical with this when $\bar{y} = (\Delta_D - \Delta_A)/\lambda'$. This $\bar{y}$ is the value at the crossing point of the surfaces. That the wave function decay should be driving force (i.e., Δ_A) dependent is neglected in the standard Condon approach, where a single $\bar{y}$ is assumed.[6a,7c,23]

The interpretation of this result is simple but important. With coupling on the donor, the exact donor wave function included admixtures of many $\tilde{\epsilon}_j$'s. However, the acceptor can only access the portion of the wave function which propagates leaving $\epsilon/\hbar\Omega$ vibrations on the donor. This particular part of the wave function decays as $(\beta/\Delta_A)^N$. The Born–Oppenheimer/Condon approximations matches the exact result in this limit because energy conservation forces the decay to the correct value. More profound problems with these approximations arise when there is coupling on both the donor and acceptor sites.

One-Nuclear Mode on Both Donor and Acceptor. Exact Calculation. In many instances there is substantial electronic coupling to both donor and acceptor vibrational modes. As an example of such a case, we solve a two-oscillator problem with equal frequencies and coupling on donor and acceptor. Generalizations of the problem are straightforward. In this model the initial and final states are

$$\Psi^D = [\sum_j g_j^{(0)}\chi_j^D(\bar{r})\phi_j^D(y^D)]\phi_0^A(y^A) \tag{4.38a}$$

$$\Psi_{n,m}^A = \phi_n^D(y^D)[\sum_j h_j^{(m)}\chi_j^A(\bar{r})\phi_j^A(y^A)] \tag{4.38b}$$

$M = \epsilon/\hbar\Omega = n + m$ where n is the number of vibrations left on the donor. Since excitation can be left on both oscillators and there are M quanta of vibrational energy to distribute, the rate now includes a sum of squared matrix elements

$$\sum_F |\langle\Psi_D|H|\Psi_A^F\rangle|^2 = \left(\frac{\beta_A\beta_D}{\beta}\right)^2 \sum_{j=0}^{M}\left[\tilde{\epsilon}_j^{N+1}\left(\frac{e^{-\gamma}\gamma^j}{j!}\right)^{1/2}\left(\frac{e^{-\gamma}\gamma^{M-j}}{(M-j)!}\right)^{1/2}\right]^2 \tag{4.39}$$

where

$$\tilde{\epsilon}_j = \frac{\beta}{\Delta_D - \lambda^2/\hbar\Omega - j\hbar\Omega} \tag{4.40}$$

Born–Oppenheimer/Condon Approach. The sum of Born–Oppenheimer matrix element when one mode is placed on each site is

$$\sum_F |\langle\Psi_D|H|\Psi_A^F\rangle|^2 = \sum_j |\langle\Psi_D(x;y^D)\phi_0(y^D)\phi_0(y^A) \times |\beta_A a_N^{\dagger} a_A|\Psi_A(x;y^A)\phi_k(y^D - 2y_0^D)\phi_m(y^A - 2y_0^A)\rangle|^2 \tag{4.41}$$

For $\epsilon = M\hbar\Omega$ and $|\tilde{\epsilon}| \ll 1$, the Condon approximation gives

$$\left|\frac{\beta_A\beta_D}{\beta}\left(\frac{\beta}{\Delta - \lambda'\bar{y}^D}\right)^{N+1}\right|^2 \sum_j |\langle\phi_0(y^D)|\phi_j(y^D - 2y_0^D)\rangle\langle\phi_0(y^A) \times |\phi_{M-j}(y^A - 2y_0^A)\rangle|^2 \tag{4.42}$$

for this sum. The minimum crossing of the two nuclear potential surfaces occurs at

$$y^D = \frac{\lambda'}{2k} + \frac{\Delta_A - \Delta_D}{2\lambda'} \tag{4.43a}$$

The decay constant at this point is

$$\tilde{\epsilon}(\bar{y}) \simeq \frac{\beta}{(\Delta_D + \Delta_A)/2 - \lambda^2/\hbar\Omega} \tag{4.43b}$$

The nuclear factor in the Condon expression is maximized when half of the vibrational excitation is left on the donor and half on the acceptor (because couplings were chosen equal), or $j\hbar\Omega = (\Delta_D - \Delta_A)/2$. $\tilde{\epsilon}_j^{\text{exact}}$ for this value of j, and this value only, is equal to the approximate value. Because many $\tilde{\epsilon}_j$'s enter the sum, as transfer distance increases the large $\tilde{\epsilon}$'s (with smaller j's) may dominate and the driving force dependence of the rate (and other details) may vary with transfer distances. This is addressed in section V. No choice of $\bar{y}$ gives the Born–Oppenheimer/Condon rate the proper distance dependence.

In summary, there are two kinds of errors in the Born–Oppenheimer/Condon approach to the problem: (1) The incorrect functional form of the Born–Oppenheimer decay length. The true electronic decay is not modulated by the reaction coordinate position when the electron is on the bridge orbitals. It is sensitive only to the vibrational energy left behind. (2) The assumption that $\tilde{\epsilon}$ is ϵ-independent (Condon approximation). This is clearly false even in the one-mode case since $\tilde{\epsilon} \propto \beta/\Delta_A$. Examples of these errors and constraints on their importance are given in section V.

Exact Vibronic States for Models with Two or More Modes per Site. The exact wave functions can be found when more than one-nuclear coordinate exists on the donor or acceptor. Consider a two-nuclear coordinate problem where one mode might correspond to an inner sphere (chemical bond) reaction coordinate and one to an outer sphere (solvent) coordinate. Thus

$$H_{D,M} = H^e + H_2^n + H_2^{e-n} \tag{4.44a}$$

where

$$H_2^n = (b_1^{\dagger}b_1 + \tfrac{1}{2})\hbar\Omega_1 + (b_2^{\dagger}b_2 + \tfrac{1}{2})\hbar\Omega_2 \tag{4.44b}$$

$$H_2^{n-e} = -a_0^{\dagger}a_0[\lambda_1(b_1^{\dagger} + b_1) + \lambda_2(b_2^{\dagger} + b_2)] \tag{4.44c}$$

and the electronic Hamiltonian is as previously described (eq 4.5a). Two *independent* oscillators are each coupled to the electron. This problem is the simplest one which includes an electron with reaction coordinates of differing time scales.

The two-mode problem is solved by analogy with the one-mode problem. Taking

$$\Psi(\bar{r}, y_1, y_2) = \sum_{j,k} g_{j,k}\chi_{j,k}(\bar{r})\phi_j(y_1)\Phi_k(y_2) \tag{4.45a}$$

one finds

$$g_{j,k}\left[\Delta_D - \frac{\beta_D{}^2}{[E_{j,k}{}^2 - 4\beta^2]^{1/2}} - E_{j,k}\right] - \lambda_1[g_{j+1,k}(j+1)^{1/2} + g_{j-1,k}j^{1/2}] - \lambda_2[g_{j,k+1}(k+1)^{1/2} + g_{j,k-1}k^{1/2}] = 0 \tag{4.45b}$$

where

$$E_{j,k} = E^{\text{total}} - (j + \tfrac{1}{2})\hbar\Omega_1 - (k + \tfrac{1}{2})\hbar\Omega_2 \tag{4.45c}$$

Since the recursion relation relates each g_{jk} to at least two other mixing constants, only the matrix approach to calculating eigenvalues is useful. The secular equation is now

$$\begin{pmatrix} \Delta_D - E_{0,0} & -\lambda_2 & -\lambda_1 & 0 & 0 & \cdots \\ -\lambda_2 & \Delta_D - E_{0,1} & -\lambda_1 & 0 & 0 & \cdots \\ -\lambda_1 & 0 & \Delta_D - E_{1,0} & -\lambda_2 & 0 & \cdots \\ 0 & -\lambda_1 & \Delta_D - E_{1,1} & -\lambda_2 & 0 & \cdots \\ \vdots & \vdots & \vdots & \vdots & \vdots & \ddots \end{pmatrix} \begin{pmatrix} g_{0,0} \\ g_{0,1} \\ g_{1,0} \\ g_{1,1} \\ \vdots \end{pmatrix} = 0 \quad (4.46)$$

This approach can be generalized to any number of modes. As the number increases, so does the number of off-diagonal elements in the matrix equation and truncations of the matrix must be made with consideration of the sizes of the g's, which can be estimated by using Appendix C.

V. Discussion and Conclusions

The dependence of the electron-transfer rate on distance, reorganization energy, and redox energy of donor and acceptor is strongly dependent on the details of the model. The electronic structure of the donor, acceptor, and bridge is crucial as well as the frequency and coupling of the reaction coordinates. Qualitative theoretical estimates of driving force and distance dependence[6a,7b,23] can now be scrutinized, at least in the limits of the simple models presented here. We ourselves are interested primarily in the nonadiabatic theory because of its relevance to the long distance biological electron-transfer problem. We have found that there are three ways that simple nonadiabatic electron-transfer theories fail. (1) The electronic decay length may be driving-force-dependent. (2) The decay length dependence on driving force depends on the details of the vibronic coupling. (3) Coupling between electronic and nuclear motion, treated incorrectly in the Born–Oppenheimer/Condon approach, may cause different rate–driving force dependences at different donor–acceptor distances.

Systems like those of Miller, Beitz, and Huddleston[28] (radiolysis initiated transfer through glassy MTHF), and Joran, Leland, Geller, Dervan, and Hopfield[29] (photoexcited transfer from porphyrin to rigidly linked quinones), are examples of electron-transfer systems where the periodic approximation may apply. Amino acid residues in a protein may effectively create a periodic bonded medium through which transfer might occur in biological systems.[8,30] The "band" which assists electron tunneling is determined primarily by the energetic proximity to the donor and acceptor states. In the case of hydrocarbon linkers, the bands of interest are very narrow compared to the energetic distance of the localized states from the band. Because mediation via one band apparently dominates in most cases, the one orbital per site model is appropriate. More elaborate treatments of the bridging medium have been discussed.[16] For hole transfer, the formalism presented in section IV is valid if the electron operators are replaced with hole operators.

The distance dependence of electron-transfer rates has been measured in a few instances. In radiolysis initiated tunneling from biphenyl radical anion to various acceptors it was found that $\tilde{\epsilon} \simeq 0.09$ assuming a unit size of ~ 4 Å ($\alpha \simeq 0.6$ Å^{-1}, where $T_{DA} \propto \exp(-\alpha R_{DA})$). In the rigid porphyrin–(linker)$_n$–quinone systems theory predicts[31] $\tilde{\epsilon} \simeq 0.026$ (experiment[29] gives $\tilde{\epsilon} \leq 0.045$). Given the reduction potentials of biphenyl and benzoquinone, the biphenyl radical anion is about 3 eV from the band of [2.2.2] linker states and the acceptor energy varies from 1 to 3 eV from the [2.2.2] states. It is not clear exactly where the corresponding MTHF "band" sits but we expect it to be close to that of other saturated hydrocarbon. Forward electron transfer in the rigid model compounds occurs at ~ 2 eV from the valence band of the linker.[31] Because the bands are so narrow, we find $\beta[2.2.2] \simeq 0.05$ eV for the σ-bonded systems and $\beta \sim 0.2$ eV for the glassy system. To fit the radiolysis date, Miller found reorganization

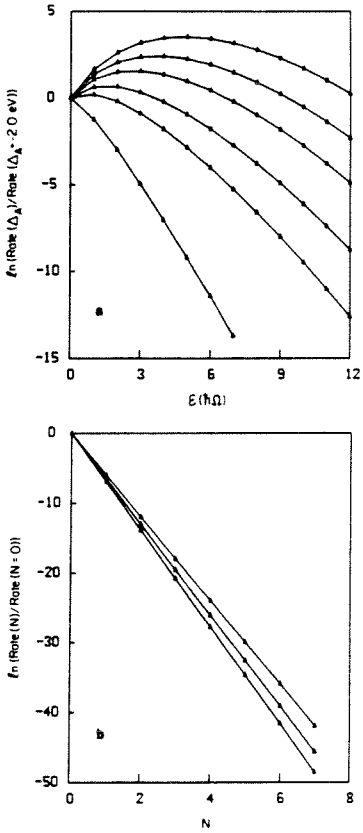

Figure 3. (a) Plots of ln (rate(Δ_A)/rate($\Delta_A = -2.0$ eV)) for different values of N, for the case of one mode coupled only to the donor, and fixed donor energy ($\Delta_D - \lambda^2/\hbar\Omega = -2.0$ eV). The horizontal axis gives $\epsilon = \Delta_D - \lambda^2/\hbar\Omega - \Delta_A$ in units of $\hbar\Omega$. The plots from top to bottom correspond to $N = 0$, 2, 4, 7, 10, and 20, respectively. The parameters are defined in the text. (b) Same as Figure 3a for plots of ln (rate(N)/rate($N = 0$)) for different values of Δ_A. The horizontal axis shows the value of N. The plots from top to bottom correspond to $\Delta_A = -2.0$, -2.6, and -3.2 eV, respectively.

energies of ~ 0.8 eV and $\hbar\Omega \sim 0.18$ eV. Given the proximity of these states to the valence levels of the bridge, hole transfer is believed to dominate.[16c,16d]

Consider electron transfer through an orbital bridge when only one mode on the donor is coupled to the transfer event. The rate in this case ($\tilde{\epsilon}^2 \ll 1$) is

$$\Gamma_{ba}{}^f = \frac{2\pi}{\hbar}\left(\frac{\beta}{\Delta_A}\right)^{2N+2}\left(\frac{\beta_D\beta_A}{\beta}\right)^2 \times \frac{\exp[-(\lambda/\hbar\Omega)^2][\lambda/\hbar\Omega]^{2\epsilon/\hbar\Omega}}{(\epsilon/\hbar\Omega)!}\hbar(E_D - E_A) \quad (5.1)$$

Writing

$$\left(\frac{\beta}{\Delta_A}\right)^{N+1} = \exp(-\alpha R_{DA}) \quad (5.2a)$$

$$\alpha = -a^{-1}\ln(\beta/\Delta_A) \quad (5.2b)$$

There is only one distance decay constant ($\tilde{\epsilon}$) in this equation because the transfer occurs at the acceptor energy, which is a constant. The "electronic" decay length of the conventional theory depends on the driving force of the reaction since

$$\epsilon = \Delta_D - \lambda^2/\hbar\Omega - \Delta_A \quad (5.3)$$

(28) (a) Miller, J. R.; Beitz, J. V.; Huddleston, R. K. *J. Am. Chem. Soc.* **1984**, *106*, 5057. Similar experiments utilize time resolved emission quenching are also of interest: (b) Domingue, R. P.; Fayer, M. D. *J. Chem. Phys.* **1985**, *83*, 2242. (c) Guarr, T.; McGuire, M. E.; McLendon, G. *J. Am. Chem. Soc.* **1985**, *107*, 5104.

(29) (a) Joran, A. D.; Leland, B. A.; Geller, G. G.; Hopfield, J. J.; Dervan, P. B. *J. Am. Chem. Soc.* **1984**, *106*, 6090. (b) Leland, B. A.; Joran, A. D.; Felker, P.; Hopfield, J. J.; Zewail, A. H.; Dervan, P. B. *J. Phys. Chem.* **1985**, *89*, 5571.

(30) Isied, S. S. *Prog. Inorg. Chem.* **1984**, *32*, 443.

(31) Beratan, D. N. *J. Am. Chem. Soc.*, in press.

In the standard theories, the Condon approximation chooses the decay length to be driving-force-independent. When the coupling is entirely on the donor, changing the driving force by changing Δ_A alters the decay length, but changing Δ_D does not. In the later case the conventional theory is adequate. The reverse is true if the reaction coordinate coupling to the electron is entirely localized on the acceptor.

Figure 3 is presented as an example of the effects suggested in section IV for the one mode on donor problem. The calculations were performed with $\beta = 0.1$ eV, $\lambda^2/\hbar\Omega$ (reorganization energy) = 0.9 eV, $\hbar\Omega = 0.15$ eV, $\Delta_D = -1.1$ eV, and Δ_A varing between −2.0 and −3.8 eV. We vary the energy of the *uncoupled* site in order to see the effect of energetics on rate and decay length. Because the decay length is driving-force-dependent, the maximum rate at different transfer distances occurs at different acceptor energies.

When there is vibronic coupling to both donor and acceptor, the rate (if $\bar{\epsilon}^2 \ll 1$) is proportional to the sum in eq 4.39, or eq 4.42 in the Born–Oppenheimer/Condon limit. The "electronic" decay factor in the later case is $\beta/(\Delta_D - \lambda\bar{\nu})$, a single term. With a mode on donor and acceptor, the exact and approximate rates are different because many $\bar{\epsilon}_j$'s are required. Nonexponential decay in distance arises and the apparent decay length varies for fixed driving force as the transfer distance changes. At short transfer distance the $\bar{\epsilon}_j$ that maximizes the Franck–Condon factor dominates the rate sum. However, as the distance increases $\bar{\epsilon}_j$'s for smaller j dominate. This effect may also introduce unusual driving force dependences. Figure 4 presents an example of a problem with one mode coupled to both donor and acceptor. The parameters are similar to the ones used for Figure 3; that is, the donor and acceptor are never closer than 2.0 eV to the center of the band. The reorganization energy is equally divided between donor and acceptor (0.45 eV on each site). In Figure 4a $\Delta_D = -1.55$ eV and Δ_A is varied between −1.55 and −3.35 eV. $\Delta_A = -3.35$ eV and Δ_D is varied between −1.55 and −3.35 eV in Figure 4b.

Changing driving force by changing Δ_D (Figure 4b) instead of Δ_A (Figure 4a) can cause drastic differences in the rate vs. driving force dependence especially in the inverted region. In this region the standard Franck–Condon factor decreases exponentially as Δ_D increases but $\bar{\epsilon}_{j=0}{}^N$ *increases*. Since only $\bar{\epsilon}$'s smaller than $\bar{\epsilon}_{j=0}$ are introduced by varying Δ_A at fixed Δ_D, there are no such compensating effects in the rate vs. driving force plots of Figure 4a. Peaks of these plots are transfer distance dependent reflecting the dominance of different $\bar{\epsilon}_j$'s at different transfer distances. Figures 3b shows that in the one mode case the rate decays exponentially with distance. When one mode is coupled to both donor and acceptor, as in Figure 4c, the rate decay with distance is not purely exponential. Nonexponential decay with distance occurs because more than one $\bar{\epsilon}$ enters the rate expression.

We now comment on the spectral densities discussed in section III and Appendix A. Many fast localized vibrations satisfy the condition that friction is weak enough so that mixing between energy levels of the reaction coordinate is unimportant. Some experimental evidence to support this assumption exists. For example, for metal-free and Zn cytochrome-*c* porphyrins,[32a] the vibrational line widths have been found to be between 1 and 10 cm^{-1}, and the extent of the inhomogeneous broadening about 400 cm^{-1}. For slow reaction coordinates the opposite condition is expected. For "diffusive" motions, such as solvent polarization, gross motion of proteins, and motion of counterions, the condition of a smoothly varying density of states holds. Even the overdamped approximation is reasonable in this case. Experimental evidence to support this assumption for solvent polarization can be found in the literature, and Kosower's work[33] is an example of it. For gross motion of proteins, experimental evidence for the

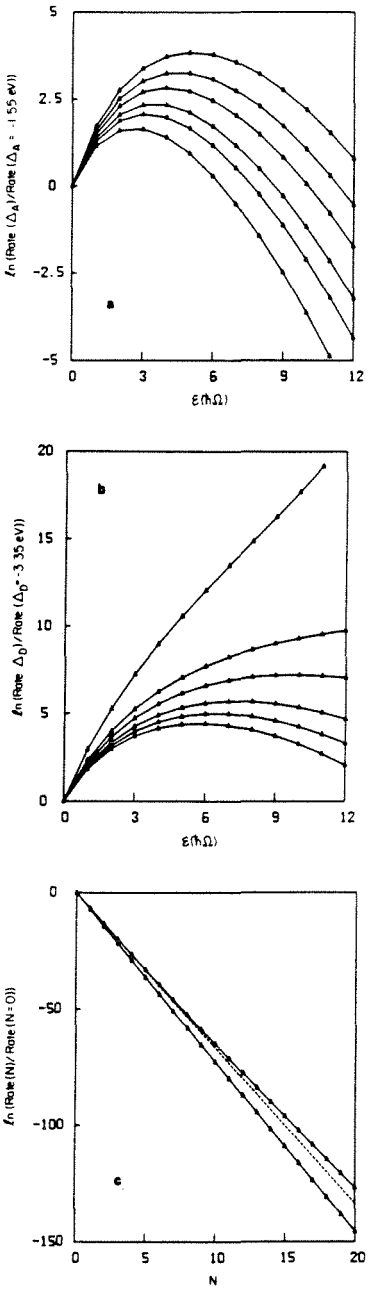

Figure 4. (a) Plots of ln (rate(Δ_A)/rate(Δ_A = −1.55 eV)) for different values of N, for the case of one mode coupled only to the donor and one to the acceptor, and fixed donor energy (Δ_D = −1.55 eV), and reorganization energy of 0.45 eV per mode. The horizontal axis gives $\epsilon = \Delta_D - \Delta_A$ in units of $\hbar\Omega$. The plots from top to bottom correspond to N = 0, 2, 4, 7, 10, and 20, respectively. The parameters are defined in the text. (b) Same as Figure 4a for plots of ln (rate(Δ_D)/rate(Δ_D = −3.35 eV)), and fixed Δ_A (Δ_A = −3.35 eV). The plots from bottom to top correspond to N = 0, 2, 4, 7, 10, and 20, respectively. (c) Same as Figure 4b for plots of ln (rate(N)/rate(N = 0)) for different values of Δ_D. The horizontal axis shows the value of N. The solid lines correspond to Δ_D = −1.55 (top) and −3.35 eV (bottom). The dashed line shows the initial slope of the upper curve.

(32) (a) Vanderkooi, J. M.; Koloczek, H. Presented at the International Conference of Excited States and Dynamics of Porphyrins, Little Rock, AR, Nov 17–19, 1985. (b) Even, U.; Magen, J.; Jortner, J.; Friedman, J.; Levanon, H. *J. Chem. Phys.* **1982**, *77*, 4374.

(33) (a) Kosower, E. M. *J. Am. Chem. Soc.* **1985**, *107*, 1114. (b) Kosower, E. M.; Huppert, D. *Chem. Phys. Lett.* **1983**, *96*, 433. (c) Kosower, E. M. *Acc. Chem. Res.* **1982**, *15*, 259.

existance of a "diffusive" mode coupled to the Fe in heme proteins has been found.[34] The relaxation time of such a mode is on the 10^{-9}-s time scale. As discussed in sections II and III, a combination of reaction coordinates, with different time scales, may be coupled to the electron-transfer problem.

To conclude the paper we describe a few experiments that may help clarify some aspects of the electron-transfer problem, and test the theoretical models. In order to estimate reorganization energies and Franck–Condon factors the following experiment should be done. Let us suppose that we have the donor without the acceptor. As proposed by Hopfield,[6b] if we irradiate this donor with monochromatic light, the electrons emitted have a kinetic energy distribution $S(E)$. This function should be peaked for the photon energy $-(E_{ion}^{D} + 2E_{R}^{D})$, where E_{ion}^{D} is the electronic ionization energy of the donor (i.e., the ionization energy if there were no vibronic coupling) and E_{R}^{D} is the donor reorganization energy. The mean square deviation of such a function should be $2kT_{eff}E_{R}^{D}$. If there is coupling on the acceptor, similar experiments should be done for A^-. Because we are suggesting optical transitions, the nuclear excitations necessary are larger than the ones for nonradiative processes. Under these circumstances the harmonic approximation is less reliable. Another problem with such experiments is that we may not be able to distinguish between homogeneous and inhomogeneous broadening, especially if the solvent is an essential part of the transfer process. In order to accomplish this, fluorescence spectroscopy experiments like those described by Vanderkooi and Koloczek are necessary.[32] The difference between adiabatic and nonadiabatic rates is mainly in the prefactors, not in the activated term. Equation 3.21 is an example of that. Thus, experiments where only prefactors can be systematically varied are ideal sources of direct dynamical information. The porphyrin–(linker)$_n$–quinone molecules synthesized by Joran, Leland, Geller, Hopfield, and Dervan are examples of such systems.[29]

Born–Oppenheimer breakdown may complicate discovery of the "inverted" region for long distance electron-transfer reactions.[28,35] The point at which the regime changes from normal to inverted was shown to depend on coupling *and* transfer distance. For this reason, a result of Miller, Beitz, and Huddleston[28a] is particularly interesting. The observed effect was a shift in the peak of the rate vs. ΔG plot to larger exothermicity for longer distance transfer (Figures 7 and 8 of ref 28a) in a radiolysis-initiated electron-transfer study. They explained this effect with time (equivalent to distance in their analysis)-dependent Franck–Condon factors arising from slow solvent relaxation around the donor ion. A shift of this sort is predicted from Born–Oppenheimer/Condon breakdown if hole transfer dominates (e.g., Figure 4b) and the hole donor (electron acceptor) energy is varied. The proposal that time-dependent solvent relaxation about the donor electron causes this shift was made.[29] Repeating the experiments at 4.2 K, where solvent motion should be considerably more restricted, might resolve this question.

Epilogue

Being at Caltech and able to interact with Rudy, and being interested in biological electron transfer, it is a special pleasure for us to join in this celebration of Rudy's seminal contributions to the field. He had the wisdom to find the right ideas and constructs, and the kindness to leave a few subtle points for others to work on.

Acknowledgment. We thank A. Garg for his collaboration in developing Appendix B. D.N.B. thanks A. Gupta for his hospitality at JPL. The research described in this paper was performed while D.N.B. held an NRC-NASA Resident Research Associateship at the Jet Propulsion Laboratory, California Institute of Technology. Support was also provided by the National Science Foundation (Grant No. PCM-8406049) and by the Brazilian Agency Conselho Nacional de Desenvolvimento Científico e Tecnológico—CNPq.

Appendix A

Calculation of Spectral Densities. Starting with the one-reaction-coordinate case, we consider the purely quadratic part of eq 3.8, i.e.

$$H_{ET} = T_{DA}\sigma_x + \frac{P_y^2}{2M_y} + \frac{1}{2}M_y\Omega^2(y + y_0\sigma_z)^2 + \frac{\epsilon}{2}\sigma_z + \sum_{b(bath)}\left\{\frac{P_b^2}{2M_b} + \frac{1}{2}M_b\omega_b^2\left[x_b + \frac{c_b}{M_b\omega_b^2}y\right]^2\right\} \quad (A.1)$$

that is not coupled to the spin, and imagine diagonalizing it via a transformation to normal modes. By doing that, we can rewrite the Hamiltonian A.1 as eq 3.12, i.e.

$$H_{ET} = T_{DA}\sigma_x + \frac{\epsilon}{2}\sigma_z + \sigma_z\sum_\beta \tilde{c}_\beta\tilde{x}_\beta + \sum_\beta\left[\frac{\tilde{p}_\beta^2}{2\tilde{m}_\beta} + \frac{1}{2}\tilde{m}_\beta\tilde{\omega}_\beta^2\tilde{x}_\beta^2 + \frac{\tilde{c}_\beta^2}{2\tilde{m}_\beta\tilde{\omega}_\beta^2}\right] \quad (A.2)$$

Our goal now is to calculate $J_{eff}(\omega)$, eq 3.13, assuming that we know $J_0(\omega)$, eq 3.9. Since the transformation for eq A.1 to eq A.2 does not involve the spin, the same $J_{eff}(\omega)$ controls the dynamics of a continuous variable q moving in some potential $U(q)$ and coupled to the coordinates y and x_α in the same way as the spin. To this end, let us consider the Hamiltonian

$$H_q = \frac{p_q^2}{2\mu} + U(q) + \frac{P_y^2}{2M_y} + \frac{1}{2}M_y\Omega^2(y + a_yq)^2 + \sum_{b(bath)}\left\{\frac{P_b^2}{2M_b} + \frac{1}{2}M_b\omega_b^2\left[x_b + \frac{c_b}{M_b\omega_b^2}y\right]^2\right\} \quad (A.3)$$

where p_q is the momentum conjugate to q. For this Hamiltonian, the classical equations of motion are

$$\mu\ddot{q} = -U'(q) - M_y\Omega^2a_y(y + a_yq)$$

$$M_y\ddot{y} = -M_y\Omega^2(y + a_yq) - \sum_{b(bath)} c_bx_b - y\sum_{b(bath)}\frac{c_b^2}{M_b\omega_b^2}$$

$$M_b\ddot{x}_b = -M_b\omega_b^2x_b - c_by \quad (A.4)$$

We now use the Leggett's prescription[36] for obtaining $J_{eff}(\omega)$. Defining the Fourier transform

$$\hat{q}(u) = \int_{-\infty}^{\infty} q(t)\exp(-iut)\,dt, \quad \mathrm{Im}\,(u) < 0 \quad (A.5)$$

and writing the equation of motion satisfied by $\hat{q}$ as

$$\hat{K}(u)\hat{q}(u) = U_u'(q) \quad (A.6)$$

where $U_u'(q)$ is the Fourier transform of $U'(q)$, $J_{eff}(\omega)$ is given by

$$J_{eff}(\omega) = \lim_{\epsilon\to 0+}\mathrm{Im}\,[\hat{K}(\omega - i\epsilon)]; \quad \omega \text{ real} \quad (A.7)$$

Carrying out these steps, we get

$$\hat{L}(u)\hat{y} = -u^2\left[M_y + \sum_{b(bath)}\frac{c_b^2}{M_b\omega_b^2(\omega_b^2 - u^2)}\right]\hat{y} = -M_y\Omega^2(\hat{y} + a_y\hat{q}) \quad (A.8)$$

$$\hat{K}(u) = -\mu u^2 + \frac{M_y\Omega^2a_y^2\hat{L}(u)}{M_y\Omega^2 + \hat{L}(u)} \quad (A.9)$$

Assuming that $J_0(\omega)/\omega$ has no singularities and a cutoff frequency Λ, we get

(34) (a) Parak, F.; Knapp, E. W. *Proc. Natl. Acad. Sci. U.S.A.* **1984**, *81*, 7088. (b) Bauminger, E. R.; Cohen, S. G.; Nowik, I.; Offer, S.; Yariv, J. *Proc. Natl. Acad. Sci. U.S.A.* **1983**, *80*, 736.

(35) Miller, J. R.; Calcaterra, L. T.; Closs, G. L. *J. Am. Chem. Soc.* **1984**, *106*, 3047.

(36) Leggett, A. J. *Phys. Rev. B* **1984**, *30*, 1208.

$$\hat{L}(u) = -u^2\left[M_y + \frac{2}{\pi}\int_0^\infty \frac{(J_0(\omega')/\omega')}{(\omega')^2 - u^2}\, d\omega' \right] = -M_y u^2 + iJ_0(u) \quad (A.10)$$

Substituting eq A.10 in eq A.9, and using eq A.7, we get

$$J_{eff}(\omega) = \frac{\Omega^4 a_y^2 J_0(\omega)}{(\Omega^2 - \omega^2)^2 + (J_0(\omega)/M_y)^2} \qquad \text{if } \Lambda \gg \Omega \quad (A.11)$$

and

$$J_{eff}(\omega) \approx a_y^2 J_0(\omega) + \frac{\pi}{2} M_y \Omega^3 a_y^2 \delta(\omega - \Omega) \qquad \text{if } \Lambda \ll \Omega \quad (A.12)$$

If instead of y being coupled to $a_y q$, it is coupled to $y_0\sigma_z$, the effective spectral density is

$$J_{eff}(\omega) = \frac{\Omega^4 y_0^2 J_0(\omega)}{(\Omega^2 - \omega^2)^2 + (J_0(\omega)/M_y)^2} \qquad \text{if } \Lambda \gg \Omega \quad (A.13)$$

and

$$J_{eff}(\omega) \approx y_0^2 J_0(\omega) + \frac{\pi}{2} M_y \Omega^3 y_0^2 \delta(\omega - \Omega) \qquad \text{if } \Lambda \ll \Omega \quad (A.14)$$

Equation A.13 becomes eq 3.14, when $J_0(\omega)$ is given by eq 3.11.

Now we consider the problem of two reaction coordinates which is given by eq 3.33, i.e.,

$$H_{ET} = T_{DA}\sigma_x + \frac{P_y^2}{2M_y} + \frac{1}{2}M_y\Omega_y^2(y + y_0\sigma_z)^2 + \frac{P_z^2}{2M_z} + \frac{1}{2}M_z\Omega_z^2(z + z_0\sigma_z)^2 + \frac{\epsilon}{2}\sigma_z + \sum_{b(bath)}\left\{ \frac{P_b^2}{2M_b} + \frac{1}{2}M_b\omega_b^2\left[x_b + \frac{c_b^y}{M_b\omega_b^2}y + \frac{c_b^z}{M_b\omega_b^2}z \right]^2 \right\} \quad (A.15)$$

This equation can be transformed in eq A.2 by using the same prescription used before. Let us consider the Hamiltonian

$$H_q = \frac{P_q^2}{2\mu} + U(q) + \frac{P_y^2}{2M_y} + \frac{1}{2}M_y\Omega_y^2(y + a_y q)^2 + \frac{P_z^2}{2M_z} + \frac{1}{2}M_z\Omega_z^2(z + a_z q)^2 + \sum_{b(bath)}\left\{ \frac{P_b^2}{2M_b} + \frac{1}{2}M_b\omega_b^2\left[x_b + \frac{c_b^y}{M_b\omega_b^2}y + \frac{c_b^z}{M_b\omega_b^2}z \right]^2 \right\} \quad (A.16)$$

which has the classical equations of motion

$$\mu\ddot{q} = -U'(q) - M_y\Omega_y^2 a_y(y + a_y q) - M_z\Omega_z^2 a_z(z + a_z q)$$

$$M_y\ddot{y} = -M_y\Omega_y^2(y + a_y q) - \sum_{b(bath)} c_b^y x_b - y\sum_{b(bath)}\frac{(c_b^y)^2}{M_b\omega_b^2} - z\sum_{b(bath)}\frac{c_b^y c_b^z}{M_b\omega_b^2}$$

$$M_z\ddot{z} = -M_z\Omega_z^2(z + a_z q) - \sum_{b(bath)} c_b^z x_b - z\sum_{b(bath)}\frac{(c_b^z)^2}{M_b\omega_b^2} - y\sum_{b(bath)}\frac{c_b^y c_b^z}{M_b\omega_b^2}$$

$$M_b\ddot{x}_b = -M_b\omega_b^2 x_b - c_b^y y - c_b^z z \quad (A.17)$$

Doing exactly as we did for the one mode case, we get

$$-u^2\left[M_y + \sum_{b(bath)}\frac{(c_b^y)^2}{M_b\omega_b^2(\omega_b^2 - u^2)}\right]\hat{y} + \sum_{b(bath)}\frac{c_b^y c_b^z}{M_b\omega_b^2(\omega_b^2 - u^2)}\hat{z} = -M_y\Omega_y^2(\hat{y} + a_y\hat{q}) \quad (A.18)$$

and the equivalent equation for z. Because the signs of c_b^y and c_b^z are random, and/or assuming that y and z are rarely coupled to the same bath mode, the terms proportional to $\sum_b c_b^y c_b^z/M_b\omega_b^2(\omega_b^2 - u^2)$ in the equation above can be neglected.

In analogy with the one-mode case, we define

$$\hat{L}^{y,z}(u) = -u^2\left[M_{y,z} + \sum_{b(bath)}\frac{(c_b^{y,z})^2}{M_b\omega_b^2(\omega_b^2 - u^2)}\right] \quad (A.19)$$

which satisfies

$$\begin{Bmatrix} \hat{L}^y(u)\hat{y} \\ \hat{L}^z(u)\hat{z} \end{Bmatrix} = -\begin{Bmatrix} M_y\Omega_y^2(\hat{y} + a_y\hat{q}) \\ M_z\Omega_z^2(\hat{z} + a_z\hat{q}) \end{Bmatrix} \quad (A.20)$$

Carrying out the algebra, we get

$$J_{eff}(\omega) = J_{eff}^y(\omega) + J_{eff}^z(\omega) \quad (A.21)$$

where $J_{eff}^{y,z}$ are the effective spectral densities for y and z, calculated by using eq A.7, A.9, and A.10, but using $\hat{L}^{y,z}$ ($J_0^{y,z}$) instead of $\hat{L}$ (J_0).

Appendix B[37]

Extreme Nonadiabatic Limit of the One-Reaction-Coordinate Electron Transfer. Let us calculate the rate of electron transfer for Hamiltonian (3.8), assuming that $J_0(\omega)$ is given by eq 3.11. We assume that friction is weak enough so that mixing between the energy levels of the reaction coordinate is unimportant.

For the electron fixed on the acceptor ($V(y; -)$ in Figure 1), the rate of decay of the m_Ath level is

$$\Gamma_{m_A} = \frac{\eta}{M_y}\left\{ m_A\frac{\exp(\hbar\Omega/kT)}{\exp(\hbar\Omega/kT) - 1} + \frac{m_A + 1}{\exp(\hbar\Omega/kT) - 1}\right\} \quad (B.1)$$

using eq 12-110 and 12-128 of ref 38. Therefore

$$\Gamma_{m_A} \approx 2m_A\gamma \qquad \text{if } kT \ll \hbar\Omega \quad (B.2)$$

$$\Gamma_{m_A} \approx \frac{2kT\gamma}{\hbar\Omega}(2m_A + 1) \text{ if } kT \gg \hbar\Omega \quad (B.3)$$

We now calculate the forward rate for electron transfer. For that, let us consider a two-level system (level n_D of the donor and m_A of the acceptor), where we have a net loss only from the acceptor at a rate Γ_{m_A}. The energy difference between these two levels is $\Delta E_{nm} = E_{n_D} - E_{m_A}$, and the coupling between them is given by $\hbar\Delta/2 = T_{DA}\langle n_D|m_A\rangle$. The wave function at time t can be written as

$$\Psi(t) = a(t)|+\rangle + b(t)|-\rangle; \quad a(0) = 1 \quad (B.4)$$

and

$$\frac{da(t)}{dt} = -i\frac{\Delta E_{nm}}{2\hbar}a(t) - i\frac{\Delta}{2}b(t) \quad (B.5a)$$

$$\frac{db(t)}{dt} = +i\frac{\Delta E_{nm}}{2\hbar}b(t) - i\frac{\Delta}{2}a(t) - \frac{1}{2}\Gamma_{m_A}b(t) \quad (B.5b)$$

Equation B.5 can be rewritten as

$$\frac{d}{dt}\begin{pmatrix} a(t) \\ b(t)\end{pmatrix} = \begin{pmatrix} -i\Delta E_{nm}/2\hbar & -i\Delta/2 \\ -i\Delta/2 & (i\Delta E_{nm} - \Gamma_{m_A})/2\end{pmatrix}\begin{pmatrix} a(t) \\ b(t)\end{pmatrix} \equiv M\begin{pmatrix} a(t) \\ b(t)\end{pmatrix} \quad (B.6)$$

and the net loss is

$$\frac{d}{dt}(|a|^2 + |b|^2) = -\Gamma_{m_A}|b|^2 \quad (B.7)$$

If the eigenvalues of M are λ_1 and λ_2, then

$$b(t) = C[\exp(\lambda_1 t) - \exp(\lambda_2 t)] \quad (B.8)$$

which ensures that $b(0) = 0$, and from eq B.5b

$$C = \frac{1}{\lambda_1 - \lambda_2}\dot{b}(0) = \frac{-i\Delta}{2(\lambda_1 - \lambda_2)} \quad (B.9)$$

(37) This appendix was developed in collaboration with A. Garg.

(38) Feynman, R. P.; Hibbs, A. R. *Quantum Mechanics and Path Integrals*; McGraw-Hill: New York, 1965.

Assuming $\Gamma_{m_A} \gg \Delta$ and/or $\Delta E_{nm} \gg \Delta$, the nonadiabatic limit is valid, and

$$\lambda_1 \approx \frac{-i\Delta E_{nm}}{2\hbar} - \frac{\hbar\Delta^2}{2(\hbar\Gamma_{m_A} - 2i\Delta E_{nm})}\left\{1 + O\left(\frac{\hbar\Delta}{\hbar\Gamma_{m_A} - 2i\Delta E_{nm}}\right)^2\right\} \quad \text{(B.10a)}$$

$$\lambda_2 \approx \frac{i\Delta E_{nm}}{2\hbar} - \frac{1}{2}\Gamma_{m_A} + O\left(\frac{\hbar\Delta^2}{\hbar\Gamma_{m_A} - 2i\Delta E_{nm}}\right) \quad \text{(B.10b)}$$

Note that λ_2 *always* has a large negative real part and λ_1 a small one. Thus after times of order $\Gamma_{m_A}^{-1}$, $|b(t)|^2$ is essentially constant, and

$$|b(t)|^2 \approx \frac{\Delta^2}{4|\lambda_1 - \lambda_2|^2} = \frac{\hbar^2\Delta^2}{4[\Delta E_{nm}^2 + \hbar^2\Gamma_{m_A}^2/4]} \quad \text{(B.11)}$$

Actually, we should also consider transitions between levels in the donor well. If the transfer rate is slow, then these transitions maintain the donor in equilibrium, guaranteeing exponential decay in time. Thus, the forward rate is

$$\Gamma_{ns}^{\,f} = \sum_{n_D m_A} \frac{\Gamma_{m_A}|T_{DA}|^2|\langle n_D|m_A\rangle|^2}{(E_{n_D} - E_{m_A})^2 + \hbar^2\Gamma_{m_A}^2/4}\rho(E_{n_D}, T) \quad \text{(B.12)}$$

To calculate the reverse rate, we invert this procedure.

The concept of relaxation time, which is used in this Appendix, assumes that the bath is always in equilibrium. This is a good assumption as long as the shift of the equilibrium position of each bath modes, due to the donor/acceptor transition, is small compared to the bath mode width. Normally this condition is satisfied because the bath is composed of a large number of oscillators. The only situation that causes problems is when the transition to the ground state of the acceptor is important and $T = 0$. In this case $\Gamma_0 = 0$ and the formalism described in this Appendix fails. Then, in order to calculate rates, we must use the procedure used to calculate eq 3.32.

Appendix C

Separation of the Coefficients in the Multimode Case and the Correspondence between Harmonic Oscillator Overlaps and Wave Function Expansion Constants. We now give an example which illustrates the nature of the wave function mixing coefficients and their interpretation in the multimode problem. Consider the two mode Hamiltonian in eq 4.44. The recursion relation is

$$g_{j,k}\left[\Delta_D - \frac{\beta_D^2}{(E_{j,k}^2 - 4\beta^2)^{1/2}} - E_{j,k}\right] - \lambda_1[g_{j+1,k}(j+1)^{1/2} + g_{j-1,k}j^{1/2}] - \lambda_2[g_{j,k+1}(k+1)^{1/2} + g_{j,k-1}k^{1/2}] = 0 \quad \text{(C.1)}$$

We write $g_{jk} = g_j^{(1)}g_k^{(2)}$. In the electron-transfer problems for which this model holds relevance

$$|\beta_D^2/(E_{jk} - 4\beta^2)^{1/2}| \ll |\Delta_D - E_{j,k}| \quad \text{(C.2)}$$

Approximating E^{total} with the Born–Oppenheimer energy and

$$\frac{\beta_D^2}{(E_\epsilon^2 - 4\beta^2)^{1/2}} \ll E^e \quad \text{(C.3a)}$$

$$E_{j,k}^{BO} \simeq \Delta_D + (j + \tfrac{1}{2})\hbar\Omega_1 - \frac{\lambda_1^2}{\hbar\Omega_1} \quad \text{(C.3b)}$$

$$+ (k + \tfrac{1}{2})\hbar\Omega_2 - \frac{\lambda_2^2}{\hbar\Omega_2} \quad \text{(C.3c)}$$

and

$$g_j^{(1)}[g_k^{(2)}|(j-n)\hbar\Omega_2 + \lambda_2^2/\hbar\Omega_2| - \lambda_2(g_{k+1}^{(2)}(k+1)^{1/2} + g_{k-1}^{(2)}k^{1/2})] + g_k^{(2)}[g_j^{(1)}|(k-n)\hbar\Omega_1 + \lambda_1^2/\hbar\Omega_1| - \lambda_1(g_{j+1}^{(1)}(j+1)^{1/2} + g_{j-1}^{(1)}j^{1/2})] = 0 \quad \text{(C.4)}$$

n is the quantum number of the coupled state. This equation may be written as

$$a(j)b(k) + c(j)d(k) = 0 \quad \text{(C.5)}$$

where $a(j) \neq 0$, $d(k) \neq 0$, and $b(k) \neq c(j)$. Therefore, $b(k) = 0$ and $c(j) = 0$ so the coefficient g_{jk} is separable into a product of two single-mode coefficients.

The mixing constants when more than two modes are present, $g_{j,k,l,\ldots}$, can be separated into as many terms as there are modes in the problem providing the corresponding limits obtain. It was shown that in the δ well limit the mixing constants (squared) in the ground-state wave function are Poisson distributed. We now show that, in general, for the mth coupled wave function $g_j \simeq \langle n|j\rangle$ where $|n\rangle$ is a harmonic oscillator eigenstate with given equilibrium geometry and $|j\rangle$ is a harmonic oscillator eigenstate with a shifted equilibrium position. We give this proof for one-nuclear mode and an orbital model for the electronic part of the problem. The possibility of separating the g's as previously described means that this fact is true for $g_j^{(1)}$, $g_k^{(2)}$, ... The recursion relation for any single mode is

$$g_{j+1}(j+1)^{1/2} - g_j[\gamma^{1/2} + (j-n)/\gamma^{1/2}] + g_{j-1}j^{1/2} = 0 \quad \text{(C.6)}$$

where $\gamma = E_R/\hbar\Omega = (\lambda/\hbar\Omega)^2$ and we approximated the energy with the Born–Oppenheimer energy. n is the quantum number of the coupled state and j is the index in the wave function expansion corresponding to the jth vibrational state. We prove that $g_j \simeq \langle n|j\rangle$, where $|n\rangle$ and $|j\rangle$ correspond to oscillators with origins at $y = 0$ and $y = 2y_0$, respectively. Defining the operator

$$P = b - \gamma^{1/2} - \frac{1}{\gamma^{1/2}}(b^+b - b_s^+b_s) + b^+ \quad \text{(C.7)}$$

$$b^+ = \frac{1}{2^{1/2}}[(M_y\Omega/\hbar)^{1/2}y - iP_y/(M_y\hbar\Omega)^{1/2}] \quad \text{(C.8a)}$$

$$b_s^+ = \frac{1}{2^{1/2}}[(M_y\Omega/\hbar)^{1/2}(y - 2y_0) - iP_y/(M_y\hbar\Omega)^{1/2}] \quad \text{(C.8b)}$$

and $b_s^+(b_s)$ creates (destroys) vibrations with equilibrium position $2y_0$. $b^+(b)$ creates (destroys) vibrations with equilibrium position at the origin (0). Clearly, $\langle j|P|n\rangle$ gives the left-hand side of eq C.6. If we can show that $P \equiv 0$, we have proven that $g_j = \langle j|n\rangle$ is the solution of eq 4.12 to the extent that the Born–Oppenheimer energy is a good estimate of the eigenvalue and

$$\beta_D^2/[(\Delta_D - \lambda' y)^2 - 4\beta^2]^{1/2} \ll \Delta_D$$

In the case of quadratic reagent and product wells

$$\gamma = (\lambda/\hbar\Omega)^2 = \frac{1}{2}\frac{M_y\Omega^2(2y_0)^2}{\hbar\Omega} = \frac{M_y\Omega}{2\hbar}(2y_0)^2 \quad \text{(C.9)}$$

Substituting $\gamma(2y_0)$ into the definition of P and using the coordinate representation for the creation and annihilation operators we see that $P \equiv 0$, as needed. Moreover, since $2y_0$ is the shift of the oscillators accompanying electron transfer the sets $|j\rangle$ and $|n\rangle$ are the eigenstates of these surfaces. The importance of including a particular mode in the Hamiltonian is proportional to γ. Whether the corresponding g's can be neglected is estimated by calculating the appropriate product of nuclear oscillator overlap functions.

II.4 Effect of Friction on Electron Transfer – The Two Reaction Coordinate Case

J. Chem. Phys., in press

by

José Nelson Onuchic[a]

Division of Chemistry and Chemical Engineering[b]

California Institute of Technology

Pasadena, California 91125

---

[a] on leave of absence from Instituto de Física e Química de São Carlos, Universidade de São Paulo, 13560, São Carlos, SP, Brazil.

[b] Contribution No. 7470.

Abstract

Electron transfer is a very important reaction in many biological processes such as photosynthesis and oxidative phosphorylation. In many of these reactions, most of the interesting dynamics can be included by using two reaction coordinates: one fast (local high–frequency vibration modes) and one slow (outer-sphere modes such as solvent polarization). We report a model to describe this problem, which uses path integral techniques to calculate electron transfer rates, and also to obtain the Fokker–Planck equations associated with this model. Different limiting cases lead to qualitatively different results such as exponential or non-exponential time decay for the donor survival probability. Conditions for the validity of the adiabatic or the non-adiabatic limits will be discussed. Application of this model to real systems is proposed, in particular for a porphyrin rigidly linked to a quinone, which is a very interesting model compound for primary events of photosysthesis. This model can also be used for other multi–coordinate biological reactions such as ligand binding to heme proteins. Also, in the concluding part of Sec. 3, we discuss the important limit where the fast vibronic mode is much faster than all the other nuclear modes coupled to the problem. In this limit the fast mode "renormalizes" the electronic matrix element, and this considerably simplifies the treatment of the problem, reducing it to coupling only to the slow modes.

1. Introduction

This paper is a continuation of the work begun in the paper "Effect of Friction on Electron Transfer in Biomolecules,"[1] in which we developed a theoretical model for electron transfer reactions coupled to one reaction coordinate. Electron transfer reactions are very important in biological and chemical processes such as oxidative phosporylation, photosynthesis, and oxy–reduction reactions.[2] In this paper we expand our understanding of the role played by friction in these reactions, generalizing the results obtained in the previous paper for one reaction coordinate, and we develop a solution for the case of transfer coupled to two reaction coordinates. The results obtained by Agmon and Hopfield[3] suggest that the formalism developed here is applicable to other chemical-biological reactions, such as CO binding to heme–proteins. The results obtained here are important for two main reasons:

1– Theoretically this work presents a discussion of the validity of several existent theories; it also shows how they are related to a general Hamiltonian. Also, several new calculation methods, which may be useful when developing theoretical models for chemical reactions in condensed matter, are developed and described in detail.

2– Some applications to existing experiments of the results here obtained are described. How to apply them to some other experimental results is discussed as well.

This paper is structured as follows. Sec. 2 describes the results available for the one mode problem in several different limits. A discussion of the validity of each limit and a comparison to existing theroretical results is given. Also,

a description of the important time scales of the problem is presented. Sec. 3 introduces the two mode problem. The electron transfer rate is calculated in several limits. A discussion is given of exponential and non–exponential decay in time of donor survival probability. Some possible applications of the results to experimental systems are described. Sec. 4 presents the Fokker–Planck equation associated with the Hamiltonian of Sec. 3. Sec. 5 discusses some introductory ideas of how to include anharmonic effects when they are necessary to describe the problem at hand. A model to interpret electron transfer between a linked porphyrin and quinone is then presented. A preliminary discussion of the available experimental data is given. Sec. 6 discusses the relevance of the results here obtained.

2. The One Mode Problem – Review and Generalization

The concepts of adiabaticity and reaction rate for electron transfer reactions have been extensively discussed in the literature (Refs. 3-11, for example). Because they have not been presented in a complete and clear way, there is a need to connect and to compile this available information, to clarify some dubious points, as well as to develop a discussion addressing the validity of each one of these models. This is the main aim of this section in which, for reasons of simplicity, we consider electron transfer coupled to only one reaction coordinate.

The electron transfer Hamiltonian in this case, in the Born–Oppenheimer and Condon approximations, is

$$H_{ET} = \frac{\hbar\Delta_0}{2}\sigma_x + \frac{P_y^2}{2M_y} + \frac{1}{2}M_y\Omega_y^2(y + y_0\sigma_z)^2 + \frac{\varepsilon}{2}\sigma_z$$
$$+\frac{1}{2}\sum_\alpha \left[\frac{p_\alpha^2}{m_\alpha} + m_\alpha\omega_\alpha^2\left(x_\alpha + \frac{c_\alpha y}{m_\alpha\omega_\alpha^2}\right)^2\right] \quad . \tag{2.1}$$

Here the electron in the donor and acceptor states is associated with $\sigma_z = 1$ and -1, respectively. y is the reaction coordinate, and $\{x_\alpha\}$'s are the bath coordinates. As discussed by Caldeira and Leggett[12] and in Ref. 1, details of the bath are unnecessary, and only how the "reduced dynamics" of electron and reaction coordinate are affected by the bath is important. Therefore, the bath oscillators' influence on the reaction coordinate is determined by the following relation, which is known as spectral density,

$$J_0(\omega) = \frac{\pi}{2}\sum_\alpha \frac{c_\alpha^2}{m_\alpha\omega_\alpha}\delta(\omega - \omega_\alpha) \quad . \tag{2.2}$$

In this section we restrict ourselves to the ohmic form of the spectral density

$$J_0(\omega) = \eta\omega\exp(-\omega/\Lambda),, \quad \text{and } \gamma = \eta/2M_y \quad . \tag{2.3}$$

Λ is a high frequency cutoff that is required on both physical and mathematical grounds. It must be much faster than any time scale associated with the problem. As discussed elsewhere[4], if other forms for the spectral density were considered, a frequency–dependent damping constant η would be necessary. Because at this level of theory there is no reason to further complicate the problem, we use in this section the ohmic form for the spectral density. It also has a simple connection with linear damping of the classical limit of the reaction coordinate[1]. Also, in the non–adiabatic limit, details of the spectral density are irrelevant, and only the strengh of the bath coupling to the reaction coordinate is important[4]. To avoid confusion, we recall that we use the standard convention for the non–adiabatic term; i.e., the rate is non–adiabatic if it is proportional to the square of the electronic matrix element, $|\hbar\Delta_0/2|^2$.

Initially we consider the case in which the coupling between the bath and the reaction coordinate is weak; i.e., the width of the reaction coordinate energy levels is much smaller than $\hbar\Omega_y$, but large enough that the non–adiabatic limit still holds. (By that we mean that the non–adiabatic rate is much slower than the reaction coordinate relaxation. See Appendix B of Ref. 4 for quantitative estimates of this condition.) Under these circumstances the non–adiabatic electron transfer rate is

$$\Gamma_{na}^{f;r} = \sum_{n_D,m_A} \frac{\gamma_{m_A;n_D}|\hbar\Delta_0/2|^2| < n_D|m_A > |^2}{(E_{n_D} - E_{m_A})^2 + \hbar^2\gamma_{m_A;n_D}^2/4}\rho(E_{n_D;m_A},T) \quad , \tag{2.4}$$

where

$$\gamma_{m_A} = \frac{\eta}{M_y}\left\{m_A\frac{\exp(\hbar\Omega_y/kT)}{\exp(\hbar\Omega_y/kT)-1} + \frac{m_A+1}{\exp(\hbar\Omega_y/kT)-1}\right\} \quad , \tag{2.5}$$

and similarly for γ_{n_D}. $\rho(E_{n_D;m_A},T)$ is the thermal density of states for the donor/acceptor reaction coordinate levels. In the high and low T limits, re-

spectively,

$$\gamma_{m_A} \approx 2m_A\gamma \quad \text{if} \quad kT \ll \hbar\Omega_y \ , \tag{2.6a}$$

and

$$\gamma_{m_A} \approx \frac{2kT\gamma}{\hbar\Omega_y}\,(2m_A+1) \quad \text{if} \quad kT \gg \hbar\Omega_y \ . \tag{2.6b}$$

Details about how these rates were computed are found in Refs. 4 and 10. For clarity we now show how the rate above is connected with the conventional "quantum mechanical" rate developed by Jortner and collaborators[9]. If $\gamma_{m_A}(\gamma_{n_D})$ is much smaller than Ω_y, the rate 2.4 is highly peaked when $E_{n_D} = E_{m_A}$. Therefore, if we take the limit $\gamma_{m_A}(\gamma_{n_D}) \longrightarrow 0$, Eq. 2.4 becomes

$$\Gamma_{na}^{f;r} = \sum_{n_D,m_A} \frac{2\pi}{\hbar}|\hbar\Delta_0/2|^2| < n_D|m_A > |^2 \ \delta(E_{n_D} - E_{m_A}) \ \rho(E_{n_D;m_A},T) \ . \tag{2.7}$$

These delta functions are purely formal (only show conservation of energy) because, as discussed previously, $\gamma_{m_A}(\gamma_{n_D})$ have to be large enough so that the non-adiabatic rate is slower than the reaction coordinate relaxation[4].

Next we consider the limit where the coupling to the bath is strong enough so that the density of states of the reaction coordinate is a smooth function of energy. From Eqs. 2.5 and 2.6 we know that this condition is satisfied when $\gamma_{m_A;n_D} > \Omega_y/2$ for the levels involved in the transfer. In this limit, the electron transfer rate is calculated for two cases, one when the reaction coordinate is underdamped and the other when it is overdamped.

In this strong coupling limit, the rates are obtained using the formalism developed by Garg, Onuchic and Ambegaokar[1]. Following that work, we calculate the inclusive probability, $W(t)$, defined as follows. Suppose that for $t \leq 0$, the electron is held on the donor (spin up), and the reaction coordinate and

bath are in thermal equilibrium. At time $t = 0$ the electron is released, and the entire system evolves according to the full Hamiltonian, H_{ET}. $W(t)$ is the probability that the spin is found in the up state at time t. The conditional expectation value $< \sigma_z(t) >$, denoted by $P(t)$, is then given by

$$P(t) = 2W(t) - 1 \quad . \tag{2.8}$$

The purely quadratic part of the Hamiltonian (2.1) can be diagonalized via a transformation to normal modes. The Hamiltonian H_{ET} is then rewritten as

$$H_{ET} = \frac{\hbar\Delta_0}{2}\sigma_x + \frac{\varepsilon}{2}\sigma_z + \sigma_z \sum_\alpha \tilde{c}_\alpha \tilde{x}_\alpha$$

$$+ \sum_\alpha \left\{ \frac{\tilde{p}_\alpha^2}{2\tilde{m}_\alpha} + \frac{1}{2}\tilde{m}_\alpha \tilde{\omega}_\alpha^2 \tilde{x}_\alpha^2 + \frac{\tilde{c}_\alpha^2}{2\tilde{m}_\alpha \tilde{\omega}_\alpha^2} \right\} \quad , \tag{2.9}$$

where $\tilde{x}_\alpha$ are the normal coordinates, and $\tilde{p}_\alpha$, $\tilde{m}_\alpha$, and $\tilde{\omega}_\alpha$ are the corresponding canonical momenta, masses, and frequencies. In exact analogy to Eqs. 2.2, we now have

$$J_{eff}(\omega) = \frac{\pi}{2} \sum_\alpha \frac{\tilde{c}_\alpha^2}{\tilde{m}_\alpha \tilde{\omega}_\alpha} \delta(\omega - \tilde{\omega}_\alpha) = \frac{\eta \Omega_y^4 y_0^2 \omega}{(\Omega_y^2 - \omega^2)^2 + 4\omega^2\gamma^2} \tag{2.10a}$$

$$= M_y^2 \Omega_y^4 y_0^2 \chi''(\omega) \quad , \tag{2.10b}$$

where χ'' is the imaginary part of the dynamic response function (susceptibility) of a damped harmonic oscillator. Therefore, when treating real systems, we need to obtain the response function of the medium modes due to electron transfer. Also, as discussed in Refs. 1 and 4, if there are medium degrees of freedom that are strongly excited, the linear treatment of the environment discussed here may break down and anharmonic corrections become necessary.

Using the results obtained in Ref. 1, after integrating over all the harmonic coordinates, we get

$$W(t) = \int D\sigma \int D\lambda A[\sigma]A^*[\lambda]$$

$$\times \exp\left\{\frac{-4}{\pi\hbar}\int_{-\infty}^{t} d\tau \int_{-\infty}^{\tau} ds\xi(\tau)\left[\xi(s)K_2(\tau-s) - i\chi(s)K_1(\tau-s)\right]\right\} \quad , \quad (2.11)$$

where $D\sigma$ denotes the integral over all spin trajectories $\sigma(\tau)$, and $A(\sigma)$ is the amplitude that any given trajectory $\sigma(\tau)$ would have in the absence of coupling to the reaction coordinate. (See Ref. 1 for details.) Also,

$$\xi(\tau) = \left[\sigma(\tau) - \lambda(\tau)\right]/2 \quad , \quad \chi(\tau) = \left[\sigma(\tau) + \lambda(\tau)\right]/2 \quad , \quad (2.12)$$

and

$$K_1(\tau) = \int_0^{\infty} d\omega J_{eff}(\omega)\ \sin(\omega\tau) \quad , \quad (2.13a)$$

$$K_2(\tau) = \int_0^{\infty} d\omega J_{eff}(\omega)\ \cos(\omega\tau)\coth\left(\frac{\beta\hbar\omega}{2}\right) \quad . \quad (2.13b)$$

Using the results above, we can write $P(t)$ in terms of a sum over all possible paths $\{\sigma(\tau),\ \lambda(\tau)\}$. $\xi(\tau) = \pm 1$ we call a blip and $\chi = \pm 1$ a sojourn[13]. Using this notation we can write the conditional expectation as

$$P(t) = \sum_{n=0}^{\infty} (-\Delta_0^2)^n \int_0^t dt_{2n} \int_0^{t_{2n}} dt_{2n-1} \cdots \int_0^{t_2} dt_1\ \tilde{F}_n(t_1, t_2, \cdots, t_{2n}) \ , \quad (2.14)$$

where

$$\tilde{F}_n(\{t_i\}) = 2^{-n}\ \exp\Big(-\sum_{j=1}^{n} A_j\Big) \sum_{\{\varsigma_i\}}\Big[\exp\Big(-\sum_{k>j=1}^{n} \varsigma_j\varsigma_k B_{jk}\Big)$$

$$\times \prod_{k=1}^{n-1} \cos\Big(\sum_{j=k+1}^{n} \varsigma_j\Phi_{kj}\Big) \prod_{j=1}^{n} \exp\Big\{-i\varsigma_j\big(\frac{\epsilon}{\hbar}\ t_{2j,2j-1} + \Phi_{0j}\big)\Big\}\Big] \ . \quad (2.15)$$

Here, $t_{n,m} \equiv t_n - t_m$, and the ζ_i's are variables indicating the signs of the blips; each of them can equal $+1$ or -1. Further,

$$A_j = G_2(t_{2j,2j-1}) , \tag{2.16a}$$

$$B_{jk} = G_2(t_{2k,2j-1}) + G_2(t_{2k-1,2j}) - G_2(t_{2k,2j}) - G_2(t_{2k-1,2j-1}) , \tag{2.16b}$$

$$\Phi_{kj} = G_1(t_{2j,2k}) + G_1(t_{2j-1,2k+1}) - G_1(t_{2j-1,2k}) - G_1(t_{2j,2k+1}) , \tag{2.16c}$$

where G_1 and G_2 are second integrals of the kernels K_1 and K_2 :

$$G_1(t) = \frac{4}{\pi\hbar} \int_0^\infty d\omega \, \frac{J_{eff}(\omega)}{\omega^2} \, \sin(\omega t) , \tag{2.17a}$$

$$G_2(t) = \frac{4}{\pi\hbar} \int_0^\infty d\omega \, \frac{J_{eff}(\omega)}{\omega^2} \, (1 - \cos(\omega t)) \, \coth\Big(\frac{\beta\hbar\omega}{2}\Big) , \tag{2.17b}$$

and the limit $t_0 \to -\infty$ is to be taken when evaluating Φ_{0j}.

In Fig. 1 we show a schematic representation of blips and sojourns. In this figure the short horizontal segments are the blips, which, as discussed, are associated with the "non-diagonal" states of the density matrix. The blips are separated by the sojourns, which represent the diagonal states of the density matrix. When the system is in a blip, $\chi(\tau) = 0$, and when it is in a sojourn, $\xi(\tau) = 0$.

When the reaction coordinate is underdamped, but in the strong coupling limit, every "transit" through the Landau–Zener region is uncorrelated to all the other transits; i.e., there is no precise relation between the times at which these transits occur. The Landau Zener region[14] is the region along the y coordinate where transitions occur. In Fig. 2, it is the region around y^*, where the difference of potential energy between the two wells varies about $\hbar\Delta_0$, i.e.,

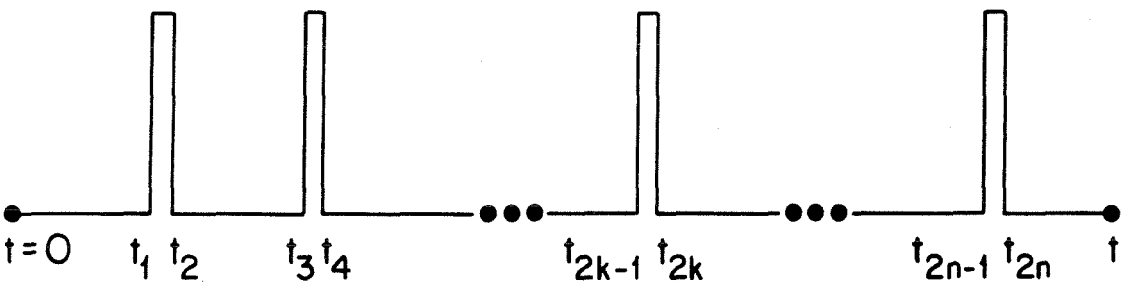

Figure 1 – Schematic representation of the electronic trajectories. The short horizontal segments are the blips. Different blips are separated by intervals called sojourns.

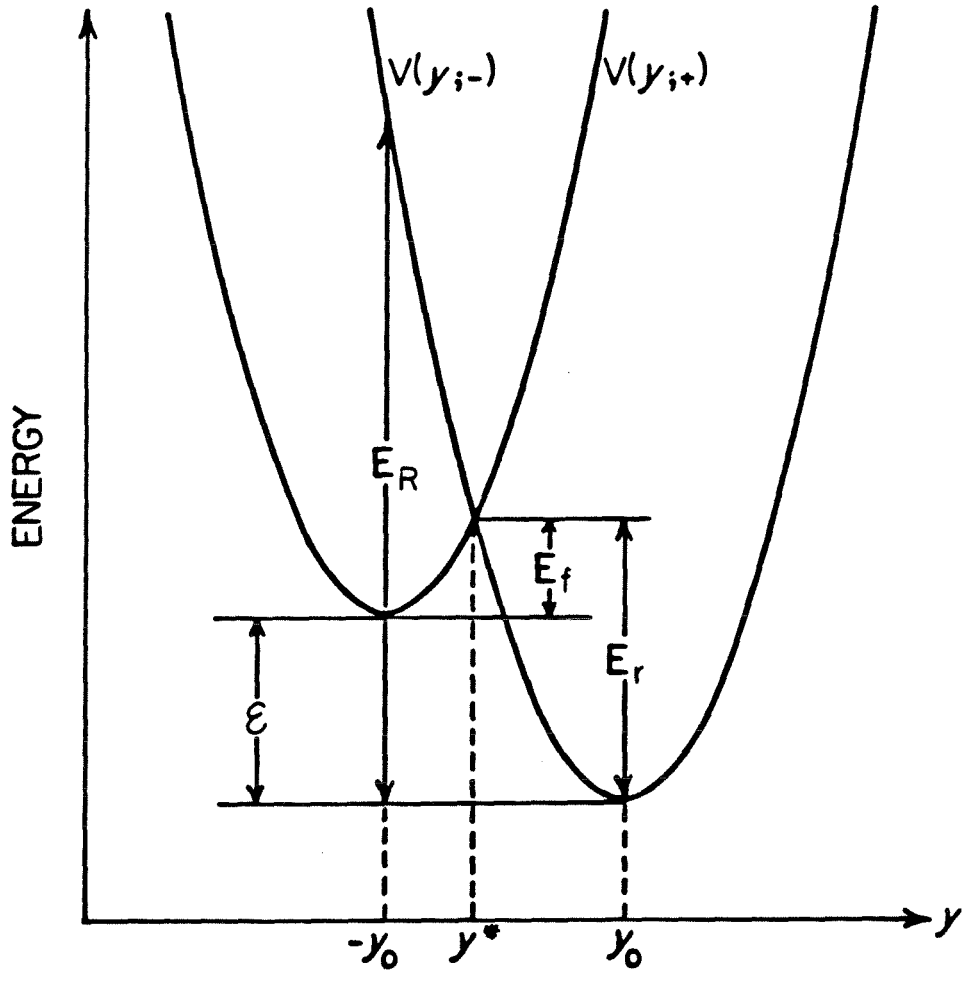

Figure 2 – Potential energy surfaces for the reaction coordinate. The labels + and − refer to the donor and acceptor sites. The energies E_f, E_r, and E_R are the forward and reverse activation energies, and the reorganization energy, respectively.

has a size $\ell_{LZ} = \hbar\Delta_0/2M_y\Omega_y^2 y_0$. This limit is the moderate friction limit. Under these conditions, in the non–adiabatic limit[1],

$$P(t) = P_\infty + (1 - P_\infty)\exp -\Big\{(\Gamma_{na}^f + \Gamma_{na}^r)t\Big\} \quad , \tag{2.18}$$

where the forward and reverse electron transfer rates are

$$\Gamma_{na}^{f;r} = \frac{\Delta_0^2}{4}\left(\frac{\pi\hbar^2}{E_R k T_{eff}}\right)^{1/2} \exp -\left\{\frac{(\varepsilon \mp E_R)^2}{4kT_{eff}E_R}\right\} \quad , \tag{2.19a}$$

and P_∞, the equilibrium value of σ_z, is

$$P_\infty \;=\; -\tanh(\varepsilon/2kT_{eff}) \quad . \tag{2.19b}$$

Here $E_R = 2M_y\Omega_y^2 y_0^2$ is the reorganization energy, and $kT_{eff} = M_y\Omega_y^2\mu^2(\eta, T)$, where μ^2 is the mean square displacement of the reaction coordinate y. Fig. 2 gives a graphical representation of the parameters in Eq. 2.19. We have used the concept of effective temperature, T_{eff}. Appendix A provides details of how to calculate G_1 and G_2, and a better understanding of T_{eff}. It follows from Appendix A that $T_{eff} \approx T$ at high temperatures.

From Appendix A, we know that for short times the expressions for G_1 and G_2 are

$$G_1(t) \;=\; \frac{E_R t}{\hbar} \quad , \tag{2.20a}$$

and

$$G_2(t) = \frac{t^2}{2\tau_0^2} \quad \text{where} \quad \tau_0^{-2} = \frac{2E_R kT_{eff}}{\hbar^2} \quad . \tag{2.20b}$$

Because G_2 appears in the exponential of Eq. 2.15, τ_0 is approximately the duration of a blip, t_{blip}. The non-adiabatic limit used above is valid when in each transit only one transition is possible. This condition is obtained self–consistently in the following way. Within each transit of the Landau–Zener

region, which can involve several tunneling events, the mean blip–plus–sojourn length, t_{b+s}, is of the order of the inverse of Γ_{na} divided by the activation factor ($\approx \exp[-E_f/kT_{eff}]$). It follows from Eqs. 2.16 and 2.17 that if $t_{blip} \ll t_{b+s}$, it is reasonable to neglect the interblip interactions B_{jk}, and all phase factors Φ_{kj} except those with $j = k+1$. These are the conditions used to compute the above rate. If we can self–consistently impose that $t_{blip} \ll t_{b+s}$, Eq. 2.19 is valid, and this condition reads[1] approximately

$$\left(\frac{\hbar^2\Delta_0^2}{2kT_{eff}E_R}\right) \ll 1 \ . \tag{2.21}$$

This condition is similar to the one of Goldstein and Bialek[10],

$$\Gamma_{na} \ll \Delta_0 \ , \tag{2.22}$$

but they did not consider the effect of activation energies, which divide the rate in the criteria above.

Next, we discuss the overdamped limit. This limit is valid when $\omega_c = \Omega_y^2/2\gamma \ll \gamma$, and may be used to describe reaction coordinates such as solvent polarization[15,16], gross protein motions[17], and motion of counter–ions. This limit is called the high friction limit. In this case, if the activation energies are at least a few kT, $P(t)$ has exponential decay in time as given by Eq. 2.18, but the electron transfer rate, Γ, can be calculated for the general case, not only for the non–adiabatic limit. Under these circumstances the rate is given by

$$\Gamma^{f;r} = \frac{\Delta_0^2}{4}\left(\frac{\pi\hbar^2}{E_R kT}\right)^{1/2}\left[\frac{1}{1+\Delta_0^2(\pi\hbar/2\omega_c E_R)}\right]\exp-\left\{\frac{(\varepsilon \mp E_R)^2}{4kTE_R}\right\} \ , \tag{2.23}$$

where

$$g = \frac{\Delta_0^2\pi\hbar}{2\omega_c E_R} \tag{2.24}$$

is the adiabaticity parameter. If $g \ll 1$, the rates reduce to the non–adiabatic limit, while if $g \gg 1$, we get the Δ_0 independent adiabatic rate. An application of this result to understand solvent polarization in electron transfer reactions is described in Ref. 18.

The condition given by Eq. 2.23 is very interesting because it provides a quantitative estimate for the validity of the non–adiabatic limit. In order to simplify the discussion, we now define two times:

$$t_{drift}^{LZ} \approx \frac{\hbar\Delta_0}{E_R\omega_c} = \frac{\ell_{LZ}}{y_0\omega_c} \quad , \tag{2.25}$$

which is the average time the "particle" stays in the Landau–Zener region each time it reaches it, and

$$t_{diff}^{LZ} \approx \frac{(\hbar\Delta_0)^2}{E_R kT\ \omega_c} \quad , \tag{2.26}$$

which is the time taken by the particle for each transit through the Landau–Zener region. Also, it is important to point out that, because $\hbar\Delta_0 \ll kT$ for the problems we are interested in, $t_{drift}^{LZ} \gg t_{diff}^{LZ}$.

Considering the two time scales above, we note the adiabaticity condition, $g \gg 1$, is satisfied when $t_{drift}^{LZ} \gg \Delta_0^{-1}$, and we do not need to meet the condition $t_{diff}^{LZ} \gg \Delta_0^{-1}$. The latter condition, $t_{diff}^{LZ} \gg \Delta_0^{-1}$, is the conventional adiabatic limit, and when it is true, the conventional picture of split nuclear wells is valid. (Also, the validity of Eq. 2.23 becomes questionable when this last limit is valid[1,15].) But, as we showed in the case $t_{drift}^{LZ} \gg \Delta_0^{-1}$, "adiabaticity" holds under a much weaker condition than the conventional one.

As can be seen from Ref. 1, Eq. 2.23 was developed assuming that the motion of the particle is diffusive even when it is in the Landau–Zener region. Thus, if $t_{diff}^{LZ} \ll \Delta_0^{-1} \ll t_{drift}^{LZ}$, when the particle crosses the Landau–Zener

region, each of its transits is associated with a very small transfer probability proportional to Δ_0^2, but adiabaticity results because the particle crosses this region many times before it drifts away. Otherwise, i.e., if $t_{diff}^{LZ} \gg \Delta_0^{-1}$, it is simpler to look at the problem in the conventional way, in which we have the "adiabatic" splitting of the nuclear wells.

3. The Two Mode Problem

As discussed in Sec. 1, if only harmonic "nuclear" modes with linear coupling between them are considered, the electron transfer Hamiltonian for the two reaction coordinates case, in the Condon and Born-Oppenheimer approximations, can be written as

$$H_{ET} = \frac{\hbar\Delta_0}{2}\sigma_x + \frac{P_y^2}{2M_y} + \frac{1}{2}M_y\Omega_y^2(y + y_0\sigma_z)^2 + \frac{\varepsilon}{2}\sigma_z$$

$$+\frac{P_z^2}{2M_z} + \frac{1}{2}M_z\Omega_z^2(z + z_0\sigma_z)^2 + \frac{1}{2}\sum_\alpha \left[\frac{p_\alpha^2}{m_\alpha} + m_\alpha\omega_\alpha^2\left(x_\alpha + \frac{c_\alpha y}{m_\alpha\omega_\alpha^2}\right)^2\right]$$

$$+\frac{1}{2}\sum_\beta \left[\frac{p_\beta^2}{m_\beta} + m_\beta\omega_\beta^2\left(x_\beta + \frac{c_\beta z}{m_\beta\omega_\beta^2}\right)^2\right] \quad . \tag{3.1}$$

The two reaction coordinate problem of electron transfer is interesting because it is the simplest model that is able to describe the effect of a fast localized vibration and a slow (sometimes diffusive) motion on electron transfer. In the above Hamiltonian the coordinates y and z represent the fast and slow coordinates, respectively. Although this problem has already been partially addressed in the literature (Refs. 3, 4, 9, 19, and 20, for example), the aim of this section is to study it beginning with a general Hamiltonian, understanding all of its important time scales, verifying how friction affects them, and finally discussing the validity of each of the approximations that are commonly used. The reasons for assuming independent baths for the y and z coordinates are addressed in Appendix A of Ref. 4.

As discussed in Sec. 2, we do not need to know details about the parame-

ters describing the bath oscillators, but only the spectral densities

$$\begin{pmatrix} J_0^y(\omega) \\ J_0^z(\omega) \end{pmatrix} = \begin{pmatrix} \frac{\pi}{2}\sum_\alpha \frac{c_\alpha^2}{m_\alpha\omega_\alpha}\delta(\omega-\omega_\alpha) \\ \frac{\pi}{2}\sum_\beta \frac{c_\beta^2}{m_\beta\omega_\beta}\delta(\omega-\omega_\beta) \end{pmatrix} . \tag{3.2}$$

Also, as in Sec. 2, in most of this section we restrict ourselves to the well–known ohmic forms of the spectral density for both coordinates

$$J_0^{y,z} = \eta_{y,z}\omega\exp(-\omega/\Lambda), \quad \text{and} \quad \gamma_{y,z} = \eta_{y,z}/2M_{y,z} . \tag{3.3}$$

Λ is a cutoff frequency, which was discussed is Sec. 2.

Now, we calculate electron transfer rates for the following situations:

a) When the coupling between bath and reaction coordinates is strong. In this case the moderate and high friction limits are considered.

b) When the coupling of the bath to both coordinates is weak.

c) When the coupling of the bath to the fast coordinate is weak, but coupling to the slow one is strong.

d) When the fast coordinate y has Ω_y that is much faster than all the other nuclear frequencies of the problem including the cutoff frequency Λ. Recall that Λ is the fastest frequency of the problem in the three case above.

First, we consider the strong coupling situation. As in Sec. 2, the purely quadratic part of Hamiltonian 3.1 can be diagonalized via a transformation to normal modes, and H_{ET} is rewritten as Eq. 2.9, but now we have the following spectral density

$$J_{eff}(\omega) = \frac{\pi}{2}\sum_\alpha \frac{\tilde{c}_\alpha^2}{\tilde{m}_\alpha\tilde{\omega}_\alpha}\delta(\omega-\tilde{\omega}_\alpha)$$

$$= \frac{\eta_y\Omega_y^4 y_0^2\omega}{(\Omega_y^2-\omega^2)^2+4\omega^2\gamma_y^2} + \frac{\eta_z\Omega_z^4 z_0^2\omega}{(\Omega_z^2-\omega^2)^2+4\omega^2\gamma_z^2} . \tag{3.4}$$

Details of this diagonalization are described in Appendix A of Ref. 4.

Next we calculate $P(t)$ using the formalism described in Sec. 2. Formulas for G_1 and G_2, which we need in this section, are given in Appendix A and Ref. 1.

Exponential Non–Adiabatic Limit (Moderate Friction)

First we work in the moderate friction limit for the two reaction coordinates y and z. In the short time limit (which is true for a blip duration), as discussed in Appendix A, G_1 and G_2 can be written as follows:

$$G_1(t) \approx \frac{(E_R^y + E_R^z)}{\hbar} t \quad , \tag{3.5a}$$

and

$$G_2(t) \approx \frac{t^2}{2\tau_0^2}, \quad \text{where } \frac{1}{\tau_0^2} = \frac{1}{(\tau_0^y)^2} + \frac{1}{(\tau_0^z)^2} \quad \text{and} \quad (\tau_0^{y,z})^{-2} = \frac{2E_R^{y,z} k T_{eff}^{y,z}}{\hbar^2} \quad . \tag{3.5b}$$

Here, $E_R^y = 2M_y\Omega_y^2 y_0^2$ and $E_R^z = 2M_z\Omega_z^2 z_0^2$ are the reorganization energies for the y and z coordinates. The concept of effective temperature was introduced in Sec. 2. The above expressions are used for calculations only in short time intervals, i.e., during blips (which are of order τ_0).

Let us assume for now that $P(t)$ decays exponentially in time with a non–adiabatic decay rate, Γ_{na}, which must be computed. This assumption is valid when two conditions are met. First, at least one of the modes has to satisfy the criteria for non–adiabaticity given by Eq. 2.21. Also, both modes must have a relaxation time much faster than the electron transfer rate; i.e., $\gamma_y, \gamma_z \gg \Gamma_{na}$. If both of these conditons are satisfied, then (as in the last

section) it is reasonable to neglect the interblip interactions B_{jk}, and all phase factors Φ_{kj} except those with $j = k + 1$. Under these circumstances, similar to Ref. 1,

$$\Phi_{k,k+1} \approx -G_1(t_{2k+2} - t_{2k+1}) \quad , \tag{3.6}$$

and Eq. 2.14 becomes

$$P(t) = P_\infty + (1 - P_\infty)\exp(-\Gamma_{na}t) \quad , \tag{3.7}$$

where

$$\Gamma_{na} = \Delta_0^2 \int_0^\infty \exp[-G_2(t)]\cos[G_1(t)]\cos(\varepsilon t/\hbar)dt \quad , \tag{3.8a}$$

$$P_\infty = 1 - \frac{\Delta_0^2}{\Gamma_{na}} \int_0^\infty \exp[-G_2(t)]\cos[G_1(t) - \varepsilon t/\hbar]dt \quad . \tag{3.8b}$$

We can now calculate Γ_{na} when Eqs. 3.5 are good approximations for G_1 and G_2 during the blips duration, and the electron transfer rate is

$$\Gamma_{na} = \Gamma_{na}^f + \Gamma_{na}^r \quad , \tag{3.9}$$

where

$$\Gamma_{na}^{f;r} = \frac{\Delta_0^2}{4}\left(\frac{\pi\hbar^2}{E_R k T_{eff}}\right)^{1/2} \exp\left\{-\frac{(\varepsilon \mp E_R)^2}{4kT_{eff}E_R}\right\} \quad . \tag{3.10}$$

Here $E_R = E_R^y + E_R^z$, and $T_{eff} = (T_{eff}^y E_R^y + T_{eff}^z E_R^z)/(E_R^y + E_R^z)$.

An interesting comment to be made about the equation above is that if some experimental data for electron transfer are fit using only one reaction coordinate, at low temperatures T_{eff} represents an average of all modes instead of a real physical mode; i.e., at zero temperature the mode frequency which we estimate from T_{eff} is the weighted average frequency, not a real mode frequency. In cases such as the electron transfer between hemes in hemoglobin[21]

and in Cytochrome c oxidation in *Chromatium*[2a], which was fit with a low temperature $T_{eff} = 350^o K$ by Hopfield[8a], effects like this may be important.

As an example let us plot the forward rate given Eq. 3.10 using parameters similar to the ones given by Goldstein and Bearden[22] for the Chromatium problem. (They fit the experimental result using a one mode model.) In Fig. 3 we show two plots. The first one considers only one nuclear mode of $\hbar\Omega_y = 250\text{cm}^{-1}$, $E_R = 1200\text{cm}^{-1}$, and $\varepsilon = 3600\text{cm}^{-1}$. The second plot considers two nuclear modes, 100 and 400 cm^{-1}, and the reorganization energy is divided between the two modes, $E_R^y = E_R^z = 600\text{cm}^{-1}$. T_{eff} was calculated using Eq. A.9. From Fig. 3 we conclude that the two plots are very similar, and therefore crude analysis of the experiments described in the last paragraph using one mode models will lead to a frequency that is the average frequency of all modes coupled to the problem instead of a physically significant one. Eq. 3.10 is valid for modes in the strong coupling limit. High–frequency modes, such as CO vibrations, do not satisfy this limit, and how to include them in the problem is discussed at the end of this section.

At this point it is interesting to notice that because we are in the non-adiabatic limit and both modes relax much faster than the electron transfer rate, Eq. 3.10 can be written as

$$\Gamma_{na}^{f;r} = \int_{-\infty}^{\infty} k_{y,na}^{f;r}(z) P_{eq}^{+,-}(z)\, dz \quad , \tag{3.11}$$

where $k_{y,na}^{f;r}(z)$ are the forward and reverse rates if we freeze the system in a particular position of the coordinate z, and $P_{eq}^{+,-}(z)$ are the equilibrium distributions of z when the electron is on the donor $(+)$ or acceptor $(-)$, respectively. $k_{y,na}^{f;r}(z)$ is calculated exactly as in the one mode case (Eq. 2.19a), but uses a z dependent driving force, $\varepsilon^y(z) = \varepsilon + 2M_z\Omega_z^2 z_0 z$. This expression

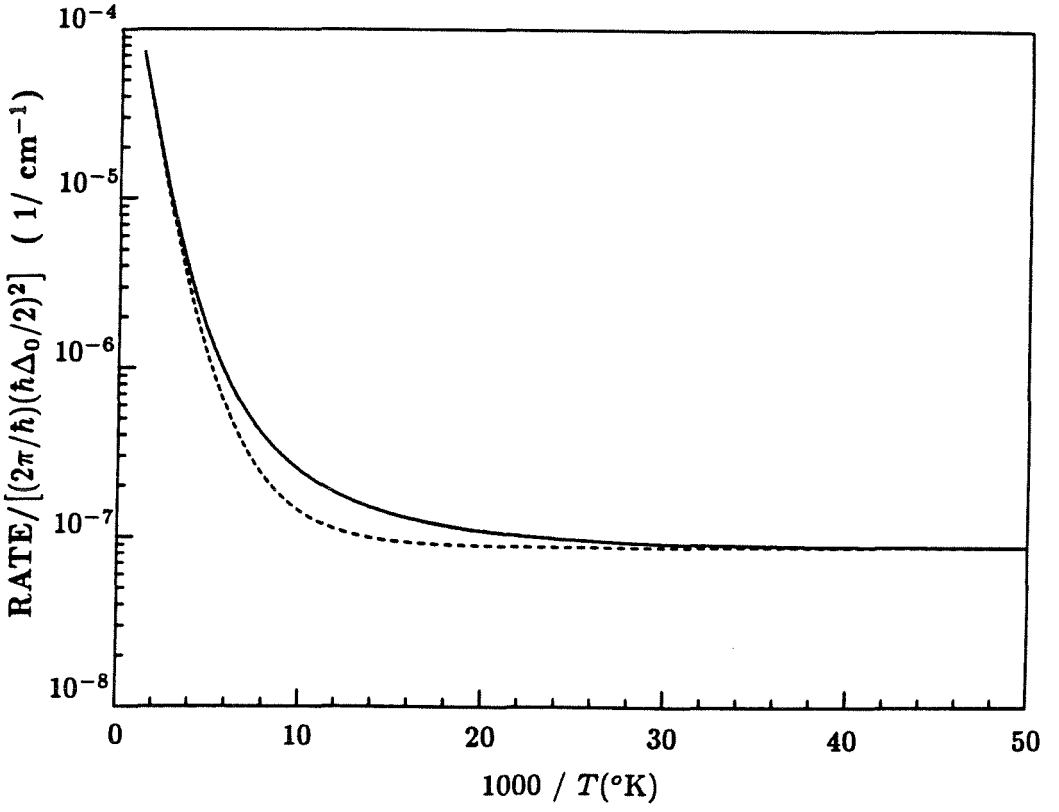

Figure 3 – Temperature dependence of the forward rate given by Eq. 3.10. We plot $\Gamma^f_{na}/[(2\pi\hbar)(\hbar\Delta_0/2)^2]$ in units of $(1/\text{cm}^{-1}$ vs $1000/T(^o\text{K})$. The solid plot uses $E^y_R = E^z_R = 600\text{cm}^{-1}$, $\varepsilon = 3600\text{cm}^{-1}$, $\hbar\Omega_y = 100\text{cm}^{-1}$, and $\hbar\Omega_z = 400\text{cm}^{-1}$. The dashed plot uses the same energies but $\hbar\Omega_y = \hbar\Omega_z = 250\text{cm}^{-1}$.

is a generalization of the result obtained by Agmon and Hopfield[3] or Sumi and Marcus[20] when the transfer is exponential in time, since in their case the z coordinate is classical and diffusive.

Eq. 3.11 is written in the form above because we assumed the z coordinate to be the slow one, but the result given by Eq. 3.10 is general for any modes y and z as long they satisfy the conditions stated at the beginning of this subsection. For example, the rate 3.10 can be obtained by considering $k^{fir}_{z,na}(y)$ and the equilibrium distributions for the y coordinate. A more detailed discussion, also including the case when the non-adiabatic limit is not valid, is given in the following subsection.

Exponential Limit (High Friction)

Now we consider both coordinates overdamped; i.e., $\gamma_y \gg \Omega_y$ and $\gamma_z \gg \Omega_z$. Then the relaxation frequencies for the y and z modes are $\omega_c^y = \Omega_y^2/2\gamma_y$ and $\omega_c^z = \Omega_z^2/2\gamma_z$, respectively. Also, we work in the limit $\hbar\omega_c^y,\ \hbar\omega_c^z \ll kT$.

Assuming that

$$\frac{1}{\omega_c^y},\ \frac{1}{\omega_c^z} \ll \frac{1}{\omega_c^y}\exp\left\{\frac{(\varepsilon^y \mp E_R^y)^2}{4kTE_R^y}\right\},\ \frac{1}{\omega_c^z}\exp\left\{\frac{(\varepsilon^z \mp E_R^z)^2}{4kTE_R^z}\right\}, \qquad (3.12)$$

the electron trajectories, which contribute appreciably to $P(t)$, consist of well–separated "blocks" of closed spaced blips (similar to Ref. 1). In the above limit we can neglect interaction between blips in different blocks. Also, the average duration of these blocks is much smaller than $(\omega_c^y)^{-1}$ or $(\omega_c^z)^{-1}$. Under these conditions $P(t)$ can be calculated analytically.

Defining

$$b_j = t_{2j} - t_{2j-1} \tag{3.13a}$$

$$s_j = t_{2j+1} - t_{2j} \ , \tag{3.13b}$$

and using Eqs. 2.16, it is straightforward to show that (see Ref. 1 for details)

$$A_j = \frac{E_R kT}{\hbar^2} b_j^2 \tag{3.14}$$

and

$$B_{jk} = \begin{cases} \frac{2E_R kT}{\hbar^2} b_j b_k, & \text{if } b_j \text{ and } b_k \text{ are in the same block;} \\ 0 & \text{otherwise.} \end{cases} \tag{3.15}$$

For the phase factors, if the blip b_j and the sojourn s_k are in the same block,

$$\Phi_{kj} \ = \ -\left(\frac{\omega_c^y E_R^y}{\hbar} + \frac{\omega_c^z E_R^z}{\hbar} \right) b_j s_k \ . \tag{3.16}$$

If they are in different blocks the phase factors vanish, unless s_k is a long sojourn separating "blocks" (super–sojourn in Ref. 1), and b_j lies in the block immediately following it. In this case,

$$\Phi_{kj} = -E_R b_j / \hbar \ . \tag{3.17}$$

In Eq. 3.16 we have to keep terms up to t^2 in $G_1(t)$ (see Eqs. A.3 and A.11).

The series 2.14 is calculated in a way similar to that described in Ref. 1. $P(t)$ is given by an expression similar to Eq. 3.7, although the rates do not have to be restricted to the non–adiabatic limit. Here, the electron transfer rates rates are

$$\Gamma^{f;r} \ = \ \frac{\Delta_0^2}{4} \left[\frac{\pi \hbar^2}{(E_R^y + E_R^z) kT} \right]^{1/2}$$

$$\times \left\{ \frac{1}{1 + \Delta_0^2 \left[\pi \hbar / (2\omega_c^y E_R^y + 2\omega_c^z E_R^z) \right]} \right\} \ \exp\left\{ -\frac{E_{f;r}}{kT} \right\} \ , \tag{3.18a}$$

where

$$E_{f;r} = \frac{\left[\varepsilon \mp (E_R^y + E_R^z)\right]^2}{4kT(E_R^y + E_R^z)} \quad . \tag{3.18b}$$

As in Sec. 2, we define the adiabaticity parameter $\bar{g}$,

$$\bar{g} = \frac{\Delta_0^2 \pi \hbar}{2\omega_c^y E_R^y + 2\omega_c^z E_R^z} \quad , \tag{3.19}$$

which can be written as

$$\frac{1}{\bar{g}} = \frac{1}{g_y} + \frac{1}{g_z} \quad , \tag{3.20}$$

where g_y and g_z are the adiabaticity parameters for the y and z modes, respectively.

If $\bar{g} \ll 1$, the non–adiabatic limit is valid, and the rates 3.18 can be given by Eq. 3.11; i.e., the final rate is the rate in the y direction averaged over the z coordinate. Otherwise, we can use Eq. 3.11 to calculate the rate only if $g_y \ll g_z$. This means that every crossing through the Landau–Zener region is basically in the y direction or that Eq. 3.11 is not valid. The reason why the non–adiabatic limit can be calculated using Eq. 3.11, independently of the y and z modes chosen, is that the dynamics of the nuclear coordinates is not important when this limit is valid ($\bar{g} \ll 1$ anyway).

This condition, $g_y \ll g_z$, gives us a quantitative estimate of when the formalism presented by Agmon and Hopfield[3], and later extended by Sumi and Marcus[20], is valid. This condition can be generalized for other dynamical situations by saying that in order for Refs. 3 and 20 to be valid, it is necessary that every cross through the Landau–Zener region be basically in the y direction. Also, in the overdamped limit, we can notice that only one fast mode is sufficient to guarantee "non–adiabaticity."

Non–Exponential Limit

We now consider the situation in which the z mode is much slower than the electron transfer. The average frequency with which the electron switches sides is much faster than any important motion of the z coordinate. Under these circumstances we can consider the short–time limit expressions given in Appendix A valid during the entire duration of the electron transfer reaction for G_1^z and G_2^z.

Let us initially consider the situation in which $t_{blip} \ll t_{b+s}$, and therefore the non–adiabatic limit is valid. As discussed earlier, this latter condition has to be imposed self–consistently. When this condition is valid and z is very slow (using Eq. 2.16 and expressions for G_1 and G_2 given in Appendix A), we can write:

$$A_j = \frac{k(T_{eff}^y E_R^y + T_{eff}^z E_R^z)}{\hbar^2}(t_{2j} - t_{2j-1})^2 \quad , \tag{3.21a}$$

$$B_{jk} = \frac{2E_R^z k T_{eff}^z}{\hbar^2}(t_{2j} - t_{2j-1})(t_{2k} - t_{2k-1}) \quad , \tag{3.21b}$$

$$\Phi_{0j} = -\frac{E_R^y + E_R^z}{\hbar}(t_2 - t_1) \text{ for } j = 1 \text{ and } -\frac{E_R^z}{\hbar}(t_{2j} - t_{2j-1}) \text{ for } j \neq 1, \tag{3.21c}$$

$$\Phi_{k,k+1} = -\frac{E_R^y}{\hbar}(t_{2k+2} - t_{2k+1}) \text{ and} \tag{3.21d}$$

$$\Phi_{kj} = 0 \text{ for } k \neq 0 \text{ and } j \geq k+2 \quad . \tag{3.21e}$$

Here the short–time approximation was used during blips of both coordinates, and also for the z coordinate during the sojourns. For the y coordinate, the long–time approximation has been used for the sojourns.

Assuming that at $t = 0$, the electron is in the donor and all nuclear modes are in thermal equilibrium, we can now calculate the electron transfer

expectation value $P(t)$ ($< \sigma_z(t) >$). Using Eqs. 2.14 and 2.15, we find

$$P(t) = \int_{-\infty}^{\infty} dz \left[P_{\infty}^{y}(z) + \left(1 - P_{\infty}^{y}(z)\right) \exp\left(-k_{y,na}(z)t\right) \right] \times P_{eq}^{+}(z) \quad , \quad (3.22a)$$

where

$$k_{y,na} = k_{y,na}^{f} + k_{y,na}^{r} \quad . \quad (3.22b)$$

Here $P_{\infty}^{y}(z)$ and $k_{y,na}$ are, respectively, the equilibrium value for $< \sigma_z >$ and the electron transfer rate when we freeze the system in a particular value for coordinate z. $P_{eq}^{+}(z)$, which was defined in Eq. 3.11, is the equilibrium distribution for z when the electron is on the donor. Because the z coordinate is very slow, we sometimes may not use an equilibrium distribution for z, but whatever is the appropriate distribution when the electron transfer process is initiated. Exactly as in Eq. 3.11,

$$k_{y,na}^{f;r}(z) = \frac{\Delta_0^2}{4} \left(\frac{\pi\hbar^2}{E_R^y k T_{eff}^y} \right)^{1/2} \exp - \left\{ \frac{(\varepsilon^y(z) \mp E_R^y)^2}{4kT_{eff}^y E_R^y} \right\} \quad , \quad (3.23a)$$

where

$$\varepsilon^y(z) = \varepsilon + 2M_z\Omega_z^2 z_0 z \quad . \quad (3.23b)$$

As in Eq. 2.19b,

$$P_{\infty}^{y}(z) = -\tanh\left(\varepsilon^y(z)/2kT_{eff}^y\right) \quad . \quad (3.24)$$

The result above is shown by comparing the perturbation series 2.14 term by term with the series expansion of Eq. 3.22 in powers of $(\Delta_0^2)^n$. Details of this calculation are given in Appendix B. Current work in Hoffman's group[23] is looking for this non–exponential behavior in electron transfer between heme groups in hemoglobin at low temperatures.

We now calculate an example of a typical distribution of driving forces $\varepsilon^y(z)$ for systems where non–exponential behavior may occur. The width of

this distribution gives us information about the size of the non–exponentiallity in Eq. 3.22. From typical values of solvent polarization or protein medium reorganization energies, a reasonable example is to calculate this distribution for a slow mode with reorganization energy $E_R^z = 0.3\text{eV}$. In Fig. 4 the probability distribution of $\varepsilon^y(z)$ with z at equilibrium is shown for $T = 300^o\text{K}$ and 77^oK. From this figure we obtain a mean–square displacement for the driving force distribution of $(0.12\text{eV})^2$ and $(0.06\text{eV})^2$, respectively. Because non–exponentiality is probably important only at low temperature, if z is at equilibrium, we should look at the low temperature distribution, but, if we cool down the experimental system very rapidly, the z coordinate will not relax, and therefore a distribution similar to the one at room temperature may be observed at lower temperatures. Also, phase transitions of polar solvents to a solid phase will give a fixed distribution of driving forces for temperatures below freezing.

Theoretically speaking, the above result is interesting because we were able to sum up the entire perturbation series 2.14 in a situation in which the decay is non-exponential in time, and to obtain an analytical result. Generalization of this expression to the overdamped regime (high friction) is straightforward, with the only difference that $k_{y,na}(z)$ is replaced by $k_y(z)$ where

$$k_y(z) = k_y^f(z) + k_y^r(z) \quad , \tag{3.25a}$$

and

$$k_y^{f;r} = \frac{\Delta_0^2}{4}\left(\frac{\pi\hbar^2}{E_R^y kT}\right)^{1/2}\left[\frac{1}{1+\Delta_0^2(\pi\hbar/2\omega_c^y E_R^y)}\right]\exp-\left\{\frac{(\varepsilon^y(z)\mp E_R^y)^2}{4kTE_R^y}\right\} \quad . \tag{3.25b}$$

In this subsection the formalism presented by Agmon and Hopfield[3] and Sumi and Marcus[20] works without any difficulties because the z coordinate is much

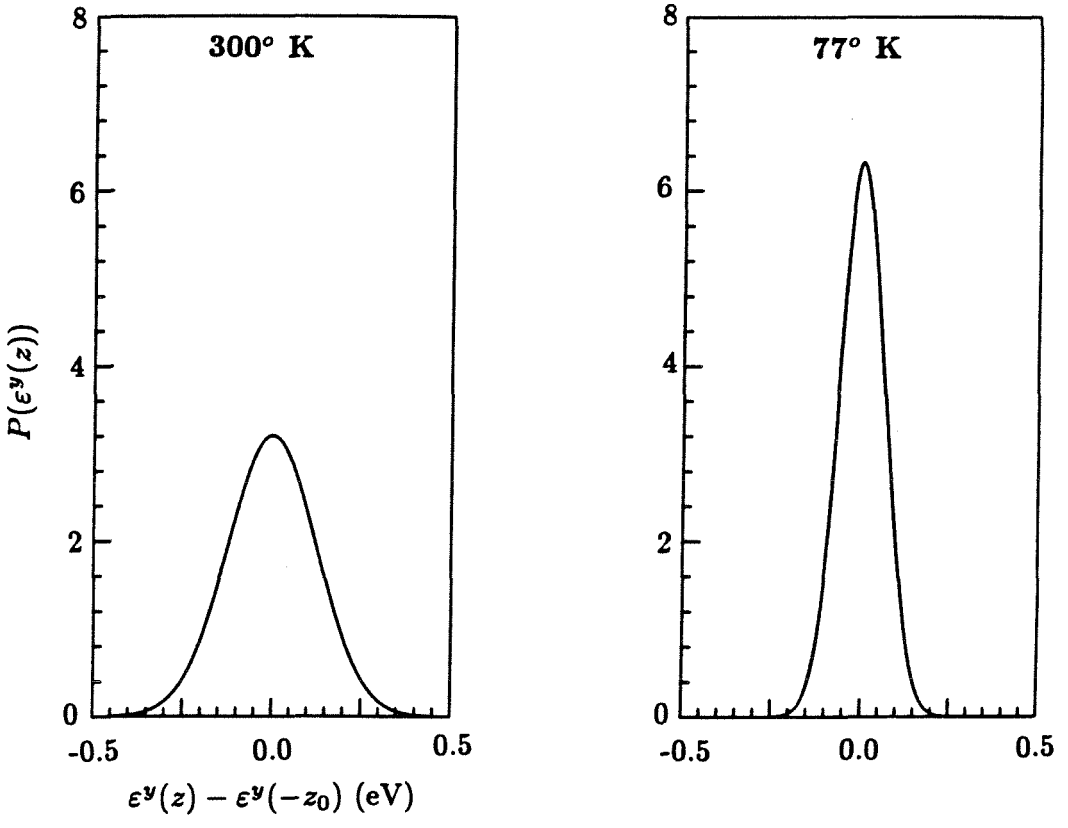

Figure 4 – Distribution of driving forces, $\varepsilon^y(z)$, assuming that z has an equilibrium distribution (see Eqs. 3.22 and 3.23). E_R^z is assumed to be 0.3 eV.

slower than y, and therefore every crossing through the Landau–Zener region is basically in the y direction. It is also important to point out that because $\varepsilon^y(z)$ appears only in the exponent of Eq. 3.25b, the non–exponential behavior is going to be the same for the adiabatic and non-adibatic limits.

In this section, and in Sec. 2, we present results for which the the series 2.14 can be summed analytically, so closed expressions are obtained for the electron transfer rate. It is important to point out the power of this technique when analytical results are impossible. In this case, numerical integration of the terms of the series 2.14 is an achievable task, and it can be performed when quantitative results are needed for situations out of the limits presented here. An example of this occurs when z is not fast enough so that the exponential non–adiabatic limit is valid, but z is also not slow enough so that we can assume z to be static during the whole electron transfer process. In the next section, we obtain the Fokker–Planck equation associated with this problem in the limit that the nuclear modes can be treated classically. In this case, numerical solutions are much simpler.

The Weak Coupling Limit

In the next two subsections, we consider the following situations: one in which the two modes of Hamiltonian 3.1 are in the weak coupling limit, and another in which one is in the weak coupling limit and the other is in the strong one.

Let us consider the first case and also assume that the relaxation of both modes is fast enough compared to the electron transfer rate so that the donor

survival probability decays exponentially in time, and also the non–adiabatic limit is valid. (See Appendix B of Ref. 4 for details.) For simplicity, we assume that $\hbar\Omega_y = k\hbar\Omega_z$ and $\varepsilon = m\hbar\Omega_y$, where k and m are integers. In this case, the electron transfer rate is calculated by generalizing the one mode result (Eq. 2.4) to two modes. In order to do that clearly, we rewrite Eq. 2.4 as

$$\Gamma_{na}^{f;r} = \frac{2\pi}{\hbar}\left(\frac{\hbar\Delta_0}{2}\right)^2 (FC)^{f;r}(\varepsilon) \quad , \tag{3.26}$$

where the Franck–Condon factor, (FC), is

$$(FC)^{f;r}(\varepsilon) = \frac{1}{2\pi}\sum_{n_D,m_A} \frac{\hbar\gamma_{m_A;n_D}|\hbar\Delta_0/2|^2|<n_D|m_A>|^2}{(E_{n_D}-E_{m_A})^2+\hbar^2\gamma_{m_A;n_D}^2/4}\rho(E_{n_D;m_A},T) \quad , \tag{3.27a}$$

and

$$E_{n_D=0} - E_{m_A=0} = \varepsilon \quad . \tag{3.27b}$$

The notation is defined in Eqs. 2.4, 2.5 and 2.6.

In the two mode case, we have to convolute the Franck–Condon factors for the modes. Doing this, we get for the electron transfer rate

$$\Gamma_{na}^{f;r} = \frac{2\pi}{\hbar}\left(\frac{\hbar\Delta_0}{2}\right)^2 \sum_n (FC)_y^{f;r}(\varepsilon - n\hbar\Omega_y)\ (FC)_z^{f;r}(n\hbar\Omega_y) \quad . \tag{3.28}$$

The above result can be easily generalized for as many nuclear coordinates as necessary.

As in Eq. 3.11, the rate given by Eq. 3.28 may be written as

$$\Gamma_{na}^{f;r} = \sum_{n_{D;A}^z} k_{na}^{f;r}(n_{D;A}^z)\rho(E_{n_{D;A}^z},T) \quad , \tag{3.29}$$

where $k_{na}^{f;r}(n_{D;A}^z)$ is the forward/reverse electron transfer rate when the z mode is in a fixed donor/acceptor state. $\rho(E_{n_{D;A}^z},T)$ is the equilibrium density of states of the z mode when the electron is on the donor/acceptor.

One Strongly Coupled and One Weakly Coupled Mode

Now we consider the second case, in which the coupling of y to the bath is weak and that of z is strong. We also assume that z is much slower than y, and therefore $\hbar\Omega_y \gg \hbar\Omega_z$. In these circumstances, the electron transfer rate can be calculated using Eq. 3.11 if the decay is exponential in time, or Eq. 3.22, if z is extremely slow. Here we present the calculation for the exponential case.

Using Eq. 3.11,

$$\Gamma_{na}^{f;r} = \int_{-\infty}^{\infty} k_{y,na}^{f;r}(z) P_{eq}^{+,-}(z)\, dz \quad , \tag{3.30a}$$

where

$$k_{y,na}^{f;r}(z) \;=\; \frac{2\pi}{\hbar}\left(\frac{\hbar\Delta_0}{2}\right)^2 (FC)^{f;r}\left(\varepsilon^y(z)\right) \quad . \tag{3.30b}$$

The Franck–Condon factor is

$$(FC)^{f;r}\left(\varepsilon^y(z)\right) \;=\; \frac{1}{2\pi}\sum_{n_D^y, m_A^y} \frac{\hbar\gamma_{m_A^y;n_D^y}\,|\hbar\Delta_0/2|^2|\, < n_D^y|m_A^y > |^2}{(E_{n_D^y} - E_{m_A^y})^2 + \hbar^2\gamma_{m_A^y;n_D^y}^2/4}\rho(E_{n_D^y;m_A^y}, T), \tag{3.31a}$$

and

$$E_{n_D^y=0} - E_{m_A^y=0} \;=\; \varepsilon^y(z) \quad , \tag{3.31b}$$

where $\varepsilon^y(z) = \varepsilon + 2M_z\Omega_z^2 z_0 z$. For details of the notation, the reader should see Eqs. 2.4 and 3.11.

Separation of Fast and Slow Modes

To conclude this section we consider the interesting situation in which y is the fastest nuclear frequency of the system; i.e, Ω_y is even much faster than

the cutoff frequency Λ. Also, the coupling of the y coordinate to the bath is weak. (In Appendix A of Ref. 4, we show that the latter conditon is not necessary but simplifies the algebra.) We also assume that the slow mode z is strongly coupled to the bath. We now discuss how to renormalize the effect of the fast mode, and then to reduce our problem to a situation in which it is coupled only to the slow modes (z and bath modes in this particular case). This situation was discussed is Ref. 4, and the effective spectral density is

$$J_{eff}(\omega) \approx J^z_{eff}(\omega) + \frac{\pi}{2} M_y \Omega_y^3 y_0^2 \delta(\omega - \Omega_y) \quad . \tag{3.32}$$

In this regime, the final rate expression is similar to Eq. 2.4, but the broadening of the y energy levels, rather than being due to the bath coupling(Lorentzian shape), is due to the z coordinate (therefore, Gaussian shape). In particular, as is shown in Ref. 4, if $\hbar\Omega_y \gg \varepsilon, kT$ (excited states of y are not important), the electron tranfer rate is

$$\Gamma^{f;r}_{na} = \frac{|\Delta_0^{eff}|^2}{4} \left(\frac{\pi\hbar^2}{E_R^z k T^z_{eff}} \right)^{1/2} \exp - \left\{ \frac{(\varepsilon \mp E_R^z)^2}{4kT^z_{eff} E_R^z} \right\} \quad , \tag{3.33a}$$

where

$$\Delta_0^{eff} = \Delta_0 < n_D^y = 0 | m_A^y = 0 > \quad . \tag{3.33b}$$

The notation, Δ_0^{eff}, is used in Eq. 3.33, because we may think of the fast mode as *renormalizing* the electronic matrix element, and then the problem is reduced to a one mode problem again. In the case of z overdamped, the rate can be calculated, using Eq. 2.23, if Δ_0 is replaced by Δ_0^{eff} and E_R by E_R^z.

Because $\hbar\Omega_y$ is much larger than the energy fluctuations of the z mode, we can generalize the above result (recall that $\hbar\Omega_y \gg kT$). In this situation, the forward rate for electron transfer can be written as a sum of several two–level system problems coupled to only one nuclear mode (z mode), in which

each one of them has a matrix element $\Delta_0^{eff}(m_A) = \Delta_0 < n_D^y = 0|m_A^y >$ and driving force $\varepsilon^y(m_A) = \varepsilon - m_A^y \hbar\Omega_y$, instead of one single two–level problem coupled to two nuclear modes (same procedure to calculate the backward rate). The prescription described in this subsection is simplistic and further work is necessary, but it gives us some initial understanding of this problem. This natural separation of the problem into fast and slow modes has also been used by Jortner and collaborators[9] and by Goldstein and Bialek[19], but only in the non-adiabatic limit. Then, in the non–adiabatic limit, the forward electron transfer rate is

$$\Gamma_{na}^f = \sum_{m_A} \frac{|\Delta_0^{eff}(m_A)|^2}{4} \left(\frac{\pi\hbar^2}{E_R^z k T_{eff}^z} \right)^{1/2} \exp - \left\{ \frac{(\varepsilon^y(m_A) - E_R^z)^2}{4kT_{eff}^z E_R^z} \right\} , \tag{3.34a}$$

where

$$|\Delta_0^{eff}(m_A)|^2 = \Delta_0^2 \left\{ \frac{\exp(-S)\ S^{m_A}}{m_A!} \right\} \quad \text{with} \quad S = \frac{E_R^y}{\hbar\Omega_y} . \tag{3.34b}$$

This description in which we separate the influence of fast modes from that of slow modes may be very important for describing electron transfer in real systems. It will be especially useful when the electron transfer problem is coupled to fast modes, such as CO vibrations, and also to slow, sometimes diffusive, modes, such as solvent polarization. After separating these fast modes, the "slow" modes left in the problem can normally be treated in the strong coupling limit, and therefore the entire formalism developed by us for this limit can then be applied. As an example here, Eq. 3.34 is a reasonable first model to understand the ε (ΔG) dependence of the recent experimental results such as the electron transfer rate between quinones and the oxidized bacteriochlorophyll dimer[24] (E_R^y =0.2 eV, $\hbar\Omega_y$ =0.2 eV, and E_R^z =0.375 eV), and between

rigidly linked porphyrin and quinone systems[25], (E_R^y =0.3 eV, $\hbar\Omega_y$ =0.2 eV, and E_R^z =0.2 eV). Fig. 5 shows the molecule used in Ref. 25. The values used for E_R^y and $\hbar\Omega_y$ in the systems above are reasonable, because the main fast mode coupled to the electron transfer process is the CO vibration of the quinone[25]. In Fig. 6a we plot Eq. 3.34, using the second set of parameters for $T = 77°$K and $T = 300°$K. From this figure we notice that the electron transfer rate has a strong temperature and ε dependence for small values of ε, and a weak one for large values of ε. This prediction for the systems above awaits experimental confirmation.

If the z mode is diffusive, the condition for adiabaticity is different for each term of the sum because *each has different* Δ_0^{eff}. The forward rate can be written as

$$\Gamma^f = \sum_{m_A} \frac{|\Delta_0^{eff}(m_A)|^2}{4} \left(\frac{\pi\hbar^2}{E_R^z kT}\right)^{1/2} \left[\frac{1}{1+|\Delta_0^{eff}(m_A)|^2(\pi\hbar/2\omega_c^z E_R^z)}\right] \times \exp - \left\{\frac{(\varepsilon^y(m_A) - E_R^z)^2}{4kTE_R^z}\right\} . \quad (3.35)$$

In Fig. 6b we show a plot of Eq. 3.35 in the adiabatic limit for the same parameters of Fig. 6a. Because in this figure ε varies from 0 to 1.2 eV, Fig. 6b is valid only if the adiabaticity condition is valid for $\Delta_0^{eff}(m_A)$ with m_A varying at least from 0 to 5. Because the rate does not depend on Δ_0^{eff} in this limit, it is basically ε independent for large values of ε.

An experimental system in which Eq. 3.35 applies is the intramolecular electron transfers in 6–(4–methylphenyl)amino–2–naphthalenesulfon–N,N–dimethylamide (TNSDMA) and 1–cyano–4–dimethyl–aminobenzene (DMAB) [26,18]. As we see from Refs. 18 and 27, solvent polarization can be represented by a diffusive mode with $(\omega_c^z)^{-1} = (\epsilon_\infty/\epsilon_0)\tau_D$, where ϵ_∞ and ϵ_0 are the optical

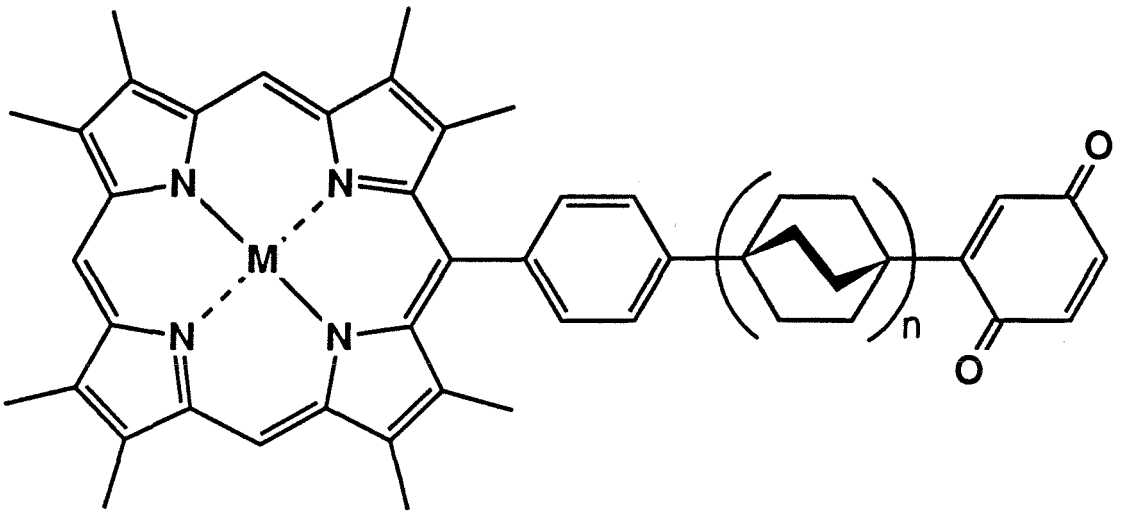

Figure 5 – Structure of the molecule Porphyrin–(Bicyclo[2.2.2.]octane)$_n$–Quinone[25]. **n** = 0, 1, 2. **M** is a metal, normally Zn.

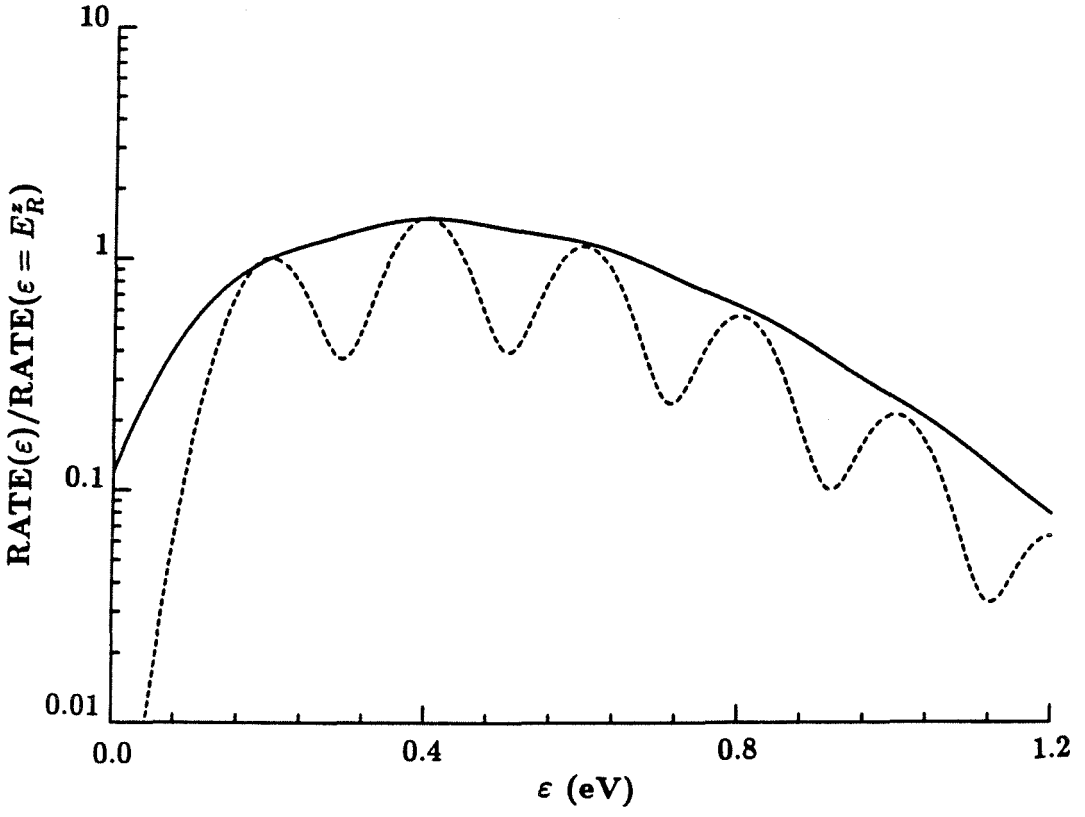

Figure 6a – Plot of rate vs. ε for the case that we can separate fast and slow modes. $E_R^y = 0.3\text{eV}$, $E_R^z = 0.2\text{eV}$, and $\hbar\Omega_y = 0.2\text{eV}$. This plot shows the non–adiabatic limit given by Eq. 3.34. The dashed line uses $T = 77°\text{K}$ and the solid one $T = 300°\text{K}$.

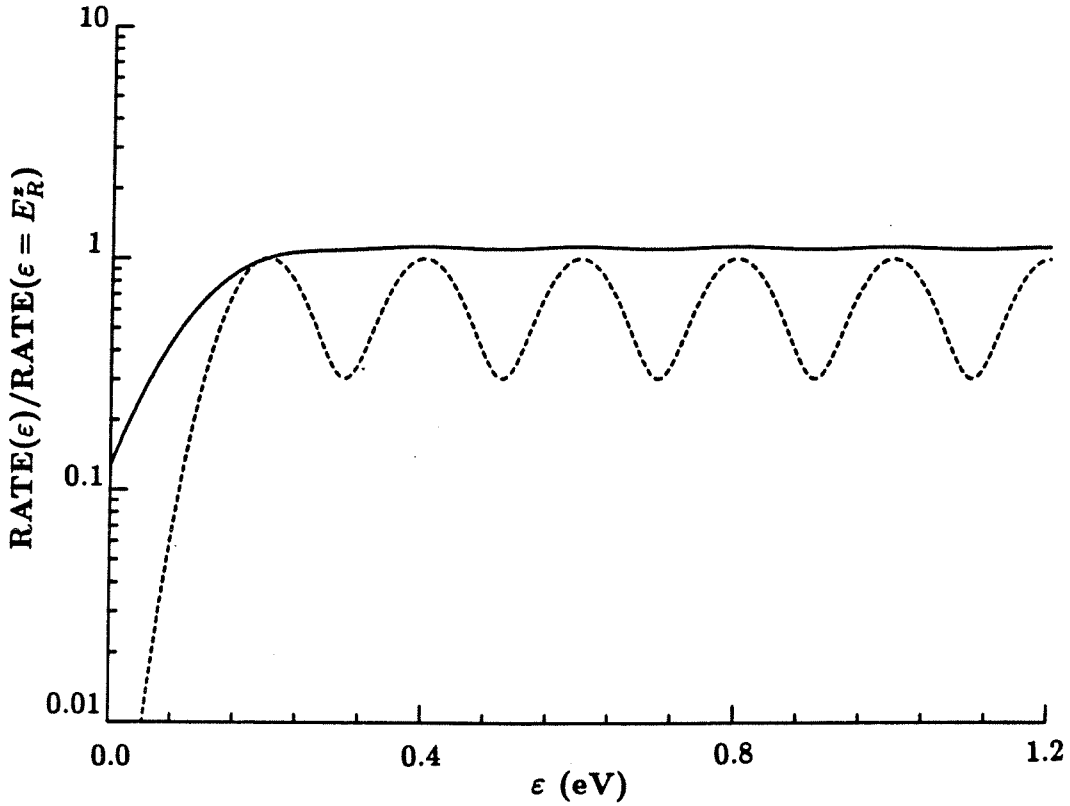

Figure 6b – Same as Fig. 6a, but it shows the adiabatic limit of Eq. 3.35.

and static dielectric constants, and τ_D is the Debye relaxation time. In the systems above the electron transfer rates are proportional to ω_c^z for different aliphatic alcohols solvents. The proportionality factor is basically one. This tells us that the rate is adiabatic and therefore independent of Δ_0^{eff} (it does not depend on the overlap of the fast mode wave functions). Also, because the proportionality factor is about one, ϵ probably lies in the region where the rate is basically ϵ independent. A ϵ dependence study of the electron transfer rate in such a systems would be interesting.

4. The Fokker–Planck Equation

In analogy to what was done in Ref. 1 by Garg, Onuchic and Ambegaokar, we now develop the Fokker–Planck equation associated with Hamiltonian 3.1. This representation of the problem is very useful since it is much clearer than a path integral, and also much simpler if numerical solutions are necessary. The only major restriction is that in order to achieve this formalism the nuclear coordinates have to be classsical; i.e., $kT/\hbar$ must be much larger than $(\Omega_{y,z}^2 - \gamma_{y,z}^2)^{1/2}$ in the underdamped case, and $\omega_c^{y,z}$ in the overdamped one.

Suppose that at time $t = t_0$, the total density matrix can be factored into a part for each bath alone (taken at temperature T), and a part for the spin plus reaction coordinates $(s + r)$. (The validity of this separation is discussed in Ref. 28, and it is correct for our problem.) Doing that, the spin reduced matrix $\rho_{\sigma,\lambda}(y_1, y_2; z_1, z_2; t)$ is given by

$$\rho_{\sigma,\lambda}(y_1, y_2; x_1, x_2; t) \;=\; \sum_{\sigma',\lambda'} \int_{-\infty}^{\infty} \int\int\int dy_1' dy_2' dz_1' dz_2'$$

$$\cdot\; \hat{J}_{\sigma,\lambda;\sigma',\lambda'}(y_1, y_2; z_1, z_2; t : y_1', y_2'; z_1', z_2'; t_0)\; \rho_{\sigma',\lambda'}(y_1', y_2'; z_1', z_2'; t_0), \qquad (4.1a)$$

where

$$\hat{J} \;=\; \int_{\sigma'}^{\sigma} D\sigma \int_{\lambda'}^{\lambda} D\lambda \int_{y_1'}^{y_1} Dy_1 \int_{y_2'}^{y_2} Dy_2 \int_{z_1'}^{z_1} Dz_1 \int_{z_2'}^{z_2} Dz_2\; A[\sigma]A^*[\lambda]$$

$$\times \exp \frac{i}{\hbar} \{S_{s+r}[y_1, z_1, \sigma] - S_{s+r}[y_2, z_2, \lambda]\} \;\cdot\; \mathcal{F}_y[y_1, y_2] \;\cdot\; \mathcal{F}_z[z_1, z_2] \;. \qquad (4.1b)$$

Here $\mathcal{F}$ is the influence functional

$$\mathcal{F}_y[y_1,y_2] \;=\; \int_{-\infty}^{\infty}\int\int dR'dQ'dR\rho_{bath}(R',Q';t_0)\int_{r'}^{R}DR\int_{Q'}^{Q}DQ$$

$$\times\ \exp\frac{i}{\hbar}\left[S_{bath}(R)-S_{bath}(Q)+S_{bath+y}(R,y_1)-S_{bath+y}(Q,y_2)\right]\ , \qquad (4.2)$$

where R,Q refers to the bath collection $\{x_\alpha\}$. A similar equation is obtained for the z mode influence functional. Doing the calculation in the way proposed by Caldeira and Leggett[12], we get

$$\mathcal{F}_y[(y_1,y_2] \;=\; \exp\left\{\frac{-i\eta_y}{2\hbar}\int_{t_0}^{t}(y_1-y_2)\frac{d}{d\tau}(y_1+y_2)d\tau\right.$$

$$\left.-\ \frac{\eta_y kT}{\hbar^2}\int_{t_0}^{t}(y_1-y_2)^2d\tau\right\}\ . \qquad (4.3)$$

Also, we recall that $A[\sigma]$, as described in Sec. 2, is the amplitude that any given trajectory $\sigma(\tau)$ would have in the absence of coupling to any nuclear coordinate.

Because the propagator $\hat{J}$ has no non–local terms, the reduced density matrix of interest, $\rho_{\sigma,\lambda}(y_1,y_2;x_1,x_2;t)$, at any time t can be related to itself at any earlier time t_0, which means that we can find a differential equation of motion for it. Thus, if for an infinitesimal time interval δ,

$$\hat{J}(t+\delta;t) \;=\; \hat{1}+\delta\hat{\mathcal{L}}+\mathcal{O}(\delta^2)\ , \qquad (4.4)$$

then

$$\frac{\partial\rho}{\partial t} \;=\; \hat{\mathcal{L}}\rho\ . \qquad (4.5)$$

Calculation of $\hat{\mathcal{L}}$ is performed using the prescription described in Sec. V of Ref. 1. Doing this we get

$$\frac{\partial\rho}{\partial t} = \frac{i\hbar}{2M_y}\left(\frac{\partial^2\rho}{\partial y_1^2} - \frac{\partial^2\rho}{\partial y_2^2}\right) - \frac{i}{\hbar}\Big(U_y(y_1) - U_y(y_2)\Big)\rho - \frac{\eta_y kT}{\hbar^2}(y_1 - y_2)^2\rho$$
$$+ \frac{i\hbar}{2M_z}\left(\frac{\partial^2\rho}{\partial z_1^2} - \frac{\partial^2\rho}{\partial z_2^2}\right) - \frac{i}{\hbar}\Big(U_z(z_1) - U_z(z_2)\Big)\rho - \frac{\eta_z kT}{\hbar^2}(z_1 - z_2)^2\rho$$
$$- \gamma_y(y_1 - y_2)\left(\frac{\partial\rho}{\partial y_1} - \frac{\partial\rho}{\partial y_2}\right) - \gamma_z(z_1 - z_2)\left(\frac{\partial\rho}{\partial z_1} - \frac{\partial\rho}{\partial z_2}\right)$$
$$- \frac{i}{\hbar}\Big(\sigma_z f(y_1, z_1)\rho - \rho\sigma_z f(y_2, z_2)\Big) - \frac{i}{\hbar}\big[H_\sigma\ ,\ \rho\big]\ , \qquad (4.6)$$

where

$$H_\sigma = \frac{\varepsilon}{2}\sigma_z + \frac{\hbar\Delta_0}{2}\sigma_x\ , \qquad (4.7a)$$

$$U_y(y) = \frac{1}{2}M_y\Omega_y^2(y^2 + y_0^2)\ , \qquad (4.7b)$$

and

$$f(y, z) = M_y\Omega_y^2 y_0 y + M_z\Omega_z^2 z_0 z\ . \qquad (4.7c)$$

In order to convert to a more familiar form we can take the Wigner transform of $\rho_{\alpha,\beta}(y_1, y_2; z_1, z_2)$ and obtain $W_{\alpha,\beta}(y, p_y; z, p_z)$. Doing this, Eq. 4.6 becomes

$$\frac{\partial W}{\partial t} = -\frac{1}{M_y}\frac{\partial}{\partial y}\Big(p_y W\Big) + \frac{\partial}{\partial p_y}\Big(U_y'(y)W\Big) - \frac{1}{M_z}\frac{\partial}{\partial z}\Big(p_z W\Big) + \frac{\partial}{\partial p_z}\Big(U_z'(z)W\Big)$$
$$+ \eta_y kT\frac{\partial^2}{\partial p_y^2}W + \eta_z kT\frac{\partial^2}{\partial p_z^2}W + 2\gamma_y\frac{\partial}{\partial p_y}\Big(p_y W\Big) + 2\gamma_z\frac{\partial}{\partial p_z}\Big(p_z W\Big)$$
$$+ \frac{1}{2}\frac{df}{dy}\frac{\partial}{\partial p_y}\{\sigma_z, W\} + \frac{1}{2}\frac{df}{dz}\frac{\partial}{\partial p_z}\{\sigma_z, W\} - \frac{i}{\hbar}\big[H_\sigma + \sigma_z f(y, z), W\big]\ , \qquad (4.8)$$

where the commutators and anticommutators now involve only the spin degrees of freedom.

The equation above is the complete Fokker–Planck equation associated with Hamiltonian 3.1. For reasons of simplicity we consider only the overdamped limit in the remainder of this section. It is important to point out

that the overdamped limit is not the only important one associated with this problem, but that it is one of the important ones, and it is also sufficient for a preliminary understanding of this equation. The underdamped problem is a much harder one, and it requires future study.

The High Friction Limit

If the friction is very high for both modes, we can assume that the momentum equilibrates to a Maxwellian distribution at each point (y, z) independently so that W takes the form

$$W_{\alpha,\beta}(y,z,p_y,p_z;t) = \frac{1}{2\pi kT\sqrt{M_yM_z}} \times \exp\left\{-\frac{p_y^2}{2M_ykT} - \frac{p_z^2}{2M_zkT}\right\} n_{\alpha,\beta}(y,z,t) \quad . \tag{4.9}$$

The conditions for the validity of the overdamped approximation are discussed in Sec. 2, and in Ref. 1.

After doing the standard transformation[29], and performing the momentum integration of Eq. 4.8, we generate the Smoluchowski–like equations

$$\frac{\partial n_{11}}{\partial t} = \left(D_y\frac{\partial^2}{\partial y^2} + D_z\frac{\partial^2}{\partial z^2}\right)n_{11} + \frac{\partial}{\partial y}\left(\frac{M_y\Omega_y^2}{\eta_y}(y+y_0)n_{11}\right) + \frac{\partial}{\partial z}\left(\frac{M_z\Omega_z^2}{\eta_z}(z+z_0)n_{11}\right) + \frac{i\Delta_0}{2}(n_{12}-n_{21}) \quad , \tag{4.10a}$$

$$\frac{\partial n_{22}}{\partial t} = \left(D_y\frac{\partial^2}{\partial y^2} + D_z\frac{\partial^2}{\partial z^2}\right)n_{22} + \frac{\partial}{\partial y}\left(\frac{M_y\Omega_y^2}{\eta_y}(y-y_0)n_{22}\right) + \frac{\partial}{\partial z}\left(\frac{M_z\Omega_z^2}{\eta_z}(z-z_0)n_{22}\right) - \frac{i\Delta_0}{2}(n_{12}-n_{21}) \quad , \tag{4.10b}$$

$$\frac{\partial n_{12}}{\partial t} = \left(D_y \frac{\partial^2}{\partial y^2} + D_z \frac{\partial^2}{\partial z^2}\right) n_{12} + \frac{\partial}{\partial y}\left(\frac{M_y \Omega_y^2}{\eta_y} y \; n_{12}\right) + \frac{\partial}{\partial z}\left(\frac{M_z \Omega_z^2}{\eta_z} z \; n_{12}\right)$$

$$-\frac{i}{\hbar}(\varepsilon + 2M_y\Omega_y^2 y_o y + 2M_z\Omega_z^2 z_o z) n_{12} - \frac{i\Delta_0}{2}(n_{22} - n_{11}) \quad , \qquad (4.10c)$$

where $n_{21} = n_{12}^*$, $D_y = kT/\eta_y$, and $D_z = kT/\eta_z$.

The first step in solving Eqs. 4.10 is to Laplace–transform them with respect to time. Therefore, if

$$n_{\alpha,\beta}(y,z,t) \;=\; \sum_i a_i \; n_{\alpha,\beta}^{(i)}(y,z) \; \exp(-\Gamma_i t) \quad , \qquad (4.11)$$

where $Re(\Gamma_i) \geq 0$, its Laplace transform is

$$\tilde{n}_{\alpha,\beta}(y,z,\lambda) \;=\; \sum_i a_i \; n_{\alpha,\beta}^{(i)}(y,z)/(\lambda + \Gamma_i) \quad . \qquad (4.12)$$

The crucial step is to argue that $\tilde{n}_{12}$ varies on a length scale that is much shorter than the length scale for $\tilde{n}_{11}$ and $\tilde{n}_{22}$. This assumption is reasonable for this problem, and details about its validity are given in Refs. 1 and 15. Under this assumption, we can write

$$Im[\tilde{n}_{12}(y,z,\lambda)] \;=\; \pi\left(\frac{\hbar\Delta_0}{2}\right) \; \delta\left(\varepsilon + 2M_y\Omega_y^2 y_0 y + 2M_z\Omega_z^2 z_0 z\right) \; [\tilde{n}_{11} - \tilde{n}_{22}] \quad . \qquad (4.13)$$

Using the above equation, Eqs. 4.10 can be reduced to

$$\frac{\partial n_{11}}{\partial t} = \left(D_y \frac{\partial^2}{\partial y^2} + D_z \frac{\partial^2}{\partial z^2}\right) n_{11}$$

$$+\frac{\partial}{\partial y}\left(\frac{M_y \Omega_y^2}{\eta_y}(y + y_0) n_{11}\right) + \frac{\partial}{\partial z}\left(\frac{M_z \Omega_z^2}{\eta_z}(z + z_0) n_{11}\right)$$

$$-2\pi\hbar \left(\frac{\Delta_0}{2}\right)^2 \delta\left(\varepsilon + 2M_y \Omega_y^2 y_o y + 2M_z \Omega_z^2 z_o z\right)(n_{11} - n_{22}) \quad , \qquad (4.14a)$$

$$\frac{\partial n_{22}}{\partial t} = \left(D_y \frac{\partial^2}{\partial y^2} + D_z \frac{\partial^2}{\partial z^2}\right) n_{22}$$

$$+\frac{\partial}{\partial y}\left(\frac{M_y \Omega_y^2}{\eta_y}(y - y_0) n_{22}\right) + \frac{\partial}{\partial z}\left(\frac{M_z \Omega_z^2}{\eta_z}(z - z_0) n_{22}\right)$$

$$+2\pi\hbar \left(\frac{\Delta_0}{2}\right)^2 \delta\left(\varepsilon + 2M_y \Omega_y^2 y_o y + 2M_z \Omega_z^2 z_o z\right)(n_{11} - n_{22}) \quad . \qquad (4.14b)$$

These equations may be solved by a variety of different techniques. For example, if the transfer is exponential in time, the calculation of the first eigenvalue gives the rate. Otherwise, we can use techniques such as time integration or the generalized momentum expansion[30].

In order to compare our results to the ones obtained by Agmon and Hopfield[3] and Sumi and Marcus[20], we consider in the remainder of this section only the limit at which the z coordinate moves much more slowly than y. (The validity of this approximation is discussed in Sec. 3.) Thus, similar to a Born–Oppenheimer approximation, the zeroth order solution assumes z as a parameter. Because z is a parameter, the problem reduces to the one mode case, and the set of equations we have to solve is

$$\frac{\partial n_{11}}{\partial t} = D_y \frac{\partial^2}{\partial y^2} n_{11} + \frac{\partial}{\partial y}\left(\frac{M_y \Omega_y^2}{\eta_y}(y + y_0) n_{11}\right)$$

$$-2\pi\hbar \left(\frac{\Delta_0}{2}\right)^2 \delta\left(\varepsilon^y(z) + 2M_y \Omega_y^2 y_o y\right)(n_{11} - n_{22}) \quad , \qquad (4.15a)$$

$$\frac{\partial n_{22}}{\partial t} = D_y \frac{\partial^2}{\partial y^2} n_{22} + \frac{\partial}{\partial y}\left(\frac{M_y \Omega_y^2}{\eta_y}(y - y_0) n_{22}\right)$$

$$+2\pi\hbar\left(\frac{\Delta_0}{2}\right)^2 \delta\left(\varepsilon^y(z) + 2M_y\Omega_y^2 y_o y\right)(n_{11} - n_{22}) \quad , \tag{4.15b}$$

where, as in Sec. 3, $\varepsilon^y(z) = \varepsilon + 2M_z\Omega_z^2 z_0 z$. The solution for the one mode problem can be found in Refs. 1 and 15, and it is used here. After performing the integration of the fast y coordinate,

$$\bar{n}_{\alpha,\beta}(z,t) \;=\; \int_{-\infty}^{\infty} n_{\alpha,\beta}(y,t;z)\;\; dy \quad , \tag{4.16}$$

the set of Eqs. 4.15 become

$$\frac{\partial}{\partial t}\bar{n}_{11}(z,t) \;=\; -k_y^f(z)\bar{n}_{11} \;+\; k_y^r(z)\bar{n}_{22} \quad , \tag{4.17a}$$

$$\frac{\partial}{\partial t}\bar{n}_{22}(z,t) \;=\; +k_y^f(z)\bar{n}_{11} \;-\; k_y^r(z)\bar{n}_{22} \quad , \tag{4.17b}$$

where

$$k_y^{f;r} \;=\; \frac{\Delta_0^2}{4}\left(\frac{\pi\hbar^2}{E_R^y kT}\right)^{1/2}\left[\frac{1}{1+g'}\right]\exp-\left\{\frac{(\varepsilon^y(z) \mp E_R^y)^2}{4kTE_R^y}\right\} \quad , \tag{4.18a}$$

and

$$g' \;=\; \frac{\Delta_0^2\pi\hbar}{2E_R^y\omega_c^y}\left(\frac{y_0}{|y^*(z)+y_0|} + \frac{y_0}{|y^*(z)-y_0|}\right) \quad . \tag{4.18b}$$

Here $y^*(z)$ is the crossing point of the donor and acceptor curves for a fixed value of z. Note that the rates presented here are very similar to the ones given by Eq. 3.25. Substituting Eqs. 4.16 and 4.17 into Eq. 4.14, the final set of equations we have to solve is

$$\frac{\partial}{\partial t}\bar{n}_{11}(z,t) \;=\; D_z\frac{\partial^2}{\partial z^2}\bar{n}_{11} + \frac{\partial}{\partial z}\left(\frac{M_z\Omega_z^2}{\eta_z}(z+z_0)\bar{n}_{11}\right) - k_y^f(z)\bar{n}_{11} \;+\; k_y^r(z)\bar{n}_{22} \quad , \tag{4.19a}$$

$$\frac{\partial}{\partial t}\bar{n}_{22}(z,t) \;=\; D_z\frac{\partial^2}{\partial z^2}\bar{n}_{22}+\frac{\partial}{\partial z}\left(\frac{M_z\Omega_z^2}{\eta_z}(z-z_0)\bar{n}_{22}\right)+k_y^f(z)\bar{n}_{11}\;-\;k_y^r(z)\bar{n}_{22}\;. \tag{4.19b}$$

When $\varepsilon \gg kT$, the equations above are exactly the problem addressed by Agmon and Hopfield[3] and Sumi and Marcus[15]. As we can note from the development of this paper, these equations are only a particular limit of the more general problem described by Hamiltonian 3.1.

Solutions for Eq. 4.19 are straightforward in two situations. First, when z is fast compared to the transfer rate,

$$P(t) \;=\; P_\infty \;+\; (1-P_\infty)\exp\left[-(\Gamma^f+\Gamma^r)t\right]\;, \tag{4.20a}$$

where

$$\Gamma^{f;r} \;=\; \int_{-\infty}^{\infty} k_y^{f;r}(z)\;P_{eq}^{+,-}(z)\;dz\;. \tag{4.20b}$$

The rates $k_y^{f;r}$ are given by Eq. 4.18 (See Eq. 3.11 for description of the notation.) Also, when z is very slow compared to the transfer rate,

$$P(t)=\int_{-\infty}^{\infty}dz\left[P_\infty^y(z)+\Big(1-P_\infty^y(z)\Big)\exp\left\{-\big(k_y^f(z)+k_y^r(z)\big)t\right\}\right]\times P_{eq}^{+}(z)\;. \tag{4.21}$$

(See Eq. 3.22 for description of the notation.)

Here we have considered both modes overdamped for mathematical simplicity, but similarly to the work developed in Sec. 3, if y is much faster than z, Eqs. 4.19 have a broader validity, and it is necessary only to replace $k_y^{f;r}$ by the correct expression, depending on the dynamics of the y coordinate. For example, if y is underdamped, Eq. 3.30b can be used.

5. Anharmonic effects

In this section we consider a few situations where the harmonic approximation fails for the problems of interest. By anharmonic we mean that the nuclear modes are not quadratic and/or the coupling to the nuclear coordinate is not linear in this coordinate.

Non–Linear Coupling to Δ_0 (σ_x):
Example: Electron Transfer in Porphyrins Linked to Quinones

In this subsection we develop the formalism that we shall use to understand the temperature dependence of the electron transfer reactions where the slow coordinate is coupled to σ_x instead of σ_z, as in Secs. 3 and 4. We are also interested in situations in which the coupling is not necessarily linear in the slow coordinate. This formalism is important when there is a slow coordinate that modulates the matrix element instead of the activation barrier as in the last two sections. Although the formalism we describe in this subsection can be applied to any system that satisfies the conditions above, in order to make this subsection clearer, we discuss electron transfer in the porphyrin–bridge–quinone molecule[31] (see Fig. 5), which is a good example of this problem. This transfer shows exponential decay in time at high temperatures (room temperature) and non–exponential decay at low temperatures (liquid nitrogen)[31b]. Although the full temperature analysis of this system has not yet been performed, we present here the formalism that we will probably use to understand the data when they become available, but which already provide us with some

understanding of this electron transfer reaction.

The simplest Hamiltonian we can write to describe the basic features of this system must contain at least two nuclear coordinates. From Fig. 5 we can see that the electronic matrix element depends on the orientation of the quinone relative to the porphyrin. Therefore, the dihedral angle θ between the porphyrin and the quinone is one of the nuclear coordinates. At this level of theory it is reasonable to assume that this coordinate is diffusive. The other nuclear coordinate, x, represents the normal vibronic coupling to the problem. As already discussed, the slow coordinate in this subsection, θ, is coupled to the problem in a completely different way than the slow coordinate in the last two sections. Here θ is coupled to σ_x, i.e., modulates the matrix element, instead of σ_z. (This Hamiltonian is oversimplified for this problem, but it is sufficient for the conclusions we want to draw in this section. To better describe this system we need more than one local "slow mode," and a matrix element renormalized by the fast modes[32].) Thus, the simplest Hamiltonian we can write is

$$H_{ET} = \frac{\hbar\Delta_0(\theta)}{2}\sigma_x + \frac{\varepsilon}{2}\sigma_z + \frac{P_x^2}{2M_x} + V_x(x) + \sigma_z f(x) + Bath_x$$

$$+\frac{P_\theta^2}{2M_\theta} + U_\theta(\theta) + Bath_\theta \quad . \tag{5.1}$$

Here, V_x and U_θ are the potentials associated with x and θ. $f(x)$ is the coupling of coordinate x to the spin. As in the last section, the equivalent of Eq. 4.6 is developed, and we obtain

$$\frac{\partial \rho}{\partial t} = \frac{i\hbar}{2M_x}\left(\frac{\partial^2\rho}{\partial x_1^2} - \frac{\partial^2\rho}{\partial x_2^2}\right) - \frac{i}{\hbar}\Big(V_x(x_1) - V_x(x_2)\Big)\rho - \frac{\eta_x kT}{\hbar^2}(x_1 - x_2)^2\rho$$

$$+ \frac{i\hbar}{2M_\theta}\left(\frac{\partial^2\rho}{\partial \theta_1^2} - \frac{\partial^2\rho}{\partial \theta_2^2}\right) - \frac{i}{\hbar}\Big(U_\theta(\theta_1) - U_\theta(\theta_2)\Big)\rho - \frac{\eta_\theta kT}{\hbar^2}(\theta_1 - \theta_2)^2\rho$$

$$- \gamma_x(x_1 - x_2)\left(\frac{\partial\rho}{\partial x_1} - \frac{\partial\rho}{\partial x_2}\right) - \gamma_\theta(\theta_1 - \theta_2)\left(\frac{\partial\rho}{\partial\theta_1} - \frac{\partial\rho}{\partial\theta_2}\right)$$

$$- \frac{i}{\hbar}\Big(\sigma_z f(x_1)\rho - \rho\sigma_z f(x_2)\Big) - \frac{i}{\hbar}\big[H_\sigma\ ,\ \rho\big]\ , \qquad (5.2)$$

where

$$H_\sigma = \frac{\varepsilon}{2}\sigma_z + \frac{\hbar\Delta_0(\theta)}{2}\sigma_x\ . \qquad (5.3)$$

The simplest model for $\Delta_0(\theta)$ gives $\Delta_0(\theta) = \Delta_0^{max}\cos(\theta)$ because of the π cloud orientation of the quinone and porphyrin[33].

If we take the Wigner transformation of ρ,

$$W_{\alpha,\beta}(x, p_x, \theta, p_\theta) = \frac{1}{(2\pi\hbar)^2}\int_{-\infty}^{\infty}\int_{-\infty}^{\infty}\exp\left(\frac{ip_x y}{\hbar} + \frac{ip_\theta\vartheta}{\hbar}\right)$$

$$\times\ \rho_{\alpha,\beta}(x - y/2, x + y/2; \theta - \vartheta/2, \theta + \vartheta/2)dyd\vartheta\ , \qquad (5.4)$$

we obtain the momentum/coordinate representation of Eq. 5.2

$$\frac{\partial W}{\partial t} = -\frac{1}{M_x}\frac{\partial}{\partial x}\Big(p_x W\Big) + \frac{\partial}{\partial p_x}\Big(V_x'(x)W\Big) - \frac{1}{M_\theta}\frac{\partial}{\partial\theta}\Big(p_\theta W\Big) + \frac{\partial}{\partial p_\theta}\Big(U_\theta'(\theta)W\Big)$$

$$+ \eta_x kT\frac{\partial^2}{\partial p_x^2}W + \eta_\theta kT\frac{\partial^2}{\partial p_\theta^2}W + 2\gamma_x\frac{\partial}{\partial p_x}\Big(p_x W\Big) + 2\gamma_\theta\frac{\partial}{\partial p_\theta}\Big(p_\theta W\Big)$$

$$+ \frac{1}{2}\frac{df(x)}{dx}\frac{\partial}{\partial p_x}\{\sigma_z, W\} - \frac{i}{\hbar}\big[H_\sigma + \sigma_z f(x), W\big]\ . \qquad (5.5)$$

Higher–order coordinate derivatives are neglected because of fluctuations[34a]. This transformation is exact for harmonic coordinates. Also, because we are

interested in the situation in which θ is much slower than x, we have neglected all terms containing derivatives of Δ_0. If this latter condition is not valid, the problem becomes extremely difficult.

As discussed in the beginning of this section, it is reasonable to treat θ as an overdamped coordinate. For mathematical simplicity, we now also consider x overdamped as well as harmonic. This is not a major problem for what we want to achieve, i.e., how θ affects the transfer. This point is addressed at the end of this subsection. Because we are assuming x harmonic, $V_x(x) = M_x\Omega_x^2(x^2+x_0^2)/2$ and $f(x) = M_x\Omega_x^2 x_0 x$. In this limit we generate the Smoluchowski–like equations

$$\frac{\partial n_{11}}{\partial t} = \left(D_x\frac{\partial^2}{\partial x^2} + D_\theta\frac{\partial^2}{\partial\theta^2}\right)n_{11} + \frac{\partial}{\partial x}\left(\frac{M_x\Omega_x^2}{\eta_x}(x+x_0)n_{11}\right)$$

$$+\frac{\partial}{\partial\theta}\left(\frac{U'_\theta(\theta)}{\eta_\theta}n_{11}\right) + \frac{i\Delta_0(\theta)}{2}(n_{12}-n_{21}) \quad , \tag{5.6a}$$

$$\frac{\partial n_{22}}{\partial t} = \left(D_x\frac{\partial^2}{\partial x^2} + D_\theta\frac{\partial^2}{\partial\theta^2}\right)n_{22} + \frac{\partial}{\partial x}\left(\frac{M_x\Omega_x^2}{\eta_x}(x-x_0)n_{22}\right)$$

$$+\frac{\partial}{\partial\theta}\left(\frac{U'_\theta(\theta)}{\eta_\theta}n_{22}\right) - \frac{i\Delta_0(\theta)}{2}(n_{12}-n_{21}) \quad , \tag{5.6b}$$

$$\frac{\partial n_{12}}{\partial t} = \left(D_x\frac{\partial^2}{\partial x^2} + D_\theta\frac{\partial^2}{\partial\theta^2}\right)n_{12} + \frac{\partial}{\partial x}\left(\frac{M_x\Omega_x^2}{\eta_x}x\, n_{12}\right) + \frac{\partial}{\partial\theta}\left(\frac{U'_\theta}{\eta_\theta}\, n_{12}\right)$$

$$-\frac{i}{\hbar}(\varepsilon + 2M_x\Omega_x^2 x_o x)n_{12} - \frac{i\Delta_0(\theta)}{2}(n_{22}-n_{11}) \quad , \tag{5.6c}$$

and $n_{21} = n_{12}^*$. Here $D_x = kT/\eta_x$ and $D_\theta = kT/\eta_\theta$.

Because θ is much slower than x, the zero$^{\text{th}}$ order solution assumes θ as a parameter, and therefore the problem reduces to the following one mode problem

$$\frac{\partial n_{11}(x,t;\theta)}{\partial t} = D_x \frac{\partial^2}{\partial x^2} n_{11} + \frac{\partial}{\partial x}\left(\frac{M_x \Omega_x^2}{\eta_x}(x+x_0) n_{11}\right) + \frac{i\Delta_0(\theta)}{2}(n_{12}-n_{21}) \ , \tag{5.7a}$$

$$\frac{\partial n_{22}(x,t;\theta)}{\partial t} = D_x \frac{\partial^2}{\partial x^2} n_{22} + \frac{\partial}{\partial x}\left(\frac{M_x \Omega_x^2}{\eta_x}(x-x_0) n_{22}\right) - \frac{i\Delta_0(\theta)}{2}(n_{12}-n_{21}) \ , \tag{5.7b}$$

$$\frac{\partial n_{12}}{\partial t} = D_x \frac{\partial^2}{\partial x^2} n_{12} + \frac{\partial}{\partial x}\left(\frac{M_x \Omega_x^2}{\eta_x} x\, n_{12}\right)$$

$$-\frac{i}{\hbar}(\varepsilon + 2M_x \Omega_x^2 x_o x) n_{12} - \frac{i\Delta_0(\theta)}{2}(n_{22}-n_{11}) \ , \tag{5.7c}$$

which, as in the last section, can be reduced to

$$\frac{\partial n_{11}}{\partial t} = D_x \frac{\partial^2}{\partial x^2} n_{11} + \frac{\partial}{\partial x}\left(\frac{M_x \Omega_x^2}{\eta_x}(x+x_0) n_{11}\right)$$

$$-2\pi\hbar\left(\frac{\Delta_0(\theta)}{2}\right)^2 \delta(\varepsilon + 2M_x\Omega_x^2 x_o x)(n_{11}-n_{22}) \ , \tag{5.8a}$$

$$\frac{\partial n_{22}}{\partial t} = D_x \frac{\partial^2}{\partial x^2} n_{22} + \frac{\partial}{\partial x}\left(\frac{M_x \Omega_x^2}{\eta_x}(x-x_0) n_{22}\right)$$

$$+2\pi\hbar\left(\frac{\Delta_0(\theta)}{2}\right)^2 \delta(\varepsilon + 2M_x\Omega_x^2 x_o x)(n_{11}-n_{22}) \ . \tag{5.8b}$$

The solution of these equations is

$$\frac{\partial}{\partial t}\bar{n}_{11}(\theta,t) = -k_x^f(\theta)\bar{n}_{11} + k_x^r(\theta)\bar{n}_{22} \ , \tag{5.9a}$$

$$\frac{\partial}{\partial t}\bar{n}_{22}(\theta,t) = +k_x^f(\theta)\bar{n}_{11} - k_x^r(\theta)\bar{n}_{22} \ , \tag{5.9b}$$

where

$$k_x^{f;r} = \frac{\Delta_0^2(\theta)}{4}\left(\frac{\pi\hbar^2}{E_R^x kT}\right)^{1/2}\left[\frac{1}{1+g'}\right] \exp -\left\{\frac{(\varepsilon \mp E_R^x)^2}{4kTE_R^x}\right\} \ , \tag{5.10a}$$

and

$$g' = \frac{\Delta_0^2(\theta)\pi\hbar}{2E_R^x \omega_c^x}\left(\frac{x_0}{|x^* + x_0|} + \frac{x_0}{|x^* - x_0|}\right) \ . \tag{5.10b}$$

Here x^* is the crossing point for the donor and acceptor curves, and

$$\bar{n}_{\alpha,\beta}(\theta,t) \;=\; \int_{-\infty}^{\infty} n_{\alpha,\beta}(x,t;\theta)\;\; dx \;\; . \tag{5.11}$$

Thus, the final set of equations we have to solve is

$$\frac{\partial}{\partial t}\bar{n}_{11}(\theta,t) \;=\; D_\theta \frac{\partial^2}{\partial\theta^2}\bar{n}_{11} + \frac{\partial}{\partial\theta}\left(\frac{U'_\theta(\theta)}{\eta_z}\bar{n}_{11}\right) - k_x^f(\theta)\bar{n}_{11} \,+\, k_x^r(\theta)\bar{n}_{22} \;\; , \tag{5.12a}$$

$$\frac{\partial}{\partial t}\bar{n}_{22}(\theta,t) \;=\; D_\theta \frac{\partial^2}{\partial\theta^2}\bar{n}_{22} + \frac{\partial}{\partial\theta}\left(\frac{U'_\theta(\theta)}{\eta_z}\bar{n}_{22}\right) + k_x^f(\theta)\bar{n}_{11} \,-\, k_x^r(\theta)\bar{n}_{22} \;\; . \tag{5.12b}$$

Solutions for Eqs. 5.12 are straightforward when the transfer rate is much slower or much faster than the θ coordinate. In the first case,

$$P(t) \;=\; P_\infty \;+\; (1-P_\infty)\exp\left[-(\Gamma^f+\Gamma^r)t\right] \;\; , \tag{5.13a}$$

where

$$\Gamma^{f;r} \;=\; \int_0^{2\pi} k_x^{f;r}(\theta)\; P_{eq}(\theta)\; d\theta \;\; . \tag{5.13b}$$

(See Eq. 3.11 for a description of the notation.) In the second case,

$$P(t) = \int_0^{2\pi} d\theta \left[P_\infty + \Big(1-P_\infty\Big)\exp\left\{-\big(k_x^f(\theta)+k_x^r(\theta)\big)t\right\}\right] \times P_{eq}(\theta) \;\; . \tag{5.14}$$

When the transfer is adiabatic, the rates $k_x^{f;r}$ become independent of Δ_0, and therefore of θ. In this limit, therefore, Eqs. 5.13 and 5.14 are exactly the same, and the decay is exponential in time.

We now discuss a result that, although very simple, is interesting in order to understand the difference between a slow mode coupled to σ_z (Secs. 3 and 4) and a slow mode coupled to σ_x (this section). Because here the slow mode modulates only the matrix element, in the adiabatic limit the rate will not be modulated by the slow coordinate. Therefore, in the adiabatic limit and if

the slow mode is coupled to σ_x, the donor survival probability always decays exponentially in time. This is not true when the slow mode is coupled to σ_z (see discussion after Eq. 3.25 or Eqs. 4.20 and 4.21). Thus, the non–exponential behavior at low temperatures for the electron transfer in the porphyrin–bridge–quinone with one linker group[31b] (see Fig. 5 with n=1) shows us that the rate is probably not adiabatic, because it appears to depend on the slow coordinate, θ. It would be interesting to perform the experiment at low temperature with n=0, where the rate is expected to be adiabatic. Thus, the low temperature transfer should present a decay exponential in time. If we observe non–exponential decay in this case, it would mean that some other slow mode (coupled to σ_z) besides θ is modulating the electron transfer process.

An interesting problem to pursue now is to try to obtain the potential U_θ. Whether this potential has only one minimum or many minima may lead to different dynamics at low temperatures. For example, if this potential has two minima, non–exponentiality will appear when the barrier between the two minima becomes larger than kT. Non–exponentiality will exist independently of the dynamics of the slow mode. If there is only one minimum[3], non–exponentiality is due to a dynamical effect; i.e., it appears only when the electron transfer rate is much faster than the slow coordinate.

As discussed in the beginning of this subsection, the porphyrin–bridge–quinone system is only an example, and the formalism described here can be applied to any electron transfer process that has the electronic matrix element, Δ_0, modulated by a slow coordinate. Also, as in the last section, this formalism can be generalized for x underdamped. In this case we have only to replace the expressions for $k_x^{f,r}(\theta)$ by the correct ones.

Some Initial Ideas About How to Treat
An Anharmonic Nuclear Coordinate Coupled to σ_z

Another way that anharmonic effects may be important is the situation in which we have nuclear modes that are strongly excited. In the limit in which we have been working, the nuclear modes are harmonic, the coupling is linear, and therefore the nuclear potential wells before and after the transfer are parabolic. In this subsection we present an initial discussion of how to treat this problem when the parabolic approximation is no longer valid, but the nuclear potential wells are still binding.

Initially, let us consider the underdamped situation. In this limit, the nuclear mode oscillates many times before the electron transfer. Thus, the simplest way to include corrections to this problem is by a "temperature–dependent" harmonic approximation. In order to do that, all we have to know is the mean–square displacement of the nuclear coordinate (μ). In the classical regime, $\mu^2 = kT/M\Omega^2$ for a harmonic oscillator. Real nuclear potentials are more like Morse functions, and therefore μ^2 grows faster than linearly with T. Thus, the first correction due to anharmonic effects would be to consider the coordinate as harmonic but with a temperature–dependent frequency (decreases with T). If the nuclear potential could behave as a square well, then the effective frequency should increase with T, but this is not a physical situation.

Also, it may necessary to consider different "effective" frequencies for some nuclear modes before and after the electron transfer. The simplest way we can achieve that is by introducing quadratic coupling in the nuclear coordinate when we couple it to the spin (electron) coordinate. This really complicates

the mathematics, but we will have to attack this problem in the near future.

In the overdamped regime, the anharmonic situation is simpler. Because we were able to develop the Fokker–Planck equations associated with the electron transfer problem (Eqs. 4.14, for example), all we have to consider is diffusion in potentials that are not harmonic. This is a well–known problem, and methods to solve it may be found in several books, such as in Ref. 34.

Thus, we have tried to show in this subsection that when non–linear effects are important, we must first try to see how they will affect our problem differently than in the harmonic approximation. Then we should try to include these effects in the simplest way possible. As we have seen here for the underdamped and overdamped regimes, different approaches are necessary, depending on the problem that has to be solved.

6. Conclusions

The main goal of this paper is to describe how electron transfer rates can be calculated in a variety of situations depending on the electronic coupling and the dynamics of the nuclear coordinates. We believe this has been done for various interesting situations. As we have seen during the development of this paper, different nuclear dynamics will lead to completely different expressions. For the one mode problem we have seen that the strength of the coupling between the bath and the reaction coordinate may completely change the dynamics of this coordinate and may strongly affect the rate expressions. In the overdamped regime we can actually calculate how this rate goes from the non–adiabatic to the adiabatic limit. In the two mode problem the results are even more interesting. Besides changes of rate expressions and discussion about adiabaticity and non–adiabaticity, we can also verify whether or not the transfer probability is exponential in time. We also present conditions for the validity of the results obtained by Agmon and Hopfield[3] and Sumi and Marcus[20].

From the theoretical point of view, we have continued in this paper what we started in Ref 1, where a complete Hamiltonian was considered from the beginning, without having to create artificial broadening of the energy levels, therefore giving a better understanding of the nuclear dynamics. Because we work in a density matrix formalism, when the effect of the bath is local in time (classical limit), we can develop the Fokker–Planck equations associated with our Hamiltonian, and therefore can compare our model with the existing classical ones.

An important result concerns the non-exponential decay of $P(t)$. In the adiabatic limit, the decay will be non-exponential in time for very slow nuclear coordinates, depending upon whether this coordinate is coupled to σ_z or σ_x. If it is coupled to σ_x, it will show exponential behavior in this limit. This conclusion is very important when we analyze the temperature dependence of the electron transfer rate for different systems. In the case of porphyrin–linker–quinone[31b], the coupling to σ_x is the correct one. But in systems where the slow mode is the solvent polarization or the protein medium[23], or in the problem of CO binding to heme proteins[3], the coupling to σ_z is probably the most adequate. In order to better understand this non–exponential behavior in time, it would be interesting if low temperature experiments were performed on some other protein systems such as the Ru–protein developed in Gray's laboratory[35].

We want to emphasize the fact that because most of the electron transfer problems are coupled to fast localized vibrations, and also to several slow vibrations (solvent polarization, gross motion of proteins, etc.), the separation of the problem into fast and slow modes as proposed at the end of Sec. 3 is a good way to approach the problem. After the fast motion is separated, we are left only with the slow motions, and for each combination of fast vibration energy levels we have a different effective matrix element (Δ_0^{eff}) and driving force. This separation of time scales really simplifies the problem, and it is reasonable to consider the slow modes in the strong coupling limit; i.e, their density of states is a smooth function of the energy. After the effect of the fast modes is included, all we need is the response function (susceptibility) of the "slow" medium modes due to the electron transfer. How to obtain a realistic

description for these response functions in complex media such as proteins awaits an answer that lies in the future.

As a final conclusion we would like to point out that, as we have described in this paper, with the amount of new experimental data which will be available in the near future, it is the natural step to try to verify which of these results will be explained by the theoretical models presented here.

Acknowledgments

I thank J.J. Hopfield, and D.N. Beratan for many fruitful discussions. I also thank A. Garg and J. Jortner for many informative and thought–provoking conversations. The work was supported by the Brazilian Agency CNPq, and by the NSF (Grant No. PCM–8406049).

Appendix A – Formulas for $G_1(t)$ and $G_2(t)$

We start this appendix with a short review of the appendix of Ref. 1. For the one mode problem, $G_1(t)$ is given by

$$G_1(t) = \frac{2M_y y_0^2}{\hbar}\left\{\omega_0 \sin(\omega_0 t)\exp(-\gamma t) + 2\gamma\Big[1 - \cos(\omega_0 t)\exp(-\gamma t)\Big]\right\} , \tag{A.1}$$

where $\omega_0 = (\Omega_y^2 - \gamma^2)^{1/2}$, in the underdamped limit, and by

$$G_1(t) \approx \frac{4M_y y_0^2 \gamma}{\hbar}\left[1 - \exp(-\omega_c t)\right] , \tag{A.2}$$

where $\omega_c = \Omega_y^2/2\gamma$, in the overdamped limit.

At short times [$t \ll \omega_c^{-1}(\Omega_y^{-1})$ in the overdamped (underdamped) case]

$$G_1(t) \approx \frac{E_R^y t}{\hbar} . \tag{A.3}$$

At long times, $G_1(t)$ goes to zero.

Calculation of $G_2(t)$ is not as simple, but in the short time limit[1], it is given by

$$G_2(t) \approx \frac{t^2}{2\tau_0^2} , \tag{A.4}$$

where

$$\tau_0^{-2} = \frac{4}{\pi\hbar}\int_0^\infty d\omega\ J_{eff}(\omega)\coth(\beta\hbar\omega/2) . \tag{A.5}$$

Eq. A.5 can be related to the mean–square displacement of the nuclear coordinate y, μ^2, by

$$\tau_0^{-2} = \left(\frac{2M_y\Omega_y^2 y_0}{\hbar}\right)^2 \mu^2 . \tag{A.6}$$

Because at high enough temperatures μ^2 acquires its "equipartition theorem" value $kT/M_y\Omega_y^2$, we define T_{eff} as

$$T_{eff} \equiv \frac{M_y\Omega_y^2\mu^2}{k} , \tag{A.7}$$

and therefore

$$\tau_0^{-2} = \frac{2E_R kT_{eff}}{\hbar^2} \quad , \qquad (A.8)$$

where $E_R = 2M_y\Omega_y^2 y_0^2$. For very long times, it follows from Eq. 2.17 that $G_2(t)$ becomes a constant. Note that T_{eff} is a function of both the temperature and the friction. For any given temperature, T_{eff} is allways less than its zero–friction value:

$$kT_{eff} = \frac{\hbar\Omega_y}{2}\coth(\hbar\Omega_y/2kT) \quad . \qquad (A.9)$$

The equation above can be used as a first–order approximation for T_{eff} in the underdamped limit.

For the two mode case the situation is straightforward. Because

$$J_{eff}(\omega) = J^y_{eff}(\omega) + J^z_{eff}(\omega) \quad , \qquad (A.10)$$

then

$$G_1(t) = G_1(t)^y + G_1(t)^z \quad , \qquad (A.11)$$

and

$$G_2(t) = G_2(t)^y + G_2(t)^z \quad . \qquad (A.12)$$

Thus, the expressions given in this appendix, using the definitions given by Eq. 2.16, are used to calculate Eqs. 3.5, 3.14, 3.15, 3.16. 3.17, and 3.12.

Appendix B – Probability for Transfer in the Non–Adiabatic and Non-Exponential Limit

In this appendix, a calculation for $P(t)$ is performed in the limit that z is very slow and the transfer rate is non-adiabatic. Also, both modes are in the moderate friction limit. This is the result given in Eqs. 3.22, 3.23 and 3.24. We also restrict ourselves to the situation in which the driving force is large compared to kT, so that we do not have to worry about back transfer, a condition that makes the algebra less tedious.

Thus, we have to show that if $kT^y_{eff} \ll \varepsilon$ and if the limit above is obeyed, then Eq. 3.22 is valid and

$$P(t) \;=\; \int_{-\infty}^{\infty} dz \;\left[2\,\exp\left(-k^f_{y,na}(z)t\right) \;-\; 1\right] \;\times P^+_{eq}(z) \;\;, \qquad (B.1)$$

where

$$P^+_{eq}(z) \;=\; \sqrt{\frac{M_z\Omega_z^2}{2\pi kT^z_{eff}}}\;\exp\left\{-\frac{M_z\Omega_z^2(z+z_0)^2}{2kT^z_{eff}}\right\} \;\;. \qquad (B.2)$$

Here

$$k^f_{y,na} \;=\; \frac{\Delta_0^2}{4}\left(\frac{\pi\hbar^2}{E^y_R kT^y_{eff}}\right)^{1/2}\;\exp\left\{-\frac{(\varepsilon^y(z)-E^y_R)^2}{4kT^y_{eff}E^y_R}\right\} \;\;, \qquad (B.3a)$$

where

$$\varepsilon^y(z) \;= \varepsilon + 2M_z\Omega_z^2 z_0 z \;\;. \qquad (B.3b)$$

If Eq. B.1 is now written as a series in Δ_0^2, we get

$$P(t) \;= \sum_{n=0}^{\infty} \frac{a_n}{n!}\,(-\Delta_0^2)^n \;\;, \qquad (B.4)$$

where

$$a_0 = 1 \;\;, \qquad (B.5a)$$

and for $n > 0$

$$a_n = \int_{-\infty}^{\infty} dz \, \frac{2}{4^n} \left(\frac{\pi\hbar^2}{E_R^y k T_{eff}^y} \right)^{n/2} \left(\frac{M_z \Omega_z^2}{2\pi k T_{eff}^z} \right)^{1/2} \exp\left\{ - \frac{n(\varepsilon^y(z) - E_R^y)^2}{4kT_{eff}^y E_R^y} \right\}$$

$$\times \exp\left\{ - \frac{M_z \Omega_z^2 (z + z_0)^2}{2kT_{eff}^z} \right\} . \qquad (B.5b)$$

For algebraic simplicity we show the calculation only for the classical limit; i.e., $T = T_{eff}^y = T_{eff}^z$. In this limit

$$a_n = \frac{2}{4^n} \left(\frac{\pi\hbar^2}{E_R^y kT} \right)^{n/2} \left(\frac{E_R^y}{E_R^y + nE_R^z} \right)^{1/2} \exp\left\{ - \frac{n(\varepsilon - E_R^y - E_R^z)^2}{4kT(E_R^y + nE_R^z)} \right\} . \qquad (B.6)$$

Now our goal is to calculate the series given by Eq. 2.14, using the terms given by Eq. 3.21 when writing $\tilde{F}_n(\{t_i\})$, and show that this series is exactly the one given by Eq. B.4, defining the Laplace–transform of $P(t)$ as

$$\tilde{P}(\lambda) = \sum_{n=0}^{\infty} \tilde{P}_n(\lambda) = \int_0^{\infty} P(t) \, \exp(-\lambda t) \, . \qquad (B.7)$$

From Eq. 2.14 we can show that

$$\tilde{P}_0(\lambda) = \frac{1}{\lambda} \, , \qquad (B.8a)$$

and for $n > 0$

$$\tilde{P}_n(\lambda) = (-\Delta_0^2)^n \int_0^{\infty} \ldots \int_0^{\infty} ds_0 \ldots ds_n \, db_1 \ldots db_n$$

$$\times \exp\left[- \lambda(s_0 + \ldots + s_n + b_1 + \ldots + b_n) \right] \tilde{F}_n(\{b_i\}) \, , \qquad (B.8b)$$

where $b_j = t_{2j} - t_{2j-1}$ and $s_j = t_{2j+1} - t_{2j}$, and $\tilde{F}_n$ is given by Eq. 2.15.

If we now put Eq. 3.21 into Eq. B.8, integrate over the s variables, and make the change of variables $b_i = \varsigma_i b_i$, we get

$$\tilde{P}_n(\lambda) = \frac{(-\Delta_0^2)^n}{2^n}\frac{1}{\lambda^{n+1}}\int_{-\infty}^{\infty}\cdots\int_{-\infty}^{\infty} db_1\ldots db_n \exp\left\{-\frac{(E_R^y+E_R^z)kT}{\hbar^2}(b_1^2+\ldots \right.$$

$$\left.\ldots+b_n^2)\right\}\ \exp\left\{-\frac{2E_R^z kT}{\hbar^2}(b_1b_2+\ldots+b_{n-1}b_n)\right\}$$

$$\times\cos\left(\frac{E_R^y b_2}{\hbar}\right)\ldots\cos\left(\frac{E_R^y b_n}{\hbar}\right)\ \exp\left\{-\frac{ib_1}{\hbar}(\varepsilon-E_R^y-E_R^z)\right\}$$

$$\exp\left\{-\frac{ib_2}{\hbar}(\varepsilon-E_R^z)\right\}\ldots\exp\left\{-\frac{ib_n}{\hbar}(\varepsilon-E_R^z)\right\}\quad . \qquad (B.9)$$

Since the blips occupy a very short fraction of the total time, in the above equation we have taken the limit $\lambda b_i \to 0$. Performing the b integrals, Eq. B.9 becomes

$$\tilde{P}_n(\lambda) = \frac{2}{\lambda^{n+1}}\frac{(-\Delta_0^2)^n}{4^n}\left(\frac{\pi\hbar^2}{kT}\right)^{n/2}$$

$$\times\left(\frac{E_R^y}{(E_R^y+E_R^z)E_R^y}\right)^{1/2}\left(\frac{E_R^y+E_R^z}{(E_R^y+2E_R^z)E_R^y}\right)^{1/2}\cdots\left(\frac{E_R^y+(n-1)E_R^z}{(E_R^y+nE_R^z)E_R^y}\right)^{1/2}$$

$$\times\ \exp\left\{-\frac{(\varepsilon-E_R^y-E_R^z)^2E_R^y}{4kT}\left[\frac{1}{(E_R^y)(E_R^y+E_R^z)}\right.\right.$$

$$\left.\left.+\frac{1}{(E_R^y+E_R^z)(E_R^y+2E_R^z)}+\ldots+\frac{1}{(E_R^y+(n-1)E_R^z)(E_R^y+nE_R^z)}\right]\right\}\ . \qquad (B.10)$$

Using the fact that

$$\frac{1}{(E_R^y)(E_R^y+E_R^z)}+\frac{1}{(E_R^y+E_R^z)(E_R^y+2E_R^z)}+\cdots$$

$$\ldots+\frac{1}{(E_R^y+(n-1)E_R^z)(E_R^y+nE_R^z)} = \frac{n}{(E_R^y+nE_R^z)E_R^y}\ , \qquad (B.11)$$

we get

$$\tilde{P}_n(\lambda) = \frac{2}{\lambda^{n+1}}\frac{(-\Delta_0^2)^n}{4^n}\left(\frac{\pi\hbar^2}{kTE_R^y}\right)^{n/2}\left(\frac{E_R^y}{E_R^y+nE_R^z}\right)^{1/2}$$

$$\times\ \exp\left\{-\frac{n(\varepsilon-E_R^y-E_R^z)^2}{4kT(E_R^y+nE_R^z)}\right\}\quad . \qquad (B.12)$$

Comparing Eq. B.12 with Eq. B.6, we notice that

$$\tilde{P}_n(\lambda) \;=\; a_n \frac{(-\Delta_0^2)^n}{\lambda^{n+1}} \quad . \qquad (B.13)$$

Thus, we prove that Eq. B.1 is the exact solution of the series 2.14 when the conditions described above are valid.

References

(1) A. Garg, J.N. Onuchic, and V. Ambegaokar, *J. Chem. Phys.* **83**, 4491 (1985).

(2) (a) D.DeVault, *Quantum Mechanical Tunneling in Biological Systems*, 2nd edition; Cambridge Univ. Press: New York, 1984; (b) B. Chance, D.C. DeVault, H. Frauenfelder, R.A. Marcus, J.R. Schrieffer, and N. Sutin, eds., *Tunneling in Biological Systems*; Academic Press: New York, 1979; (c) R.A. Marcus and N. Sutin, *Biochim. Biophys. Acta* **811**, 265 (1985); (d) M.D. Newton and N. Sutin, *Ann. Rev. Phys. Chem.* **35**, 437 (1984).

(3) (a) N. Agmon and J.J. Hopfield, *J. Chem. Phys.* **78**, 6947 (1983); (b) *J. Chem. Phys.* **79**, 2042 (1983).

(4) J.N. Onuchic, D.N. Beratan, and J.J. Hopfield, *J. Phys. Chem.* **90**, 3707 (1986).

(5) R.A. Marcus, (a) *J. Chem. Phys.* **24**, 966 (1956); (b) *Discuss. Faraday Soc.* **29**, 21 (1960); (c) *J. Phys. Chem.* **67**, 853, 2889 (1963); (d) *Ann. Rev. Phys. Chem.* **15**, 155 (1964); (e) *J. Chem. Phys.* **43**, 679 (1963); (f) in *Oxidases and Related Redox Systems*, T.E. King, H.S. Mason, and M. Morrison, eds.; Pergamon Press: New York, 1982, p. 3.

(6) N.S. Hush, (a) *Trans. Faraday Soc.* **57**, 557 (1961); (b) *Electrochim. Acta* **13**, 1005 (1965).

(7) (a) V.G. Levich and R.R. Dogonadze, *Dokl. Acad. Nauk SSSR* **124**, 123 (1959); (b) V.G. Levich, *Adv. Electroch. Electroch. Eng.* **4**, 249 (1965).

(8) (a) J.J. Hopfield, *Proc. Nat. Acad. Sci. (USA)* **7**, 3640 (1974); (b) J.J. Hopfield, *Biophys. J.* **18**, 311 (1977); (c) M. Redi and J.J. Hopfield, *J. Chem. Phys.* **72**, 6651 (1980).

(9) (a) N.R. Kestner, J. Logan, and J. Jortner, *J. Phys. Chem.* **78**, 2148 (1974); (b) J. Jortner, *J. Chem. Phys.* **64**, 4860 (1976); (c) J. Jortner, *Biochim. Biophys. Acta* **594**, 193 (1980); (d) M. Bixon and J. Jortner, *Faraday Discuss. Chem. Soc.* **74**, 17 (1982).

(10) R.F. Goldstein and W. Bialek, *Phys. Rev. B* **27**, 7431 (1983).

(11) H. Frauenfelder and P.G. Wolynes, *Science* **229**, 337 (1985); (b) P.G. Wolynes, *J. Chem. Phys.* , in press.

(12) A.O. Caldeira and A.J. Leggett (a) *Ann. Phys (N.Y.)* **149**, 374 (1983); (b) *Physica A* **121**, 587 (1983).

(13) (a) A.J. Leggett, S. Chakravarty, A. Dorsey, M.P.A. Fisher, A. Garg, and W. Zwerger, *Rev. Mod. Phys.*, in press; (b) S. Chakravarty and A. J. Leggett, *Phys. Rev. Lett.* **53**, 5 (1984).

(14) L.D. Landau and E.M. Lifshitz, *Quantum Mechanics*, 3rd edition; Pergamon Press: New York, 1977, § 90.

(15) L.D. Zusman, *Chem. Phys.* **49**, 295 (1980).

(16) D.F. Calef and P.G. Wolynes, *J. Phys. Chem.* **87**, 3387 (1983).

(17) (a) F. Parak and E.W. Knapp, *Proc. Nat. Acad. Sci. (USA)* **81**, 7088 (1984); (b) E.R. Bauminger, S.G. Cohen, I. Nowik, S. Ofer, and J. Yariv, *Proc. Nat. Acad. Sci. (USA)* **80**, 736 (1983).

(18) I. Rips and J. Jortner, submitted to J. Chem. Phys.

(19) R.F. Goldstein and W. Bialek, preprint (1986).

(20) H. Sumi and R.A. Marcus, *J. Chem. Phys.* **84**, 4272 (1986).

(21) S.E. Peterson–Kennedy, J.L. McGourty, J.A. Kalweit, and B.M. Hoffman, *J. Am. Chem. Soc.* **108**, 1739 (1986).

(22) R.F. Goldstein and A. Bearden, *Proc. Nat. Acad. Sci. (USA)* **81**, 135 (1984).

(23) B.M. Hoffman, personal communication.

(24) M.R. Gunner, D.E. Robertson, and P.L. Dutton, *J. Phys. Chem.* **90**, 3783 (1986).

(25) A.D. Joran, B.A. Leland, P.M. Felker, A.H. Zewail, J.J. Hopfield, and P.B. Dervan, preprint (1986).

(26) E.M. Kosower and D. Huppert, *Chem. Phys. Lett.* **96**, 433 (1983).

(27) D.F. Calef and P.G. Wolynes, *J. Phys. Chem.* **87**, 3387 (1983).

(28) V. Hakim and V. Ambegaokar, *Phys. Rev. A* **32**, 423 (1985).

(29) (a) H.A. Kramers, *Physica(Utrecht)* **7**, 284 (1940); (b) S. Chandrasekhar, *Rev. Mod. Phys.* **15**, 3 (1943).

(30) W. Nadler and K. Schulten, *J. Chem. Phys.* **84**, 4015 (1986).

(31) (a) A.D. Joran, B.A. Leland, G.G. Geller, J.J. Hopfield, and P.B. Dervan, *J. Am. Chem. Soc.* **106**, 6090 (1984); (b) B.A. Leland, A.D. Joran, P.M. Felker, J.J. Hopfield, A.H. Zewail, and P.B. Dervan, *J. Phys. Chem.* **89**, 5571 (1985).

(32) J.N. Onuchic, Ph.D. thesis in preparation.

(33) (a) D.N. Beratan, *J. Am. Chem. Soc.* **108**, 4321 (1986); (b) R.J. Cave, Ph.D. Thesis, California Institute of Technology (1986).

(34) (a) N.G. van Kampen, *Stochastic Processes in Physics and Chemistry*; North–Holland: Amsterdam, 1981; (b) H. Risken, *The Fokker–Planck Equation*; Springer–Verlag: Berlin, 1984.

(35) S.L. Mayo, W.R. Ellis, R.J. Crutchley, and H.B. Gray, *Science* **233**, 948 (1986).

II.5 Reaction Rates in Biomolecules: Adiabatic Limit Revisited

to be submitted

William Bialek* and **José Nelson Onuchic****

*Institute for Theoretical Physics

University of California

Santa Barbara, California 93106

**Division of Chemistry and Chemical Engineering

California Institute of Technology

Pasadena, California 91125

ABSTRACT

Several important chemical reactions in biomolecules have been described as phonon-assisted transitions between two electronic states. It is widely believed that the reaction rate saturates at an "adiabatic limit" as the matrix element V between these states becomes large. We show that this is incorrect for large energy gaps between reactants and products, where the rate *decreases* at large V. Applications are suggested and limitations of approximate rate theories are emphasized.

The simplest model of a chemical reaction is that of two electronic states, identified as reactants and products, coupled to a single damped molecular vibrational mode. This picture, schematized in Fig. 1a, is an example of the family of spin-boson models which have been applied to a variety of physical processes and which have received renewed attention in connection with macroscopic quantum phenomena.[1] These models have been used to interpret the kinetics of several biomolecular reactions in terms of rather simple descriptions of the molecular dynamics, and in some instances important features of these models have subsequently been confirmed in spectroscopic studies.[2] There is, however, a strong prejudice that simple models cannot possibly capture the essential dynamical features of such obviously complex molecules, and several specific observations have been offered as evidence against the applicability of these models to real biomolecules.[3] It is not our intention to offer comments on these issues that are in any way conclusive, but rather to provide a more firm foundation for discussion by re-examining the predictions of the simplest model. We find that there is a large range of parameters over which these predictions diverge substantially from folklore regarding the theory of reaction rates, and that this unexpected richness of the simple models parallels certain unexpected features in the kinetics of the best-studied biomolecular reaction, ligand binding to heme proteins.

Chemical reactions are usually categorized as "adiabatic" or "non–adiabatic" depending on the extent of mixing between the two electronic states. In Fig. 1a we have drawn potential surfaces that neglect this mixing altogether, and from this point of view the reaction is seen to occur through some small perturbation, which allows a transition from one surface to another; if this perturbation is $\sim V$, the rate, from the Golden rule, is $\sim V^2$. In Fig. 1c we show potential surfaces obtained by solving the full electronic Hamiltonian, including mixing, at each value of the vibrational coordinate. The crossing is

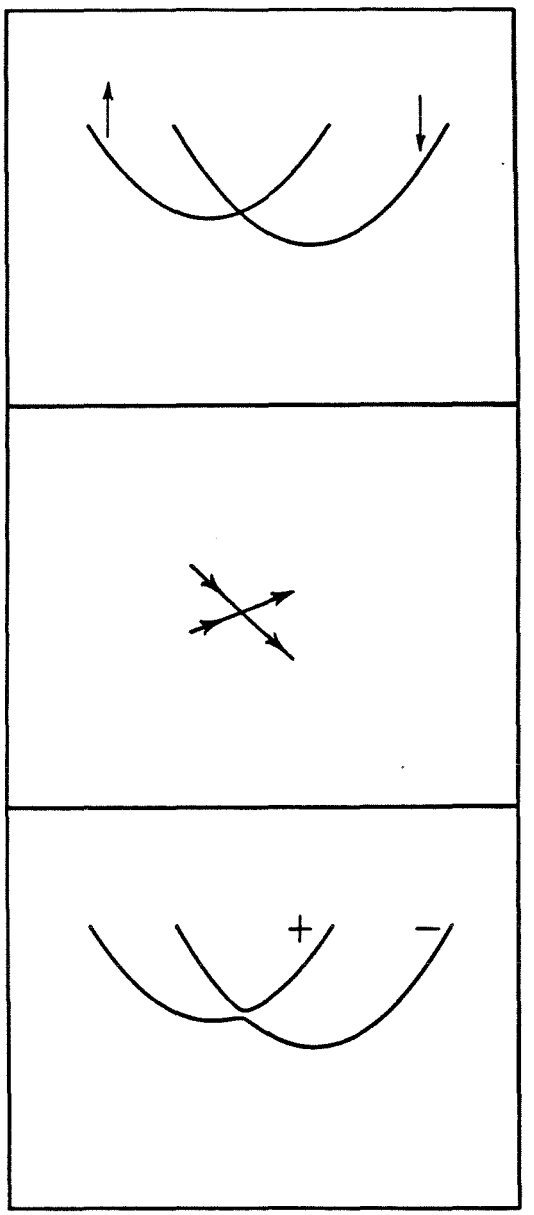

Figure 1 – (a) Upper panel. Energies of two electronic states $|\uparrow\rangle$ and $|\downarrow\rangle$ as a function of some molecular vibrational coordinate Q. (b) Middle panel. The region where the potential surfaces in (a) cross, with arrows denoting a reactive trajectory. (c) Lower panel. Adiabatic surfaces corresponding to the zero-order surfaces in (a); note the avoiding crossing.

avoided, and one expects that as the matrix element becomes large and the two adiabatic surfaces separate, the reaction should be viewed as a problem of thermally activated escape over a barrier, or possibly tunneling through the barrier at low temperatures. In this case the precise magnitude of the matrix element is irrelevant (unless it is so large as to significantly change the activation energy, but this is unlikely), and the rate saturates at an adiabatic limit.

The crossover between adiabatic and non-adiabatic regimes has generally been studied in the context of the Landau-Zener[4] model. The idea is to focus on the region where the zero-order surfaces cross (Fig. 1b), which is the only place where the reaction can occur in a semi-classical approximation. One then replaces the dynamical evolution of the vibrational degrees of freedom by motion through the crossing region at a fixed velocity v, so that the electronic states see a Hamiltonian that is time–dependent: the energy difference between the states varies linearly in time and there is a constant matrix element V mixing the two states. Given that the system enters the crossing region on the reactants' surface, the probability that it leaves on the products surface is $P(v) = 1 - e^{-\pi V^2/2\hbar vF}$, where F has the units of force and measures the difference in slopes of the two potential surfaces at the point where they cross. Thus, if $V \ll (2\hbar vF/\pi)^{1/2}$, the probability is $\sim V^2$, suggesting that a simple perturbative calculation of the reaction rate is possible, while if $V \gg (2\hbar vF/\pi)^{1/2}$, the system is essentially stuck on the single potential surface corresponding to the adiabatic ground state. This crossover from adiabatic to non-adiabatic behavior can be understood intuitively as the point where the system spends just enough time δt in the mixing region for the perturbation to have an effect $\sim V\delta t$ of order unity. This intuitive picture allows one to extend the Landau-Zener argument to more complex situations, although some care is required.

While many limitations of the Landau-Zener approximation are obvious, what concerns us here is that Fig. 1 is not the only possible picture that can be drawn. Imagine that the structural change between reactants and products — the horizontal displacement of the potential surface minima — is held fixed, and we change the energy gap ϵ between the two states. Then as this energy gap increases, Fig. 1a gradually becomes Fig. 2a. This situation is termed the "inverted region" in the theory of electron transfer reactions,[5] inverted because increasing the driving force for the reaction decreases the reaction rate; quantum mechanically, it is the case in which the electron–phonon coupling is too small to achieve the maximal rate, so this situation is also called "undercoupled."

The adiabatic limit of an undercoupled problem is shown in Fig. 2c. We observe that, if the dynamics is exactly adiabatic, so that there is no jumping from one surface to the other, there is *no* reaction. This can also be seen in a Landau-Zener picture, Fig. 2b, where one finds that as the matrix element becomes large, the probability of a reactive trajectory through the crossing region *decreases* exponentially in V; for small V the rate remains proportional to V^2.

These pictorial arguments suggest rather different behavior in the adiabatic limit, depending on whether the reaction is overcoupled or undercoupled: saturation of the rate constant in the adiabatic limit appears not to be universal. To see this more precisely, we would like to do a dynamical calculation of the rate constant in the adiabatic, undercoupled regime.

The model Hamiltonian that corresponds to both Figs. 1 and 2 is

$$\mathbf{H} = \frac{\epsilon}{2}\sigma_z + V\sigma_x + \frac{1}{2}[\dot{Q}^2 + \omega^2(Q + g\sigma_z)^2] + \text{damping}, \qquad (1)$$

where ω is the vibrational frequency, $2g$ is the change in the equilibrium position of the coordinate Q during the reaction, and damping[6] denotes terms that couple Q to a heat bath and generate vibrational relaxation at a rate γ. The

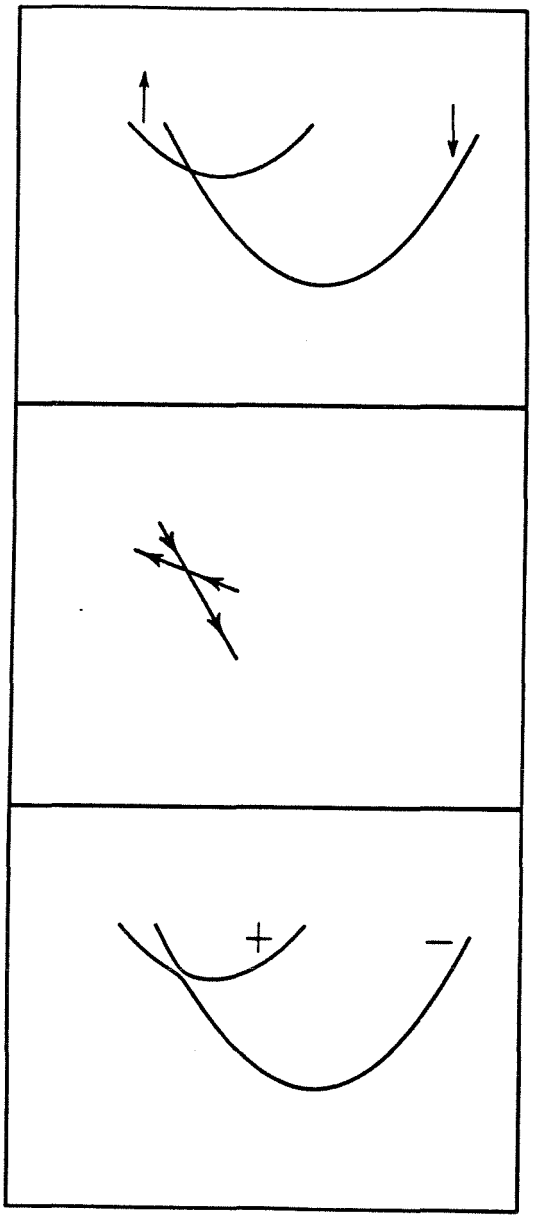

Figure 2 – As in Fig. 1, but for large energy gaps between reactants and products.

rate we are interested in calculating is that of a spin flip, $|\uparrow\rangle \longrightarrow |\downarrow\rangle$, where the eigenstates are those of σ_z. For small V we can do this perturbatively in V, and the rate is $\sim V^2$ as indicated above.

To calculate at large V, we first transform to the adiabatic basis schematized in Figs. 1c and 2c. The eigenstates in this basis are $|\pm>$, and the Pauli operators over this basis are σ'. The Hamiltonian becomes

$$\mathbf{H} = E(Q)\sigma_z' + \frac{1}{2}[(\dot{Q} - \hat{A})^2 + \omega^2 Q^2] + \text{damping}, \tag{2}$$

where $E(Q) = [(\epsilon/2 + \omega^2 gQ)^2 + V^2]^{1/2}$ and $\hat{A}$ is an operator

$$\hat{A} = i\hbar \sum_{\mu,\nu=\pm} |\mu\rangle\langle\mu|\frac{\partial}{\partial Q}|\nu\rangle\langle\nu|. \tag{3}$$

We emphasize that this is an exact transformation of the Hamiltonian[7]; the standard Born-Oppenheimer approximation is to set $\hat{A} = 0$. As one might expect from Fig. 2, at large V the slowest rate in the problem is the transition between the Born-Oppenheimer eigenstates, and we identify this as the reaction rate. This rate can be calculated perturbatively in $\hat{A}$, which turns out to be an expansion in V^{-1}.

The leading contribution to the rate constant $k(+ \rightarrow -)$ comes from terms $\sim \dot{Q}\hat{A}$, and the Golden rule gives

$$k = 2\pi\hbar \sum_{mn} P_{n+}|\langle m - |\Delta(Q)\dot{Q} + \dot{Q}\Delta(Q)|n+\rangle|^2 \delta(E_{m-} - E_{n+}), \tag{4}$$

where $|n\pm\rangle$ denotes the n^{th} vibrational state on the potential surface $(1/2)\omega^2 Q^2 \pm E(Q)$ with energy $E_{n\pm}$. P_{n+} is the Boltzmann probability for occupying this state, given that one is the electronic state $|+\rangle$, and

$$\Delta(Q) = [\omega^2 g - E'(Q)][\epsilon/2 + \omega^2 g + E(Q)]/D_+ D_-,$$

$$D_\pm = \{V^2 + [\epsilon/2 + \omega^2 gQ \mp E(Q)]^2\}^{1/2}.$$

This expression for the rate is purely formal, because of the delta functions, but can be transformed into an integral over a well–behaved correlation function using standard methods[8].

To keep our calculation as close as possible to the intuitive semi-classical pictures associated with the Landau-Zener argument, we will evaluate this correlation function in a semi-classical approximation. Since semi-classically the reaction can occur only in the crossing region, we approximate the matrix element $\Delta(Q)$ by its value at the crossing point Q_0 and expand all exponential factors to quadratic order around Q_0. The result is

$$k = \left(\frac{\omega^2 g}{V}\right)^2 \int d\tau \left\langle \dot{Q}(\tau)\mathbf{T}\exp\left[2iV\tau/\hbar \right.\right.$$
$$\left.\left. +i\frac{(\omega^2 g)^2}{\hbar V}\int_0^\tau dt(Q(t)-Q_0)^2\right]\dot{Q}(0)\right\rangle_+, \qquad (5)$$

where $\langle\cdots\rangle_+$ denotes an expectation value in an equilibrium vibrational ensemble constrained to electronic state $|+\rangle$, and $\mathbf{T}$ is the time-ordering operator. Contributions to the integral in Eq. (5) on time scales comparable to ω^{-1} give rise to quantum effects associated with resonances at multiples of the phonon energy $\hbar\omega$;[9] to have a consistent semi-classical approximation we must therefore assume that the times that are significant are short compared to these vibrational time scales. In practice the quantum resonances are attenuated by both the vibrational damping and by coupling to several modes with incommensurate frequencies. We make one further approximation, and this is that the crossing occurs at a displacement Q_0 much larger than typical fluctuations in Q, which is equivalent to the assumption that the activation energy for the reaction is large compared to k_BT or $\hbar\omega$. The semi-classical rate constant is then

$$k = \frac{\hbar\tilde{\omega}^2}{V}\sqrt{\frac{2\pi\langle(\delta Q)^2\rangle}{(Q_0-Q_+)^2}}\exp\left[\frac{-1}{2\langle(\delta Q)^2\rangle}\left(|Q_0-Q_+|+\frac{2V^2}{\omega^4 g^2|Q_0-Q_+|}\right)^2\right], \qquad (6)$$

where Q_+ is the equilibrium coordinate in state $|+\rangle$, $\langle(\delta Q)^2\rangle$ is the mean-square coordinate fluctuation in this state, and $\tilde{\omega}^2 = \langle(\delta\dot{Q})^2\rangle/\langle(\delta Q)^2\rangle$.

To understand this result, recall that the classical activation energy is, from Fig. 2, roughly proportional to $(Q_0 - Q_+)^2$, with corrections of order V, while at high temperatures $\langle(\delta Q)^2\rangle$ is proportional to the absolute temperature T. Thus, we have the approximate result

$$k \sim \frac{\hbar\tilde{\omega}^2}{V}\sqrt{\frac{2\pi k_B T}{E_a}}e^{-E_a/k_B T}, \tag{7}$$

which should be contrasted with the corresponding result at small V,[10]

$$k \sim \frac{V^2}{\hbar}\sqrt{\frac{\pi}{2\omega^2 g^2 k_B T}}e^{-E_a/k_B T}. \tag{8}$$

These expressions are equal at $V \sim \alpha\hbar\tilde{\omega}$, with α of order unity for reasonable parameter values. This is exactly what we expect: the crossover from small V to large V occurs when this matrix element is comparable to the spacing $\hbar\tilde{\omega}$ between vibrational energy levels.

We emphasize that our large V results are valid only in the undercoupled regime. There is excellent evidence that this regime is in fact relevant for at least some biomolecular reactions.[2] In one photosynthetic electron transfer reaction there are measurements not just of temperature–dependent reaction rates but also of the direct optical transition between reactants and products;[11] while the kinetic data can be explained with either undercoupled or overcoupled models, the spectroscopic data are only consistent with the undercoupled case. In the binding of small ligands to heme proteins, the energy gaps reported for the last (intramolecular) step of the binding reaction are so large[12] that the reaction is almost certainly undercoupled, and this is supported by estimates of g and ω from available spectroscopic and structural data.[13] Finally, studies of other photosynthetic electron transfer reactions using chemical substitutions to vary the energy gap strongly suggest that these reactions are undercoupled under normal conditions.[14]

The heme protein reactions may provide an example of the effects discussed here.[15] The binding of oxygen (O_2) or carbon monoxide (CO) to the heme iron (Fe) is accompanied by a change in spin states from high–spin ($S = 2$) iron in the unbound to a low-spin ($S = 0$) diamagnetic iron-ligand complex. In the case of CO, which is itself diamagnetic, this can occur only at second order in the spin-orbit coupling, so we expect $V_{CO} \sim \lambda_{SO}^2/\Delta$, with the spin-orbit splitting $\lambda_{SO} \sim 100\ cm^{-1}$ and the crystal field $\Delta \sim 10^4\ cm^{-1}$, so $V_{CO} \sim 1\ cm^{-1}$. With O_2, on the other hand, the Fe spin needs to change by only one unit to $S = 1$ and then couple anti-ferromagnetically to the triplet O_2; this suggests $V_{O_2} \sim \lambda_{SO} \sim 100\ cm^{-1}$. As emphasized by Frauenfelder and Wolynes,[3] if one could calculate the reaction rates in perturbation theory for both ligands, O_2 would bind approximately 10^4 times faster than CO. In fact, from 40 K to 160 K the kinetics of the two ligands are rather similar.

The fact that ligand binding to heme proteins is temperature–dependent down to $T \sim 20$ K suggests coupling of the electronic state changes to modes in the $\hbar\omega \sim 20\ cm^{-1}$ range,[13] and a mode at $\hbar\omega = 25\ cm^{-1}$ has been identified in Mössbauer spectra as coupling strongly to motions of the heme iron in both the O_2 and CO bound states of myoglobin.[16] It is clear that, if this mode is the dominant one, $V_{CO} \ll \hbar\tilde{\omega}$ while $V_{O_2} > \hbar\tilde{\omega}$. Since, from Eqs. (7) and (8), the rate increases at small V and decreases at large V, with the crossover at $V \sim \hbar\omega$, we see that CO binding will be slow because the matrix element is small, but O_2 binding will also be slow, this time because the matric element is too large — in going from CO to O_2 we have increased the matrix element beyond the value $V \sim \hbar\tilde{\omega}$ required for the maximal rate.

We emphasize that these considerations are rather qualitative and that much more work is required to have a quantitative theory of either CO or O_2 binding. We might also point out that the kinetic similarity of CO and O_2 is much less evident[17] if one looks at room temperature or at very low temper-

atures. Our point is that the simplest dynamical model of chemical reaction rates predicts, in the undercoupled regime, a non-monotonic dependence of the reaction rate on the electronic matrix element, with a maximum rate at some finite V. The parameters of the heme proteins are such that CO and O_2 plausibly fall on opposite sides of this maximum, so that both ligands can have small — and roughly similar — binding rates even though they are very different in electronic structure.

As a final remark we note that the correct semi-classical rate at large V and ϵ, Eq. (6), differs substantially from the naive Landau-Zener prediction $k \sim e^{-\pi V^2/2\hbar v F}$. The Landau-Zener picture is of course not dynamical, and does not correctly treat the possibility of coherence between electronic states as one enters the crossing region; the latter effect seems to be the most important in our case, where the adiabatic basis embodies maximum coherence. These results suggest that the rate would be very different if dissipation (in this case vibrational relaxation) were very strong, so that coherence is destroyed, and that even in the more conventional overcoupled case the rate constant approaches the adiabatic limit with corrections $\sim \hbar\tilde{\omega}/V$, not $\sim e^{-\pi V^2/2\hbar v F}$.

We thank J. Friedman, R.F. Goldstein J.J. Hopfield, J.S. Langer, J. Moody, J.R. Schrieffer, and F. Wilczek for helpful discussions. Work in Santa Barbara was supported by the National Science Foundation under Grant No. PHY82-17853, supplemented by NASA. Work at Caltech was supported by the Brazilian Agency CNPq and by the National Science Foundation under Grant No. PCM84-06049.

* Present address: Departments of Physics and Biophysics, University of California, Berkeley, California 94720.

** On leave of absence from the Instituto de Física e Química de São Carlos, USP, São Carlos, SP 13560, Brazil.

References

(1) For a review, see A.J. Leggett, S. Chakravarty, A. Dorsey, M.P.A. Fisher, A. Garg, and W. Zwerger, *Revs. Mod. Phys.* (in press).

(2) J.J. Hopfield, *Proc. Nat. Acad. Sci. (USA)* **71**, 3640 (1974); R.F. Goldstein and A. Bearden, *Proc. Nat. Acad. Sci. (USA)* **81**, 135 (1984); W. Bialek and R.F. Goldstein, *Biophys. J.* **48**, 1027 (1985). For reviews see W. Bialek and R.F. Goldstein, *Physica Scripta* (in press); R.F. Goldstein and W. Bialek, *Comments Mol. Cell. Biophys.* **3**, 407 (1986).

(3) A. Ansari, J. Berendzen, S.F. Bowne, H. Frauenfelder, I.E.T. Iben, T. Sauke, E. Shyamsunder, and R.D. Young, *Proc. Nat. Acad. Sci. (USA)* **82**, 5000 (1985); H. Frauenfelder and P..Wolynes, *Science* **229**, 337 (1985).

(4) L.D. Landau, *Sov. Phys.* **1**, 89 (1932); C. Zener, *Proc. Roy. Soc. Lond.* **A137**, 696 (1932).

(5) R.A. Marcus *Ann. Rev. Phys. Chem.* **15**, 155 (1964).

(6) A.O. Caldeira and A.J. Leggett, *Ann. Phys.* **149**, 374 (1983).

(7) This "gauge potential" formulation of the adiabatic approximation is essentially that given by F. Wilczek and A. Zee, *Phys. Rev. Lett.* **52**, 2111 (1984); see also J. Moody, A. Shapere, and F. Wilczek, unpublished.

(8) R. Kubo, *Phys. Rev.* **86**, 929 (1952).

(9) See, for example, the discussion by W. Bialek and R.F. Goldstein, Ref. 2.

(10) J.J. Hopfield, Ref. 2.

(11) R.F. Goldstein and A. Bearden, Ref. 2.

(12) R.H. Austin, K.W. Beeson, L. Eisenstein, H. Frauenfelder, and

I.G. Guasalus, *Biochemistry* **14**, 5355 (1975).

(13) W. Bialek and R.F. Goldstein, Ref. 2.

(14) M.R. Gunner, D.E. Robertson and P.L. Dutton, *J. Phys. Chem.* **90**, 3783 (1986).

(15) All of the kinetic data relevant to this discussion is given by Austin *et al.*, Ref. 12. The significance of the problem was emphasized by H. Frauenfelder and P.G. Wolynes, Ref. 3, although the suggestion of using electronically different ligands to probe the dynamics of the reaction is due to J.R. Schrieffer, in *Tunneling in Biological Systems*, B. Chance, D.C. DeVault, H. Frauenfelder, R.A. Marcus, J.R. Scheriffer, and N. Sutin, eds.; Academic Press: New York, 1979. Estimates of the matrix elements were made by M.H. Redi, B.S. Gerstman, and J.J. Hopfield, *Biophys. J.* **35**, 471 (1986).

(16) W.W. Wise, G.C. Wagner, and P.G. Debrunner, to be published.

(17) J.M. Friedman, unpublished.

CHAPTER III – Electron Tunneling Matrix Elements; Application to Electron Transfer in Proteins

III.1 Through-Bond and Through-Space Pathways – Protein Pathways and Modulation of Matrix Elements

As proposed by Hopfield[1] in 1974 and discussed in Chapter I, several biological electron transfers, which control the primary steps of bacteria photosynthesis, are non–adiabatic. For non–adiabatic rates it is important to know the electronic matrix element connecting the two states involved in the transfer. Because of that, to calculate this matrix element became an important problem in the field. The basic problem is to understand how the medium affects the transfer rate. Is the electronic matrix element due to direct overlap between donor and acceptor states (through-space), or do the orbitals of the medium between them facilitate the transfer?

From Hopfield's work, we notice that the distance decay of the matrix element, T_{DA}, is too slow in order to believe that the electron transfer occurs through-space, i.e., direct interaction between donor and acceptor orbitals. To give an idea about numbers, the decay per distance given by Hopfield[1,2] in his early work is $\alpha \sim 0.72\text{Å}^{-1}$ when, if we had through-space transfer, α should be around 1.7Å^{-1} (see discussion in Secs. III.2 and III.4). This fast through-space decay arises from completely neglecting the bridge. Therefore, in the biological electron transfers described in Chapter I, the medium orbitals must be facilitating the electron tunneling.

Trying to understand how the medium orbitals affect the electron transfer matrix elements (through-bond transfer), much experimental and theoretical work was performed. In the experimental area, several compounds were built where the distance between donor and acceptor is adjustable. In several of

them one is able to change the transfer electron energy. A list of such systems is given in Ref. 3.

From the theoretical point of view, the pioneering work was done by Halpern and Orgel,[4] who first identified the importance of bridge mediation in the electron transfer interaction. Since then, an extensive literature that estimates the effect of the bridge (electron or hole transfer, depending on the bridge orbitals and donor/acceptor redox energies) has emerged[5]. The work developed in our group by Beratan and Hopfield[5d,5i] is particularly interesting because of its quantitative predictions. They calculate matrix elements for systems where the bridge is composed by several units of some linkers. The dependence of the matrix element on the energetics of the system and on the number of linkers is the aim of their work. A tight–binding Hückel Hamiltonian was used for their calculations, and a periodic approximation was made so that the wave functions behave as Bloch states. Examples of systems studied by this method are the prophyrin–bridge–quinone molecule where the bridge is composed by bicyclo[2.2.2]octane linkers[3a] (Figure II.2) and mixed–valence dithiaspirocyclobutane molecules.[3h] From their work we expect that most of the electron transfers mediated by organic bridges are actually hole transfer. This is due to the fact that the transfer electron energy lies much closer to the valence band.

In Sec. III.2 we present a model that allows us to define when the through-space transfer or through-bond transfer limits are reasonable models. (We do not present the model in this section because it is carefully described in Sec. III.2, which is a short enough section.) Also, in the case of through-bond transfer, two limits are possible, weak or strong interaction between the

bridge units. The functional dependence of the matrix element on the tunneling electron energy for the three cases is discussed, and this was used to explain a controversy that existed in this field. The periodic approximation assumed by Beratan and Hopfield is discussed and justified in this section and Sec. III.3. Substituting some reasonable parameters in the expressions obtained in Sec. III.2, we come to the conclusion that the tight binding model is a good approximation for the bridges in these model compounds. Therefore, based on the results of Sec. III.2, we calculate how different hydrocarbon bridges affect the electronic matrix element, using a tight binding Hamiltonian. These results are presented in Sec. III.3, and they show calculations for several model compounds now existent. The basic conclusion of this work is how, compared to a single linear alkane chain, constructive or destructive interference, increases or decreases the electron transfer rate.

If we are interested in biology, model compounds are not enough, and trying to understand electron transfer through a protein environment is a natural next step. From the model compounds we learned that covalent pathways really assist electron transfer. Therefore, they must be important for electron transfer in proteins. However, if we look at protein structures,we come to the conclusion that covalent pathways are, in most cases, prohibitively long, and some through-space electron "jumps" are probably occurring. We therefore developed a model that includes both possibilities: the electron transfer pathway is composed of covalent legs connected with a few through-space jumps. Systems for which we intend to perform calculations using this model are described in Sec. III.4. A more detailed discussion of how we intend to do the calculations is given in Sec. IV.2.

This model for electron transfer in proteins is presented in Sec. III.4. Here we summarize its most important results. Sec. III.4 is basically divided into two parts. The first one assumes that the medium through which the electron tunnels is rigid, and for this condition it develops a prescription for calculating the electron transfer rate. In the second part, we include thermal mobility for the tunneling medium and discuss how it affects the rate. This second part is an improvement of the model proposed in Sec. III.5. We now describe the prescription to calculate the electron transfer rate for a rigid protein medium. Here we recall the fact that through-space decay is much faster than through-bond decay ($\sim$ 1.7 Å^{-1} vs. $\sim$ 0.6 Å^{-1}). In most of the protein electron transfer cases, however, the "complete" through-bond pathways (covalent) are prohibitively long. Therefore, as already discussed, in our model we consider electron transfer pathways that are composed of through-space and through-bond parts. For the through-bond parts, as in the matrix element calculations for covalent chains, a tight binding Hückel Hamiltonian is used. The electronic donor Hamiltonian is then written as

$$H_D^{el} = \Delta_D a_D^\dagger a_D + \beta_D (a_D^\dagger a_1 + a_1^\dagger a_D) + \sum_{i=1}^{N-1} \beta_i (a_i^\dagger a_{i+1} + a_{i+1}^\dagger a_i) \quad . \quad (III.1)$$

If the covalent chain is periodic, the decay of the wave function can be calculated using the method proposed by Beratan and Hopfield.[5d] In Sec. III.4 we developed a method that we call "decay per bond." This formalism is useful when we can neglect "backscattering" between bonds. Calling β the interaction between (sp^3) and (sp^3) or (sp^2) orbitals on different atoms, γ_i the interaction between hybrid orbitals on the same atom i, and α_i the self-energy of the hybrid orbital on atom i, the decay of the wave function on bond i is

$$\epsilon_i = \frac{\gamma_i \beta}{(\alpha_i - E)(\alpha_{i+1} - E) - \beta^2} \quad . \quad (III.2)$$

As we see in Sec. III.4, this method is very efficient when $\epsilon_i^2 \ll 1$, and works quite reasonably for protein backbone and alkanes. Reasonable parameters for all the important through-bond interactions are given in Sec. III.4.

As already discussed, through-space interactions are also going to be important in proteins. Because they decay with distance much faster than the through-bond ones, when performing calculations we will be looking for the shortest possible through-space jumps. By shortest we mean that we can not go to prohibitively long through-space distances. The simplest way to calculate the interaction between the two orbitals through which the electron is going to transfer "through-space" is by using the Hückel approach,[6] and therefore calculating the coupling between these two non–covalent contacts, for orbitals with the same binding energy V_b, by

$$\beta^{n-c} = V_b \, S_{12} \quad , \qquad (III.3)$$

where S_{12} is the overlap between them. Now let us assume, for example, that these two terminal groups are two carbon–carbon sigma bonds. If we approximate these bonds by a 1S hydrogen–like orbital with binding energy of 10 eV, we obtain at a separation of 5.5 Å a $\beta^{n-c} \approx 0.03eV$. This interaction has a distance decay of $1.7\mathring{A}^{-1}$. At this separation we have $\epsilon^{n-c} \approx 0.005$. At this level it is important to point out that this model is very crude, but the distance decay in the weak coupling limit is model–independent and depends only on the binding energy. Also, this 1S approximation overestimates the interaction.

Putting these two sorts of interactions together, the simplest expression

we can get for the electron transfer matrix element is

$$T_{DA} = (\beta_D \beta_A / E) \prod_{i=1}^{N_B} \epsilon_i^c \prod_{j=1}^{N_S} \epsilon_j^{n-c} \quad . \qquad (III.4)$$

Here the energy, E, is measured with respect to the first "orbital" (bond) that the donor interacts with. N_B is the number of covalent bonds and N_S is the number of non–covalent jumps along a given pathway.

We now give a summary of the second part of this model, which discusses how temperature affects the matrix element. The model described until now considers a rigid medium through which the electron tunnels. This may not always be appropriate, and we now show how mobility of the medium groups may alter (modify the usual temperature dependence) the electron transfer rate.

As an example, consider an ideal electron transfer pathway composed of identical orbitals, where only one of the interactions is allowed to fluctuate. The Hamiltonian for such a system is

$$H = H^{el} + H^{nuc} + H^{int} \quad , \qquad (III.5)$$

where

$$H^{el} = H_D^{el} + H_A^{el} \qquad (III.6a)$$

$$H^{nuc} = H_D^{nuc} + H_A^{nuc} + H_N^{nuc} \qquad (III.6b)$$

$$H_D^{el} = \Delta_D a_D^\dagger a_D + \beta_D (a_D^\dagger a_1 + a_1^\dagger a_D) + \beta \sum_{i=1}^{N} (a_i^\dagger a_{i+1} + a_i^\dagger a_{i-1}) \qquad (III.6c)$$

$$H_A^{el} = \Delta_A a_A^\dagger a_A + \beta_A (a_A^\dagger a_{N_T} + a_{N_T}^\dagger a_A) + \beta \sum_{j=N+1}^{N_T} (a_j^\dagger a_{j+1} + a_j^\dagger a_{j-1}) \qquad (III.6d)$$

$$H^{int} = \beta_1^{eq} \exp\left\{-\alpha'[(R_{N+1} - R_N) - R^0]\right\} (a_N^\dagger a_{N+1} + a_{N+1}^\dagger a_N) \qquad (III.6e)$$

$$H_D^{nuc} = \left(b_D^\dagger b_D + \frac{1}{2}\right)\hbar\Omega_D + \lambda_D a_D^\dagger a_D (b_D^\dagger + b_D) \qquad (III.6f)$$

$$H_A^{nuc} = \left(b_A^\dagger b_A + \frac{1}{2}\right)\hbar\Omega_A + \lambda_A a_A^\dagger a_A (b_A^\dagger + b_A) \qquad (III.6g)$$

$$H_N^{nuc} = \left(b_N^\dagger b_N + \frac{1}{2}\right)\hbar\omega \quad , \qquad (III.6h)$$

where β_1^{eq} is the interaction between sites N and $N+1$ at their equilibrium separation. Also, we define $y_N = (R_{N+1} - R_N) - R^0$ as the deviation from equilibrium of the distance between these two sites. In the simplest approximation, y_N is considered harmonic.

We can calculate the temperature dependence due to fluctuations of y_N. Doing a semiclassical calculation, we find that the electron transfer rate change due to this fluctuation is

$$\langle \exp(-2\alpha' y_N) \rangle = \int \exp(-2\alpha' y_N) P(y_N) dy_N \quad , \qquad (III.7)$$

where $P(y_N)$ is the probability distribution function for this coordinate. By semiclassical we mean that quantum mechanics is included only through the distribution function. (See Sec. III.4 for details.) Here we assume that the relaxation of this nuclear mode is fast enough (see Secs. II.1 and II.4) so that the donor survival probability decays exponentially in time. If y_N is harmonic, Eq. 2.7 can be calculated exactly, and

$$\langle \exp(-2\alpha' y_N) \rangle = \exp(2\alpha'^2 \mu_N^2) \quad , \qquad (III.8a)$$

where

$$\mu_N^2 = \frac{\hbar}{2m\omega} \coth \frac{\hbar\omega}{2\kappa T} = \frac{\kappa T^{eff}}{m\omega^2} \qquad (III.8b)$$

is the mean-square deviation of y_N. This is equivalent to writing

$$P(y) = \frac{1}{\sqrt{2\pi\mu_N^2}} \exp\left[-\frac{y_N^2}{2\mu_N^2}\right] . \qquad (III.9)$$

The final semi-classical rate is then written as

$$k_{ET} = \frac{2\pi}{\hbar}|T^0_{DA}|^2 \langle \exp(-2\alpha' y_N)\rangle \, F.C(\text{local modes}) \quad , \qquad (III.10)$$

where T^0_{DA} is the matrix element for a rigid medium. In Sec. III.4 we show that this contribution due to fluctuations of the distance between covalently bonded groups is going to be negligible. Therefore, if this effect is important, it will be due to fluctuations of the distance between non-covalent groups along the electron transfer pathway. A discussion about their possible effect on the rate is given in Sec. III.4.

References – Section III.1

(1) J.J. Hopfield, *Proc. Nat. Acad. Sci. (USA)* **7**, 3640 (1974).

(2) M. Redi and J.J. Hopfield, *J. Chem. Phys.* **72**, 6651 (1980).

(3) (a) B.A. Leland, A.D. Joran, P.M. Felker, J.J. Hopfield, A.H. Zewail, and P.B. Dervan, *J. Phys. Chem.* **89**, 5571 (1985); (b) S.S. Isied and A. Vassilian, *J. Am. Chem. Soc.* **106**, 1732 (1984); (c) H. Heitele and M.E. Michel–Beyerle, *J. Am. Chem. Soc.* **107**, 8286 (1985); (d) M.R. Wasielewski and M.P. Niemczyk, *J. Am. Chem. Soc.* **106**, 5043 (1984); (e) D.E. Richardson and H. Taube, *J. Am. Chem. Soc.* **105**, 40 (1985); (f) G.L. Closs, L.T. Calcaterra, N.J. Green, K.W. Penfield, and J.R. Miller, *J. Phys. Chem.* **90**, 3673 (1986); (g) J. Verhoeven *J. Pure and Appl. Chem* **58**, 1285 (1986); (h) C.A. Stein, N.A. Lewis, and G.J. Seitz, *J. Am. Chem. Soc.* **104**, 2596 (1982).

(4) J. Halpern and L. Orgel, *Discuss. Faraday Soc.* **29**, 32 (1960).

(5) (a) H.M. McConnell, *J. Chem. Phys.* **35**, 508 (1961); (b) S. Larsson, *J. Chem. Soc., Faraday Trans. 2* **79**, 1375 (1983); (c) S. Larsson, *J. Am. Chem. Soc.* **103**, 4034 (1981); (d) D.N. Beratan and J.J. Hopfield, *J. Am. Chem. Soc.* **106**, 1584 (1984); (e) P.D. Hale and M.A. Ratner, *Int. J. Quantum Chem.: Quantum Chem. Symp.* **18**, 195 (1984); (f) A.A.S. da Gama, *Theor. Chim. Acta* **68**, 159 (1985); (g) D.E. Richardson and H. Taube, *J. Am. Chem. Soc.* **105**, 40 (1983); (h) D.E. Richardson and H. Taube, *Coord. Chem. Revs.* **60**, 107 (1984); (i) D.N. Beratan, *J. Am. Chem. Soc.* **108**, 4321 (1986).

(6) (a) K. Yates, *Hückel Molecular Orbital Theory*; Academic Press: New York, 1971; (b) C.J. Ballhausen and H.B. Gray, *Molecular Orbital Theory*; Academic Press: New York, 1978.

III.2 Limiting Forms of the Tunneling Matrix Element in the Long Distance Bridge Mediated Electron Transfer Problem

J. Chem. Phys. **83**, 5325 (1985)

Limiting forms of the tunneling matrix element in the long distance bridge mediated electron transfer problem

David N. Beratan, José Nelson Onuchic,[a] and J. J. Hopfield[b]
Division of Chemistry and Chemical Engineering,[c] California Institute of Technology, Pasadena, California 91125

(Received 6 May 1985; accepted 7 August 1985)

A simple model is presented for long distance electron transfer through a bridging medium. Assumptions about the bridge mediated interaction, inherent in many other models, are shown to be limits of the more general problem. The relative importance of through bond and through space coupling is discussed.

I. INTRODUCTION

The rate of long distance (nonadiabatic) electron transfer depends critically on the electronic exchange interaction (tunneling matrix element) between donor and acceptor.[1-4] The exchange interaction is usually calculated by one of three methods. One method assumes that the interaction occurs directly *through space* and ignores the presence of the bridge altogether. The other methods assume that all interactions are mediated by the intervening medium (bonds). The "medium" includes any atomic or molecular species between donor and acceptor. In real systems this medium may be protein, halide atom, or hydrocarbon, for example. The donor–acceptor *through bond* interaction depends on the detailed molecular structure of the bridge. For example, electron transfer through an unsaturated hydrocarbon bridge may be considerably faster than through a saturated bridge. Two through bond mechanisms exist. They differ in their treatment of the interactions between neighboring bridge units. One assumes very strong and the other assumes weak electronic interactions between bridging groups. Each of these methods is an approximation of the correct donor–acceptor interaction which is assisted by interactions with both bound and continuum states.

In both the through bond and through space calculations the tunneling matrix element decays approximately exponentially with distance.[3] The various mechanisms predict decay lengths with different functional dependences on the electronic binding energy of the tunneling electron.[5-12]

The aim of this paper is to present a model which connects these three methods. The through bond and through space treatments in common use are shown to be distinct limits of the electron tunneling problem. A model problem is solved and it is shown under which circumstances the limits are obtained. The validity of selecting one limit for a calculation depends on the relative energetics of the donor, acceptor, and bridging medium and on the interaction between the neighboring bridging units.

II. STATEMENT OF THE MODEL

The decay of the donor wave function with distance is now found in an exactly soluble model system which does not restrict the decay to a purely through bond or through space pathway. The rate of distant electron transfer is proportional to a product of electronic and nuclear factors. The electronic term is related to the electronic exchange interaction between donor and acceptor. The nuclear factor is related to the nuclear activation barrier to electron transfer. The electron tunnels between the donor and acceptor in an "activated complex" of *fixed* nuclear geometry reached by atomic distortions to a configuration with matching donor and acceptor electronic energy levels (within the Born–Oppenheimer and Franck–Condon approximations). The models for electron tunneling describe the *electronic* potential in the activated complex and do not address the nuclear motion needed to reach that configuration. The exchange interaction can be found if the eigenstates of the electronic Schrödinger equations [Eq. (1)] can be found.

$$(T^e + V^D + V^M)\Psi_D = E_D\Psi_D,$$
$$(T^e + V^A + V^M)\Psi_A = E_A\Psi_A. \quad (1)$$

This is a one electron representation of the problem. The nuclear coordinates enter only as *parameters* in the electronic potentials V^D, V^A, and V^M. V^D is the potential of the isolated donor, V^M is the potential of the intervening medium, and V^A is the potential of the isolated acceptor. T^e is the electronic kinetic energy operator. The exchange matrix element, T_{ab}, is then $\langle\Psi_D|V^A|\Psi_A\rangle$ where V^A is the perturbation which mixes donor and acceptor electronic states. In this example, V^A is constant and less than zero on the acceptor and zero elsewhere. Since $V^A|\Psi_A\rangle$ is not dependent on the transfer distance in this model, the decay of the exchange interaction with distance is determined by the decay of Ψ_D.[6,7] (A more detailed explanation is presented in Appendix A.)

The simplest possible model for a bridging medium is a one dimensional chain of equally spaced constant potential wells.[13-15] Constant one dimensional potentials are poor substitutes for more realistic potentials if details of the states near the nuclei are needed. However, the asymptotic behavior of square well or Dirac delta function eigenstates correctly reproduce the decay of more complicated states far from the wells if the potentials are of finite range. Actual Coulom-

[a] On leave of absence from Instituto de Física e Química de São Carlos, Universidade de São Paulo, 13560, São Carlos, SP, Brazil.
[b] Also Division of Biology and AT&T Bell Laboratories, Murray Hill, NJ 07974.
[c] Contribution No. 7105.

bic potentials will only change the square well result by a polynomial factor. Also, shielding effects in many electron systems may make "muffin tin" potentials appropriate for one electron calculations.[16] The asymptotic behavior of the states, not the details in the high probability regions, is crucial for the calculation of tunneling matrix elements.

Modeling the medium with an infinite periodic potential is a useful first approximation for systems which have donor and acceptor connected by repeating groups such as synthetic organic linkers[18–22] or peptide units,[17] for example. The fact that the potential is infinite means that the donor and acceptor states will not include small corrections due to wave function reflection at a boundary (see Appendix A). The decay of a donor localized state in an otherwise periodic bridge is determined by the energy of the donor and the associated decay length determined by the bridge for that energy. The model Hamiltonian (Fig. 1) considered for the initial state (donor plus bridge) is

$$H^D = -\frac{\hbar^2}{2m}\frac{\partial^2}{\partial x^2} + \begin{cases} -U, & \text{if } na < x < na + b,\ n \neq 0 \\ -(U + U_{imp}), & \text{if } 0 < x < b \\ 0, & \text{elsewhere} \end{cases} \quad (2)$$

where $U>0$, $U_{imp}>0$, and n is an integer. $-U$ is the potential on each of the bridging units. The spacing between the two left (and two right) walls of adjacent wells is a. $-U_{imp}$ is the potential of the isolated donor relative to the potential of all other bridging potential wells. The choice of these well depths for a specific system depends on the chemical properties of the donor and bridge as well as the properties of the surrounding solvent or protein. When $U=0$ there is no bonded network to assist transfer and the problem reduces to one of purely through space propagation. When $U_{imp}=0$ each well is identical and the Schrödinger equation reduces to Kronig–Penney form.[13,14] In the latter case all states are delocalized and all "atoms" in the model are equivalent. The general solution for the trap plus bridge states could be written ignoring the translational symmetry of the bridge. However, because the potential away from the donor is periodic, both the donor localized and bridge delocalized wave functions change only by a decay factor per chain unit. The donor state of interest, Ψ_D, is a localized *bound* state with $E<0$. However, in this model one also finds the delocalized bridge states ($E<0$) and the continuum states ($E>0$). Defining $\kappa = \sqrt{-2mE/\hbar^2}$ and $Q = \sqrt{2m(U+E)/\hbar^2}$ where E is the energy eigenvalue for the bound state (and is, therefore, negative), the Kronig–Penney relation for the wave function decay is

$$\epsilon + 1/\epsilon = 2\cosh[\kappa(a-b)]\cos(Qb) + \frac{\kappa^2 - Q^2}{\kappa Q}\sinh[\kappa(a-b)]\sin(Qb). \quad (3)$$

ϵ is the Bloch factor[12–14] by which the wave function changes upon translation by one repeating unit in the bridge. The donor localized ground state is even with respect to the trap site ($x=0$) and the amplitude on the donor is nonzero. For the donor localized state ϵ is real and $|\epsilon|<1$. A boundary condition dependent on the trap energy determines the actual energy eigenvalues of the states. In the remainder of the paper, we use E only to represent the ground state energy of the Hamiltonian in Eq. (2). This is the energy of the transferring electron which is shown schematically in Fig. 1.

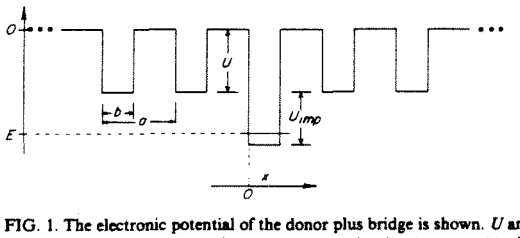

FIG. 1. The electronic potential of the donor plus bridge is shown. U and U_{imp} are positive. E is shown for a bound donor localized state and is the ground state of the Hamiltonian in Eq. (2).

Two limiting cases of this square well problem will be considered. In the first case the wave function decay in the bridge has characteristic decay length ($1/\kappa$) larger than the bridge unit spacing ($a-b$). In this case $\kappa(a-b)\ll 1$. We call this situation the loose binding limit. In this limit Eq. (3) becomes

$$\epsilon + 1/\epsilon = 2\cosh|Q|b \quad (4)$$

since $|E|>U$. Hence $\epsilon = \exp(-|Q|b)$ for the decaying states. This is the limit in which one works when assuming constant potential between donor and acceptor and trap well depth so that the electron has binding energy less than the true ionization potential of the trap.[5,6] When $\kappa(a-b)\ll 1$ a tight binding (molecular orbital) treatment of the bridging medium is invalid.[13] The precise size of the bridge–bridge interactions is irrelevant because it is so large. The second limit is discussed in Sec. III.

III. THROUGH BOND AND THROUGH SPACE LIMITS FOR A TIGHT BINDING BRIDGE

In contrast to the previous limit of strong interaction between bridging traps is the tight binding limit of the problem. In this case $\kappa(a-b)$ is not small and the wave function in the bridge has sharp peaks near the bridging atoms. Because the interaction between sites is small and wave function details near the nuclei are unimportant, we pass to the limit $b\to 0$, $U\to\infty$, $Ub\to\sqrt{V_b(2\hbar^2/m)}$, and $(U+U_{imp})b\to\sqrt{(V_b+\Delta)(2\hbar^2/m)}$. This is the Dirac delta function potential limit which is shown in Fig. 2 and is useful when $b\ll a$. V_b is the binding energy of an electron bound to an isolated bridge unit Dirac delta function potential well. V_b and Δ are both positive quantities. $V_b+\Delta$ is the binding energy of the isolated donor. We emphasize that when $\kappa(a-b)\to 0$ the delta function limit is no longer valid. The tunneling problem is simpler in the delta well limit and more easily compared with previous calculations. By resorting to delta wells we will find only one bound state per isolated bridge atom. In the more realistic square well model many bound states may exist in each isolated well. When a chain of delta wells is formed only one "band" of states results. In "real" systems many bands of states exist. However, electron mediation is usually dominated by interaction of donor and

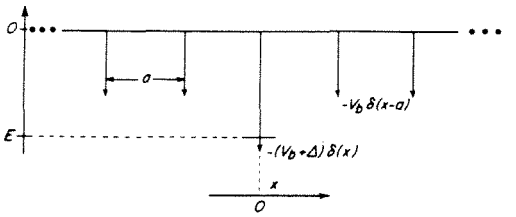

FIG. 2. A schematic representation of the potential in Fig. 1 is shown in the delta function limit. V_b and Δ are positive. E is the energy of the bound donor localized state of the Hamiltonian in Eq. (2) in the delta function limit.

acceptor with a single band of either valence (bonding) or conduction (antibonding) bridging states.[8] The delta function model is appropriate when hole transfer through a valence band or electron transfer through a conduction band dominates. Analysis of the problem for the general square wells is also possible.

Equation (3) may be written in the delta well limit as

$$\epsilon + 1/\epsilon = e^{\kappa a}(1-\lambda) + e^{-\kappa a}(1+\lambda), \tag{5}$$

where $\lambda = \sqrt{V_b/|E|}$. The boundary condition which determines the energy of the single donor localized state is

$$(2m/\hbar^2)\kappa\sqrt{(2\hbar^2/m)V_b}\coth(\kappa a) = \kappa^2 + (4m/\hbar^2)\sqrt{V_b(V_b+\Delta)} - (2m/\hbar^2)(\Delta + V_b). \tag{6}$$

Using the fact that in this section $\exp(\kappa a) \gg 1$,

$$\kappa = \sqrt{-2mE/\hbar^2} \simeq \sqrt{2m(V_b+\Delta)/\hbar^2}. \tag{7}$$

In the limit of $\lambda \ll 1$, i.e., $V_b \ll |E|$, the first order expansion of Eq. (5) is

$$\epsilon + 1/\epsilon \simeq e^{\kappa a} + e^{-\kappa a}. \tag{8}$$

This is the same result expected from the square well model [Eq. (3)] with $U \to 0$. The localized wave function decays by the amount $\epsilon \simeq e^{\kappa a}$ per repeating unit. This is exactly the energy dependence of the decay predicted in through space calculations ($U = 0$). To the extent that the bridge weakly perturbs the donor, the energy of the state is approximately $V_b + \Delta$ in both the through bond and through space limits.

Consider now the case where λ is not much less than one. Because $e^{\kappa a} \gg 1$ and writing $|E| = V_b + \delta E$, the expansion of Eq. (5) to second order in δE is

$$(\epsilon + 1/\epsilon) = \frac{\delta E}{2V_b \exp(-a\sqrt{2mV_b/\hbar^2})}\left[1 - \frac{3}{4}\frac{\delta E}{V_b}\right] \cdot \left[1 + a\delta E\sqrt{\frac{m}{2\hbar^2 V_b}}\right]. \tag{9}$$

The interaction between wells is small, i.e.,

$$\exp(-a\sqrt{2mV_b/\hbar^2}) \ll \exp(a\sqrt{2mV_b/\hbar^2})$$

so:

$$\epsilon + 1/\epsilon \simeq \frac{\delta E}{2V_b \exp(a\sqrt{2mV_b/\hbar^2})} \tag{10}$$

to first order in

$$\delta E a\sqrt{m/(2\hbar^2)}/\sqrt{V_b}. \tag{11}$$

δE is the energy of the donor localized state below the center of the band (which occurs at energy $-V_b$) of bridging states. The exchange interaction between two isolated delta wells in the weak interaction limit is[5]

$$-2V_b \exp(-\sqrt{2mV_b/\hbar^2}a) = \beta. \tag{12}$$

Thus $\epsilon + 1/\epsilon \simeq (E + V_b)/\beta$, exactly the decay of a local state interacting with an infinite chain of identical orbitals when only nearest neighbors interactions are included.[8-10] The nearest neighbor limit of the decay is indeed expected when the interactions between wells are weak.

IV. DISCUSSION

The through bond and through space tight binding limits are well defined. The through space tight binding limit is valid when the binding energy of the bridging units is small compared to the energy of the donor state. The through bond tight binding limit is valid when δE is small compared to $\sqrt{V_b}/(a\sqrt{m/2\hbar^2})$ and $\exp(\kappa a) \gg 1$. Increasing the binding energy of the bridge wells or decreasing the spacing between bridge atoms is expected to increase the validity of the through bond approximation (retaining κa large). In the tight binding limit $-V_b$ is the energy of the band center and δE is the energy difference between an electron (or a hole) trap and that band center. Hence, this analysis applies to both electron and hole tunneling. Indeed, recent evidence for hole transfer has been reported.[24]

In the three limiting cases the tunneling matrix element decays with distance as

$$\exp[-\sqrt{(2m/\hbar^2)|E+U|}R] \tag{13a}$$

for the loose binding through bond case,

$$\exp\left[\ln\left(\frac{\beta}{E+V_b}\right)R/a\right], \tag{13b}$$

when ($\epsilon \ll 1/\epsilon$) for the tight binding through bond case, and

$$\exp[-\sqrt{(2m/\hbar^2)|E|}R] \tag{13c}$$

for the tight binding shallow bridge well ($V_b \ll |E|$) case. E is the energy of the initially occupied donor localized bound state and is determined by a, b, U, and U_{imp}. Note that both the absolute sizes of these decay constants and their functional dependences on electronic energy are different.

At this point it is useful to describe the origin of the difference in the functional form of Eq. (13b) compared to Eqs. (13a) and (13c). In order to understand this difference we must compare the nearest neighbor bridge group interaction, the donor-bridge and acceptor-bridge interaction, and δE with the depth of the bridge group well U (V_b in the delta function limit). If these energies are small enough compared to U (V_b), only nearest neighbor interactions need to be considered and the problem can be solved by making a first order expansion. The expansion yields, as expected, the well known functional dependence found with the tight binding method when the bridge unit exchange interaction energy [β, Eq. (12)] is identified. Equation (13b) and related equations for more complicated linkers are used as starting points in several examples in the literature.[8,24] We now understand

the limits of validity for these methods. On the other hand, if one of these conditions is not satisfied, the functional dependence of the tunneling matrix element on distance cannot be expressed by a simple analytical expression and equations like Eq. (3) or Eq. (5) must be solved for ϵ and $T_{ab} \propto \exp[(\ln \epsilon)R/a]$. This is true until the opposite limit is reached, i.e., $U(V_b$ in the delta function limit) becomes small compared to the nearest neighbor bridging group interaction and the problem is reduced to tunneling through a square barrier. This limit may be reached in two ways: (1) by increasing the neighboring group interaction, i.e., $(a - b) \rightarrow 0$, and we obtain Eq. (13a); or (2) by decreasing $U(V_b)$, i.e., $U(V_b) \rightarrow 0$, and we obtain Eq. (13c).

Tight binding calculations of tunneling matrix elements are expected to be most appropriate when the energy of the localized state is close to a band of linker states (δE small). V_b, the binding energy of a bridging unit in the delta model, should be large. Finally, the spacing between bridging units should be small, but not so small that the condition $\exp(\kappa a) \gg 1$ is violated. Appendix B discusses the range of validity of this approximation in the square well model. References 8–12, 23, and 25 work in this limit. When the loose binding approximation is used U is understood to be no more than a parameter. Tight binding calculations (e.g., extended Hückel) permit the use of independently determined parameters and are expected to give a more realistic functional dependence of the tunneling matrix element on energy when the tight binding limit is valid (see Appendix B).

In real systems, such as proteins, the dominant tunneling pathway between donor and acceptor may not include bonded atoms, and the bonded pathway may be considerably longer.[17] In this situation the important tunneling pathways may include both bonded and nonbonded neighboring groups so a more elaborate model is required which includes all of the different interactions. In such a case the tunneling is still mediated by the medium groups. The direct donor–acceptor (through space) interaction is expected to be negligible. (If through space interactions were of importance *much* more rapid decays of T_{ab} with distance than commonly observed would be expected.[24]) The true interaction energy may have a rather complicated dependence on the donor and acceptor energetics and subunit interactions. The subunit–subunit interactions depend on the chemical properties of the groups including their separation, geometry, symmetry, and energy, for example.

This one dimensional model is an obvious oversimplification. Three dimensional effects and orientational effects may complicate the analysis of real systems. However, these details are not expected to cause qualitative changes in the wave function decay with distance in the bridging medium. Introduction of polar solvent may alter the effective ionization energy of the donor. It is not known to what extent intervening solvent may act as a through bond pathway. Boundary effects due to the finite length of real bridging groups are not expected to be large when $\epsilon^N \ll 1$ where N is the number of bridge units between donor and acceptor (see Appendix A).[26]

In the one delta function trap per repeating unit model a single band of bridge states is found. Transport is enhanced by energetic proximity of the donor and acceptor to bands of bound states of the bridging medium or to the continuum states. In real systems there are multiple bands. The band with edge closest to the donor and acceptor energies will dominate electron (hole) mediation. Depending upon whether the states in the band are bonding or antibonding, the transfer mechanism will be hole or electron exchange, respectively. The importance of bond mediated interactions between donors and acceptors has been shown recently in several experimental systems.[17–24] More realistic theoretical models for the bridging medium are under investigation.

ACKNOWLEDGMENTS

The authors are most grateful to Professor R. A. Marcus for suggesting investigations of the link between through bond and through space transfer. This work was supported in part by the National Science Foundation (Grant PCM-8406049) and by the Brazilian Agency CNPq.

APPENDIX A

In this formulation of the problem the acceptor appears to have an unimportant role. This is certainly not the case. Indeed, the problem may be analogously formulated considering hole transport from the electron acceptor to the electron donor. The details of the acceptor appear unimportant because only the *electronic* tunneling matrix element and not the Franck–Condon factor was discussed. Within the Born–Oppenheimer and Franck–Condon approximations

$$\begin{aligned} k &\propto \sum_{i,f} B_i |\langle \Psi_D(x; y_D, y_A)\phi_D^i \phi_A^i | V_A | \\ &\quad \times \Psi_A(x; y_D, y_A)\chi_D^f \chi_A^f \rangle|^2 \delta(E_i - E_f) \\ &\propto |\langle \Psi_D(x; \bar{y}_D, \bar{y}_A)| V_A |\Psi_A(x; \bar{y}_D, \bar{y}_A)\rangle|^2 \\ &\quad \times \sum_{i,f} B_i |\langle \phi_D^i \phi_A^i | \chi_D^f \chi_A^f \rangle|^2 \delta(E_i - E_f). \end{aligned} \tag{A1}$$

B_i is a Boltzmann weighting factor, Ψ_D is the donor electronic wave function, Ψ_A is the acceptor electronic wave function, ϕ^i is the donor (D) or acceptor (A) initial vibrational wave function, and χ^f is the donor or acceptor final vibrational wave function. x is the electronic coordinate. y is the donor or acceptor nuclear coordinate. The bar above the y coordinate represents a particular value for y chosen when making the Franck–Condon approximation. The vibronic coupling on the donor and acceptor determines $\bar{y}_D$ and $\bar{y}_A$ which maximize the product $(\phi_D^i \phi_A^i)^*(\chi_D^f \chi_A^f)$. As such, the vibronic coupling on donor *and* acceptor determine the tunneling energy, E.

Results for the dependence of the tunneling matrix element on distance for finite length bridges are not substantially different from the results for the infinite bridge model in the tight binding limit if: (1) $\epsilon^N \ll 1$ and (2) the addition of bridge groups does not significantly alter the energy of the localized state (perturbation theory suggests energy changes of the order ϵ^N) as the bridge is increased from N to $N + 1$ units. For a donor linked to a one orbital per site bridge of N repeating units the amplitude on the Nth site, C_N, is[26]

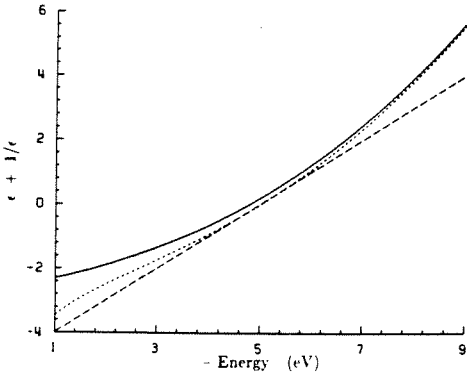

FIG. B1. The lower curve is a plot of Eq. (10) for $V_b = 5$ eV and $a = 2$ Å. The upper curve is the exact result [Eq. (5)]. The central curve is Eq. (5) neglecting the $\exp(-\kappa a)$ term. The lower curve corresponds to the through bond tight binding limit of the problem.

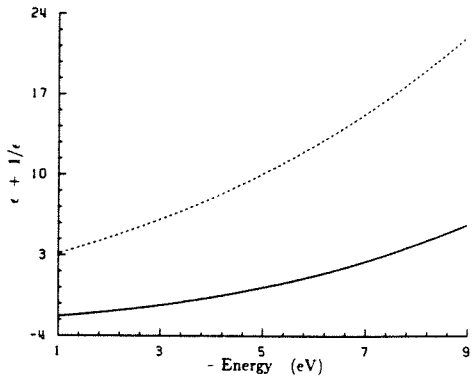

FIG. B2. The lower curve is the exact result [Eq. (5)] for the same parameters as in Fig. 1. The upper curve is a plot of Eq. (8), the limit of neglecting the bridging wells.

$$C_N = (1-\epsilon^2)\left(\frac{E-\Delta}{\beta'}\right)\left(\frac{\epsilon^N}{\epsilon-\epsilon^{2N-1}}\right). \quad \text{(A2)}$$

The decay of the tunneling matrix element with the number of bridging groups (N) is proportional to this amplitude. β' is the interaction energy of the donor orbital at site zero with the nearest bridge orbital at site one. The finite bridge contains N identical units. In this model, as in the constant potential bridge models, the electronic tunneling matrix element is proportional to the donor wave function overlap with the acceptor wave function on the acceptor site. For this reason, the spatial extent of V_A is important. The width and depth of the acceptor potential are expected to enter the rate at *all* distances as a distance *independent* prefactor.

One final condition must be imposed on the acceptor potential. It is required that energy be conserved. Because V_A is the potential felt by the electron on the acceptor in the activated complex, it must be chosen such that the electronic energy of the acceptor plus bridge in the activated complex coincides with the initial state (donor plus bridge) electronic energy.

APPENDIX B

As a numerical example parameters were chosen which are typical of values which might be chosen to model a hydrocarbon bridge between donor and acceptor. At this level of theory it is not possible to unambiguously choose parameters. It is vital to stress that no quantitative predictions of tunneling matrix elements should be extracted from this example. The parameters are $V_b = 5$ eV and $a = 2$ Å. V_b was chosen to give the approximate distance from the mediating band to the trap (~ 1 eV) and a reasonable value for the ionization energy of the trap (~ 8 eV). a was chosen to give -1 eV for β. The quality of the linear approximation for $\epsilon + 1/\epsilon$ [Eq. (10)] is shown in Fig. B1. A comparison of the exact result [Eq. (5)] with the result obtained by complete neglect [Eq. (8)] of the bridging atoms is shown in Fig. B2. Calculation of $\epsilon + 1/\epsilon$ for this set of parameters demonstrates that in typical bonded systems the transfer is mediated considerably more by the bonded than by the through space interactions along the same pathway. The linear dependence of ϵ on E is only valid when $\epsilon \ll 1$, however as ϵ becomes too small the linear approximation itself [Eq. (9)] becomes a poor estimate of the decay. Figure B1 shows that the through bond picture for electron transport gives a linear relation between $\epsilon + 1/\epsilon$ and E in the one orbital per repeating unit limit. This approximation is best close to the band. Further from the band the relation is roughly linear but the slope is not exactly the β which comes directly from molecular orbital theory. For donor states far from the band a correction to standard values of β may be necessary.

[1]D. DeVault, Q. Rev. Biophys. **13**, 387 (1980).
[2]R. A. Marcus, in *Oxidases and Related Redox Systems*, edited by T. E. King, H. S. Mason, and M. Morrison (Pergamon, New York, 1982), p. 3.
[3]J. J. Hopfield, Proc. Natl. Acad. Sci. U.S.A. **71**, 3640 (1974).
[4]*Tunneling in Biological Systems*, edited by B. Chance, D. C. DeVault, H. Frauenfelder, R. A. Marcus, J. R. Schrieffer, and N. Sutin (Academic, New York, 1979).
[5]M. Redi and J. J. Hopfield, J. Chem. Phys. **72**, 6651 (1980).
[6]P. Siders, R. J. Cave, and R. A. Marcus, J. Chem. Phys. **81**, 5613 (1984).
[7]P. Siders, Thesis, California Institute of Technology, 1983.
[8]D. N. Beratan and J. J. Hopfield, J. Am. Chem. Soc. **106**, 1584 (1984).
[9]A. A. S. da Gama, Theor. Chim. Acta (in press).
[10]A. S. Davydov, Phys. Status Solidi B **90**, 457 (1978).
[11]S. Larsson, J. Chem. Soc., Faraday Trans. 2 **79**, 1375 (1983).
[12]S. Larsson, J. Am. Chem. Soc. **103**, 4034 (1981).
[13]D. S. Saxon and R. A. Hunter, Philips Res. Rep. **4**, 81 (1949).
[14]C. Kittel, *Introduction to Solid State Physics*, 5th ed. (Wiley, New York, 1976).
[15]F. Kuliasko, Physica **30**, 2180, 2185 (1964).
[16]J. M. Ziman, *Theory of Solids*, 2nd ed. (Cambridge University, New York, 1979), Sec. 3.7.
[17]S. S. Isied and A. Vassilian, J. Am. Chem. Soc. **106**, 1732 (1984).
[18]D. E. Richardson and H. Taube, J. Am. Chem. Soc. **105**, 40 (1983).
[19]D. E. Richardson and H. Taube, Coord. Chem. Rev. **60**, 107 (1984).
[20]M. N. Paddon-Row, Acc. Chem. Res. **15**, 245 (1982).
[21]V. Balaji, K. D. Jordan, P. D. Burrow, M. N. Paddon-Row, and H. K. Patney, J. Am. Chem. Soc. **104**, 6849 (1982).
[22]A. D. Joran, B. A. Leland, G. G. Geller, J. J. Hopfield, and P. B. Dervan, J. Am. Chem. Soc. **106**, 6090 (1984).
[23]J. R. Miller, J. V. Beitz, and R. K. Huddleston, J. Am. Chem. Soc. **106**, 5057 (1984).
[24]J. R. Miller and J. V. Beitz, J. Chem. Phys. **74**, 6746 (1981).
[25]H. M. McConnell, J. Chem. Phys. **35**, 508 (1961).
[26]D. N. Beratan, Thesis, California Institute of Technology, 1986.

III.3 Molecular Bridge Effects on Distant Charge Tunneling

to be submitted

José Nelson Onuchic[a]

Division of Chemistry and Chemical Engineering[b]

California Institute of Technology

Pasadena, CA 91125

and

David N. Beratan

Jet Propulsion Laboratory

California Institute of Technology

Pasadena, CA 91109

---

[a] on leave of absence from the Instituto de Física e Química de São Carlos, Universidade de São Paulo, 13560, São Carlos, SP, Brazil

[b] Contribution No. 7546

Abstract

Why should different hydrocarbon bridges give different electron transfer rates? We answer this question based on energetic and topological (interference) effects that can be gleaned from one-electron models. A discussion of model compound electron transfer rates based on this interpretation is given. The approximations implicit in the periodic models used here (and in previous work) are carefully justified.

I. Introduction

In previous studies, we presented predictions for the tunneling matrix element dependence on donor, acceptor, and bridge energetics and topology for several linkers[1]. We also distinguished the nature and importance of through-bond vs. through-space pathways for some model potentials[2]. Here we simplify and unify the results for tunneling through organic linkers. We begin by discussing considerable simplifications that arise when charge mediation by either the bonding (valence) or the antibonding (conduction) states dominates the donor-acceptor interaction. We discuss the validity of the periodic, weak coupling, and small "back-scattering" approximations. Next, we compare tunneling matrix elements for several linkers and show, analytically, how topological effects in cyclic bridges can enhance or decrease the matrix element. Both constructive and destructive interference effects are found to be important. An understanding of how these effects influence the distance decay of the matrix element for different organic donor-acceptor bridges of current experimental interest is the main goal of this paper. (Recall that the rate is proportional to the square of the matrix element in the non-adiabatic limit[3].) We also discuss the predictions of Hush[4] and Schipper[5], that electron transfer matrix elements decay in a polynomial rather than in an exponential fashion with distance.

The goal of this work is to show why different hydrocarbon bridges are expected to give different electron transfer rates even for the same donors, acceptors, and transfer distance. A consistent method is given to predict the efficiency of different bridges for mediating the donor-acceptor interaction. This

method is given in a simple enough form so that it can be directly applied by experimentalists when considering target bridging molecules and it is also of use for understanding electron transfer rates in existing model compounds. It may also be useful for designing new molecules with novel applications to microelectronics [6]

II. One band model for bond mediated electron tunneling

In the first part of this section we show how the electron transfer rate dependence on distance for a linear alkane bridge can be described with a one orbital per bond model. This description permits a clearer understanding of the terms electron and hole transfer. It also identifies the contributions of different "tunneling pathways" to the tunneling matrix element.

Let us represent an alkane chain by a set of $sp^{(3)}$ orbitals. Orbitals on the same carbon atom have an interaction γ, and orbitals in the same bond have an interaction β. For simplicity we neglect the C–H bonds in this section. For realistic parameters, $|\beta| \gg |\gamma|$. Thus, if the donor is coupled to an n–alkane with with $2N$ carbon atoms, the Hamiltonian is

$$H_D = \Delta_D a_D^\dagger a_D + \beta_D(a_D^\dagger a_1 + a_1^\dagger a_D) + \sum_{i=1}^{N} \gamma(a_{2i-1}^\dagger a_{2i} + a_{2i}^\dagger a_{2i-1}) + \sum_{i=1}^{N-1} \beta(a_{2i}^\dagger a_{2i+1} + a_{2i+1}^\dagger a_{2i}) \; . \tag{2.1}$$

The zero of the energy scale is chosen so that $\alpha_{sp^{(3)}} = 0$. Also, β and γ are defined as negative quantities in the usual Hückel convention, which follows from the assumption that the basis functions all have the same phase[7].

The above Hamiltonian employs a one–electron model. Discussions of the reasons that this approximation works for the electron transfer problem have been given by several authors[8,9]. Because we are working in the weak coupling limit (donor-bridge and bridge-bridge orbital interactions are "small"), many electron effects are expected to be unimportant. Assuming that orbitals in the bridge can be represented well in the tight binding limit[2], the one electron wave function is a good approximation for the donor and acceptor states far from

the nuclei. This is because the electrons of the bridge are closed shell "core" electrons[8]. Electron correlation strongly affects the orbital energies, but the hopping matrix element between bridge sites is basically a one electron matrix element. A similar argument has been given for the electron exchange process in aqueous $Fe^{2+} - Fe^{3+}$.[9]

If the alkane chain were infinite, we could use Bloch conditions and write the donor wave function at bonding orbital k as

$$\Phi_k^D = \epsilon^k \left(a\phi_{2k} + b\phi_{2k+1}\right) \quad . \tag{2.2}$$

Here ϕ_k is the orbital wave function of the k-th $sp^{(3)}$ orbital. The ϵ^k term arises from the translational symmetry.

We now calculate the donor localized state of Hamiltonian 2.1 for $N \to \infty$. The system of equations to solve is then

$$\begin{pmatrix} 0 & \beta + \gamma/\epsilon \\ \beta + \gamma\epsilon & 0 \end{pmatrix} \begin{pmatrix} a \\ b \end{pmatrix} = E \begin{pmatrix} a \\ b \end{pmatrix} \quad , \tag{2.3}$$

where E is the energy of the donor state. If the donor interacts weakly with the chain, then $E \approx \Delta_D$ for the localized state. This approximation is reasonable, and its validity is discussed later in this section. The equation above gives

$$\epsilon + \frac{1}{\epsilon} = \frac{E^2 - \gamma^2 - \beta^2}{\gamma\beta} \quad . \tag{2.4}$$

In the case of an alkane chain, $|\beta| \gg |\gamma|$. If we had an infinite chain of alkane (without the donor), the solution of Eq. 2.4 would lead to two bands: one with energy states between $\beta + \gamma$ and $\beta - \gamma$, and the other, between $-(\beta - \gamma)$ and $-(\beta + \gamma)$. The first band is composed of the bonding states of the chain and is called the valence band, and the second one is composed of the anti-bonding states and is called the conduction band. The donor state interacts mainly

with the band which is energetically closer to it. From Eq. 2.4, we see that any state in the band gap ($|E| < |\beta|$) has a negative value for ϵ. Because the gap between the two bands is large (about 10 eV), one band generally dominates the interaction. In most of the systems discussed in the next section, the energy level of the transfer electron is near the valence band. Now we show how to formally neglect the effect of the energetically distant band and include only the donor interaction with the closest one.

Assume that the donor state energy E is close to the valence band. Then, E is negative and $|E-\beta|, |\gamma| \ll |\beta|$. Because the donor state is in the band gap (localized), $|E-\beta| > |\gamma|$. Using the approximations above, Eq. 2.4 can be rewritten as

$$\epsilon + \frac{1}{\epsilon} \simeq \frac{2(E-\beta)\beta}{\gamma\beta} \simeq \frac{E-\beta}{\gamma/2} \ . \tag{2.5}$$

Eq. 2.5 is exactly the result we would get from a one orbital per site chain model with the Hamiltonian

$$H_D = \Delta_D a_D^\dagger a_D + \beta_D(a_D^\dagger a_1 + a_1^\dagger a_D) + \sum_{i=1}^{N} \beta a_i^\dagger a_i + \sum_{i=1}^{N-1} \gamma/2(a_i^\dagger a_{i+1} + a_{i+1}^\dagger a_i) \ . \tag{2.6}$$

This Hamiltonian represents a chain of orbitals with self–energy β and nearest neighbor interaction $\gamma/2$. Now the "orbitals" represent the C–C bonding orbitals rather than the carbon atomic (hybrid) orbitals. This is equivalent to saying that the donor interacts with a chain of bonding orbitals of self-energy β, which form a band of width 2γ. This approximation neglects the donor interaction with an entire band of states, not individual states within a band. In the appendix we give a comparison of the σ band calculation with the complete calculation for n-alkane.

In order to validate the above discussion we must carefully address two points. The first is that the bridges we are considering are finite, so the infinite chain limit is not exact. The second point is that we assumed that the donor weakly interacts with the chain. As in Eq. 2.2, but for finite N, let us write the (exact) donor wave function for Eq. 2.6 as

$$\Psi_D \;=\; \frac{1}{\mathcal{N}}\left\{\phi_D + \sum_{i=1}^{N}(a\epsilon^i + b\epsilon^{N+1-i})\phi_i\right\} \quad . \tag{2.7}$$

where $\mathcal{N}$ is the normalization factor. Here ϕ_j is the j-th bond orbital. Also, for reasons of simplification, we fix the zero of the energy scale in the center of the band, and define $\gamma' = \gamma/2$. This form for the wave function is completely general as long as the finite bridge is periodic except at its edges. Multiplying $H_D\ \Psi_D = E_D\ \Psi_D$ by ϕ_j^*, and integrating we have

$$< D| : \quad \beta_D\ (a\epsilon + b\epsilon^N) = (E - \Delta_D) \tag{2.8a}$$

$$< 1| : \quad \beta_D + (a\epsilon^2 + b\epsilon^{N-1})\gamma' = E(a\epsilon + b\epsilon^N) \tag{2.8b}$$

$$< i| : \quad (a\epsilon^{i-1} + b\epsilon^{N-i+2})\gamma' + (a\epsilon^{i+1} + b\epsilon^{N-i})\gamma' \;=$$

$$= \; E(a\epsilon^i + b\epsilon^{N-i+1}) \;\text{ for }\; i = 2, N-1 \tag{2.8c}$$

$$< N| : \; (a\epsilon^{N-1} + b\epsilon^2)\gamma' = E(a\epsilon^N + b\epsilon) \quad . \tag{2.8d}$$

From Eq. 2.8c, we obtain the same $E - \epsilon$ relation that we found for the infinite bridge,

$$\epsilon + \frac{1}{\epsilon} \;=\; \frac{E}{\gamma'} \quad . \tag{2.9}$$

Combining Eq. 2.8d and 2.9,

$$\frac{a}{b} \;=\; -\frac{1}{\epsilon^{N+1}} \quad . \tag{2.10}$$

From Eq. 2.10, we see that the coefficient multiplying ϕ_j in Ψ_D is

$$C_j = a\epsilon^j + b\epsilon^{N-j+1} = a\epsilon^j\left(1 - \frac{\epsilon^{2N+2}}{\epsilon^{2j}}\right) . \tag{2.11}$$

From Eq. 2.11 we obtain two conclusions. First, the infinite chain approximation becomes worse near the ends of the chain. Second, the terminal orbital coefficient, C_N, is always equal to the infinite chain result, $a\epsilon^N$, multiplied by $1-\epsilon^2$, independent of N (a is chain length independent in the weak coupling limit, discussed below). Thus, if we link an acceptor to the N^{th} bridge unit, the amplitude of the matrix element is proportional to $(1-\epsilon^2)\epsilon^N$, and therefore shows a distance dependence proportional to ϵ^N. Also, if $\epsilon^2 \ll 1$ (i.e., $1-(\epsilon^{2N+2}/\epsilon^{2j}) \approx 1$ for all j) we can neglect backscattering between bonds, and the infinite chain result becomes exact for a finite chain. It is important to stress that the $\epsilon^2 \ll 1$ condition is not necessary to guarantee a chain length dependence of ϵ^N.

Assuming that $\epsilon^N \ll 1$, we obtain from Eq. 2.8b that

$$a\epsilon = \frac{\beta_D}{E - \epsilon\gamma'} \approx \frac{\beta_D}{E} . \tag{2.12}$$

Substituting Eq. 2.12 into Eq. 2.8a

$$E = \Delta_D + \frac{\beta_D^2}{E} . \tag{2.13}$$

Therefore we can assume $E \approx \Delta_D$ as long as $\beta_D^2 \ll \Delta_D^2$. (Recall that Δ_D is the energy of the donor orbital relative to the center of the band.)

The normalization factor of Eq. 2.7 is

$$\mathcal{N}^2 = 1 + \sum_{j=1}^{N} |C_j|^2 . \tag{2.14}$$

In the weak coupling limit, if $\beta_D \ll E$, then $a\epsilon \ll 1$, so $\mathcal{N}^2 \approx 1$. In this limit, the normalization constant is chain length independent.

From Eq. 2.11, we see that if $\epsilon^2 \ll 1$, we can neglect backscattering and the wave function can be described as decaying by the factor γ'/E per bond (orbital). Because γ' is negative and E is positive for hole tunneling, the ratio γ'/E is always negative, and the sign of this ratio is important for interference effects between tunneling pathways, discussed in Sec.III. For electron rather than hole tunneling, the signs of both parameters are reversed and the ratio is still negative. More generally, if we have a chain with varying orbitals where the periodic condition is not necessarily applicable, we can define a decay per bond of

$$\epsilon(\text{bond i}) = \frac{\gamma_{i,i-1}}{E - \alpha_i} \quad , \tag{2.15}$$

where $\gamma_{i,i-1}$ is the exchange interaction between orbitals (bonds) i and $i-1$, α_i is the bond orbital energy, and E is the energy of the tunneling electron. This approximation has been discussed for electron tunneling through protein backbones.[1c]

For non-linear (cyclic) bridges, the results obtained by neglecting "backscattering" agree with the exact result for the leading term in powers of γ/E. However, in such systems other corrections, besides backscattering, appear. They are basically constructive interference of pathways of same length, or destructive interference of pathways whose lengths differ by one bond. This is shown in Section III and in the appendix.

III. Topological effects on valence band tunneling through hydrocarbon linkers

For a qualitative treatment of bridge mediated electron tunneling through hydrocarbons, the basis set of bonding orbitals (hole tunneling) or antibonding orbitals (electron tunneling) is a reasonable approximation. To include all of the states (bonding and antibonding) in the calculation is entirely possible. However, it would not permit a transparent comparison of the results (especially sources of interference) for different bridging groups – the main goal of this section. As discussed in Section II, this approximation is appropriate for saturated hydrocarbons because the bonding–anti-bonding energy gap ($2\beta \sim 17\ eV$) is much larger than the energetic distance between the tunneling electron and the center of the relevant band ($< 5eV$). In this section we include the CH bonds in our Hamiltonians because their influence on the matrix elements is comparable to many topological effects (e.g., those arising from having cyclic rather than linear bridges) as shown later in this section.

We begin this section by listing the exact $E - \epsilon$ relations for some real and imagined hydrocarbon chains. We then show that the leading terms in the relation can be identified with the tunneling pathways in the bridge. The negative sign of γ/E leads to interference between connected pathways differing in length by one bond. For this reason, edge-fused hydrocarbon states of symmetry that minimize side routes are particularly important for charge mediation. A comparison of matrix element decay with distance is made for a chain composed of cyclic hydrocarbons fused on an edge vs. those fused at an atom.

For the following systems we define the decay per unit cell or bond as ϵ or ϵ'. The value of γ used in this section is 1/2 of the valence band width discussed in Sec. 2. When discussing the parity of the bridge states one should recall that the states contribute to the tunneling matrix element only if the donor and acceptor are of the proper symmetry to mix with them (i.e., β_D and $\beta_A \neq 0$).

A. Linear alkane[1b]

The simplest molecular model for extended n-alkane is composed of one CC bond and two CH bonds per "unit cell" (see Figure 1). In this case

$$\epsilon + \frac{1}{\epsilon} = \frac{E}{\gamma}\left[\frac{1+\{4\gamma^2/[E(\alpha+\gamma-E)]\}}{1-\{2\gamma/[\alpha+\gamma-E]\}}\right]. \qquad (3.1a)$$

This was obtained by expanding the determinate that relates E to ϵ

$$det\begin{pmatrix} \gamma/\epsilon+\gamma\epsilon-E & 2\gamma/\epsilon+2\gamma \\ \gamma+\gamma\epsilon & \alpha+\gamma-E \end{pmatrix} = 0. \qquad (3.1b)$$

Figure 2 shows E vs. ϵ in the gap (above the band) for this linker ($\gamma = -1.1$, and α, the CH bond energy relative to the CC bond energy, is -.5 eV). Solving Eq. 3.1b for $\epsilon + 1/\epsilon$ and expanding the quotient for small γ,

$$\epsilon + \frac{1}{\epsilon} = \frac{E}{\gamma}\left[1 - \frac{2\gamma}{E-\alpha} + \cdots\right]. \qquad (3.1c)$$

Since $-2\gamma/(E-\alpha)$ is positive, $|\epsilon|$ is decreased due to the CH bonds (recall that without any CH bonds, $\epsilon + 1/\epsilon = E/\gamma$). This correction can be attributed to amplitude that has made a single excursion into the two CH bonds interfering with amplitude that has propagated directly along the CC backbone. Higher

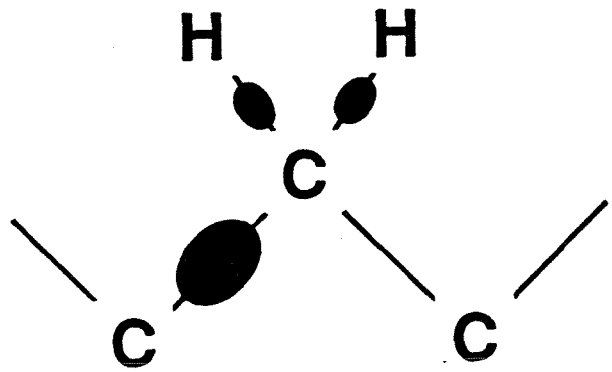

Figure 1 – The repeating unit orbital for the valence band of n–alkane is shown ($|\epsilon|$).

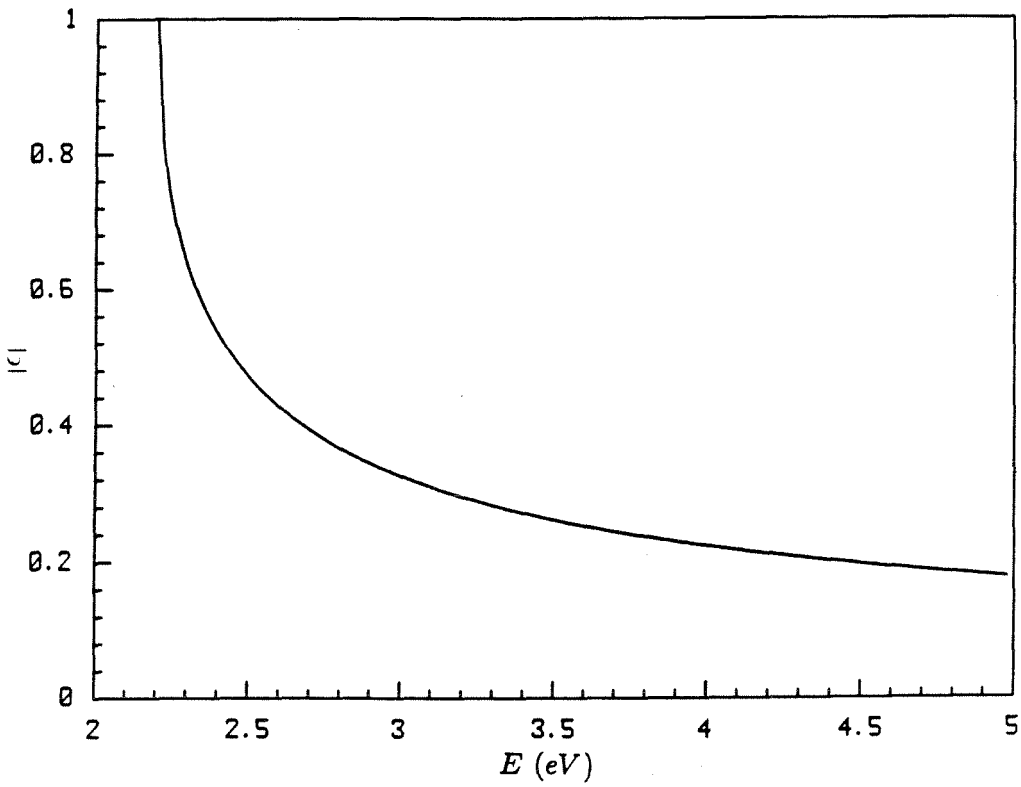

Figure 2 – Decay per repeating unit (per CC bond) in n–alkane is shown. The energies shown are tunneling energies above the band. The zero of the energy scale is the CC sigma bond energy.

order terms in the expansion can be connected with more convoluted tunneling pathways. This destructive interference is a general effect, in hydrocarbons, of bonds adjacent to the tunneling pathway.

Far from the band ($|E|$ large), the destructive interference is unimportant. Recall that we can not use these models for tunneling energies so far from the valence band that mediation by other bands becomes important. The presence of CH or other bonds with energy lower than that of CC bonds decreases hole tunneling, i.e. decrease $|\epsilon|$ (wave function decay becomes more rapid).

To illustrate further complications that arise from geometric effects of the linker, we consider chains with four member rings. These chains have pedagogical value as well as relevance to bridges described in Refs. 10 and 12. We then consider six member rings of current experimental relevance, namely, fused norbornanes and fused cyclohexanes.

B. Poly(edge-fused cyclobutane)

For the even states (Figure 3a) we find

$$\epsilon + \frac{1}{\epsilon} = \frac{E}{\gamma}\left[\frac{(\alpha - E)(1 - \frac{2\gamma}{E}) + \frac{4\gamma^2}{E}}{(\alpha - E) - \gamma}\right], \tag{3.2a}$$

and for small γ,

$$\epsilon + \frac{1}{\epsilon} = \frac{E}{\gamma}\left[1 - \frac{2\gamma}{E} - \frac{\gamma}{E - \alpha} + \cdots\right]. \tag{3.2b}$$

Interference arises from the CC bond connecting the two parallel sigma pathways as well as from the CH bond. For the odd states (Figure 3b) of the valence band, however,

$$\epsilon + \frac{1}{\epsilon} = \frac{E}{\gamma}\left[\frac{(\alpha - E) + \left(\frac{2\gamma^2}{E}\right)}{(\alpha - E) - \gamma}\right] \tag{3.3a}$$

a)

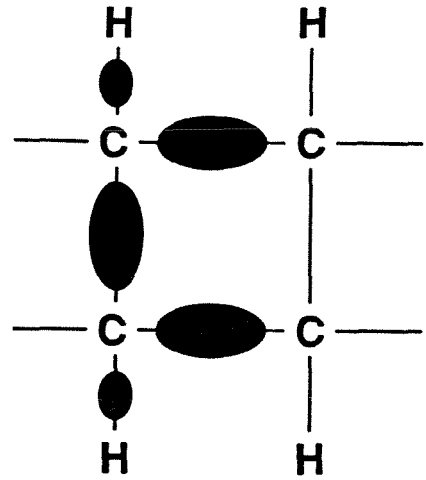

b)

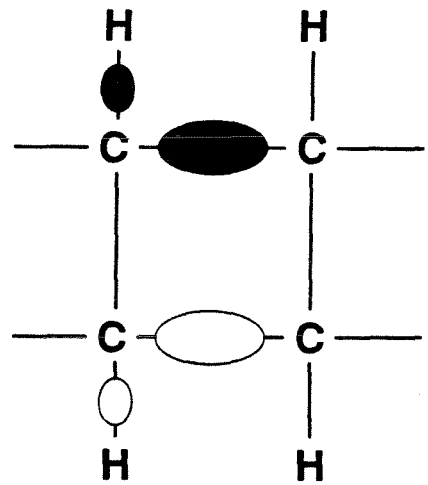

Figure 3 – (a) Same as Figure 1 for the even states of edge–fused cyclobutane; (b) same as (a) for the odd states.

and for small γ,

$$\epsilon + \frac{1}{\epsilon} = \frac{E}{\gamma}\left[1 - \frac{\gamma}{E-\alpha} + \cdots\right] \quad . \tag{3.3b}$$

In this case, interference arises only from the CH bonds because there is no interaction between the parallel σ bonding pathways. Figure 4 shows the $E-\epsilon$ relation for the even and odd states of this unit cell.

C. Poly(spirocyclobutane)[1b,10]

To illustrate the difference between edge and corner-fused cyclic alkanes, we now consider spirocyclobutanes. There are two CC bonds per unit cell and two convergent pathways for tunneling. One finds for the even states (Figure 5)

$$\epsilon + \frac{1}{\epsilon} = \frac{(\gamma-E)^3 - 9\gamma^2(\gamma-E) + \alpha(\gamma-E)^2 + 4\gamma^3 - 5\alpha\gamma^2}{2\gamma^2(\gamma-E) + 2\gamma^2\alpha - 4\gamma^3} \quad . \tag{3.4a}$$

This equation was used to plot the $E-\epsilon$ relation in Figure 6. Expanding this for small γ:

$$\epsilon + \frac{1}{\epsilon} = \frac{1}{2}\left(\frac{E}{\gamma}\right)^2\left[1 - \frac{2\gamma}{E} - \frac{2\gamma}{E-\alpha} + \cdots\right] \quad . \tag{3.4b}$$

The convergent pathways give a prefactor of 2 in the decay per unit cell, which enhances tunneling. Destructive interference arises from the CH bonds and the interactions between bonds to the quaternary carbon atoms. Far from the band, the factor of two dominates, and wave function propagation per CC bond is $\sqrt{2}$ times as efficient as in n-alkane. However, near the band edge, the extra destructive interference at the quaternary carbon is significant, and the full $\sqrt{2}$ enhancement relative to n-alkane is not realized.

From the equations for this and other unit cells we see that the valence band is split into a few closely lying bands. The one band approximation

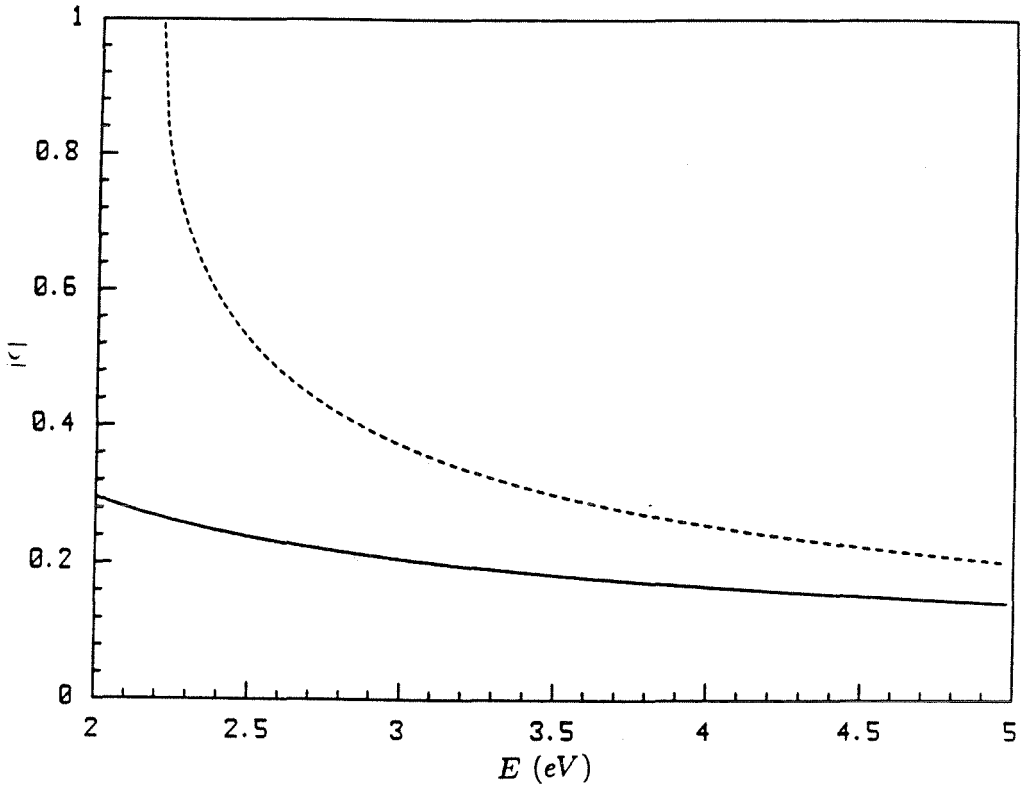

Figure 4 – Same as Figure 2 for edge–fused cyclobutane. The solid (dashed) line shows the decay for the odd (even) states.

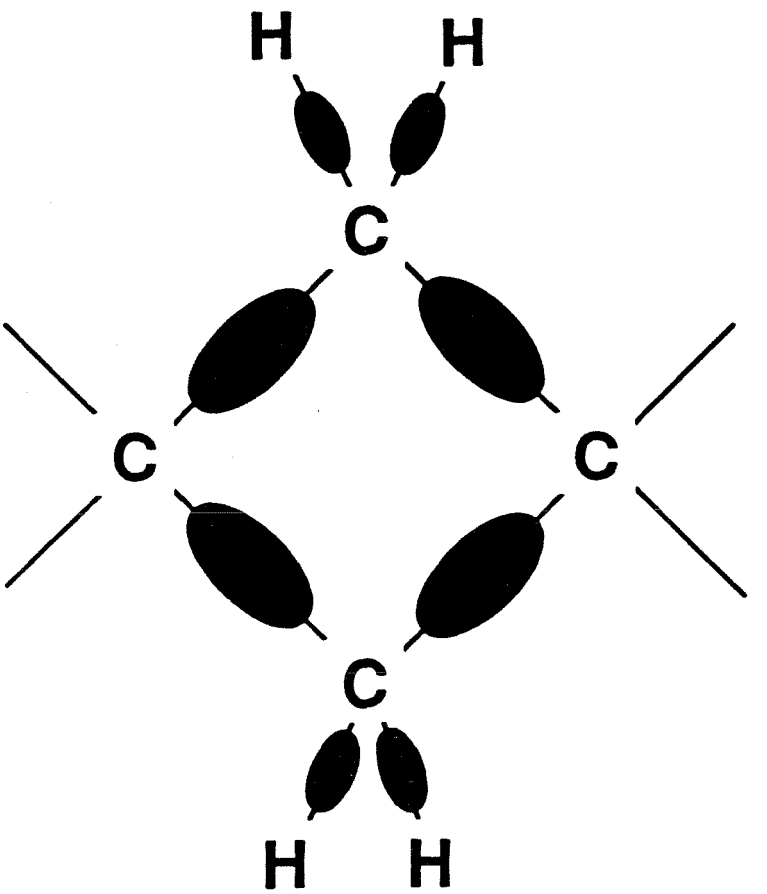

Figure 5 – Same as Figure 1 for the even states of spirocyclobutane.

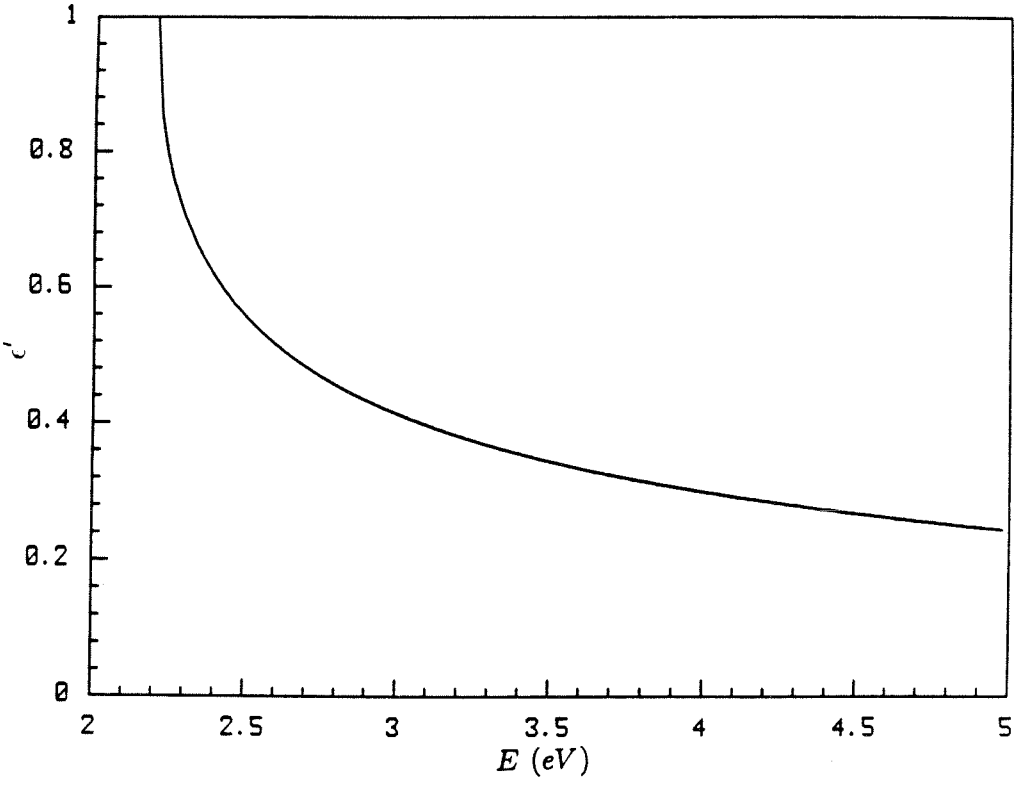

Figure 6 – Same as Figure 2 for spirocyclobutane (even states). In all the following molecules there are two CC bonds per repeating unit. The decay per bond is shown ($\epsilon' = \sqrt{|\epsilon|}$).

discussed in the previous section cannot be applied further to these bands because the gaps are smaller than the energetic distance of the transfer state to the bands. The sole inclusion of CC σ bonds, however, remains valid and is discussed further in the appendix. The bridge states odd with respect to either mirror plane of spirocyclobutane, give zero contribution to electron tunneling due to the molecular symmetry.[1b]

D. Poly(edge-fused cyclohexane)

A model for the steroidal and cyclohexyl donor-accepter linkers of Closs and co-workers[11] is a chain of edge-fused cyclohexane rings (Figure 7). As in the edge-fused cyclobutanes, the leading term in the $\epsilon + 1/\epsilon$ equation is E/γ raised to the power of the number of bonds in the unit cell along the most direct tunneling route. The next higher order terms arise from the destructive interference due to the CH bonds and the one bond connection between the two parallel direct tunneling routes. The $2\gamma/E$ factor arises from destructive interference between amplitude propagating along the edge of the molecule with that propagating between the two edge pathways (for even bridge states). For the even states, we solved (Figure 8)

$$det \begin{pmatrix} \alpha - E & \gamma & \gamma & 0 & \gamma/E \\ 2\gamma & -E & 2\gamma & 0 & 2\gamma/\epsilon \\ \gamma & \gamma & -E & 2\gamma & \gamma/\epsilon + \gamma \\ 0 & 0 & \gamma & \gamma + \alpha - E & \gamma \\ \gamma\epsilon & \gamma\epsilon & \gamma + \gamma\epsilon & 2\gamma & -E \end{pmatrix} = 0 \quad . \tag{3.5a}$$

Also, for small γ (even states),

$$\epsilon + \frac{1}{\epsilon} = \left[\frac{E}{\gamma}\right]^2 \left(1 - \frac{3\gamma}{E - \alpha} - \frac{2\gamma}{E} + \cdots\right) \quad . \tag{3.5b}$$

a)

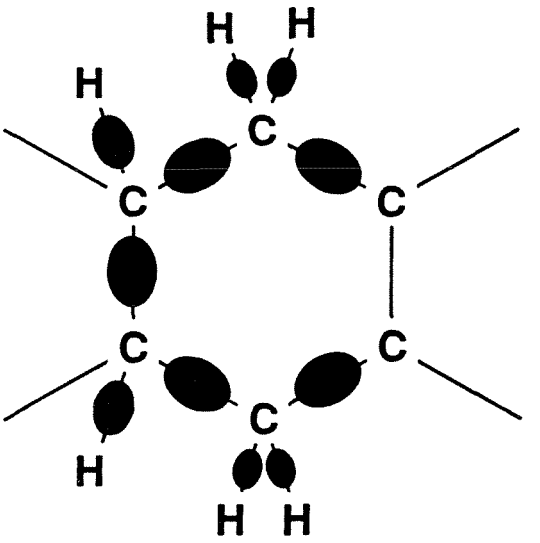

b)

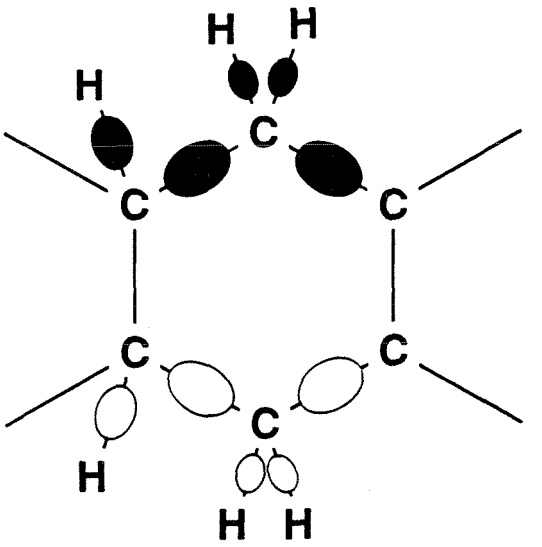

Figure 7 – Same as Figure 3 for edge–fused cyclohexane.

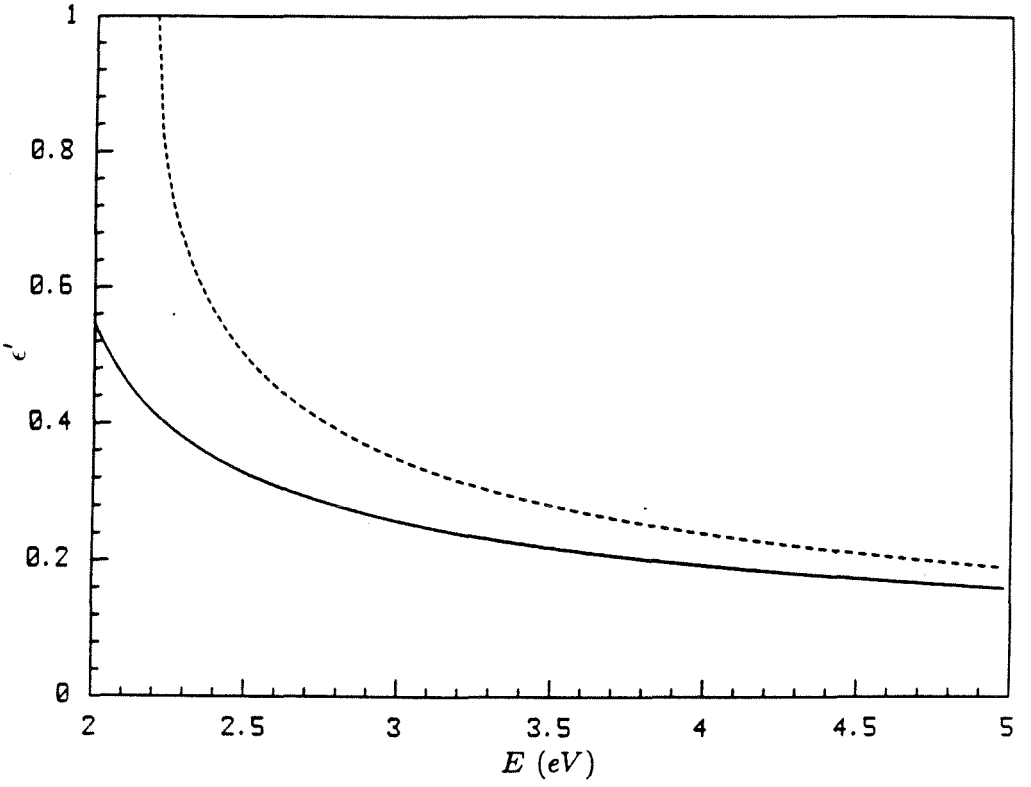

Figure 8 – Same as Figure 4 for edge–fused cyclohexane.

For the odd states, the decay per unit cell is given by (Figure 8)

$$det \begin{pmatrix} -E & \gamma/\epsilon+\gamma & 2\gamma & \gamma/\epsilon \\ \gamma\epsilon+\gamma & -E & 2\gamma & \gamma \\ \gamma & \gamma & \alpha+\gamma-E & 0 \\ \gamma\epsilon & \gamma & 0 & \alpha-E \end{pmatrix} = 0 \quad . \tag{3.6a}$$

For these odd states, the bridge functions as two independent n-alkane chains with one less CH bond every other carbon atom. For small γ,

$$\epsilon + \frac{1}{\epsilon} = \left[\frac{E}{\gamma}\right]^2 \left(1 - \frac{3\gamma}{E-\alpha} + \cdots\right) \quad . \tag{3.6b}$$

E. Poly(norbornane)[12]

In this case (shown in Figure 9), a model for the linkers of Verhoeven and co-workers, the propagation is similar to that through fused cyclohexane. The differences arise (to first order) from the presence of two CC bonds in the place of two CH bonds in the unit cell.

For the even states (Figure 10),

$$det \begin{pmatrix} -E & 2\gamma & 2\gamma & 0 & 0 & 2\gamma/\epsilon & 0 \\ \gamma & \alpha-E & \gamma & 0 & 0 & \gamma/\epsilon & 0 \\ \gamma & \gamma & -E & \gamma & \gamma & \gamma+\gamma/\epsilon & 0 \\ 0 & 0 & \gamma & \alpha-E & \gamma & \gamma & 0 \\ 0 & 0 & \gamma & \gamma & \gamma-E & \gamma & 2\gamma \\ \gamma\epsilon & \gamma\epsilon & \gamma+\gamma\epsilon & \gamma & \gamma & -E & 0 \\ 0 & 0 & 0 & 0 & 2\gamma & 0 & \gamma+\alpha-E \end{pmatrix} = 0 \tag{3.7a}$$

and

$$\epsilon + \frac{1}{\epsilon} = \left[\frac{E}{\gamma}\right]^2 \left(1 - \frac{2\gamma}{E-\alpha} - 3\frac{\gamma}{E} + \cdots\right) \quad . \tag{3.7b}$$

For the odd states (Figure 10),

$$det \begin{pmatrix} \alpha-E & \gamma & 0 & 0 & \gamma/\epsilon \\ \gamma & -E & \gamma & \gamma & \gamma+\gamma/\epsilon \\ 0 & \gamma & \alpha-E & \gamma & \gamma \\ 0 & \gamma & \gamma & -\gamma-E & \gamma \\ \gamma\epsilon & \gamma+\gamma\epsilon & \gamma & \gamma & -E \end{pmatrix} = 0 \tag{3.8a}$$

a)

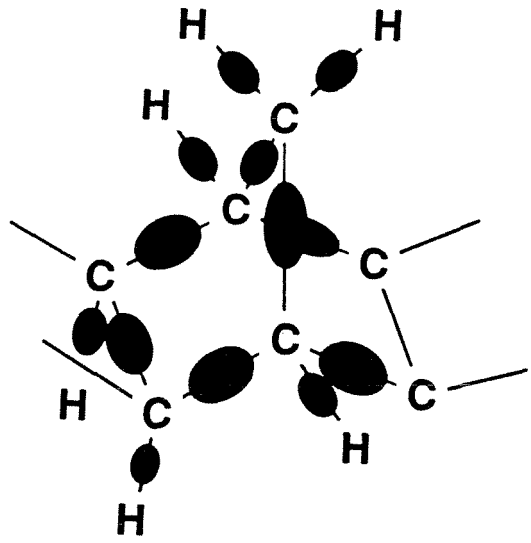

b)

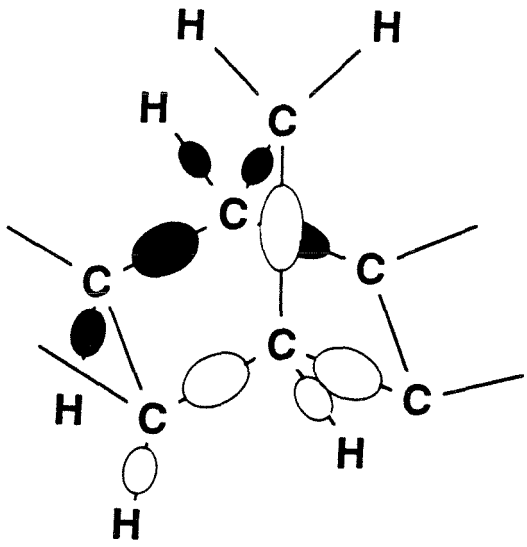

Figure 9 – Same as Figure 3 for norbornane.

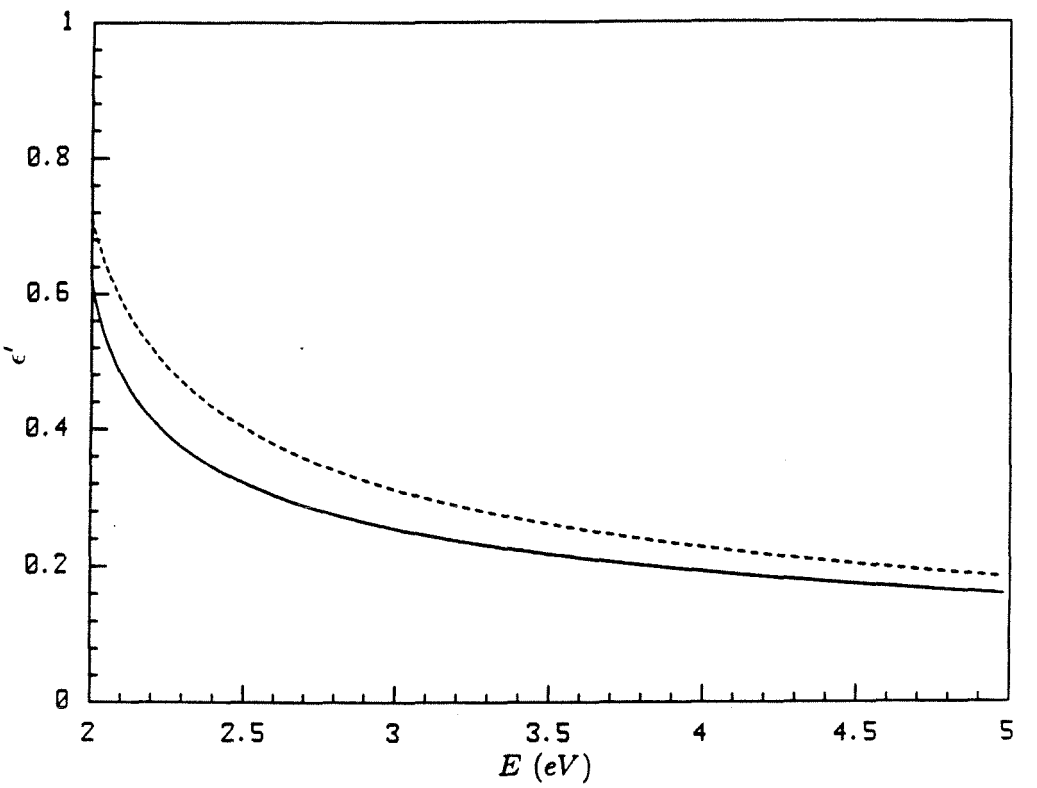

Figure 10 – Same as Figure 4 for norbornane.

and

$$\epsilon + \frac{1}{\epsilon} = \left[\frac{E}{\gamma}\right]^2 \left(1 - \frac{2\gamma}{E-\alpha} - \frac{\gamma}{E} + \cdots\right) \quad . \tag{3.8b}$$

As in the case of fused cyclohexanes, the odd states assist electron transport more than the even ones due to the absence of destructive interference from the bond common to adjacent rings. The presence of the CC bond in place of the CH bond compared to cyclohexane decreases the electron propagation.

We now discuss the simple interpretation of the above results. Let us assume that the shortest pathway in the unit cell is composed of x CC bonds. If we neglect pathways with more than x bonds, the decay can be written as

$$\epsilon + \frac{1}{\epsilon} = \frac{1}{P}(\gamma/E)^x \quad , \tag{3.9a}$$

where P is the number of convergent pathways in the unit cell. This factor P enhances the rate due to constructive interference of multiple pathways of x bonds. The next correction we can include in Eq. 3.9a arises from the destructive interference of pathways of length x with those of length $x+1$. To this order of correction, the decay can be written

$$\epsilon + \frac{1}{\epsilon} = \frac{1}{P}(\gamma/E)^x \left[1 - \sum_i \gamma/(E-\alpha_i)\right] \quad , \tag{3.9b}$$

where the sum on i extends over the extra bond of all $x+1$ bond pathway. α_i is zero if this extra bond is CC and -0.5 eV if it is CH. Eq. 3.9b yields exactly the first order expansions presented in this section up to this point.

It is important to recall that these corrections arise from the several possible tunneling pathways, not from backscattering. As discussed in Sec. II, the backscattering corrections for periodic systems are the corrections to the approximation $\epsilon + 1/\epsilon \approx 1/\epsilon$.

The leading terms in the expansions for small γ may not be adequate for calculating ϵ in some experimentally important cases because γ/E need not be small compared to one, and prefactors of these and higher-order terms may need to be included. However, they give a qualitative indication of which bridges are more favorable for mediating electron transfer at a given tunneling energy. The discussion to first order about constructive and destructive interference can be generalized. Pathways that differ by an odd number of bonds interfere destructively, but those that differ by an even number of bonds interfere constructively. Convergent tunneling routes such as those in spirocyclobutane give $\epsilon + 1/\epsilon$ a prefactor equal to the number of these routes. Parallel pathways joined occasionally, such as in edge-fused cyclohexane or cyclobutane, introduce destructive interference due to pathways one bond longer than the "main" path. For σ band tunneling, the odd states in edge-fused molecules assist tunneling more than the even states. For electron tunneling through the anti-bonding bands, the reverse is true (even states assist tunneling more than odd states).

IV. Discussion

We have seen that different destructive and/or constructive interference for different bridges leads to different matrix elements. Because of destructive interference, odd (even) states for edge–fused single ring hydrocarbons have a slower (faster) decay than n–alkane. Norbornane, due to the additional CC bridging bonds, is the least favorable bridge considered within a few eV of the band. Donor and acceptor states may mix with both even and odd bridge states. At large transfer distances, the wave–function amplitude will be dominatated by the odd symmetry bridge states. Constructive interference is important in spiro–cyclic alkanes, and it will always slow the matrix element decay with distance.

Figure 11 shows the energy dependence of the average wave function decay per bond for the linkers discussed in the previous section (odd symmetry states). Normal donors and acceptors lie a few eV from the band edge. At these energies the relative mediation efficiencies can be understood from the interference effects described in the previous section. The constructive interference in spirocyclobutane makes it the most effective hydrocarbon charge mediator that we have considered.

Experimental results show that the model systems are about 2-4 eV from the band. In order to determine this position more precisely, we need the full ΔG study at all distances. (Experiments at fixed ΔG but with <u>both</u> donor and acceptor energies moved up or down in the absolute sense would be particularly useful.) From these experiments, it will be possible to obtain ϵ as a function of energy and ΔG. This will permit connection of the redox energy

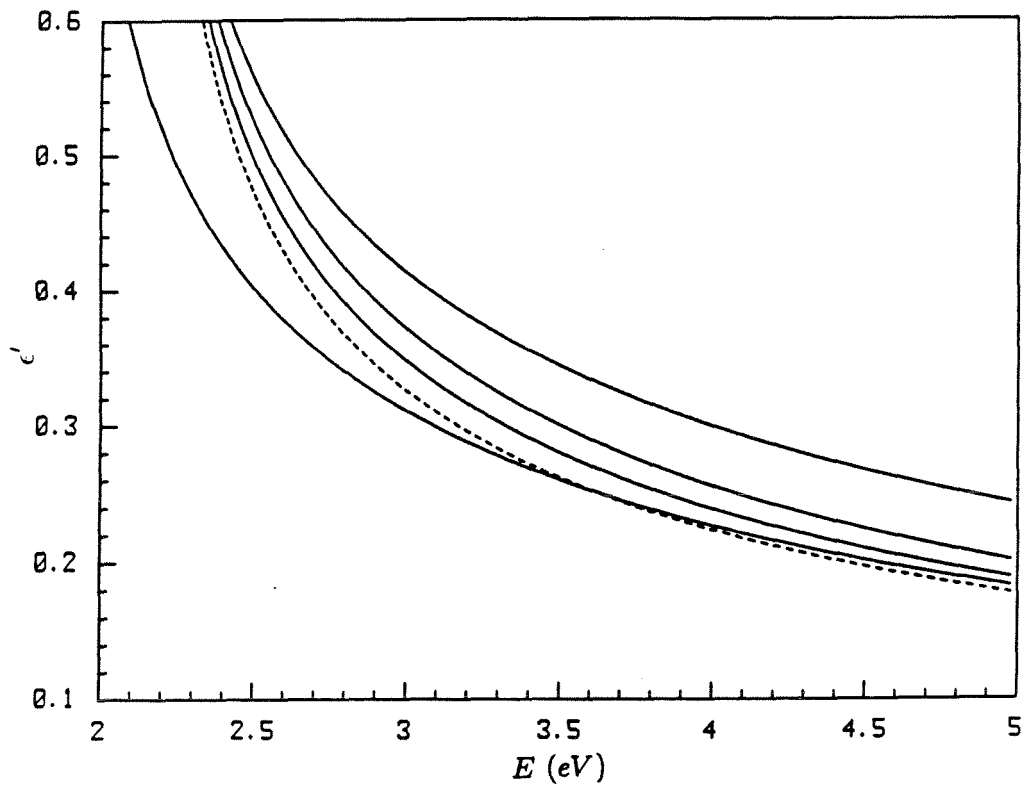

Figure 11 – The decay per bond is shown for n–alkane (dashed lines), for the even states of spirocyclobutane, and for the odd states of all other linkers. The solid curves, from top to bottom, correspond to spirocyclobutane, edge-fused cyclobutane, edge-fused cyclohexane, and edge-fused norbornane.

scale with the energetic distance to the center of the band. For systems where the donor and acceptor are both initially neutral, the importance of the ΔG study is even greater because ΔG is transfer distance dependent (ΔG is smaller for longer transfer distances). This problem appears in the norbornyl model systems (actually, these systems are composed of both edge-fused norbornyl and cyclobutyl groups) of Verhoeven and co-workers.[12] For the recently reported systems of Closs and co-workers[11] (biphenyl radical anion donor, fused cyclohexyl bridges, and napthylene acceptor) we expect the tunneling energy to be about 2.5 eV on our energy scale. This result is preliminary and a real quantitative prediction should include all of the bridge orbitals and will require more experiments.

If a full experimental study as prescribed above were performed, it would permit us to quantify precisely the redox energy scale. Comparison of the results for spirocyclobutane, fused norbornanes, and fused cyclohexanes for fixed donors and acceptors would allow a check of the effectiveness of this calculation. Also, the ΔG/distance study would permit a test of our early prediction that hole tunneling (valence band tunneling) rather than electron (conduction band) tunneling dominates the charge mediation process in hydrocarbons.

Other complex bridges of biological relevance can be studied with similar techniques. They do not necessarily need to be composed of hydrocarbon for this method to be useful. Such an example has been given for electron transfer through a protein backbone.[1c] Indeed, these methods can be extended and applied to aperiodic systems if backscattering can be neglected.[1c]

If the donor is weakly coupled to the bridge, the tunneling matrix element decay is strictly exponential in the number of bridge groups independent of

the size of ϵ. This finding runs counter to claims of Hush[4] and Schipper[5], that matrix element decays such as $1/R^m$ with $m \simeq 3$ are anticipated. Although the origin of the Hush result is unclear, the $1/R^3$ prediction of Schipper arises from faulty analysis of the problem. The wave function amplitude on unmixed bridge orbital j on the N^{th} (terminal) bridge orbital in a one orbital per bridge unit representation is[13]

$$\sqrt{\frac{2}{N+1}} \sin\left(\frac{jN\pi}{N+1}\right). \tag{4.1}$$

Considering electron (rather than hole) transfer through this band, the energetically nearest state is the $j = 1$ state, and as a function of N, the amplitude on the N^{th} site is:

$$C_{1,N} \propto \frac{1}{(N+1)^3}, \text{ as } N \to \infty \ . \tag{4.2}$$

As the chain length increases, the density of states near the band edge changes and one expects very many bridge state to mix with the donor and acceptor. Indeed, we know the exact result in the $N \longrightarrow \infty$ limit[14] for the amplitude of the donor localized wave function at the N^{th} bridge site is

$$C_N \propto \epsilon^{N-1} \ , \tag{4.3a}$$

where

$$\epsilon + \frac{1}{\epsilon} = \frac{E}{\beta}. \tag{4.3b}$$

Hence, in the long chain limit the analytical form for the localized wave function (and hence the tunneling matrix element) decay is a pure exponential. This is the case even if backscattering can not be ignored (ϵ^2 not much smaller than 1), in which case we solve the $E - \epsilon$ quadratic equation exactly. That the decay must be exponential in the long chain limit is known from Bloch's theorem.

The error in the analysis of Schipper is a common problem, which arises from summing incomplete perturbation series. To obtain the exponential decay, the sum over all the N states of the band must be included. It is of interest that neglect of an entire band with energy far from the donor, acceptor, and "relevant" band does not introduce functional errors to the modeling. Indeed, if the interaction parameters are judiciously chosen and the band gaps are large enough, quite satisfactory results can be obtained from one orbital per bond models.

Finally, we emphasize the fundamental energy and orbital symmetry dependence of the tunneling matrix element. Its value depends on the tunneling energy and so, for a given linker, depends on the donor and acceptor energetics and vibronic coupling. Individual calculations of the tunneling splitting can not be used to predict the distance decay of the tunneling matrix element for different donors and acceptors on the same bridge. Sources of both constructive and destructive interference in saturated tunneling bridges can be readily identified. Generally speaking, pathways of equal length converging at a single atom enhance the matrix element more than if these pathways converge at a bond.

Appendix

This appendix shows the validity of the σ band approximation and presents preliminary results for tunneling through unsaturated linkers. First, we show the validity of separating the saturated linker tunneling problem into independent bonding and anti-bonding mediated transport problems. That is, we show that the use of just the bonding CC and CH orbitals reproduces the band structure of the bonding states obtained from the more "complete" calculation, which uses a full set of atomic orbitals and finds both the bonding and anti-bonding bands. Second, we discuss tunneling in unsaturated periodic linkers.

For n-alkane, the full (bonding and anti-bonding) band structure is calculated from the equation

$$det \begin{pmatrix} -E & \gamma+\beta/\epsilon & 2\gamma & 0 \\ \gamma+\beta\epsilon & -E & 2\gamma & 0 \\ \gamma & \gamma & \gamma-E & \beta_{CH} \\ 0 & 0 & \beta_{CH} & \alpha_H-E \end{pmatrix} = 0. \qquad (A1)$$

β_{CH} is the carbon sp^3 orbital exchange interaction with hydrogen and α_H is the diagonal energy of hydrogen relative to carbon sp^3. Figure A1 plots this equation for[1a] $\beta_{CH} = -9.14$ eV, $\beta_{CC} = -8.5$ eV, and $\alpha_H = .35$ eV.[1c] Also shown is a plot of Eq. 3.1a (offset by 8.5 eV).

Para-poly(phenyl) (Figure A2) is a linker of increasing interest.[15,16] It is difficult to obtain quantitative predictions for unsaturated linkers because, in contrast to the saturated linker problem, a consistent set of experiments does not exist on which we can "normalize" ϵ for a given tunneling energy. Also, dynamical effects due to phenyl ring rotation may be significant in systems without locked geometries. For para-poly(phenyl) chains we find for the

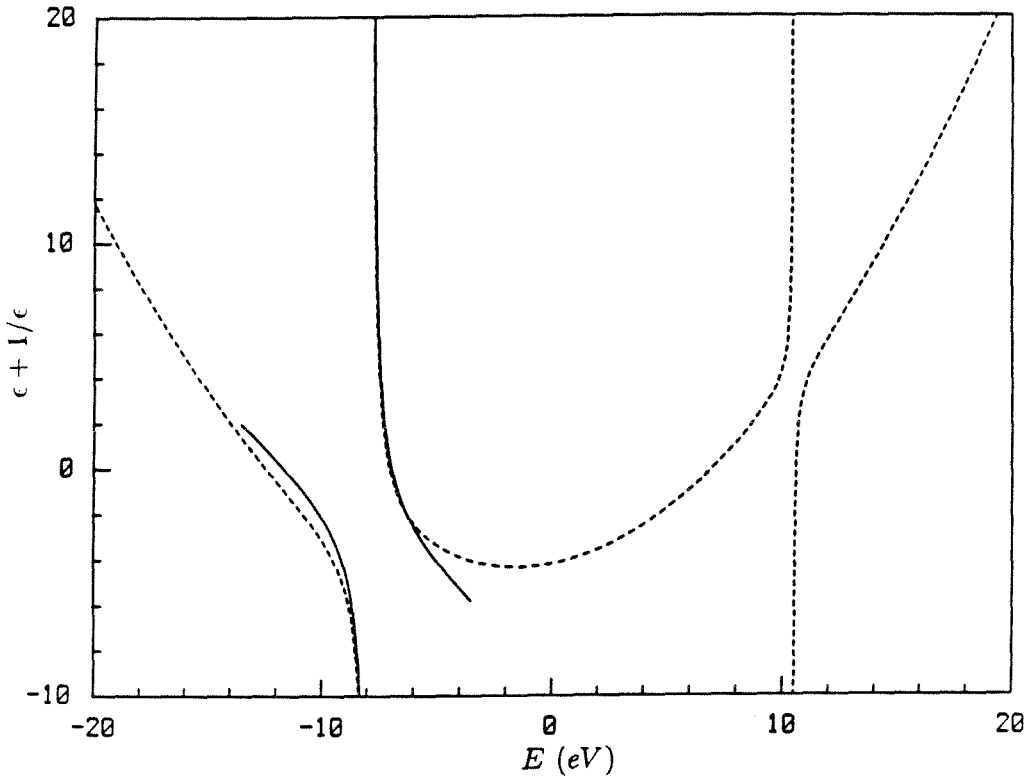

Figure A1 – The band structure determined for n-alkane using only bonding orbitals is shown with a dashed line. The band structure determined for n-alkane[1a] including both bonding and antibonding states is shown with a solid line. The structure of the bonding bands determined with the simple model (solid line) reasonably reproduces those determined from the full model. Recall that for $-2 < \epsilon + 1/\epsilon < 2$, the states are delocalized over the bridge. The sigma band energies were shifted by 8.5 eV for direct comparison with the full model.

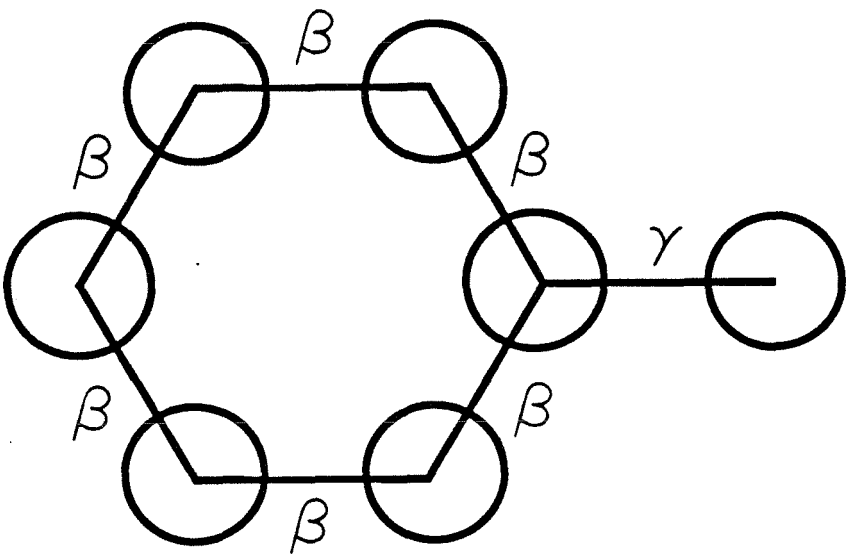

Figure A2 – The geometry and interactions in the para-poly(phenyl) chains are shown.

geometry of rings in Figure A3

$$\epsilon + \frac{1}{\epsilon} = \frac{(E/\beta)^4 - (E/\beta)^2(5+\nu^2) + (4+\nu^2)}{2\nu}. \qquad (A2)$$

The interaction between p orbitals in the ring is β and the interaction between p orbitals on atoms connecting the rings is γ. The ratio of these quantities is $\nu = \gamma/\beta$.

Because the HOMO-LUMO gap is a few eV in these systems and ν on the order of the cosine of the angle between the rings, the small backscattering approximation is most likely not generally appropriate. Taking $\nu = \cos 50°$, the equilibrium geometry of biphenyl, we find the $E - \epsilon$ relation shown in Figure A3. The maximum decay of the rate with distance occurs for the tunneling energy at the center of gap ($E = 0$) where

$$\epsilon(E=0) = \frac{\nu}{2}. \qquad (A3)$$

For a 50° angle, therefore, the rate is expected to change by no more than a factor of 10 per ring. Because of the relatively small band gap, ϵ (and hence the distance decay of the rate) may be considerably different for (photoinduced) forward transfer compared to reverse (thermally activated) electron transfer in these systems.

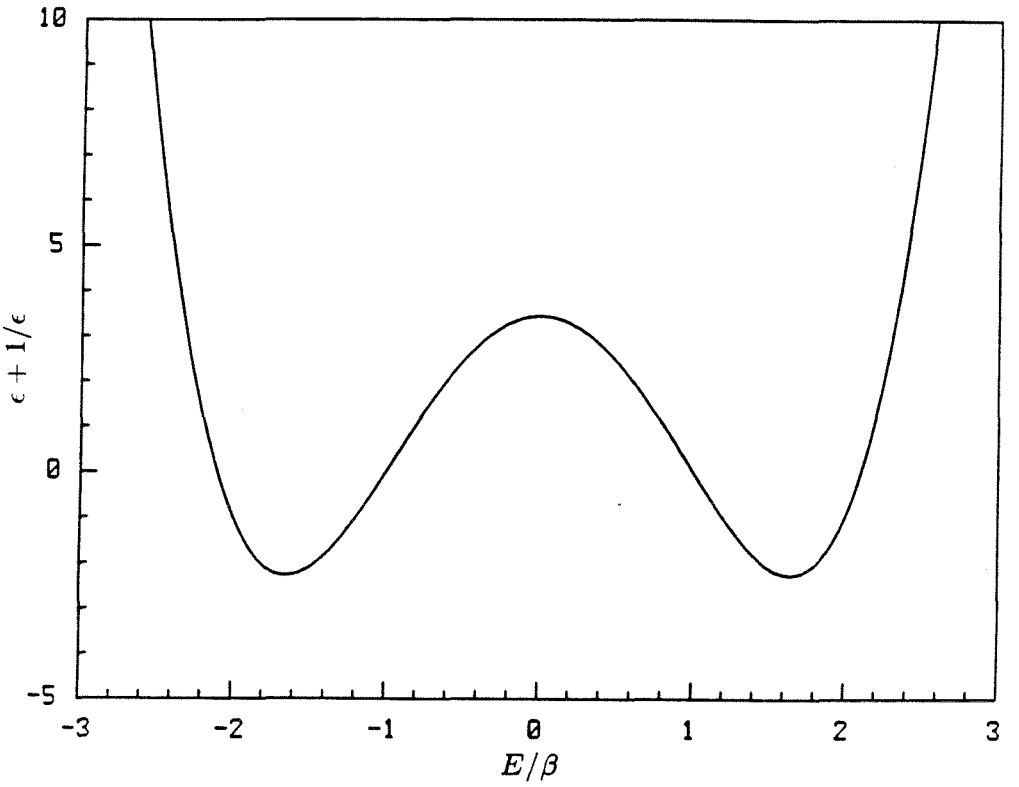

Figure A3 – The $\epsilon + 1/\epsilon$ – E/β relation for para-poly(phenyl) is shown for $\nu = \cos 50°$. ν is the ratio of the inter-ring (γ) to intra-ring exchange (β) interactions.

Acknowledgments

We thank John Hopfield for thoughtful discussions of bridge mediated tunneling. The research described in this paper was performed while D.N.B. held an NRC-NASA Resident Research Associateship at the Jet Propulsion Laboratory, California Institute of Technology. Support for this work was also provided by the Brazilian agency CNPq and the National Science Foundation (Grant No. DMB-8406049,802).

References

(1) (a) D.N. Beratan and J.J. Hopfield, *J. Am. Chem. Soc.* **106**, 1584 (1984); (b) D.N. Beratan *J. Am. Chem. Soc.* **108**, 4321 (1986); (c) D.N. Beratan, J.N. Onuchic, and J.J. Hopfield, *J. Chem. Phys.*, in press.

(2) D.N. Beratan, J.N. Onuchic, and J.J. Hopfield, *J. Chem. Phys.* **83**, 5325 (1985).

(3) (a) B. Chance, D.C. DeVault, H. Frauenfelder, R.A. Marcus, J.R. Schrieffer, and N. Sutin, eds., *Tunneling in Biological Systems*; Academic Press: New York, 1979; (b) D.DeVault, *Quantum Mechanical Tunneling in Biological Systems*, 2nd edition; Cambridge Univ. Press: New York, 1984.

(4) N.S. Hush, *Coord. Chem. Revs.* **64**, 135 (1985).

(5) P.S. Schipper, *Int. Revs. Phys. Chem.* **5**, 283 (1986).

(6) F.L. Carter,editor, *Molecular Electronic Devices*; Marcel Dekker: New York, 1982.

(7) (a) K. Yates, *Hückel Molecular Orbital Theory*; Academic Press: New York, 1971; (b) C.J. Ballhausen and H.B. Gray, *Molecular Orbital Theory*; Academic Press: New York, 1978.

(8) J.N. Onuchic, D.N. Beratan, and J.J. Hopfield, *J. Phys. Chem.* **90**, 3707 (1986).

(9) (a) J. Logan and M.D. Newton, *J. Chem. Phys.* **78**, 4086 (1983); (b) M.D. Newton, *Kinetics of electron transfer between transition metal ion complexes: insights from ab-initio studies*, presented at the 192nd Amer-

ican Chemical Society National Meeting, Anaheim, CA, September 1986.

(10) C.A. Stein, N.A. Lewis, and G.J. Seitz, *J. Am. Chem. Soc.* **104**, 2596 (1982).

(11) G.L. Closs, L.T. Calcaterra, N.J. Green, K.W. Penfield, and J.R. Miller, *J. Phys. Chem.* **90**, 3673 (1986).

(12) (a) J. Verhoeven, *J. Pure and Appl. Chem* **58**, 1285 (1986); (b) N.S. Hush, M.N. Padden-Row, E. Cotsaris, H.Hoevering, J.W. Verhoeven and M. Heppener, *Chem. Phys. Lett.* **117**, 8 (1985).

(13) I.N. Levine, *Quantum Chemistry, 2nd edition*, Allyn and Bacon: Boston, 1974.

(14) G.H. Wannier, *Elements of Solid State Theory*, Cambridge Press: London, 1959.

(15) H. Heitele and M.E. Michel-Beyerle, *J. Am. Chem. Soc.* **107**, 8286 (1985).

(16) D. Heiler, P. Rogalskyj, and G. McLendon, presented at the 192nd American Chemical Society National Meeting, Anaheim, CA, September 1986.

III.4 Electron Tunneling through Covalent and Non-Covalent Pathways in Proteins

J. Chem. Phys., in press

by

David N. Beratan

Jet Propulsion Laboratory

California Institute of Technology

Pasadena, CA 91109

José Nelson Onuchic[a] and **J. J. Hopfield**[b]

Division of Chemistry and Chemical Engineering[c]

California Institute of Technology

Pasadena, California 91125

---

[a] on leave of absence from Instituto de Física e Química de São Carlos, Universidade de São Paulo, 13560, São Carlos, SP, Brazil

[b] Also Caltech Division of Biology and AT&T Bell Laboratories, Murray Hill, NJ 07974

[c] Contribution No. 7474

Abstract

A model is presented for electron tunneling in proteins, which allows the donor-acceptor interaction to be mediated by the covalent bonds between amino acids *and* non-covalent contacts between amino acid chains. The important tunneling pathways are predicted to include mostly bonded groups with less favorable non-bonded interactions being important when the through-bond pathway is prohibitively long. In some cases, vibrational motion of non-bonded groups along the tunneling pathway strongly influences the temperature dependence of the rate. Quantitative estimates for the sizes of these non-covalent interactions are made, and their role in protein mediated electron transport is discussed.

1. Introduction

Recent experimental measurements of non-adiabatic electron transfer rates (and intervalence bands) probe the distance dependence of the donor-acceptor interaction in systems with chemically different non-biological bridging groups.[1] The distance depencence of the rates is clearly influenced by the electronic structure of the bridge. Theoretical models for tunneling through some of these bridges make a variety of qualitative and quantitative predictions about distance, energetic, orbital symmetry, and topological effects on the electron transfer rate.[2] Native electron transfer proteins and modified proteins[3] are not as easily understood as these model systems because of the ambiguity in assigning a tunneling "pathway" to the protein. In proteins, in contrast to the model compounds, direct covalent pathways may not exist between donor and acceptor or may be prohibitively long, as has been pointed out repeatedly.[1b] By a "pathway" we mean the group of atoms (orbitals) that mediates the donor-acceptor interaction. Because bond mediated interactions are expected to dominate the direct donor-acceptor "through-space" interaction so severely in most long distance charge transfer reactions, the proper picture for electron transfer in proteins (and, perhaps, in polymeric media) must include a combination of covalent (through-bond) and *short distance* through-space interactions. By "through-space" we mean interactions between groups not covalently bound but near each other in space. The non-bonded contacts may be constrained by van der Waals, hydrogen bonded, or other steric restrictions on the protein backbone. Experimental and theoretical estimates show that completely ignoring the intervening medium gives the electronic wave function (and hence the matrix element) *much* too rapid a decay with distance (see

Ref. 2a, for example). Some workers choose an effective constant potential[4] between donor and acceptor with height chosen to include the bond mediated interactions in an average sense (see discussion in Ref. 2a).

The distance dependence of bond mediated interactions is determined primarily by the atom types and bond lengths in the bridge. Fluctuations of the distances between the orbitals of the bridge that assist electron transfer may be the origin of a new type of temperature dependence for the rate. (Vibrations coupled to the donor and acceptor give rise to the standard temperature dependence.[4a]) The vibrations of the covalently linked bridge atoms (see Sec. 4) give a weak temperature dependence to the rate. The interactions between the covalent legs, however, will be temperature dependent because events such as ring flips or other relatively large amplitude motions (related to the thermal expansion of the protein) may be involved. As such, the standard picture of a constant, temperature *independent* tunneling matrix element may not be adequate.

The aim of this paper is to present a simple model, which demonstrates how a combination of through-bond and through-space donor-acceptor electron transfer interactions can modify the standard electron transfer rate expression. Consideration of both kinds of interactions gives a prescription for estimating the importance of proposed tunneling pathways in proteins. Our goal is the development of a model that allows donor-acceptor electron exchange mediated by both covalent and non-covalent interactions with the intervening medium. This problem is of interest for protein-mediated electron transfer because: (1) the predicted through-"space" interaction between donor and acceptor is infinitesimal compared to the interaction actually observed in proteins and model

systems; (2) the through-bond pathway between donor and acceptor in the proteins may be prohibitively long or even non-existent, suggesting that a combination of covalent and non-covalent interactions may be important; (3) protein structure is not frozen on the time scale of electron transfer.

The paper is organized as follows. Sec. 2 presents a model for the electron transfer matrix element dependence on the path for a combined through-bond and through-space pathway in a protein when all atoms in the bridge are held at fixed positions. The decay resulting from wave function propagation along a rigid protein backbone and between unbound protein backbone groups is discussed. An estimate of the through-space interaction is made. Next, in Sec. 3, we introduce one vibrational degree of freedom to the bridge and show how this changes the rate. Generalizations and special cases of this model are discussed in Sec. 4. We introduce vibrations between all bridge groups to generalize the one mode result. The single bridge mode calculation is then studied in the limit in where the bridge mode is used to simulate a weak, floppy, non-covalent contact between two otherwise rigid chains. We estimate the sizes of the intra- and inter- chain interaction parameters in proteins for use in the next section. Finally, we present predictions for electron tunneling in proteins with covalent and non-covalent interactions in which motion that modulates the non-covalent interaction is included in the calculation of T_{DA}, the tunneling matrix element. A simple formula is presented for the matrix element decay along a pathway composed of N_B covalent and N_S non-covalent links. We discuss plans for making more precise theoretical estimates of the tunneling matrix element in redox labeled and native electron transport proteins based on the predicted through-bond and through- space pathways. A discussion of

tunneling through covalent bonds in proteins is given in the appendix.

2. Through-Bond and Through-Space Tunneling in Rigid Proteins

A. Through-Bond Decay

Consider a donor and acceptor bound to an extended periodic poly-peptide bridge. The donor/acceptor interaction mediated by the bridge is

$$< \Psi(\text{donor} + \text{bridge})|H^{int}|\Psi(\text{acceptor}) > . \tag{2.1}$$

$\Psi(\text{donor} + \text{bridge})$ is an eigenfunction of H_D^{el}. In the interest of clarity, we will not write the local vibrational wave functions at this stage. A Born-Oppenheimer and Condon separation in these coordinates is assumed[5,7].

$$H_D^{el} = \Delta_D a_D^\dagger a_D + \beta_D(a_D^\dagger a_1 + a_1^\dagger a_D) + \sum_{i=1}^{N-1} \beta_{i,i+1}(a_i^\dagger a_{i+1} + a_{i+1}^\dagger a_i) \tag{2.2}$$

$$H^{int} = \beta_A(a_A^\dagger a_N + a_N^\dagger a_A) \ . \tag{2.3}$$

Ψ_D has non-zero amplitude on the bridge orbitals at sites 1 through N; Ψ_A has zero amplitude on the bridge. Mixing of the two states is provided by H^{int}. i sums over all orbitals on the bridge. Fig. 1 shows the arrangement of donor, acceptor, and bridge. In the weak coupling tight binding limit, the wave function is approximately:

$$\Psi_D = \theta_D(\vec{r}) + \frac{\beta_D}{E}\sum_n \epsilon^{|n|}\sum_p c_p\theta_p(\vec{r} - n\vec{a} - \vec{b}_p), \tag{2.4}$$

where $|\vec{a}|$ is the separation between unit cells and the p atoms in the unit cell are at positions $\vec{b}_p$. The donor wave function (hence the matrix element) decays by ϵ per unit cell. In a simple model for protein backbone, the six hybrid orbitals in the unit cell give a six-by-six determinant relating E to ϵ. This equation is

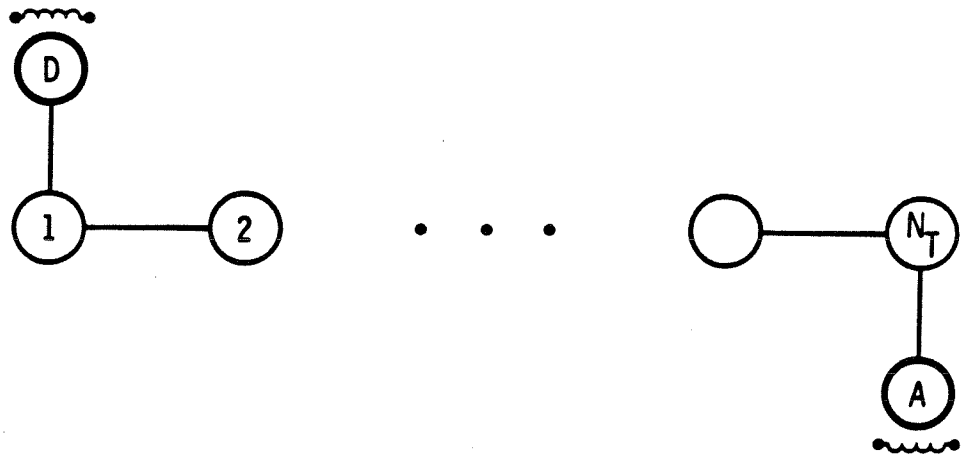

Figure 1 – Schematic representation of the orbitals that mediate charge transfer between donor and acceptor.

written in the appendix. The $E - \epsilon$ relation is shown in Fig. A1 for protein and n-alkane.

In the appendix we develop a model for the wave function decay per bond in the protein backbone and hydrocarbon chains. The relatively simple decay per bond model is an excellent approximation to the full band structure calculations for the chains and improves as the tunneling energy relative to the nearest band increases (backscattering corrections to the decay enter as the square of reciprocal of the energy to the nearest band). A comparison of the accuracy of this per bond method with the full band structure calculation in truly periodic systems is made in the appendix as well. In more detailed calculations, both the σ and π frameworks (as well as pendant groups) should be explicitly included. Because of the periodic approximation, the matrix element decays by ϵ per bridge unit. From the appendix we see that the typical wave function decay per bond, $\epsilon(\textit{per bond})$, is about 0.3-0.5. Recall that these values are tunneling energy dependent. We also show in the appendix that for large enough β (bond), we can reduce the problem to a one band problem with an effective interaction of $\gamma/2$. γ is the Hamiltonian matrix element between hybrid orbitals on a single atom.

Because the wave function decay down the chain is rapid, we may approximate the donor wave function at any site n in the above periodic chain as

$$[\beta_D/(E - \alpha_1)] \prod_{i=1}^{n} \epsilon_c(i), \tag{2.5}$$

where i includes all bonds along a chosen protein covalent (c) pathway. α_1 is the energy of the bridge orbital with which the donor interacts. The amplitude that leaks across a weak, non-covalent contact with a neighboring chain of

"periodic" protein depends on a different ϵ, determined by the interacting non-bonded groups.

B. Through-Space Decay

Assume for simplicity that the non-covalent contact through which the electron tunnels is composed of only two orbitals, one on each backbone chain (see Fig. 2). Assuming two identical orbitals, the transfer matrix element connecting them is on the order of $V_b S_{12}$, where V_b is the orbital energy and S_{12} is the orbital overlap. (This fact is commonly used to approximate Hückel parameters.[10]) In the case of the covalent pathway, where most of the bond energy is due to electron delocalization, the size of the matrix element of the tunneling electron for exchange between the two orbitals is on the order of the Hückel β for a covalent bond. As discussed previously[2a], there are some corrections because the energy of the tunneling electron is not the same as that of the backbone electrons. However, this energy difference is small relative to the ionization energy. Because of this, β's taken to fit optical spectra of $C-C$ bonds can be used to calculate electron tunneling through these covalent pathways. The non-covalent contacts do not involve a bond, so there is no simple experimental way to estimate the size of the non-covalent electron transfer interaction. Therefore, we must rely on theoretical estimates of this interaction.

In the delta function approximation to the binding potential, the exchange interaction between two atoms is $2V_b \exp(-R_{12}\sqrt{2mV_b/\hbar^2})$, where V_b is the binding energy of one delta function and R_{12} is their separation. As previously

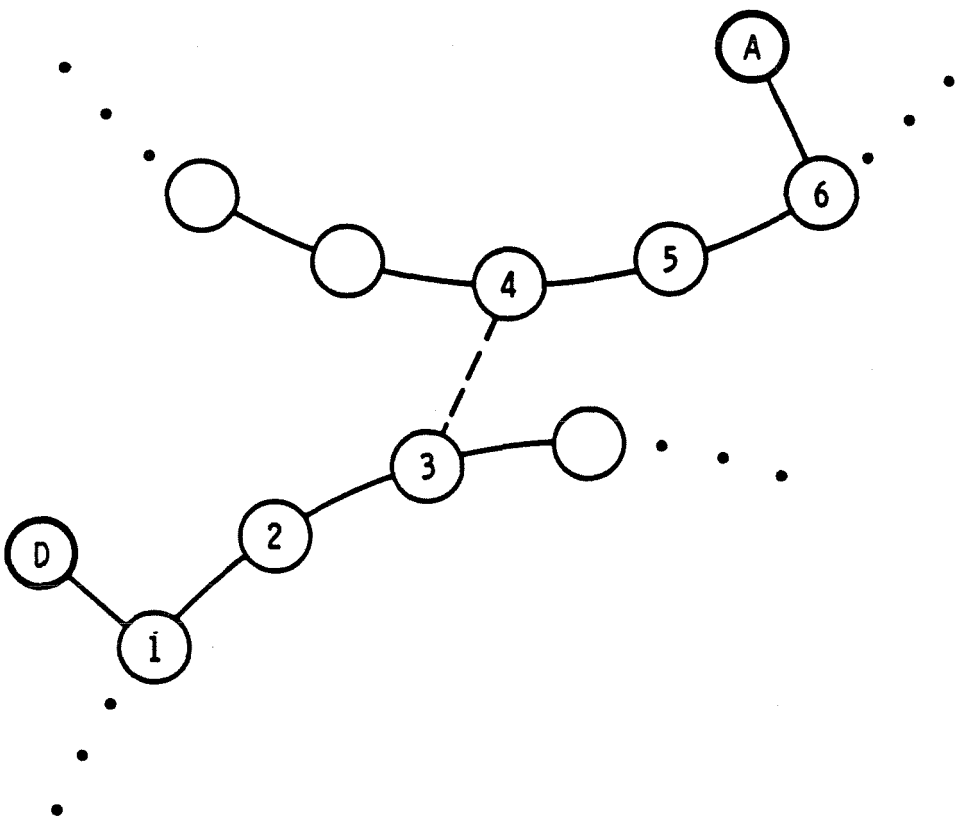

Figure 2 – Schematic representation of an electron transfer pathway composed by two covalent bridges with one significant non-covalent interaction.

mentioned, the energy may need to be corrected because of the difference between the orbital and tunneling energy, but the orbital value is a good estimate. In reality, the exchange interaction should be calculated for two more realistic orbitals. The non-bonded interaction is, again, an exchange interaction on the order of $V_b S_{12}$ where S_{12} is the overlap. S_{12} is expected to have an orbital symmetry dependence in real systems and an exponential distance decay of $\exp(-R_{12}\sqrt{2mV_b/\hbar^2})$.

As an example, assume that the two interacting orbitals are two σ carbon-carbon bonding orbitals (other orbitals, such as CH bonds, carbonyl groups, etc. may be important in real systems). Recall that E is the energy of the tunneling electron in eV relative to the orbital energy V_b and is about 10 eV. The delta function potential model for the non-covalent sites gives

$$\epsilon_{n-c}(j) \simeq (2V_b/E)\exp(-\sqrt{2mV_b/\hbar^2}R_{12_j}) \simeq (20/E)\exp(-1.7R_{12_j}), \quad (2.6)$$

where V_b is the absolute binding energy of the tunneling electron (here approximated as 10eV) and R_{12} is in Å. In a more realistic approximation, we might model the bonds with two 1S hydrogenic orbitals (orientation effects and more complicated radial wave functions may correct this with a prefactor), each with a binding energy of 10 eV. The overlap between these orbitals is

$$S_{12}(1S-1S) = \left[1+\alpha R+\frac{1}{3}(\alpha R)^2\right]\exp(-\alpha R). \quad (2.7)$$

For an orbital separation of 4Å (typical van der Waals distance for carbon atoms), this interaction energy is about 0.25 eV, which gives ϵ_{n-c} about 0.05 ($n-c$ signifies a non-covalent contact). This interaction is very sensitive to distance. A 4 Å separation between sigma orbitals is as short as may be expected. For a 5.5 Å separation, the interaction is 0.03 eV, which gives ϵ_{n-c}

about 0.005. Also, this 1S orbital approximation is rather crude, but in the weak coupling limit, the leading exponential term depends only on the energy of the state and dominates the distance dependence of the interaction. The 1S representation certainly overestimates the prefactor of the overlap because, in the real systems, the wave function is anisotropic and has less density perpendicular to the bond than parallel to it (at a given distance from its center). This effect may severely reduce the through-space interaction.

C. Combined Through-Bond and Through-Space Pathways

Assuming that there are N_B covalent bonds and N_S non-covalent jumps along a given pathway, the *simplest* expression for the tunneling matrix element is

$$T_{DA} = (\beta_D \beta_A / E) \prod_{i=1}^{N_B} \epsilon_c(i) \prod_{j=1}^{N_S} \epsilon_{n-c}(j). \tag{2.8}$$

Here the energy, E, is measured with respect to the first orbital (bond) with which the donor interacts. Estimates of ϵ_c for amino acids and linear hydrocarbon are given in the appendix. The ϵ's are tunneling energy dependent. The energy to be used to calculate ϵ (see appendix) can be approximated

$$E(eV) \simeq -[E_{1/2}(D) + E_{1/2}(A)]/2 - 5.1, \tag{2.9}$$

measuring redox potentials vs. NHE.[2c,2e]

The simplest way to improve Eq. 2.8, is to make a periodic approximation for the protein backbone and to take more accurate values for the decay per "unit cell" of the protein backbone on the tunneling pathway rather than calculate the decay per bond. A similar treatment using alkane parameters

may be applicable for some amino acid side groups. Typical values of α, where $\epsilon = A\exp(-\alpha R)$, are 0.6 $Å^{-1}$ and 1.7 $Å^{-1}$ for through-bond and through-space interactions, respectively. Predicting the number of through-bond steps giving "equivalent" decay to one through- space jump depends crucially on the different prefactors (A's) for the interactions and requires more detailed study in the future.

3. Models for Bridge Modulated Electron Tunneling

The pathways for electron transfer in proteins can be composed of both bonded and non-bonded legs. Distance fluctuations within these legs and between legs of the pathway can affect the rate and its temperature dependence.

In this section we introduce the formalism needed to calculate bridge mediated electron transfer rates when the interactions in the bridge are allowed to fluctuate. Recall that T_{DA} calculated in Sec. 2 assumed a purely static bridge. In Sec. 4 we will use the rate expressions developed here for particular kinds of bridge interactions which are expected to be important in real proteins.

Consider the Hamiltonian for the model of Fig. 2 where vibronic coupling to only one of the "bridge" interactions is included (H^{int}). This is the simplest model for understanding how bridge vibrations influence electron transfer rates. In this section and in Sec. 4 we discuss when these bridge vibrations must be explicitly included in the calculation. Local vibronic coupling on the donor and acceptor is also included. The Hamiltonian is

$$H = H^{el} + H^{nuc} + H^{int}, \tag{3.1}$$

where

$$H^{el} = H_D^{el} + H_A^{el} \tag{3.2a}$$

$$H^{nuc} = H_D^{nuc} + H_A^{nuc} + H_N^{nuc} \tag{3.2b}$$

$$H_D^{el} = \Delta_D a_D^\dagger a_D + \beta_D(a_D^\dagger a_1 + a_1^\dagger a_D) + \beta \sum_{i=1}^{N-1}(a_i^\dagger a_{i+1} + a_{i+1}^\dagger a_i) \tag{3.2c}$$

$$H_A^{el} = \Delta_A a_A^\dagger a_A + \beta_A(a_A^\dagger a_{N_T} + a_{N_T}^\dagger a_A) + \beta \sum_{j=N+1}^{N_T-1}(a_j^\dagger a_{j+1} + a_{j+1}^\dagger a_j) \tag{3.2d}$$

$$H^{int} = \beta_1^{eq} \exp\left\{-\alpha'[(R_{N+1} - R_N) - R^0]\right\} (a_N^\dagger a_{N+1} + a_{N+1}^\dagger a_N) \qquad (3.2e)$$

$$H_D^{nuc} = \left(b_D^\dagger b_D + \frac{1}{2}\right) \hbar\Omega_D + \lambda_D a_D^\dagger a_D (b_D^\dagger + b_D) \qquad (3.2f)$$

$$H_A^{nuc} = \left(b_A^\dagger b_A + \frac{1}{2}\right) \hbar\Omega_A + \lambda_A a_A^\dagger a_A (b_A^\dagger + b_A) \qquad (3.2g)$$

$$H_N^{nuc} = \left(b_N^\dagger b_N + \frac{1}{2}\right) \hbar\omega. \qquad (3.2h)$$

The donor and acceptor localized states solve

$$\{H^{el} + H^{nuc}\}\Psi = E\Psi \qquad (3.3)$$

The two localized electronic states are Ψ_D and Ψ_A. Ψ_D has non-zero amplitude on bridge sites 1 through N; Ψ_A has non-zero amplitude on bridge sites $N+1$ through N_T. H^{int} couples these two states. α' in Eq. 3.2e is the decay length for the exchange interaction betweeen residues N and $N+1$. The prime notation is used to distinguish it from the usual designation of α as the decay constant for the tunneling matrix element in a truly periodic covalently bonded medium (α' is about 1.7 Å^{-1}).[2a] A single local vibrational state is put on D and A. This can easily be extended to multiple modes per site. For simplicity, a one orbital per unit cell model has been used in Eqs. 3.2c and 3.2d.

The initial and final states involved in the transfer event are:

$$\Psi_I = \Psi_D(x; y_D; y_A)\chi_i^D(y_D)\chi_j^A(y_A)\Phi_k(y_N) \qquad (3.4a)$$

and

$$\Psi_F = \Psi_A(x; y_D; y_A)\chi_{i'}^D(y_D - y_D^0)\chi_{j'}^A(y_A - y_A^0)\Phi_{k'}(y_N) \quad , \qquad (3.4b)$$

where x is the electronic coordinate, $y's$ are nuclear coordinates, $y_N = (R_{N+1} - R_N) - R^0$, and a Born-Oppenheimer separation is made for all nuclear modes. χ's are used for local vibrational wave functions and Φ's are used for bridge mode vibrational states. This separation of time scales has been discussed previously for the local vibrations.[5] It should be valid for the bridge mode when $\beta_1^{eq}/\hbar >> \omega$. Also, we assume that the relaxation times of all nuclear modes coupled to the problem are fast enough so that the donor survival probability decays exponentially in time. The electron transfer rate, then, is given by

$$k_{ET} = \frac{2\pi}{\hbar} \sum_I B_I \sum_F | < \Psi_I | H^{int} | \Psi_F > |^2 \delta(E_I - E_F). \qquad (3.5)$$

The delta function in Eq. 3.5 is purely formal and is included to guarantee energy conservation. A discussion of how to broaden these energy levels is given elsewhere.[5] The y_N mode does not change equilibrium displacement upon charge transfer (although it may gain or lose vibrational quanta in the process) because it is spatially well removed from the sites of charge localization. In contrast to most previous studies on model systems (Ref. 6 is the exception), the perturbing Hamiltonian (H^{int}) is explicitly modulated by one nuclear coordinate (more than one such coordinate in the bridge is added in Sec. 4). In Hamiltonian 3.1 we have one bridge mode and the coordinate for this mode is the displacement from equilibrium of residues N and $N+1$ (defined as y_N). Because we are interested in the way in which the bridge mode affects the dynamics of the transfer reaction, we will consider from this point only one local mode, y_L, coupled to the donor or the acceptor. The affects described in this section are "non-Condon" in origin; i.e. they arise from matrix elements of the form

$$< \Phi_k(y_N) | exp(-\alpha' y_N) | \Phi_{k'}(y_N) > . \qquad (3.6)$$

The Condon approximation will be used to simplify the matrix element only for the local mode, not for the bridge mode(s). Non-Condon effects arising from the local modes have been discussed at length[5,7] and will result in qualitively different effects from those described in this paper.

In the one bridge mode model, the absolute $D-A$ distance, is *held fixed* and y_N varies, modulating the overall donor-acceptor interaction. This analysis can easily be extended to systems with a direct donor-acceptor interaction and a varying donor-acceptor distance, if the y_N coordinate is redefined as the donor-acceptor separation.

Approximating the bridge as a periodic chain *except* between sites N and $N+1$, the matrix element $< \Psi_I|H^{int}|\Psi_F >$ can be written ($\chi_i = |i>$)

$$< \frac{\beta_D}{E}\epsilon^N \Phi_k(y_N)|\beta_1^{eq}\exp\{-\alpha' y_N\}|\frac{\beta_A}{E}\epsilon^{N_T-N-1}\Phi_{k'}(y_N) >< i|i' >, \qquad (3.7a)$$

so

$$k_{ET} = \frac{2\pi}{\hbar}|T_{DA}^0|^2$$

$$\times \sum_{k,k'}\sum_{i,i'} B(k,T)B(i,T)|< \Phi_k(y_N)|\exp(-\alpha' y_N)|\Phi_{k'}(y_N) > |^2|< i|i' > |^2$$

$$\times \delta[(i'-i)\hbar\Omega + (k'-k)\hbar\omega - \Delta E), \qquad (3.7b)$$

where

$$|T_{DA}^0|^2 = \left(\frac{\beta_D\beta_A}{E^2}\right)^2 (\beta_1^{eq})^2\,\epsilon^{2N_T-2},$$

$$\beta_1^{eq} =< \phi_{B_N}|H_{int}|\phi_{B_{N+1}} > \text{ at } y_N = 0,$$

and

$$\epsilon \simeq \frac{\beta}{E}$$

in this (one band) model.[2a] Here E is the electronic energy of the tunneling electron relative to the center of the band of bridge orbitals. It is assumed

that this energy is weakly dependent on the local nuclear coordinates so that the Condon approximation is valid.[5] β_1^{eq} is the exchange interaction energy of orbitals N and $N+1$ at separation R^0. $< i'|i >$ is the nuclear Franck-Condon factor for the local mode. $|i' >$ and $|i >$ are eigenstates for the shifted and unshifted harmonic oscillators, respectively. ϵ is the Bloch factor by which the localized donor and acceptor states decay in the bridge. ϵ depends parametrically on y_L, the value of which is fixed when making the Condon approximation. The Condon approximation for the local modes allows any number of local modes to be added to the problem. They will factor out of the matrix element in the same way.

A special case of coupling to a bridge mode, allowing only zero or one phonon exchange with it, has been studied.[6] In that model, transfer through a potential barrier of modulating height was considered. Here, the orbital interaction between two groups in the intervening barrier is allowed to fluctuate. We next consider several specific examples for which k_{ET} may be calculated.

A. Rate Expressions

(1) Low Temperature limit (one local mode, one bridge mode)

In this case $i = 0$, $k = 0$, and $i'\hbar\Omega + k'\hbar\omega = \Delta E$. i labels the local mode (χ) and k the bridge mode (Φ). At low temperature the first integral in 3.7b is the overlap of a ground state harmonic oscillator of equilibrium displacement $\alpha'\hbar/m\omega$ with an oscillator centered at the origin (from combining $\exp[-\alpha' y_N]$ with $\Phi_0(y_N)$). At low temperature ($\kappa T \ll \hbar\omega, \hbar\Omega$), the rate is-

$$k_{ET} = \frac{2\pi}{\hbar} | < \Psi_D(x;y_L)\Phi_0(y_N)|H^{int}|\Psi_A(x;y_L)\Phi_{k'}(y_N) > |^2$$

$$\times | < 0|i' > |^2 \delta(E_I - E_F) \qquad (3.8a)$$

or

$$k_{ET} = \frac{2\pi}{\hbar}|T^0_{DA}|^2 \exp\left[\frac{\alpha'^2\hbar}{2m\omega}\right] \sum_{k'=0}^{\Delta E/\hbar\Omega} \left\{\left[\frac{\alpha'^2\hbar}{2m\omega}\right]^{k'} \frac{1}{k'!}\right\} \left\{\frac{\exp(-X)X^{i'}}{i'!}\right\}$$

$$\times \delta(i'\hbar\Omega + k'\hbar\omega - \Delta E) \quad . \qquad (3.8b)$$

X is the reorganization energy of the local mode in units of $\hbar\Omega$ and k' is the number of vibrational quanta excited in the bridge mode due to transfer.

The y_N mode gives a matrix element enhancement of $\exp[\alpha'^2\hbar/4m\omega]$ compared to the result when y_N is held fixed at zero (Condon approximation in bridge mode). Hence, the bridge enhancement is particularly important when the interaction associated with y_N decays rapidly with distance (α' large) and/or when the zero point motion of the oscillator is large. The principal effect on the low temperature rate can be written $\exp[\alpha'^2 < y^2 >]$, where $< y^2 >$ is the mean-square displacement of a ground state harmonic oscillator.

(2) General Rate (one local mode, one bridge mode)

The electron transfer rate is

$$k_{ET} = \frac{2\pi}{\hbar}|T_{DA}^0|^2 \sum_{i,i'}\sum_{k,k'} B(i,T)B(k,T)$$

$$\times|<\Phi_k(y_N)|\exp[-\alpha' y_N]|\Phi_{k'}(y_N)>|^2|<\chi_i(y_L)|\chi_{i'}(y_L - y_L^0)>|^2$$

$$\times\delta[(i'-i)\hbar\Omega + (k'-k)\hbar\omega - \Delta E]. \qquad (3.9a)$$

$B(i(k),T)$ is the probability of having $i(k)$ vibrational quanta in the local (bridge) mode prior to electron transfer. Following the standard treatment for such sums over thermally populated states[8], we find

$$k_{ET} = \frac{2\pi}{\hbar}|T_{DA}^0|^2 \sum_{m,p} \exp\left[-X(2\bar{n}_L+1)\right]\left(\frac{\bar{n}_L+1}{\bar{n}_L}\right)^{p/2}$$

$$\times I_p\left(2X\left[\bar{n}_L(\bar{n}_L+1)\right]^{1/2}\right)\exp\left[+S(2\bar{n}_B+1)\right]\left(\frac{\bar{n}_B+1}{\bar{n}_B}\right)^{m/2}$$

$$\times I_m(2S[\bar{n}_B(\bar{n}_B+1)]^{1/2})\delta\left[p\hbar\Omega + m\hbar\omega - \Delta E\right] \qquad (3.9b)$$

where we defined $m = k' - k$ and $p = i' - i$, so

$$k_{ET} = \frac{2\pi}{\hbar}|T_{DA}^0|^2 \sum_{m,p} F.C._p(\text{local mode})\mathcal{B}_m(\bar{n}_B)\delta\left[p\hbar\Omega + m\hbar\omega - \Delta E\right], \qquad (3.10)$$

where $S = \alpha'^2\hbar/(2m\omega)$. I_j is a Bessel function. Here $F.C.$ is the Franck-Condon factor for the local modes and $\mathcal{B}$ is the contribution to the rate from the bridge modes. The delta function is purely formal. To obtain numerical expressions for the rate, broadening of the energy levels must be included. Discussions of how to accomplish this have been given.[5,8b] The simplest way is to assume a uniform density of states for the acceptor levels of $1/\hbar\omega'$, where ω' is the frequency of the slowest mode of the problem. This approximation is not always valid and is discussed in Ref. 5. The low temperature rate ($\kappa T \ll \hbar\omega,\ \hbar\Omega$); i.e. Eq. 3.8, can be derived from this expression.

To compute the high temperature limit for the rate ($\kappa T \gg \hbar\Omega,\ \hbar\omega$) we use the fact that for large z,

$$I_p(z) \longrightarrow \frac{1}{\sqrt{2\pi z}} \exp\left\{z - \frac{p^2}{2z}\right\}. \tag{3.11}$$

Substituting 3.11 in 3.10 we obtain a Gaussian form for the rate,

$$k_{ET} = \frac{2\pi}{\hbar}|T^0_{DA}|^2 \exp\left[\frac{4S\kappa T}{\hbar\omega} + \frac{S\hbar\omega}{3\kappa T}\right] \exp\left\{\frac{(\Delta E - S\hbar\omega - X\hbar\Omega)^2}{4\kappa T(S\hbar\omega + X\hbar\Omega)}\right\}$$

$$\times \frac{1}{\sqrt{4\pi(S\hbar\omega + X\hbar\Omega)\kappa T}}. \tag{3.12}$$

When $X\hbar\Omega \gg S\hbar\omega$, the reorganization energy of the local mode is much greater than the "pseudo-reorganization energy" of the bridge mode (this assumption is reasonable for typical reorganization energies), we find the high temperature rate is:

$$k_{ET} = \frac{2\pi}{\hbar}|T^0_{DA}|^2 \frac{1}{\sqrt{4\pi X\hbar\Omega\kappa T}} \times \exp\left[\frac{4S\kappa T}{\hbar\omega}\right] \exp\left\{(\Delta E - X\hbar\Omega)^2/[4\kappa T X\hbar\Omega]\right\}$$

$$= \frac{2\pi}{\hbar}|T^0_{DA}|^2 \exp\left[\frac{4S\kappa T}{\hbar\omega}\right] F.C.(\text{local mode}). \tag{3.13}$$

For slow classical modes ($\hbar\omega \simeq 10\ \text{cm}^{-1}$), the above assumption is reasonable because if $S\hbar\omega$ were $\sim$ 1 eV, we would get a temperature dependence of $\exp[320\kappa T(cm^{-1})]$. This dramatic temperature dependence is non-physical and has never been observed. For example, if $< y^2 >= 1$ Å^2, this would correspond to α' of 180 Å^{-1}.

In the high temperature limit, the effect of the bridge enters the rate as $\exp[2\alpha'^2 < y^2 >]$, where $< y^2 >$ is the (temperature dependent) mean-square displacement of the bridge oscillator. In the low temperature limit this effect entered as $\exp[\alpha'^2 < y^2 >]$ (see Eq. 3.8).

(3) "Semi-classical" calculation of the rate

Eq. 3.7b, the general rate expression where one local mode and one bridge mode is included, can be written ($\Phi_k = |k>$)

$$k_{ET} = \frac{2\pi}{\hbar}|T_{DA}^0|^2$$

$$\times \sum_{k,k'}\sum_{i,i'} B(k,T)B(i,T) < k|\exp(-\alpha' y_N)|k' >< k'|\exp(-\alpha' y_N)|k >$$

$$\times| < i|i' > |^2 \ \delta[(i'-i)\hbar\Omega + (k'-k)\hbar\omega - \Delta E]. \qquad (3.14)$$

We perform the semi-classical approximation, assuming that the motion of the bridge oscillator is slow enough so that no energy is exchanged between the local and bridge modes. This is accomplished by assuming $< n|\exp(-\alpha' y_N)|m >= 0$, if $n \neq m$. This is the same as assuming that $\exp(-\alpha' y_N)$ commutes with H_N^{nuc}, the Hamiltonian of the bridge mode (Eq. 3.2h). If quantum effects are washed out by coupling to the bath, i.e., the density of states becomes a smooth function of the energy instead of being sharply peaked with peaks separated by energy $\hbar\omega$, neglecting such commutators is a reasonable approximation[5]. In this limit,

$$k_{ET} = \frac{2\pi}{\hbar}|T_{DA}^0|^2 \sum_k \sum_{i,i'} B(k,T)B(i,T) < k|\exp(-2\alpha' y_N)|k > | < i|i' > |^2$$

$$\times\delta[(i'-i)\hbar\Omega - \Delta E]. \qquad (3.15)$$

The bridge contribution to this rate, which is

$$\sum_k B(k,T) < k|\exp(-2\alpha' y_N)|k > \equiv \langle\exp(-2\alpha' y_N)\rangle\,, \qquad (3.16)$$

can be written

$$\langle \exp(-2\alpha' y_N) \rangle = \int \exp(-2\alpha' y_N) P(y_N) dy_N, \tag{3.17a}$$

where

$$P(y_N) = \sum_k B(k,T) \Phi_k^*(y_N) \Phi_k(y_N) \tag{3.17b}$$

is the probability distribution function for the bridge coordinate. We call this model "semi-classical" because this distribution function need not be a classical one, but the final rate is not the quantum result. For this probability distribution function, Eq. 3.17a can be calculated exactly[9] and

$$\langle \exp(-2\alpha' y_N) \rangle = \exp(2\alpha'^2 \mu_N^2), \tag{3.18a}$$

where

$$\mu_N^2 = \frac{\hbar}{2m\omega} \coth \frac{\hbar\omega}{2\kappa T} = \frac{\kappa T^{eff}}{m\omega^2}. \tag{3.18b}$$

This is equivalent to writing

$$P(y) = \frac{1}{\sqrt{2\pi\mu_N^2}} \exp\left[-\frac{y_N^2}{2\mu_N^2} \right]. \tag{3.19}$$

The final semi-classical rate may be written as

$$k_{ET} = \frac{2\pi}{\hbar} |T_{DA}^0|^2 \langle \exp(-2\alpha' y_N) \rangle \, F.C(\text{local modes}), \tag{3.20}$$

In the high temperature limit this is exactly Eq. 3.13. This semi-classical result gives a rate, which is an average of all bridge coordinate configurations. Therefore, Eq. 3.17a may be used in more general situations, i.e., when the bridge potential is not harmonic, and $P(y_N)$ is therefore not Gaussian. Multiple bridge modes enter the rate as products.

4. Applications of Bridge Modulated Tunneling

A. Bridges with more than one vibrational mode

We consider in this section electron transfer when the donor and acceptor are coupled to the same bridging unit and the direct through- space interaction can be neglected. As an example, this model simulates the case in which the donor and the acceptor are bonded to the same protein chain, and the through-bond pathway completely dominates the electron transfer rate. This may not be a physically meaningful picture for an *entire* protein but is certainly useful for understanding "legs" of the pathway. In Fig. 3 is shown a schematic representation of the simplest possible bridge, which includes N identical "atoms" (orbitals) connected in a ring by N identical springs ("bonds"). The donor and acceptor are rigidly linked to this bridge via "atoms" i and j, respectively ($j > i$). The equilibrium separation between neighboring bridge "atoms" is R_0, and ΔR_k is the displacement of atom k from its equilibrium position. The atomic masses are M, the spring constants are k, and $\omega_0 = \sqrt{k/M}$.

We write the total Hamiltonian in analogy with the one in Sec. 3 as:

$$H = H_D + H_A + H_{AD} + H_N \quad , \tag{4.1}$$

where

$$H_{D(A)} = \Delta_{D(A)} a^{\dagger}_{D(A)} a_{D(A)}, \tag{4.2a}$$

$$H_{AD} = \beta_{eff} \exp\{-\alpha'(\Delta R_j - \Delta R_i)\} (a^{\dagger}_D a_A + a^{\dagger}_A a_D), \tag{4.2b}$$

and

$$H_N = \sum_q \frac{p_q^2}{2M} + \frac{1}{2} M \omega_q^2 \left[(y_q^c)^2 + (y_q^s)^2 \right] \quad . \tag{4.2c}$$

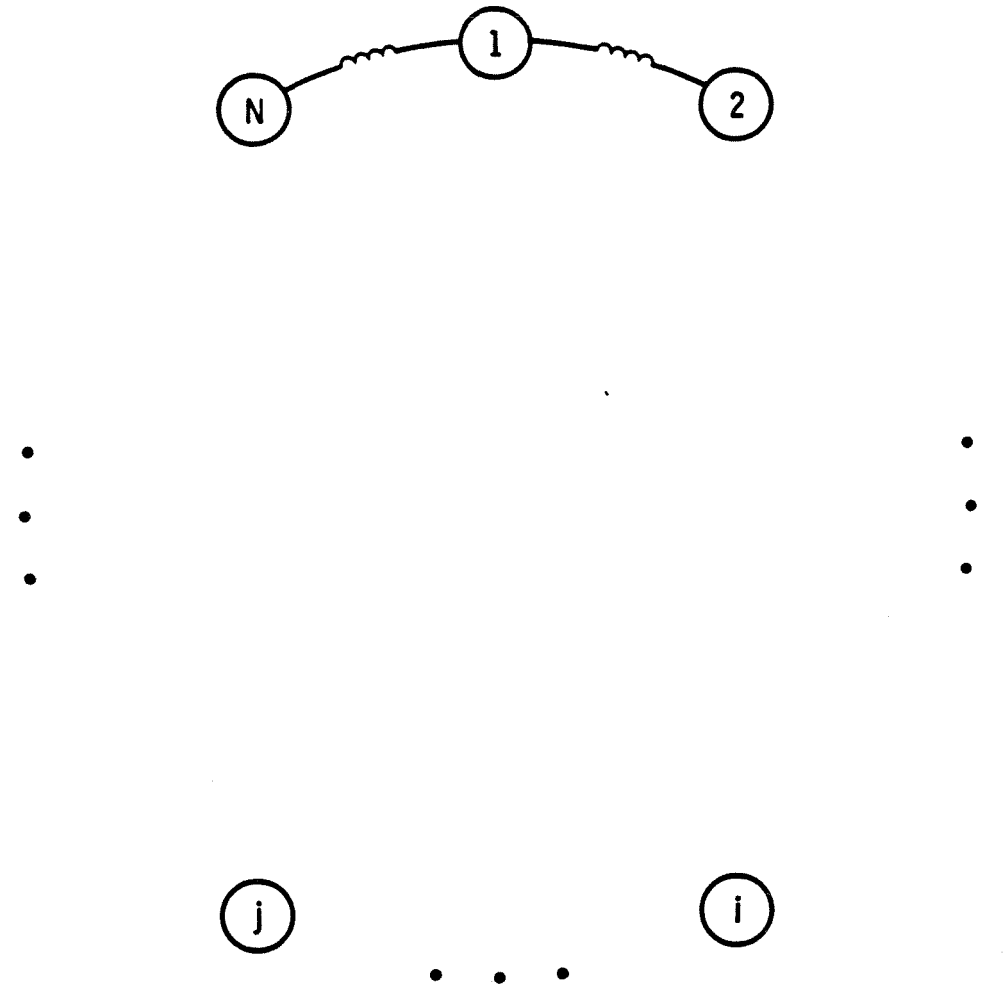

Figure 3 – Schematic representation of a chain of covalent bridge orbitals. These bridge orbitals are connected in a ring by flexible links. The mass associated with the site of each orbital is M and each link has a spring constant $k = M\omega_0^2$.

In order to keep the notation clear, if in the last section we call the interaction between two atoms in the chain

$$\beta_{i+1,i} = \beta^{eq} \exp\{-\alpha'(\Delta R_{i+1} - \Delta R_i)\} \quad , \tag{4.3}$$

then here, assuming that back scattering can be neglected, the net interaction between donor and acceptor with bridge atoms at their equilibrium positions is

$$\beta_{eff} = \frac{\beta_D \beta_A}{E} \left[\frac{\beta^{eq}}{E}\right]^{(j-i)} \quad . \tag{4.4}$$

y_q^c and y_q^s are the normal coordinates for the ring of atoms. The normal modes of vibration for the ring are (for N odd)

$$y_q^c = \frac{1}{C_q} \sum_{n=1}^{N} \cos(k_q n) \Delta R_n \quad \text{for} \quad q = 0, 1, \ldots, (N-1)/2 \quad , \tag{4.5a}$$

and

$$y_q^s = \frac{1}{C_q} \sum_{n=1}^{N} \sin(k_q n) \Delta R_n \quad \text{for} \quad q = 1, \ldots, (N-1)/2 \quad , \tag{4.5b}$$

and where C_q is a normalization factor and is equal to $\sqrt{N/2}$ if $q \neq 0$. The frequency associated with the q^{th} mode is

$$\omega_q^2 = 2\omega_0^2(1 - \cos k_q) \quad , \tag{4.6}$$

where $\cos(k_q N) = 1$. For simplicity, we consider N odd; thus, $k_q = 2\pi q/N$, where $q = 0, \cdots, (N-1)/2$, and all eigenvalues except $q = 0$ are doubly degenerate.

In order to calculate the tunneling matrix element dependence on the bridging coordinate vibrations as in the one-mode case, $\Delta R_j - \Delta R_i$ can be expanded for large N as

$$\Delta R_j - \Delta R_i = \sum_{n=1}^{(N-1)/2} \sqrt{\frac{2}{N}} \Big\{ \big[\cos(k_n j) - \cos(k_n i)\big] y_n^c + \big[\sin(k_n j) - \sin(k_n i)\big] y_n^s \Big\} \quad . \tag{4.7}$$

The $\omega_i = 0$ mode is always neglected because it is never coupled to the problem.

Substituting Eq. 4.7 into Eq. 4.2b, the problem becomes similar to the one described in Sec. 2. The difference is that instead of one bridge mode, $N-1$ independent bridge modes affect the rate. Therefore, the net effect of the bridge modes on the rate is a product $\langle \exp(-2\alpha' y_k) \rangle$ in the semi-classical limit, which in the harmonic case goes as $\exp(2\alpha'^2 < y_k^2 >)$. As an example, we calculate here the case where $j = 0$ and i=1. In our case, for large N, the density of states of the c or s modes is

$$\rho^{c;s}(\omega) = \frac{N}{2\omega_0\sqrt{2}} \quad , \tag{4.8}$$

and

$$\big(\cos\big[k(\omega)\big] - 1\big)^2 + \sin^2\big[k(\omega)\big] = \frac{\omega^2}{\omega_0^2} \quad . \tag{4.9}$$

The equation above shows us that when $j = 1$ and $i = 0$ the coupling to a mode of frequency ω is proportional to ω^2. Using Eqs. 4.8 and 4.9, we get in the semi-classical limit (Eq. 3.18) a bridge temperature dependence of

$$\exp\left\{ 2\alpha'^2 \int_0^{\sqrt{2}\omega_0} d\omega \; \rho(\omega) \frac{2\omega^2}{N\omega_0^2} < y^2(\omega) > \right\} \quad , \tag{4.10a}$$

or

$$\exp\left\{ 2\alpha'^2 \int_0^{\sqrt{2}\omega_0} d\omega \; \frac{\omega^2}{\sqrt{2}\omega_0^3} < y^2(\omega) > \right\} \quad . \tag{4.10b}$$

In the high temperature limit this term becomes $\exp\{(2\alpha'^2 kT)/(M\omega_0^2)\}$, which is equivalent to having coupling to only one mode of frequency ω_0. In the low

temperature limit it is $\exp\{2(\alpha'^2\hbar)/(2M\sqrt{2}\omega_0)\}$, which is equivalent to being coupled to only one mode of frequency $\sqrt{2}\omega_0$. Eq. 4.10 is just a particular case but it gives us an idea of the size of the effect of these chain modes.

For a covalent bond mediated tunneling pathway, the atomic vibrations are of very small amplitude, and approximating the bridge as a truly rigid structure is quite acceptable. This is discussed in more detail in the following subsections.

B. Estimates of Parameters for the Dynamical Effects

(1) Covalent bonds

Fluctuations of the interatomic distances in the covalently bridged donor–acceptor systems are expected to have small effects on the transfer rate. A value of α' for the bridge interaction (Eq. 3.2e) is of the size 1.7 Å^{-1}. This value is large because the interaction between two groups in a tight binding approximation decays as $\exp(-\sqrt{2mV_b/\hbar^2}R)$ where R is the distance between atoms and V_b is the binding energy of the electron on an isolated atom.[2a] This interaction is model dependent and depends on the symmetry and energetics of the interacting sites. The above number is just an order of magnitude estimate for the decay constant. From the above discussion we note that the bridge effect on the rate reduces to one effective oscillator with frequency on the order of a single vibration. For a $C-C$ vibration, μ^2 (Eq. 3.18) is of the order 0.002 Å^2 (T=0) and, because the frequency of the vibration is so large, this does not have a temperature dependence. Therefore, for the covalently

linked atoms, the rate correction due to the bridge covalent bond vibrations is insignificant and temperature independent. Hence, it is reasonable to treat the covalent tunneling pathway as rigid. Because of this we will approximate the through-bond decay simply with the method presented in Sec. 2.

(2) Non-covalent Contacts

Fluctuations of the through-space distances from their equilibrium values are expected to be much larger than the through-bond distance fluctuations. Hence, large fluctuations in the size of the non-covalent interaction caused by these fluctuations may occur. In the harmonic case (Eq. 3.18a), distance fluctuations giving a mean square displacement from equilibrium of 1.0 $Å^2$ enhance the rate by a factor of 400, but fluctuations of 0.15 $Å^2$ enhance it by only a factor of 2 (for a tunneling energy of 10 eV). Thus, the non-bonded groups will introduce a temperature dependence arising from thermally induced changes in the non-covalent interaction energy, depending on the magnitude of the separation fluctuations between these groups. Also, anharmonic effects on the temperature dependence may enter because of hard wall repulsion of the residues because the groups, after a certain point, may fluctuate to larger rather than shorter distances with further temperature increases. When these effects are important, we must have the proper (temperature dependent) distribution of the distance between contacts. This distribution can be determined from molecular dynamics calculations. With the correct distribution, Eq. 3.17a can be used to calculate the effect of these fluctuations on the rate.

C. Matrix elements for pathways with thermal fluctuations

We can now generalize Eq. 2.8 for the electron tunneling matrix element by including its temperature dependence. In the limit of rapid wave function decay the tunneling matrix element is

$$|T_{DA}|^2 = |T_{DA}^0|^2 \prod_{j=1}^{N_S} \langle \exp(-2\alpha' y_j) \rangle \,, \tag{4.11}$$

where N_S is the number of through-space jumps and T_{DA}^0 is the matrix element given by Eq. 2.8 for the equilibrium (zero temperature) geometry. This expression shows that systems with the same donor and acceptor (and therefore same local modes) may present completely different temperature dependences, depending on the magnitude of the fluctuations of the "through-space" distance(s).

5. Conclusions

We have introduced two important new ideas. The first is the presentation of a consistent means of calculating rates in complex systems having both through-bond and through-space elements in the tunneling pathway. Application of this model to the calculation of electron transfer rates in real protein systems is a natural extension. The second is that the temperature dependence of electron transfer rates may arise from "bridge" (tunneling medium) modes in addition to local modes.

It is important to bear in mind that the temperature dependence of the rate that we find is due to fluctuations of the interactions *within* the bridging medium. It does not arise from fluctuations of the absolute donor-acceptor separation. The observed temperature dependence of electron transfer may have contributions from these modes as well as the standard contribution from vibrational modes coupled directly to the donor and acceptor.

Weak non-bonded interactions along the tunneling pathway cause tremendous attenuations in the decaying wave functions. It is, therefore, not surprising that large rate differences may exist in transfers over similar distances, driving forces, and energetic distances from the relevant "bands" for proteins compared to other (covalent and non-covalent) model systems.[1,11]

This model is especially suited to compare rates of protein mediated electron transfer in three classes of systems: (1) those with surface attached redox probes at different locations (see Ref. 3a and references therein), (2) those with fixed donors and acceptors and the"medium" modified by chemical means[12] or by site directed mutagenesis[3a], and (3) those with identifiable competing

electron transport pathways with different rates[13]. The determination of the dominant electron transfer pathway(s) in these systems is a challenge that will be taken in the future.

Appendix

Wave function decay along covalent pathways

The $E - \epsilon$ relation for the protein backbone ($C - C$ and $C - N$ bonds only) is:

$$\begin{vmatrix} (\alpha_N - E) & \gamma_N & 0 & 0 & 0 & \beta_{CN}^{(2)}/\epsilon \\ \gamma_N & (\alpha_N - E) & \beta_{CN}^{(3)} & 0 & 0 & 0 \\ 0 & \beta_{CN}^{(3)} & \alpha^{(3)} - E & \gamma_C^{(3)} & 0 & 0 \\ 0 & 0 & \gamma_C^{(3)} & \alpha^{(3)} - E & \beta_{CC} & 0 \\ 0 & 0 & 0 & \beta_{CC} & \alpha^{(2)} - E & \gamma_C^{(2)} \\ \beta_{CN}^{(2)}\epsilon & 0 & 0 & 0 & \gamma_C^{(2)} & (\alpha^{(2)} - E) \end{vmatrix} = 0 , \tag{A1}$$

where the (2) and (3) superscripts refer to sp^2 and sp^3 orbitals, respectively. The energy of the carbon sp^3 orbital, $\alpha^{(3)}$, is taken as the energy zero. Figs. A1 and A2 show plots of $\epsilon + 1/\epsilon$ vs. E and $\epsilon^{1/3}$ vs. E for the parameters in Table 1. Fig. A3 shows the orbitals in the protein backbone unit cell. For the $C - C$ and $C(sp^3) - N$ bonds -8.5 eV is a good estimate for β.[2e] A larger value is probably appropriate for the $C(sp^2) - N$ bond due to larger overlap and binding energies. We are working at such a crude level of theory, neglecting all (variable) side groups, so we use only one β in the calculation.

If we neglect backscattering between bonds, we can calculate the matrix element decay per bond in the protein. A "bond" includes the γ interaction immediately before the bond and

$$\epsilon_i = \frac{\gamma_i \beta}{(\alpha_i - E)(\alpha_{i+1} - E) - \beta^2} . \tag{A2}$$

In this limit, the decay per unit cell in the protein is the product of the three ϵ's for the bonds.

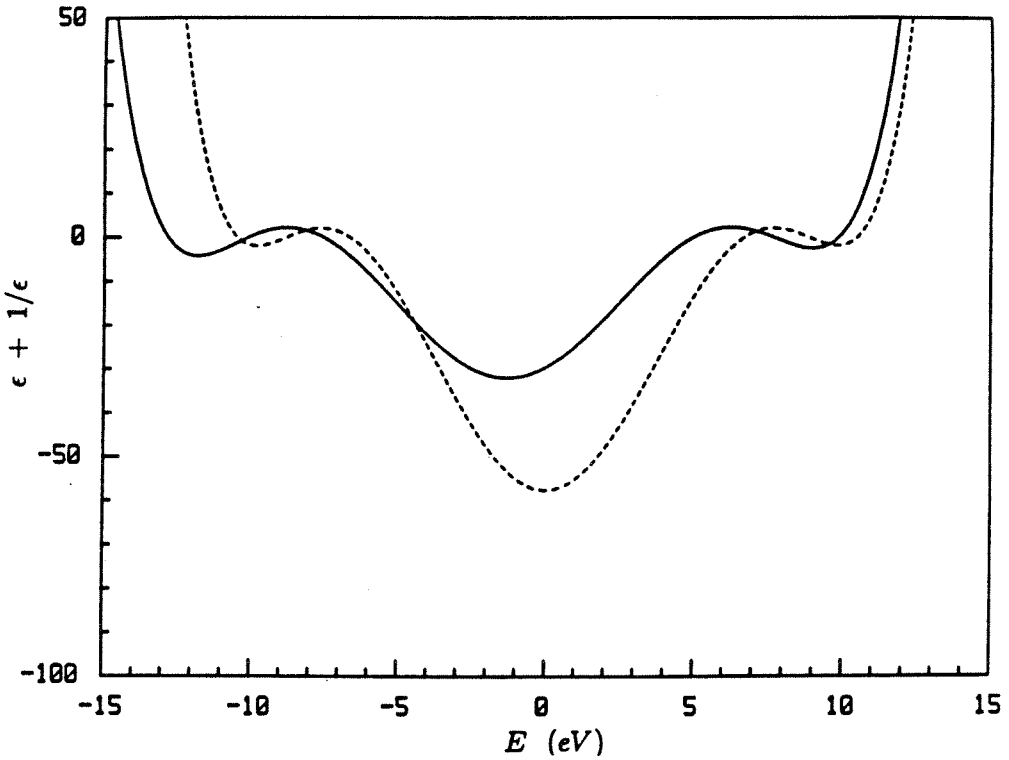

Figure A1 – $\epsilon + 1/\epsilon$ is plotted vs. energy for a six orbital per amino acid model for the protein backbone (solid line) and a two orbital per C-C bond model for the backbone of n-alkane (dashed line). The unit cells are: [N(sp^3), N(sp^3); C(sp^3), C(sp^3); C(sp^2), C(sp^3)] and [C(sp^3), C(sp^3); C(sp^3), C(sp^3); C(sp^3), C(sp^3)], respectively.

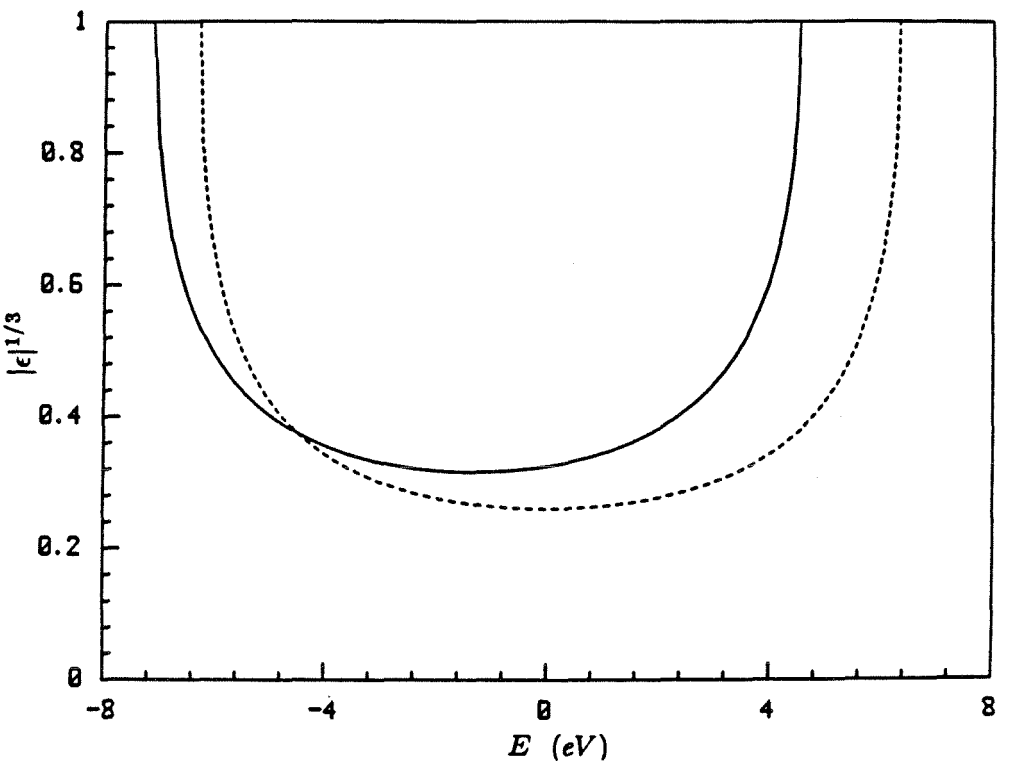

Figure A2 – $|\epsilon|^{1/3}$, the effective decay per bond for backbone tunneling, is plotted vs. energy in the band gap region for the six orbital per amino acid model for the protein backbone (solid line) and two orbital per C-C bond model (six orbitals per unit cell) for the backbone of n-alkane (dashed line).

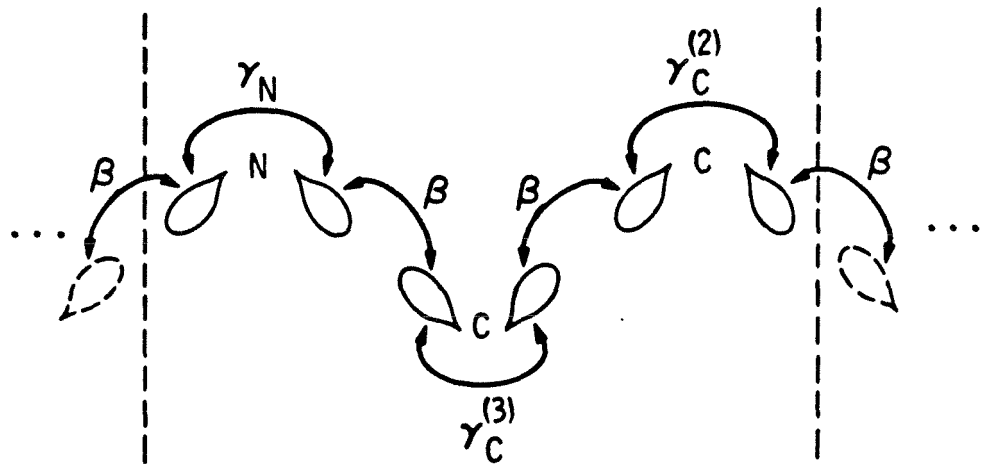

Figure A3 – Schematic representation for the orbitals in a protein backbone unit cell.

TABLE 1 - Orbital Parameters

Parameter	Energy(eV)
$\alpha^{(3)}$	0.00
$\alpha^{(2)}$	-0.70
α_N	-3.30
β	-8.50
$\gamma_C^{(3)}$	-2.20
$\gamma_C^{(2)}$	-2.93
γ_N	-3.10

From earlier work, we expect that most electron transfers at physiologically important redox potentials are mediated by the valence band of the protein. From Fig. A1, we see that the valence band edge is at about -7.1 eV. Therefore, we can check Eq. A2 for the protein backbone. For protein, Eq. A2 predicts a decay per unit cell of

$$\epsilon_1\epsilon_2\epsilon_3 = \left[\frac{\gamma_N\beta}{(\alpha_N - E)(\alpha^{(3)} - E) - \beta^2}\right] \times \left[\frac{\gamma^{(3)}\beta}{(\alpha^{(3)} - E)(\alpha^{(2)} - E) - \beta^2}\right]\left[\frac{\gamma^{(2)}\beta}{(\alpha^{(2)} - E)(\alpha_N - E) - \beta^2}\right], \qquad (A3)$$

where 1, 2, and 3 refer to $N(sp^3) - C(sp^3)$, $C(sp^3) - C(sp^2)$, and $C(sp^2) - N(sp^3)$ bonds, respectively. At $E = -5.5$ eV (1.5 eV from the band edge), this predicts a wave function decay of 14, compared to the exact band structure calculation (Eq. A1) which gives a decay of 12 per unit cell at this energy. Farther from the band (e.g., $E = -4.0$ eV), Eq. A3 predicts a decay of 23 compared to 22 for Eq. A1. This shows that neglect of backscattering gives a more rapid decay with distance than the exact result. However, it gives quite reasonable results and provides a prescription for including incomplete unit cells and aperiodic side groups in the calculation of the matrix element. This method defines a decay per bond, so when computing the rate, we need only determine the total number of each type of bond along the pathway of interest. Although this is simpler, we should use the band result (Eq. A1 and Fig. A2 in the case of protein) to calculate the wave function decay in long backbone segments.

This crude model for the protein backbone gives values for band widths and gaps on the order of those found in more extensive calculations of protein electronic structure.[14] The variations found in those calculations between proteins with different side groups or secondary structure are much smaller than

the precision that we can claim for our model. Also, side groups affect the band states more than the gap states (donor or acceptor states). For these reasons we can justify our periodic model for the backbone. Also, the validity of neglecting backscattering to give a per bond decay shows that contributions to the wave function decay from the pendant groups enter as higher order corrections to the decay.

Secondary and higher order structure will influence the quality of the periodic approximation for backbone tunneling if non-nearest neighbor interactions are important for the through-bond decay. If such interactions are determined to be important, this model will have to be improved to include these effects. Experience from model compound calculations (and other band structure calculations) suggests that these corrections are not essential to understand the main features of this problem.

A two orbital per site model of n-alkane gives

$$\det \begin{pmatrix} -E & \gamma + \beta/\epsilon' \\ \gamma + \beta\epsilon' & -E \end{pmatrix} = 0. \qquad (A4)$$

To compare this result directly to Eq. A1, we put all γ's equal to $\gamma^{(3)}$ and all α's equal to $\alpha^{(3)}$. Fig. A4 shows the orbitals in the n–alkane unit cell. This model may be useful for calculating decay in some protein side groups. The valence band edge occurs at -6.3 eV, using the parameters in Table 1. The decay of the wave function per three bonds at $E = -4.0$ eV ($\sim$ 2 eV from the band edge) is 25. Using the decay per bond equation for hydrocarbon (the analogue of Eq. A3), we predict a decay of 27. The offset of the ϵ per atom vs. E plots for protein and hydrocarbon is due mainly to the greater electron binding energy of nitrogen.

A one–band model for tunneling in a two-band system is appropriate when

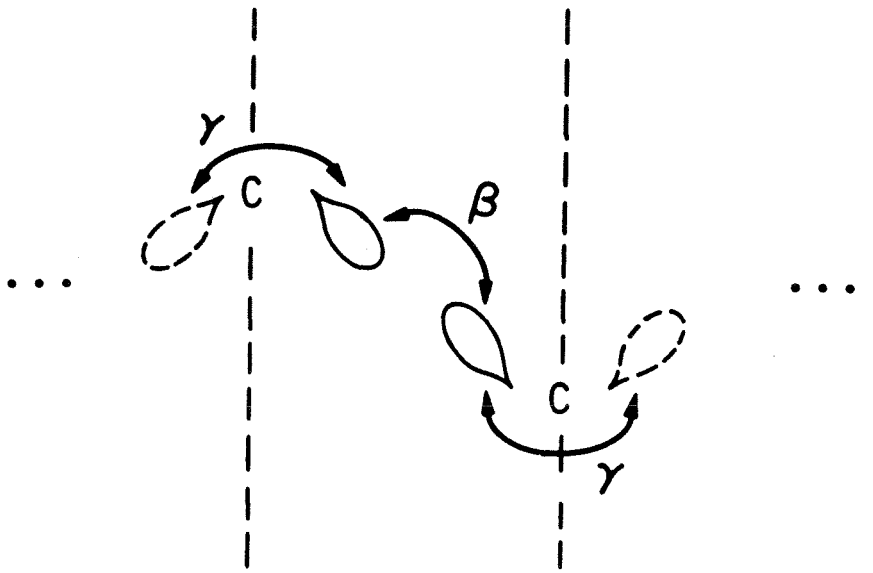

Figure A4 – Schematic representation for the orbitals in an n–alkane unit cell.

the interactions in each cell split the backbone states into bands well separated (their centers are at $\pm\beta$) in energy relative to their widths ($2|\gamma|$) and the donor (band gap) state lies close to one of the bands. This condition is $|E-\beta| \ll |\beta|$. The wave function decay, when $\gamma^2 \ll \beta^2$ in the small backscattering limit, is

$$\epsilon' = \frac{\beta\gamma}{(E-\beta)(E+\beta)} \simeq \frac{-|\gamma|}{2(E+|\beta|)}. \qquad (A5)$$

This is exactly the one band limit for wave function decay previously discussed[2a]. For the more general case of different atoms in the unit cell, if β is large enough,

$$\epsilon_i = \frac{\gamma_i\beta}{(E-\alpha_i)(E-\alpha_{i+1})-\beta^2}$$

$$= \frac{\gamma_i\beta}{\prod_{k=1,2}\left(E-\left(\frac{\alpha_i+\alpha_{i+1}}{2}\right)+(-1)^k\sqrt{\beta^2+\left[\frac{(\alpha_i-\alpha_{i+1})}{2}\right]^2}\right)}$$

$$\simeq \frac{\gamma_i/2}{E-(\alpha_i+\alpha_{i+1})/2-\beta} \qquad (A6)$$

for $E<0$ and $\beta<0$.

As an example, consider pentaamine(histidine) Ru(II/III)- ferricytochrome c, (III/II) studied by Gray and co-workers. The mean redox potential of the sites is +0.175 V vs. NHE. Converting to our energy scale (normalized as in Ref. 2e, but for the current parameters) we find a tunneling energy on the orbital energy scale of -5.3 eV (Eq. 2.8). This corresponds to $\epsilon_1 = -0.427$, $\epsilon_2 = -0.391$, $\epsilon_3 = -0.395$, and $\epsilon_1\epsilon_2\epsilon_3 = -1/15$. These three values are calculated with Eq. A6. From Eq. A1 or Fig. A1, at $E = -5.3$ eV ϵ(per amino acid) $= -1/13$. Wave function decay in n-alkane at this tunneling energy is -0.46 (exact result) and -0.42 (neglecting backscattering) per $C-C$ bond.

To conclude the discussion of the parameters, we point out that the interaction parameters presented here are an initial set, which may need to be adjusted when calculations on real proteins are performed. As discussed earlier in the appendix, this set gives reasonable band widths and gaps. Even more crucial than the interaction parameters is the choice of the tunneling energy (redox energy of the transferring electron). We have selected this scale from model system experiments. In the future this scale will receive further study.

Acknowledgments

We thank Brian Hoffman and Harry Gray for inspirational discussions, which initiated this work. The research presented in this paper was performed while D.N.B. held a NRC-NASA Resident Research Associateship at the Jet Propulsion Laboratory, California Institute of Technology. Support was also provided by the National Science Foundation (Grant No. PCM-8406049) and by the Brazilian Agency Conselho Nacional de Desenvolvimento Científico e Tecnológico–CNPq.

References

(1) (a) B.A. Leland, A.D. Joran, P.M. Felker, J.J. Hopfield, A.H. Zewail, and P.B. Dervan, *J. Phys. Chem.* **89**, 5571 (1985); (b) S.S. Isied *Prog. Inorg. Chem.* **32**, 443 (1984); (c) H. Heitele and M.E. Michel–Beyerle, *J. Am. Chem. Soc.* **107**, 8286 (1985); (d) M.R. Wasielewski and M.P. Niemczyk, *J. Am. Chem. Soc.* **106**, 5043 (1984); (e) D.E. Richardson and H. Taube, *J. Am. Chem. Soc.* **105**, 40 (1985); (f) G.L. Closs, L.T. Calcaterra, N.J. Green, K.W. Penfield, and J.R. Miller, *J. Phys. Chem.* **90**, 3673 (1986); (g) J. Verhoeven *J. Pure and Appl. Chem* **58**, 1285 (1986); (h) C.A. Stein, N.A. Lewis, and G.J. Seitz, *J. Am. Chem. Soc.* **104**, 2596 (1982).

(2) (a) D.N. Beratan, J.N. Onuchic, and J.J. Hopfield, *J. Chem. Phys.* **83**, 5325 (1985); (b) S. Larsson, *J. Chem. Soc., Faraday Trans. 2* **79**, 1375 (1983); (c) D.N. Beratan *J. Am. Chem. Soc.* **108**, 4321 (1986); (d) K. Ohta, G.L. Closs, K. Morokuma, and N.J. Green, *J. Am. Chem. Soc.* **108**, 1319 (1986); (e) D.N. Beratan and J.J. Hopfield, *J. Am. Chem. Soc.* **106**, 1584 (1984).

(3) (a) S.L. Mayo, W.R. Ellis, R.J. Crutchley, and H.B. Gray, *Science* **233**, 948 (1986); (b) S.E. Peterson–Kennedy, J.L. McGourty, J.A. Kalweit, and B.M. Hoffman, *J. Am. Chem. Soc.* **108**, 1739 (1986); (c) G. McLendon and J.R. Miller, *J. Am. Chem. Soc.* **107**, 7811 (1985); (d) S.G. Boxer, *Biochim. Biophys. Acta* **726**, 265 (1983).

(4) (a) J.J. Hopfield, *Proc. Nat. Acad. Sci. (USA)* **7**, 3640 (1974); (b) P. Siders, R.J. Cave, and R.A. Marcus, *J. Chem. Phys.* **81**, 5613 (1984).

(5) J.N. Onuchic, D.N. Beratan, and J.J. Hopfield, *J. Phys. Chem.* **90**, 3707 (1986).

(6) J.N. Onuchic and A.A.S. da Gama, *Theor. Chim. Acta* **69**, 89 (1986).

(7) D.N. Beratan and J.J. Hopfield, *J. Chem. Phys.* **81**, 5753 (1984).

(8) (a) D.DeVault, *Quantum Mechanical Tunneling in Biological Systems*, 2nd edition; Cambridge Univ. Press: New York, 1984; (b) J. Jortner, *J. Chem. Phys.* **64**, 4860 (1976).

(9) A. Messiah, *Quantum Mechanics*, vol. 1; John Wiley & Sons: New York, 1958, p.449.

(10) (a) K. Yates, *Hückel Molecular Orbital Theory*; Academic Press: New York, 1971; (b) C.J. Ballhausen and H.B. Gray, *Molecular Orbital Theory*; Academic Press: New York, 1978.

(11) (a) J.R. Winkler, D.G. Nocera, K.M. Yocom, E. Bordignon, and H.B. Gray, *J. Am. Chem. Soc.* **106**, 5145 (1984); (b) J.R. Miller, J.V. Beitz, and R.K. Huddleston, *J. Am. Chem. Soc.* **106**, 5057 (1984).

(12) B.M. Hoffman, personal communication.

(13) J. Deisenhofer, O. Epp, K. Miki, R. Huber, and H. Michel, *Nature* **318**, 618 (1985).

(14) (a) J. Ladik, M. Seel, P. Otto, A.K. Bakhshi, *Chem. Phys.* **108**, 203 (1986); (b) P. Otto, A.K. Bakhshi, J. Ladik, M. Seel, S. Chin, *Chem. Phys.* **108**, 223 (1986); (c) A.K. Bakhshi, J. Ladik, M. Seel, P. Otto, *Chem. Phys.* **108**, 233 (1986).

III.5 Influence of Intersite Modes on the Exchange Interaction in Electron Transfer at Large Distances

Theor. Chim. Acta **69**, 89 (1986)

Theor Chim Acta (1986) 69: 89-100

Theoretica Chimica Acta

Influence of intersite modes on the exchange interaction in electron transfer at large distances*

J. N. Onuchic and A. A. S. da Gama*****

Division of Chemistry and Chemical Engineering******, California Institute of Technology, Pasadena, CA, 91125, USA

(Received April 25, revised August 23/Accepted October 30, 1985)

We consider the dependence of the exchange interaction in electron transfer processes on the intersite vibrational modes. We assume, in particular, that high-frequency intramolecular modes of proteins may play this role in biological processes. We compare our model with that for tunneling through a time dependent barrier and with other works which considered the dependence of the exchange interaction on the nuclear coordinates.

Key words; Electron transfer — Metalloproteins — Medium influence in the electronic matrix element

1. Introduction

In this work we are concerned with electron transfer over large distances in biological systems, particularly proteins. In some circumstances, for example, when mixed valence or excited species are present electron transfer can take place between two localized electronic states [1, 2].

Electron localization or delocalization has been a subject of subtle interest in physics [3], chemistry [4] and biology [5] for many years. Mixed valence compounds, for example, have been classified [4] and experimentally identified [6]

* Work partially supported by the Brazilian Agency CNPq and by the NSF (Grant PCM-8406049)

** On leave of absence from Instituto de Física e Química de São Carlos, Universidade de São Paulo, 13560, São Carlos, SP, Brazil

*** On leave of absence from Departamento de Física, Universidade Federal de Pernambuco, 50000, Recife, Pe, Brazil

**** Contribution No. 7325

as completely localized (or delocalized) and partially localized, where localization or delocalization depends on the electronic interaction between the two "localized" wave functions and on the magnitude of the vibronic coupling on each trapping site. The interesting regime to be explored is the one where localization can be characterized within the time scale of some experimental measurement, and the transfer rate between the two trapping sites can be measured.

There are two proposed mechanisms for electron transfer. In one of them the transfer rate is a function of the small overlap of the two spatially localized wave functions (through space mechanism) [2]. In the other mechanism, bridging groups significantly enhance the effective overlap between the localized functions (through bond mechanism) [7]. At specially large distances, this second mechanism may assume special importance. Depending on the energy of the localized state relative to some "medium" extended states, and on the electronic hopping interaction between the bridging units, the "through bond" wave function decay with distance may be slower than the direct interaction. The role of this kind of essentially superexchange mechanism has been discussed in great detail in the recent literature [7–9]. The main aim of the present work is to discuss the possibility of the influence of the intersite "medium" modes on the electronic interaction, which can be "through space" or "through bond", since, for the latter, an effective interaction, which replaces the direct interaction, may be defined [9].

Electron migration at large distances has been observed in biological systems. Particular interest has been devoted to the photosynthetic system [1, 2]. Heme proteins, and some other systems with well established molecular structure, have been used in recent intramolecular electron transfer experiments [10–12].

In large biological systems, like proteins with mixed valence sites, the polypeptide chain has been proposed to play the role of bridging group in a "through bond" mechanism. Since the protein chain can be modeled as a 1-D periodic structure, it has been treated by solid state techniques to investigate general feature of the system [13].

To advance a theoretical model for electron migration in this kind of system we should start with a simplified model. There are, actually, three main theories for thermal electron transfer processes [1, 2]: the classical Marcus' theory [14], the semi-classical model developed by Hopfield [15] and the quantum one, first formulated by Levich, Dogonadze and collaborators [16] and later by Jortner and collaborators [17]. The differences among them are basically in the way each one treats the "nuclear" coordinates. By nuclear coordinates we mean nuclear vibrations and librations, solvent motion and any other "slow" effect which may be coupled to the transfer process. A good discussion of the differences between the electron transfer theories was presented in a recent review by Marcus [18].

All these theories have a strong relationship with the theories of radiationless processes [19] and transport of small polarons [20]. The small polaron theory follows from the molecular crystal model, which assumes negligible overlap between neighboring sites. In this model, the electron-lattice interaction plays

the role of trapping the electron by lowering the site energy when the electron is present.

Biological systems are quite complex. The states of such systems must be described by statistical operators or density matrices. Due to the large number of degrees of freedom, a dynamical description of these systems using the above theories seems to be impossible. However many processes are associated with changes in a small number of degrees of freedom, weakly coupled to the others, in an essentially irreversible process [15, 17, 21, 22]. De Vault has called attention to the special role of vibronic coupling via high-frequency modes ($\sim 400\,\mathrm{cm}^{-1}$) in biological electron transfer processes [2].

At large distances, the electron transfer process has been assumed in the conventional theories to be non-adiabatic and to respect the Franck-Condon principle. Because of the latter the electronic exchange interaction is assumed to be important for only a single nuclear configuration.

The applicability of the Born-Oppenheimer and Condon approximations to electron transfer at large distances has been questioned [23]. For very weak electronic exchange matrix elements ($\sim 10^{-4}$ eV) the influence of nuclear coordinates on this interaction energy may be of some importance. In this work we consider the influence of the intersite and intrasite modes on these matrix elements. These two types of modes are considered separately, but the influence of them together is an important problem to be studied as an extension of the present model.

2. Theoretical model

In order to obtain a reasonable model for electron migration in molecules of biological interest we shall start with a simple model and later improve it. As we already discussed, an intramolecular electron transfer between two well localized states(sites) is considered. Because we are working in the Born-Oppenheimer approximation, and considering a one electron problem, the Hamiltonian depends only parametrically on the nuclear coordinates, i.e.,

$$\mathbf{h}_{el} = h_{el}(x; \vec{X}_1, \vec{X}_2, \vec{X}_b) \tag{1}$$

where x is the electronic coordinate and $\vec{X}_1$, $\vec{X}_2$ and $\vec{X}_b$ are the nuclear coordinates of the localized modes on site 1 and site 2, and the intersite modes, respectively.

Each site is characterized by a one electron energy level plus all the localized vibrational modes. The one electron model is used because it has been shown to be adequate to describe the general features of the distant electron transfer problem, which is dependent on the long-range tail of the wave function [24]. On site 1, for example

$$H_{site1} = \varepsilon_1(\vec{X}_1) a_1^\dagger a_1 + \sum_i \hbar\omega_i (b_i^\dagger b_i + 1/2) \tag{2}$$

where $a\dagger(a)$ and $b\dagger(b)$ are respectively fermion and boson creation (anihilation) operators. The one electron energy parameter is defined as

$$\varepsilon_1(\vec{X}_1) = \int \varphi_1^*(x; \vec{X}_1)\mathbf{h}_{el}\varphi_1(x; \vec{X}_1)\, dx \tag{3}$$

where the site energy ε_1 and the site localized wavefunctions are assumed dependent only on the localized site modes.

Using the linear approximation for the expansion of $\varepsilon_1(\vec{X}_1)$ in the nuclear coordinates we obtain the "small polaron" term, i.e.,

$$\varepsilon_1(\vec{X}_1) = \varepsilon_1 + \sum_i g_i \hbar\omega_i (b_i^\dagger + b_i) \tag{4}$$

and define the electron-vibration constant as usual [25]

$$g_i = (2/M_i\hbar\omega_i^3)^{1/2}[\partial\varepsilon_1(\vec{X}_1)/\partial X_i]|X_i^0 \tag{5}$$

where X_i^0 is the equilibrium displacement of normal mode i without coupling. The "polaron" term changes the equilibrium position and energy of the site localized modes depending on whether or not the electron is on the site.

To allow the transfer of the electron between the two centers we shall include an intersite exchange perturbation

$$H_{int} = V_{12}(\vec{X}_1, \vec{X}_2, \vec{X}_b)(a_1^\dagger a_2 + a_2^\dagger a_1) \tag{6}$$

where the two centers electronic integral is

$$V_{12}(\vec{X}_1, \vec{X}_2, \vec{X}_b) = \int \varphi_2^*(x; \vec{X}_2)\mathbf{h}_{el}\varphi_1(x; \vec{X}_1)\, dx. \tag{7}$$

Putting all of the above parts together, including the energy term of the intersite modes, we obtain

$$\begin{aligned} H = {} & \varepsilon_1 a_1^\dagger a_1 + \varepsilon_2 a_2^\dagger a_2 \\ & + \sum_{i(site1)} [\hbar\omega_i(b_i^\dagger b_i + 1/2) + g_i\hbar\omega_i(b_i^\dagger + b_i)a_1^\dagger a_1] \\ & + \sum_{j(site2)} [\hbar\omega_j(b_j^\dagger b_j + 1/2) + g_j\hbar\omega_j(b_j^\dagger + b_j)a_2^\dagger a_2] \\ & + \sum_{k(bridge)} \hbar\omega_k(b_k^\dagger b_k + 1/2) + \sum_{i,j,k} V_{12}(X_i, X_j, X_k)(a_1^\dagger a_2 + a_2^\dagger a_1). \end{aligned} \tag{8}$$

In this work we intend to discuss the dependence of V_{12} on the nuclear coordinates. It is important to mention that previous works, by Ratner [25] in particular, considered the dependence of V_{12} on the nuclear coordinates. We will compare our results with the previous ones. We are also going to discuss our model in light of a result obtained by Buttiker and Landauer [26] for tunneling through a time modulated barrier, i.e.

$$V(x, t) = V_0(x) + V_1(x)\cos\omega t. \tag{9}$$

In the next section we solve two simple cases of Eq. (8): V_{12} dependent only on one site localized mode, and V_{12} dependent on one intersite mode. We will discuss how the dependence of V_{12} on the nuclear coordinate can be considered as a modulation of the zero order intersite exchange interaction and the different results when fast or slow intersite modes are coupled to the electron transfer.

3. A simple application

As a first application we consider only one localized vibration, on one of the two sites, and we suppose this nuclear coordinate affects V_{12}. This dependence of V_{12} on the localized nuclear coordinates has already been considered by Ratner [25] as $V_{12} = V_{12}(X_1 - X_2)$, where X_1 and X_2 are the coordinates of the localized vibrations at the center 1 and 2, respectively.

The two site Hamiltonian with one localized mode on site 1 is

$$H = \varepsilon_1 a_1^\dagger a_1 + \varepsilon_2 a_2^\dagger a_2 + g\hbar\omega(b_1^\dagger + b_1)a_1^\dagger a_1 + \hbar\omega(b_1^\dagger b_1 + 1/2) + V_{12}(X_1)(a_1^\dagger a_2 + a_2^\dagger a_1). \tag{10}$$

A picture of the two localized sites is shown in Fig. 1.

Since we have only a linear correction from the "polaron" coupling we can define

$$\hbar\omega(b_1^\dagger b_1 + 1/2) + g\hbar\omega(b_1^\dagger + b_1) = \hbar\omega(b_*^\dagger b_* + 1/2) + \Delta\varepsilon \tag{11}$$

where $b_*^\dagger(b_*)$ are the boson operators for the shifted oscillator, when the electron is on the donor, and for reasons of convenience, we include $\Delta\varepsilon$ in ε_1. Then we can write the time dependent eigenfunctions for each center as

$$\begin{aligned} &\textit{site } 1\text{:} |n, 1\rangle = (n!)^{-1/2} \exp\{-i[\varepsilon_1 + (n+1/2)\hbar\omega]t/\hbar\} b_*^{\dagger n} a_1^\dagger |0\rangle \\ &\textit{site } 2\text{:} |m, 2\rangle = (m!)^{-1/2} \exp\{-i[\varepsilon_2 + (m+1/2)\hbar\omega]t/\hbar\} b_1^\dagger a_2^\dagger |0\rangle \end{aligned} \tag{12}$$

where n and m represent the number of vibrational quanta in the harmonic oscillator.

By using time dependent perturbation theory, and then Fermi's golden rule, we evaluate the transition rate from the initial thermally averaged states $|n, 1\rangle$ to a manifold of final states $\{|m, 2\rangle\}$.

$$k = (2\pi/\hbar) \sum \rho(n) |\langle m | v_{12}(X_1) | n \rangle|^2 \delta[(\varepsilon_1 + n\hbar\omega) - (\varepsilon_2 + m\hbar\omega)] \tag{13}$$

where $\rho(n)$ is the thermal density of initial states.

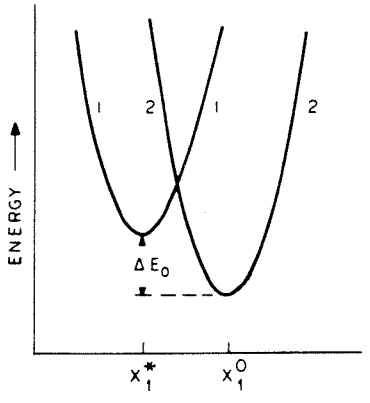

Fig. 1. A diagramatic representation of the two localized states

X_1^* – Is the minimum energy position when the eletron is insite 1

This result is equivalent to the one obtained by Ratner [25].

It is useful to assume at this point that the localized modes do not influence the exchange interaction, i.e., X_1 is treated in the Condon approximation. The dependence of V_{12} on one intersite nuclear coordinate (X_b) is now considered. Assuming we have one localized mode X_1 and one intersite mode X_b, V_{12} is expanded to first order in the intersite coordinate

$$V_{12}(X_b) = V_{12}^0 + V_{12}^{b-} - b_b^\dagger + V_{12}^{b+} b_b \tag{14}$$

where we make a Condon approximation for the X_1 coordinate. The difference between V_{12}^{b-} and V_{12}^{b+} is due to the dependence of the integral over the electronic coordinate (Eq. 7) on the nuclear configuration.

Then, we obtain the following Hamiltonian:

$$\begin{aligned} H = {} & \varepsilon_1 a_1^\dagger a_1 + \varepsilon_2 a_2^\dagger a_2 + g\hbar\omega(b_1^\dagger + b_1) a_1^\dagger a_1 + \hbar\omega(b_1^\dagger b_1 + 1/2) \\ & + \hbar\omega_b(b_b^\dagger b_b + 1/2) + [V_{12}^0 + V_{12}^{b-} b_b^\dagger + V_{12}^{b+} b_b](a_1^\dagger a_2 + a_2^\dagger a_1). \end{aligned} \tag{15}$$

The time dependent eigenfunctions for the two states are:

$$\begin{aligned} |n_b, n, 1\rangle = {} & (n_b! n!)^{-1/2} \exp\{-i[\varepsilon_1 + (n+1/2)\hbar\omega \\ & + (n_b + 1/2)\hbar\omega_b]t/\hbar\} b_b^{\dagger n_b} b_*^{\dagger n} a_1^\dagger |0\rangle \\ |m_b, m, 2\rangle = {} & (m_b! m!)^{-1/2} \exp\{-i[\varepsilon_2 + (m+1/2)\hbar\omega + (m_b + 1/2)\hbar\omega_b]t/\hbar\}. \\ & \cdot b_b^{\dagger m_b} b_1^{\dagger m} a_2^\dagger |0\rangle \end{aligned} \tag{16}$$

and the transition rate

$$\begin{aligned} k = {} & 2\pi/\hbar \sum_{n_b, m_b} \rho(n_b) \sum_{n,m} \rho(n) |V_{12}^0 \langle m|n\rangle|^2. \\ & \cdot \delta[(\varepsilon_1 + n\hbar\omega) - (\varepsilon_2 + m\hbar\omega)] + [|V_{12}^{b-} \langle m|n\rangle\langle m_b|b_b^\dagger|n_b\rangle|^2 \\ & + |V_{12}^{b+} \langle m|n\rangle\langle m_b|b_b|n_b\rangle|^2]. \\ & \cdot \delta[(\varepsilon_1 + n\hbar\omega) - (\varepsilon_2 + m\hbar\omega) + \hbar\omega_b(n_b - m_b)] \end{aligned} \tag{17}$$

where $\rho(n_b)$ is the initial thermal density of states of the bridging modes.

Looking carefully at the result of the above equation we can think about this problem forgetting the bridging modes and considering a time dependent exchange interaction, i.e.

$$V_{12} = V_{12}^0 + V_{12}^- \exp(i\omega_b t) + V_{12}^+ \exp(-i\omega_b t) \tag{18}$$

where $+/-$ is associated with absorption/emission of a vibrational quantum during the transition. We define

$$V_{12}^+ = V_{12}^{b+}\sqrt{\overline{n_b}} \quad \text{and} \quad V_{12}^- = V_{12}^{b-}\sqrt{\overline{n_b} + 1} \tag{19}$$

where $\overline{n_b} = [\exp(\hbar\omega_b/kBT) - 1]^{-1}$ is the average number of phonons in the harmonic oscillator.

The difference between V_{12}^{+} and V_{12}^{-} is due to the dependence of the integral over the electronic coordinate on the nuclear configuration. In the classical limit $\bar{n}_b \gg 1$ ($k_b T \gg \hbar\omega_b$), and without integrating over the electronic coordinate, the potentials in Eqs. (9) and (19) are equivalent. The relationship between the matrix elements of $V_{12}^{\pm}$ and V_{12}^{0} can be used to get some insight about the interaction of the "traveling" electron and the intersite medium mode.

The simplest model for electron transfer considers tunneling through a static barrier between two symmetric square wells separated by a distance R (symmetric because the energy for both sites is the same in the crossing point), as it is shown in Fig. 2. In our case instead of considering only a static barrier we include an oscillatory term $(V_1/2)(b_b^{\dagger}+b_b)$ for the coupling between the electronic and nuclear coordinate, i.e. a similar situation to the one considered by Buttiker and Landauer in [26]. Following Redi and Hopfield [27] we use the following wave functions for the barrier region between the two wells

$$\psi_1 = (2k_0^2/a\chi_1^2)^{1/2} \exp[-\chi_1(x+R/2)]$$
$$\psi_2 = (2k_0^2/a\chi_2^2)^{1/2} \exp[+\chi_2(x-R/2)] \tag{20}$$

where k_0^2 (E_0 in Fig. 2) is the energy of the infinite square well in units of $\hbar^2/2m$, R is the separation between the wells, a is the size of the wells, and χ_1^2, χ_2^2 are the binding energies of sites 1 and 2 respectively. Assuming the deep well condition $a\chi \gg 1$ (there is almost all particle density inside the well), for the static barrier (symmetric wells) the tunneling matrix element can be evaluated using Bardeen's transmission current [27];

$$V_{12}^{0} = (2\hbar^2 k_0^2/m\chi a) \exp(-\chi R) \tag{21}$$

The tunneling matrix elements for the time dependent barrier can be obtained by changing the energy of one well by $\pm\hbar\omega_b$ (for example, in the Hamiltonian of Eq. (15), it is the donor energy), and using perturbation theory. The results

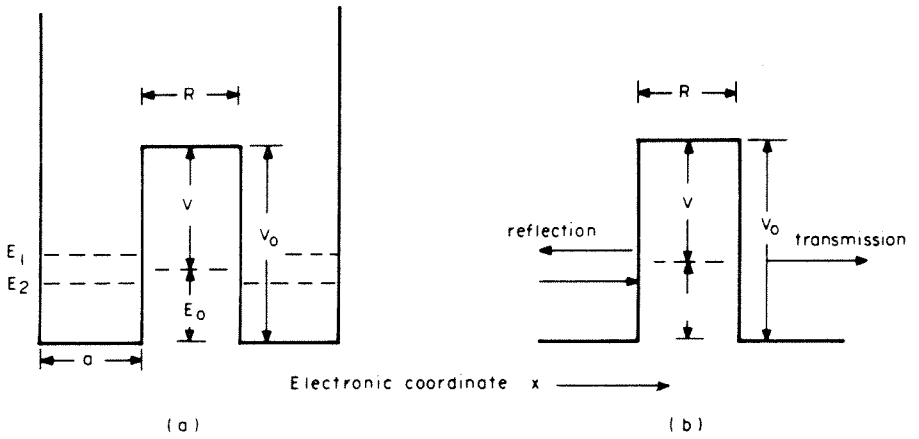

Fig. 2. a Two square wells model for electron transfer.
b Tunneling through a square barrier

obtained, shown in the next equation, can be related to the time independent matrix element by assuming $\hbar\omega_b \ll V, E_0$ (typical values for biological problems are of $\hbar\omega_b \simeq 400\ \text{cm}^{-1} = 0.05$ eV and $V \sim 2$ eV [27]):

$$\begin{aligned} V_{12}^{b\pm} &= \langle \psi_2(\chi_2) | V_1/2 | \psi_1(\chi_1) \rangle \\ &= \langle \psi_2(\hbar^2\chi_2^2/2m) | V_1/2 | \psi_1(\hbar^2\chi_2^2/2m \pm \hbar\omega_b) \\ &\sim \pm (V_1/2\hbar\omega_b)[1 - \exp(\mp mR\omega_b/\hbar\chi)] V_{12}^0 \end{aligned} \tag{22}$$

where $mR/\hbar\chi = \tau$ is the traversal time defined by Buttiker and Landauer [26] and χ_2 is equal to χ in Eq. (21).

The relation between ω_b and τ^{-1} determines the influence of the barrier modulation. At low frequencies ($\omega_b \ll \tau^{-1}$) the tunneling electron sees a static barrier. At high frequencies ($\omega_b \gg \tau^{-1}$) the tunneling occurs through an averaged barrier of mean height V_0. It is important to recall that this is valid only for this specific electronic interaction and more generally we must recognize that V_{12}^0 and $V_{12}^{\pm}$ are dependent on the model assumed for this interaction. Furthermore, the source for the barrier oscillation in our model is the electron-phonon interaction, then $V_{12}^{\pm}$ is proportional to the amplitude of vibration of the bridge coordinate, and the transmission coefficient for absorption or emission is temperature dependent.

To obtain the final rate equation we have to use a distribution function for the intrasite mode and work out the sum over the Franck-Condon overlap integrals. From Eq. (17-19) we can write each contribution as

$$k = (2\pi/\hbar)|V_{12}^{0,\pm}|^2 \sum_{n,m} |\langle m|n\rangle|^2 \rho(n) \cdot \delta[\Delta E_{0,\pm} + (n-m)\hbar\omega] \tag{23}$$

where $\Delta E_0 = \varepsilon_1 - \varepsilon_2$ and $\Delta E_{\pm} = \Delta E_0 \pm \hbar\omega_b$.

Following the conventional procedure we use the generating function method [19] and write Eq. (23) in the form

$$k = (|V_{12}^{0,\pm}|^2/\hbar^2) \exp(-G_0) \int_{-\infty}^{+\infty} dt \exp\left[-i(\Delta E_{0,\pm} t/\hbar) + G_+(t) + G_-(t)\right] \tag{24}$$

where

$$G_+(t) = (\Delta^2/2)(\bar{n}+1) \exp(i\omega t)$$

$$G_-(t) = (\Delta^2/2)\bar{n} \exp(-i\omega t)$$

$$G_0 = G_+(0) + G_-(0) = (\Delta^2/2)(2\bar{n}+1)$$

and Δ is the reduced displacement of the two site curves ($X_1^0 - X_1^{*}$) at Fig. 1. The reorganization energy of the intrasite nuclear coordinates can be expressed in terms of Δ as $E_r = \hbar\omega(\Delta^2/2)$. G_0 is often used as a parameter to quantify the magnitude of the vibronic coupling. Analytical expressions for k are in general obtained at the weak coupling limit ($G_0 \leq 1$) or at the strong coupling limit ($G_0 \gg 1$). From Jortner [17] we can obtain for the weak coupling limit (small reorganization energy, $E_r \leq \hbar\omega$ and/or low-temperature $k_B T \ll \hbar\omega$):

$$k = (2\pi|V_{12}^{0,\pm}|^2/\hbar^2\omega)(\bar{n}+1)^p \exp(-G_0)[(\Delta^2/2)^p/p!] \tag{25}$$

where $p = \Delta E_{0,\pm}/\hbar\omega$ is the reduced effective energy gap (assumed to be an integer). For $p \geq 2$ the use of the Stirling approximation for $p!$ is quite good and k can be expressed as

$$k = (2\pi|V_{12}^{0,\pm}|^2/\hbar^2\omega)\exp(-G_0)\exp(-\gamma p)/(2\pi p)^{1/2} \tag{26}$$

where $\gamma = \ln[p/(\Delta^2/2)(\bar{n}+1)] - 1$, for $\gamma > 0$ Eq. (26) expresses the energy gap law for radiationless processes.

The strong coupling limit (large reorganization energy and high temperature) reproduces the well-known activated rate equation:

$$k = (2\pi|V_{12}^{0,\pm}|^2/\hbar)(4\pi E_r k_B T^*)^{-1/2}\exp(-E_A^{0,\pm}/k_B T^*) \tag{27}$$

where the effective temperature is defined by $k_B T^* = (\hbar\omega/2)\coth(\hbar\omega/2k_B T)$ and the activation energy is $E_A^{0,\pm} = (\Delta E_{0,\pm} - E_r)^2/4E_r$. This result can also be obtained by semiclassical approximation [15] and the classical expression [14] is reproduced at sufficiently high temperatures ($k_B T \gg \hbar\omega$) when $k_B T^* = k_B T$.

4. Discussion

In this model we consider the possible influence of intersite "medium" modes on the exchange interaction (transfer matrix) of electron transfer processes. High-frequency intramolecular modes of the protein may play a special role in this "phonon assisted" transfer matrix in biological systems, i.e., the electron may be interacting with the nuclear bridging modes "while travelling" between the two trapping sites.

The coupling of the two sites to a common boson field is considered as a way to describe inelastic tunneling [28]. However, the time dependent transfer matrix leads to a different physical interpretation. The intrasite and the intersite modes play different roles in the process. In some ways this separation is similar to the one of promoting and accepting modes in the theory of radiationless processes [29]. Indeed the intrasite modes are identified as the accepting modes. The main effect of the vibronic coupling is included on the unperturbed Hamiltonian to describe the initial and final states and the intrasite modes are the ones directly coupled to the donor and acceptor centers. The intersite modes may be less sensitive to the change of charge on the two localized sites. However, in particular for electron transfer at large distances, the "electron traveling time" may be sufficiently long to make the electron-bridging modes interaction effective. To avoid higher orders of perturbation, the "promoting factor" is considered a one-phonon mechanism. The first consequence is that the conventional multiphonon factor changes only by one order ($p \pm 1$ − phonon process), and it is assigned to the intrasite modes. The second consequence is that "V_{12}" is no longer a pure electronic factor, i.e. $V_{12}^{\pm}$ are related to the vibronic coupling between the "traveling electron" and the bridging modes. The magnitude of the effect depends on V_1, which is related to the intersite mode vibronic coupling, and on the relation between ω_b and τ^{-1} in Eq. (22). For typical values of barrier height, for example, 1.5 eV, at a distance of 13 Å, and with $\hbar\omega_b = 400\,\mathrm{cm}^{-1}$, if

$V_1/2\hbar\omega_b = 10$, this effect is significantly large. However, much more experimental and theoretical work is necessary for a clearer interpretation of the mechanism of intersite mode vibronic coupling and, therefore, to obtain reasonable estimates for these parameters.

The separation of nuclear vibrations in low- and high-frequency modes has often been used in the electron transfer theory ([17], for example). However, in this work only high-frequency modes are considered because for slow-modes the validity of the non-adiabatic limit is questionable, and this is not a point we intend to discuss here.

The contribution of the term corresponding to phonon emission (with V_{12}^- and ΔE_- in Eq. (23), in particular the effect of spontaneous emission ($\overline{n_b} = 0$ in Eq. (19)), can be important when we consider some electron transfer processes on the region of validity of the "energy gap law". These processes are predicted to occur when the electron transfer is associated with a small reorganization of the nuclear coordinates [30]. In this "weak coupling limit" the electron transfer rate can display weak temperature dependence, in particular for small energy gaps. Temperature dependence of radiationless transitions in this limit has been observed experimentally to be associated with the factor $(\bar{n}+1)^p$ [31]. In biological electron transfer, weak coupling limits may be observed when the metal sites are buried inside the protein pocket, protected from interaction with a polar medium [30]. The reorganization of the first coordination shell, here associated with the intrasite mode, has been observed to be small for $Ru^{II/III}(bpy)_3$ and $Ru^{II/III}(NH_3)_6$ [32]. $Ru(NH_3)_5$-histidine modified azurin, for example, was observed to have a weak temperature dependent intramolecular electron transfer rate from -10°C to 60°C [11].

In Fig. 3, we show the dependence of the electron transfer rate on the energy gap for the terms in ΔE_0 and ΔE_- within the weak coupling limit. The two contributions have to be summed up and the absolute magnitudes will depend

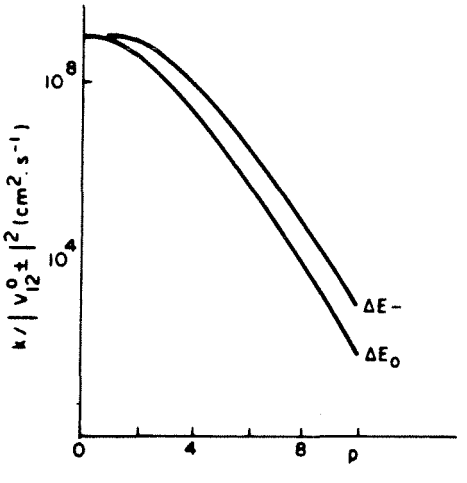

Fig. 3. Dependence of k with the energy gap on the weak coupling limit. $T = 300$°K.

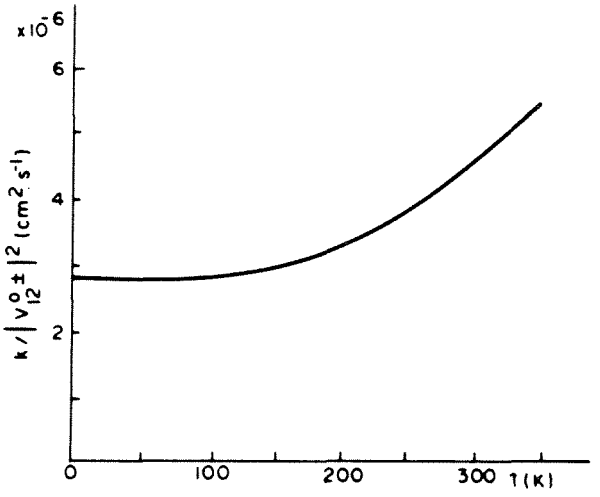

Fig. 4 Dependence of k with the temperature on the weak coupling limit. Plot for ΔE_0 and $p = 5$

on the parameter $A = (2\pi|V_{12}^{0,-}|^2/\hbar)$ which is different for each one. To illustrate the temperature dependence in this limit we also plot $k(\hbar\omega/A)$ versus T in Fig. 4. In this calculations we use the same value of 400 cm^{-1} for the intrasite modes, which is in agreement with the mean frequency of metal-ligand bonds in some metalloproteins. The reorganization energy is assumed to be $(E_r/\hbar\omega) \simeq 0.75$.

On the strong coupling limit, the reorganization energy being much larger than $\hbar\omega$, the difference in activation energy associated with ΔE_0 and ΔE_- may be very small. The interesting situation $\Delta E_0 = E_r$, which has also been used as an explanation for temperature independent electron transfer rates [17], has an activation energy associated with ΔE_- which is $E_a^{\pm} = \hbar\omega/2\Delta^2$. If, for example, we assume $E_r = 3000\ cm^{-1}$, we have $E_A^{\pm} \simeq 13.3\ cm^{-1}$ which is too small to be characterized experimentally.

Acknowlegment. The authors are grateful to Dr. H. B. Gray, Dr. J. J. Hopfield, and Dr. D. N. Beratan for very helpful suggestions with regard to this manuscript.

References

1. Chance B, De Vault DC, Frauenfelder H, Marcus RA, Schrieffer JR, Sutin N (1979) Tunneling in biological systems. Academic Press, New York
2. De Vault DC (1980) Q Rev Biophys 13:387
3. Anderson PW (1958) Phys Rev B 109:1492
4. Robin MB, Day P (1967) Adv Inorg Radiochem 10:247
5. Szent-Györgyi A (1941) Nature 148;157, (1941) Science 93:609
6. Bunker BC, Drago PS, Hendrickson DN, Richmond PN, Kessell SL (1978) J Am Chem Soc 100:3805
7. Richardson DE, Taube H (1983) J Am Chem Soc; Beratan DN, Hopfield JJ (1984) J Am Chem Soc 106;1584

8. McConnell HM (1961) J Chem Phys 35:508; Halpern J, Orgel L (1960) Discuss. Faraday Soc 29:32; Beratan DN, Onuchic JN, Hopfield JJ (1985) J Chem Phys 83:5325
9. da Gama AAS (1985) Theor Chim Acta 68:159
10. Kennedy SEP, McGourty JL, Hoffman BM (1984) J Am Chem Soc 106:1722
11. Kostić NM, Margalit R, Che CM, Gray HB J Am Chem Soc (1983) 105:7765
12. Winkler JR, Nocera DG, Yocom KM, Bordignon E, Gray HB (1982) J Am Chem Soc 104:5798; Isied SS, Kuehn C, Worosila G (1984) J Am Chem Soc 106:1722
13. Davydov AS (1978) Phys Stat Solidi(b) 90;457; Kharkyanen VN, Petrov EG, Ukrainskii II (1978) J Theor Biol 73:29; Larsson S (1983) J Chem Soc Faraday Trans 2 79:1375
14. Marcus RA, (1964) Ann Rev Phys Chem 15:155
15. Hopfield JJ (1974) Proc Natl Acad Sci (USA) 71:3640
16. Levich VG (1965) Adv Electroch Electroch Eng. 4:249
17. Jortner J (1976) J Chem Phys 64;4860, Biochim Biophys Acta (1980) 594;193
18. Marcus RA (1982) In: King TE, Morrison M, Mason HS (eds) Oxidases and related redox systems, Pergamon Press, Oxford, p 3
19. Kubo R, Toyozawa Y (1955) Prog Theor Phys 13:160
20. Holstein T (1959) Ann Phys 8:325,343
21. Davydov AS (1982) Biology and quantum mechanics. Pergamon Press, Oxford
22. Garg A, Onuchic JN, Ambegaokar V (1985) J Chem Phys 83:4491
23. Beratan DN, Hopfield JJ (1984) J Chem Phys. 81;5753
24. See, e.g.: Siders P, Cave RJ, Marcus RA (1984) J Chem Phys 81:5613
25. Ratner MA, Madhukar A (1978) Chem Phys 30;201; Lindberg J Ratner MA (1981) J Am Chem Soc 103:3265
26. Buttiker M, Landauer R (1982) Phys Rev Lett 49:1739
27. Redi M, Hopfield JJ (1980) J Chem Phys 72:6651
28. Duke CB: In [1] p 31
29. Englman R Non-radiative decay of ions and molecules in solids. North-Holland, Amsterdam
30. Marcus R: In [1] p 109
31. Auzel F (1976) Phys Rev B 13:2809
32. Taube H In [1] p 173; Sutin N In [1] p 201

CHAPTER IV – Final Remarks and Possible Future Work

IV.1 Electron Transfer between Porphyrin and Quinone Linked by a Bicyclo[2.2.2]Octane Bridge

The aim of this subsection is to present a preliminary discussion about electron transfer in the porphyrin–phenyl–$\left(\text{bicyclo[2.2.2]octane}\right)_n$–quinone system, where $n = 0, 1$ and 2 (see Fig. IV.1a). These molecules were synthesized by the Dervan–Hopfield group, and some experimental electron transfer measurements are available.[1] In this subsection we discuss the existent experimental results and try to understand them within the theory now available. Then, we conclude by describing some experiments that we believe would be helpful to resolve some conflicting points.

We now summarize the experimental results available for these systems. Initially, we describe experimental results for Zn–porphyrins. Fluorescence decay was measured for the case of $n = 1$ linker, and the electron transfer rate was calculated by comparing these lifetimes (τ_1) with the reference lifetime (τ_0) of the molecule ZnPϕ^tBu (see Figure IV.1b). The electron transfer rate is

$$k_{et} = \frac{1}{\tau_1} - \frac{1}{\tau_0} \ . \qquad (IV.1)$$

Electron transfer rate vs. driving force (ΔG) was measured. Different ΔG's were obtained by changing the substituent (R) group of the quinone of Figure IV.1a. The values of the ΔG were calculated from the measured electrochemical data for porphyrins and quinones. Details of the experimental procedures can be found in Ref. 1. All these experiments were performed in four different solvents: CH_3CN, n–PrCN, MTHF, and benzene. The rate vs. driving force results obtained at room temperature are shown in Figure IV.2 for the single linker case ($n = 1$). Also, for $n = 1$, electron transfer in 2–

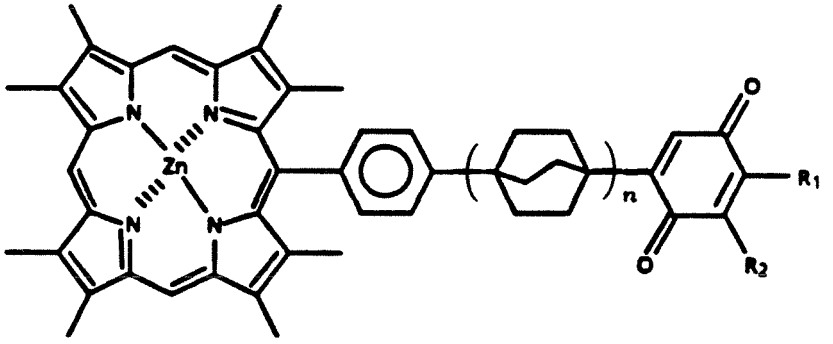

(a)

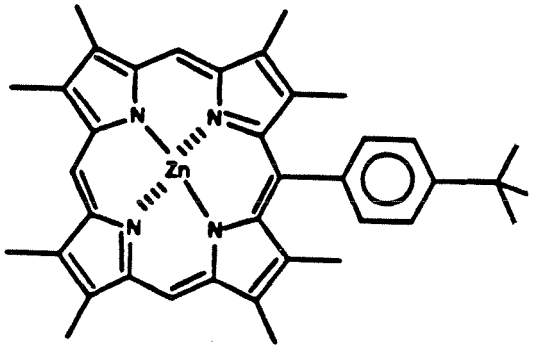

(b)

Figure IV.1 – (a) Structure of the molecule Zn–Porphyrin–Phenyl–(Bicyclo[2.2.2]octane)$_n$–Quinone. $n = 0, 1, 2$. Different R_1 and R_2 groups are used in order to obtain different driving forces ΔG (energy gap). (b) Structure of the reference molecule ZnPϕ^tBu.

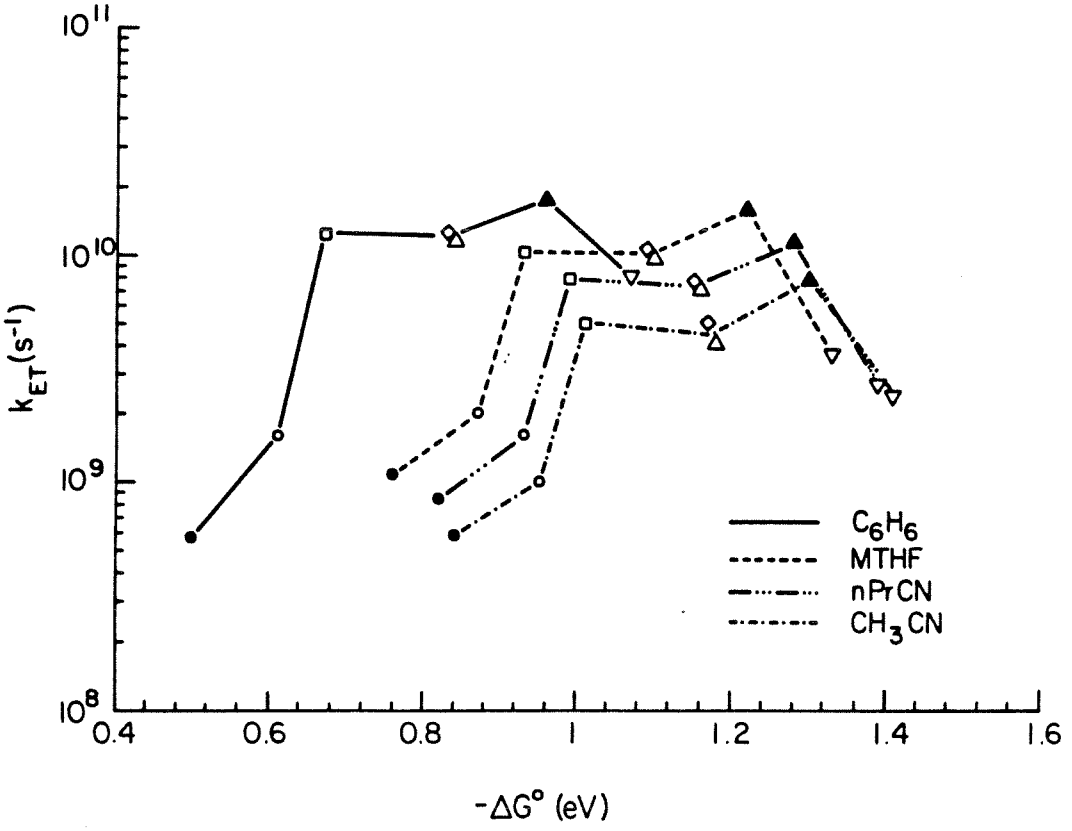

Figure IV.2 – Electron transfer rate versus exothermicity for the molecule Zn–Porphyrin–Phenyl–(Bicyclo[2.2.2]octane)–Quinone (Figure IV.1a with $n = 1$) in several solvents.

methyltetrahydrofuran glass at 77 K showed non–exponential decay in time (the reference decay is monoexponential). The experimental result is fit to

$$I(t) = a_0 \sum_{i=1}^{N} \frac{1}{N} \exp\left\{-t[\cos^2\theta_i/\tau + 1/\tau_0]\right\} + b_0 \exp\left\{-t/\tau_0\right\}, \qquad (IV.2)$$

where b_0/a_0 is the fraction of the minor component, probably due to porphyrin–linker–hydroquinone. The minor component lifetime compares well with the lifetime of the reference pophyrin ($\tau_0 \sim 1.7$ ns). Here, θ_i is the dihedral angle between porphyrin and quinone, and to assume a matrix element modulation proportional to the cosine of this angle is the simplest possible approximation (see Sec. II.4). Also, the expression above assumes an equal probability for all orientations (uniform distribution), and this is probably incorrect.

Now we discuss these experimental results. From looking at Figure 6a of Sec. II.4 and at Figure IV.2 we see that a two–mode picture (at least one fast and one slow) is needed to describe these results. In Figure IV.3 we show how this model fits the experimental result in benzene. The fast mode is probably dominated by the CO vibration. A crude estimate of the reorganization energy for this mode was made by B. Leland,[1c] and he obtained $E_R^{fast} \sim 0.25$ eV ($\hbar\Omega_{fast} \sim 0.25$eV). The reorganization energy for the slow mode E_R^{slow} was chosen to fit the low ΔG data, and it should be about 0.15 eV. All these parameters are completely preliminary. The value of the matrix element chosen to fit the data is $T_{DA} = 7 \times 10^{-4}$ eV. There is a crucial problem here; the zero of the ΔG scale obtained from the experimental data does not agree with the theoretical one. A shift of 0.6 eV must be included. This difference is probably due to two factors. The first one is the work term; the system goes from the neutral to the charged state. The second factor is the absence of the counter ions that exist in the electrolyte solution and stabilizes the ions in the

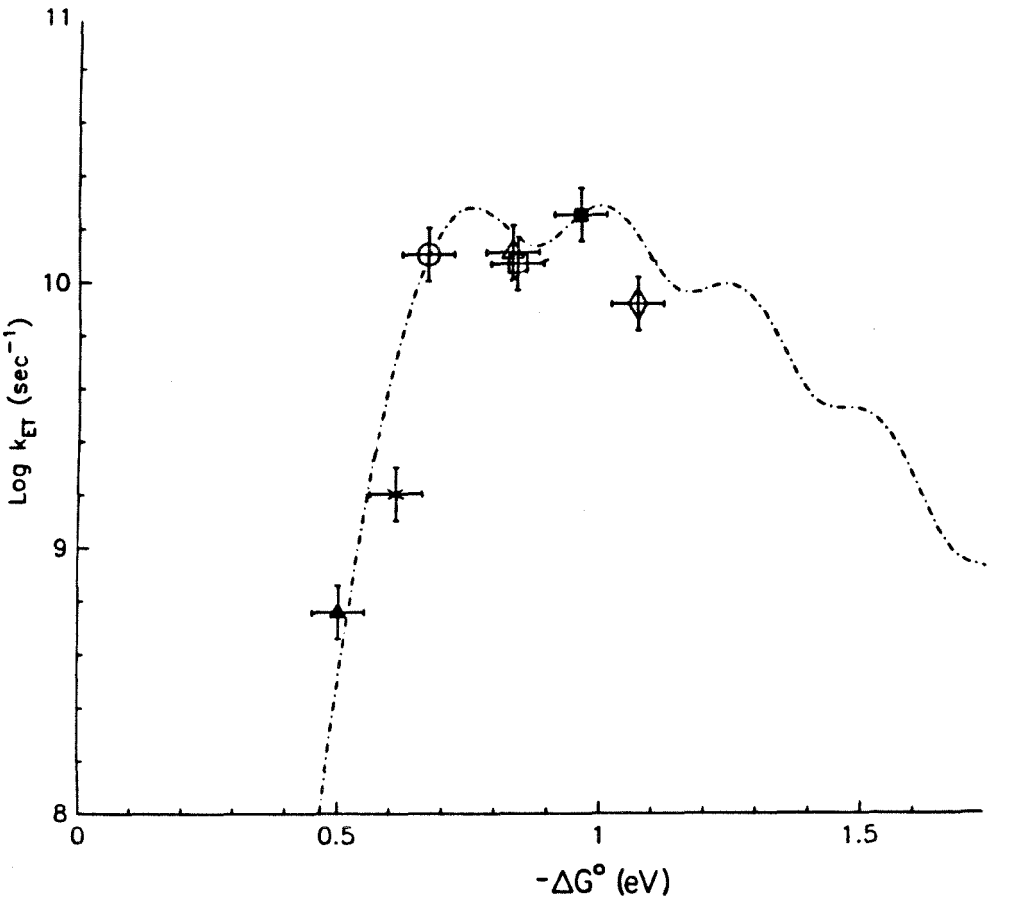

Figure IV.3 – Theoretical fit of the electron transfer rate versus exothermicity for the molecule Zn–Porphyrin–Phenyl–(Bicyclo[2.2.2]octane)–Quinone (Figure IV.1a with $n = 1$) in benzene. Eq. 3.34 of Sec. II.4 is used. The parameters used are described in the text.

electrochemical measurements. The first effect should increase ΔG, and the second one should reduce it, because the quinone is much smaller than the porphyrin. We do not discuss details about these corrections here, but they should be very similar for all molecules described in Figure IV.1a, if they are in the same solvent. Therefore, they are probably responsible for the shift we have to include in Figure IV.3. Another basic problem still exists. At very low ΔG, if our shift assumption is correct, we will have some endothermic electron transfer, and the possibility of back–transfer has to be included in the calculation (as suggested by Marcus). Here the question is the following: Which rate is faster, back–transfer to the porphyrin S_1 state or quinone transfer to the porphyrin S_0 ground state? To check this point, we propose two experiments.

To verify our value of E_R^{slow}, we should study the temperature dependence of the rate for temperatures before the solvent freezing. The mean–square deviation of the first peak (variation of the rate at low ΔG) is $\sqrt{2E_R^{slow}kT}$, and if our model is correct, this should be observed in the experiments. The other possibility is to try directly to measure the rate of quinone ion formation together with fluorescence decay.

Next, we discuss the effect of solvent on the rate (see Figure IV.2). Assuming that we have a different energy drift for each solvent, but the same E_R^{fast} and $\hbar\Omega_{fast}$, we estimate E_R^{slow} for the different solvents. Gross estimates of the value of E_R^{slow} from benzene ($\epsilon_S = 2.3$) to CH_3CN ($\epsilon_S = 38.8$) show that it varies less than 0.1 eV. This tells us two things: we have at least one other slow mode besides solvent polarization, and the macroscopic linear model for solvent polarization overestimates the value of E_R^{slow}. We have to be careful to check the values for E_R^{slow}, as proposed in the last paragraph, before making

any conclusion.

Now we discuss the low temperature result. As discussed in Sec. II.4, it would be interesting to determine the temperature dependence of the electron transfer rate and to try to observe the transition from exponential to non–exponential decay in time. Some molecular mechanics calculations[2] can be done for the porphyrin–quinone relative orientation potential as a function of the dihedral angle. If the potential obtained has several minima, we should be able to estimate (from the barrier heights) the "critical temperature" for going from exponential to non–exponential decay in time, if exponentiality is mainly a function of this mode. Comparing the theoretical prediction with the experiments would be interesting. If the potential has only one minimum (which I do not expect because of the quinone–CO bridge interaction), then a smooth transition from exponential to non–exponential behavior should be expected.

To conclude, we discuss the $n = 0$ and 2 bridge linker cases (see Figure IV.1a). Experimental measurements on the zero linker molecule at room temperature estimate that this rate is faster than 10^{12} Hz. This suggests that the rate is adiabatic. In order to study the transition from adiabatic to non–adiabatic rates, it would be interesting if this rate were measured. Also, it may be simpler to measure this rate at low temperature. If the low temperature measurements become possible, it may be possible to verify whether other modes, besides the dihedral angle modulation of the matrix element, are responsible for the non–exponential decay in time (see Sec. II.4). The $n = 2$ linker case is interesting to check the predicted matrix element dependence on distance. Also, it would help to give some estimates of the size of the work

term if a rate vs. ΔG study were made for the two linker system. Preliminary phosphorescence measurements in Pt–porphyrin predicts that k_{ET}(double linker) $< 10^6$. Comparing with the single linker rate for a similar value of ΔG, k_{ET}(single linker)/k_{ET}(double linker) > 3000 (not exactly). Theoretical predictions by Beratan[3] expect this ratio to be about 2000. This result, however, is very preliminary, and we do not want to draw any further conclusion before more reliable experimental data are available.

IV.2 Some Other Interesting Problems– Work in Progress

To conclude, we would like to comment on two other interesting problems we are starting to address now and intend to continue to investigate in the near future. Some preliminary ideas are given here. The first one, as already remarked in Chapter I, is that if we consider only a finite number of "reaction coordinates," it is impossible to account for large entropic changes that appear in some electron transfer reactions.[4] When we deal with entropic changes, we also approach the problem of dynamics on "free" energy surfaces. The second problem is to try to apply the model described in Sec. III.4 in order to understand electron transfer rates in some protein systems.

How to include entropy in simple model

The models described in this thesis assume electron transfer coupled to a finite number of reaction coordinates. In this description it is basically impossible to account for large entropic changes. Also, in many discussions of reaction rate theory, entropy is taken into account by assuming that we have "free" energy wells rather than potential energy wells. Free energy, however, is a thermodynamic property that one calculates by averaging over many dynamical trajectories, and dynamics is determined by the potential energy surface. These are the sorts of issues we are trying to address.

A free energy surface can be defined by fixing the reaction coordinate at some value Q and allowing some subset of all other degrees of freedom to

equilibrate. This results in a well–defined free energy surface, but we have to understand whether it has anything to do with the dynamics of the reaction coordinate. If we assume that our reaction coordinate moves much more slowly than the time necessary for this subset of modes to come to thermal equilibrium with their environment, the dynamics of this reaction coordinate (slow mode) can be described by motion on an effective potential surface determined by the free energy of the fast modes at each value of the slow coordinate.

This problem is being formalized in collaboration with W. Bialek. Using a simple picture, we can think about a single mode coupled to a continous background. The continuum will be responsible for damping (modes with frequency on the same order as the reaction coordinate) and "fast" modes that convert the potential energy surface of the specific modes into free energy surfaces. It is important to point out that linear coupling and a harmonic bath are sufficient for damping, but more complicated coupling and/or bath is necessary to generate large entropic changes.

Calculation of Electron Transfer Rates in Proteins

To conclude this chapter, we discuss the way in which we intend to apply the model described in Sec. III.4 in order to calculate electron transfer rates in real proteins. The systems we intend to study initially are the Ru–modified proteins that are being prepared in Harry Gray's laboratory with site–directed mutagenesis (cytochrome *c* and myoglobin).[5] The reason to study these systems is that there will be a large number of isomers, each one with a different site where the Ru–$(NH_3)_5$ groups can bind. This will be obtained by site–directed

mutogenesis, which will increase the number of histidines on the protein surface. Because of that, we will have several electron transfer systems where basically only the medium through which the electron tunnels is changed but "everything else" is the same. Some experimental results are already available for cytochrome *c* and myoglobin.[6] The problem with the actual data is that only a few different electron transfer rates are available. From the myoglobin results, a possible example of the medium structure influence on the rate is seen when we compare the transfer rates to the Ru–$(NH_3)_5$ in His–12 and His–116 from ZnP*. They are very similar ($\ln(k_{ET}) \sim 4.5$), but the edge–edge distances are 22 and 19 Å, respectively. This last comment is pure speculation.

Predicting the new form of temperature dependence introduced in Sec. III.4 for the protein pathways may be important (each isomer will have different pathway(s)). This is also a challenge that lies in the future. Another way of changing the electron transfer pathway is by changing amino acids that are "important" to the electron transfer pathway. Experimental work in this direction is starting to be done in Hoffman's group in complexes of cytochrome *c* and cytochrome peroxidase.[7]

IV.3 References – Chapter IV

(1) (a) B.A. Leland, A.D. Joran, P.M. Felker, J.J. Hopfield, A.H. Zewail, and P.B. Dervan, *J. Phys. Chem.* **89**, 5571 (1985); (b) A.D. Joran, *Ph.D. Thesis*, California Institute of Technology, 1986; (c) B.A. Leland, *Ph.D. Thesis*, California Institute of Technology, 1987.

(2) W.A. Goddard, personal communication.

(3) D.N. Beratan *J. Am. Chem. Soc.* **108**, 4321 (1986).

(4) W.R. Ellis, *Ph.D. Thesis*, California Institute of Technology, 1986.

(5) H.B. Gray, personal communication.

(6) (a) A.W. Axup, *Ph.D. Thesis*, California Institute of Technology, 1987; (b) J.R. Winkler, D.G. Nocera, K.M. Yocom, E. Bordignon, and H.B. Gray, *J. Am. Chem. Soc.* **104**, 5798 (1982); (c) S.L. Mayo, W.R. Ellis, R.J. Crutchley, and H.B. Gray, *Science* **233**, 948 (1986).